Studies on solid-state photopolymerization of styrene derivatives bearing 1,3,4-thiadiazole group

Akira Furukawa

Graduate School of Materials Science
Nara Institute of Science and Technology

2003

Contents

Chapter 4 Influence of monomer concentration in the solid-state photoinitiated polymerization of styrenyl compound bearing 1,3,4-thiadiazole group

Chapter 5 Effects of photoinitiator concentration and light intensity on the solid-state polymerization of styrenyl compound bearing thiadiazole group

Chapter 6 Effect of alkyl chain length in 2-(4'-vinylbenzyl)thio-5-alkyl-thio-1,3,4-thiadiazole on its photopolymerization in polymer matrix

Chapter 1

General introduction

Photoinitiated polymerization is one of the best controllable processes for producing polymer materials with well-defined structures. Irradiation from a suitable light source initiates polymerization at ambient temperature and precisely at the desired position of the polymerization system. The rate and degree of polymerization can be controlled simply by adjusting the intensity of the irradiation. The use of photoirradiation instead of heat to induce polymerization has rendered us a number of merits. There are a number of ecological advantages, i.e., low-energy consumption and non-volatile organic solvent. Many industrial innovations have been resulted, such as coating industry, microelectronics and photolithography. In the past decades, extensive investigations on the photoinitiated polymerization systems have been carried out aiming at finding polymerization system with higher photosensitivity. Major efforts have been devoted to develop highly photopolymerizable monomers and high-speed photoinitiating system (initiator and its sensitizer). In order to understand the polymerization mechanism and to construct improved polymerization system, many kinetic investigations have also been carried out.

Photoinitiated polymerization may be classified into two groups, i.e., photoinitiated cationic polymerization[1] and photoinitiated radical polymerization.[2] In either of them, developments of highly photosensitive systems are required and under extensive investigations. Recently, Crivello and Ortiz[3, 4] have developed highly photoactive epoxy

monomers. These undergo a fast cationic polymerization involving radical-induced decomposition of onium salt photoinitiator.[1,5-7] One of the most distinct advantages in cationic photopolymerization as compared with radical photopolymerization is the insensitivity to oxygen. As for radical photopolymerization various types of effective photoinitiators have been developed. In combination with specially designed acrylate monomers,[2,8] ultra-fast radical photopolymerization was demonstrated by Decker and Moussa.[9] In radical photopolymerization mostly acrylic monomers have been utilized due to their high polymerizability and easiness for structural modifications to be best-suited for the practical usages.

In both types of photopolymerization little attention has been paid to styrene derivatives. One of the reasons is the relatively low polymerizability of styrene derivatives. On the other hand, incorporation of styrenyl units into polyacrylates renders improved physical and chemical properties such as mechanical properties, chemical resistance and elevated T_g of the copolymers, which opens the way to industrial applications. Since styrenyl monomers could be polymerized *via* either cationic or radical mechanism, discovery of photoactive styrene monomers would create a new photopolymerization system.

Subsequently, the current status of the solid-state photopolymerization will be surveyed with special reference to the uniqueness of the present investigation.

1-1. Trends in highly photopolymerizable compounds

The relationship between the chemical structure of unsaturated compound and its photopolymerizability had not been investigated in detail until Decker[8] found that heterocyclic oxygen introduced to acrylate compound accelerated the polymerization

reactivity. Quite recently Jansen, et al.[10, 11] reported that some acrylate compounds exhibited high photopolymerization reactivity in bulk and the rates of polymerization were directly related to the dipole moment of acrylate compounds. Some preorganized structures due to dipole-dipole interactions have been put forward by them to explain the high reactivity of these acrylate compounds. The effect of preorganized structure has been observed in the photopolymerization of monomers which are capable to form intermolecular hydrogen bonding.[10]

Styrene is one of the most important unsaturated compounds in polymer industries and polystyrene is among the four major plastics (polyethylene, polypropylene, poly(vinyl chloride) and polystyrene). Polystyrene is resistant to corrosions by acid and alkali and is an excellent electric insulator. Its stiff and brittle properties are improved by copolymerization in high-impact polystyrene, SBR (styrene-butadiene copolymer) and ABS (acrylonitrile-butadiene-styrene copolymer or blend). In addition, styrene-unsaturated polyester system is an instance of the most widely used graft copolymers, which are used for flooring materials. Photoinitiated polymerization of styrene in the presence of unsaturated polyesters was reported as early as 1946[12] and currently still in active use especially for wood coatings.

In most of industrial applications, photopolymerization of styrene and its derivatives has not been paid much attention because of their low polymerization reactivity and volatility. In radical photopolymerization, various types of acrylates and methacrylates have been in major usage.

1-2. Photoinitiator and its photodecomposition process

Light-sensitive compounds including trichloromethyl-substituted 1,3,5-triazines

were found in the late 1960's[13] and are currently used in microelectronics industry and others. This types of photoinitiator can be used either as photoradical initiator[14] or as photoacid generator (PAG).[15-20] Upon UV irradiation, trichloromethyl group attached to the triazine ring undergoes homolytic cleavage of the carbon-chlorine bond and thus produced chlorine atom abstracts hydrogen atom from a donor, resulting in the formation of hydrogen chloride which acts as an acid catalyst in chemically amplified imaging system. On the other hand, the carbon radical resulting from carbon-chlorine bond cleavage adds to carbon-carbon double bond of vinyl compound to initiate radical polymerization. Buhr, et al.[16] identified the structures of photodecomposition products of similar 2-substituted-4,6-bis(trichloromethy)-1,3,5-triazines in both nonpolar aprotic and polar protic solvents. They found that the photolysis in toluene gave products of homolytic cleavage of carbon-chlorine bond, whereas in ethanol/ethyl acetate the products of heterolytic cleavage of carbon-chlorine bond were detected among those from homolytic cleavage. They also estimated the quantum yield of acid formation from triazines in a novolak resin to range from 0.29 to 0.35.[16] Pohlers, et al.[18] reported the quantum yield of acid formation from 2-substituted-3,6-bis(trichloromethyl)-1,3,5-triazines in diglyme solution was in the range of 0.009 to 0.012. They also found by laser flash photolysis studies that in a polar aprotic solvent both homolysis and heterolysis of the C-Cl bond took place.[21] They detected intermediate cationic species from heterolysis which was quenched by the addition of chloride ion. One of the very important discoveries in their studies is that the quantum yield of acid formation through the heterolytic bond cleavage is much smaller than those in homolytic bond cleavage in nonpolar solvents. These experimental results suggest that the effectiveness of trichloromethyl-substituted triazine as a PAG and/or a photoradical initiator is

strongly dependent on the environment in which it is used.

In the present investigation, the trichloromethyl-substituted 1,3,5-triazines were used as photoinitiators of solid-state polymerization of styrene derivatives carrying heterocyclic substituent.

1-3. Kinetic investigations on the photopolymerization in polymer matrix

Photoinitiator is a key material to realize a highly effective photopolymerization system. Although the rate of initiation is closely related to the decomposition rate of photoinitiator in determining the overall polymerization rate, only few have been reported on actual photodecomposition processes of photoinitiator in bulk photopolymerization system. Decker, et al.[2, 22, 23] investigated the photodecomposition behaviors of typical photoradical initiator, Lucirin TPO (2,4,6-trimethylbenzoyldiphenylphosphine oxide) and of some photoacid generators, triarylsulfonium salts, by monitoring the decrease of UV absorbance of these photoinitiators. They found that these photoinitiators disappeared according to a simple exponential law. However, spectroscopy under UV irradiation might affect photodecomposition of UV-sensitive photoinitiators so that whole measurements should be carried out without these effects. In order to relate the rate of monomer consumption with photodecomposition rate of photoinitiator, both reactions should be determined simultaneously in the polymerization system. Other methods to measure decomposition of photoinitiator have been explored such as laser flash photolysis and emission spectroscopy,[21] time-resolved electron spin resonance[24] and time-resolved electron paramagnetic resonance.[25] However, these methods cannot measure the polymerization rate simultaneously.

Recently, Decker and Moussa[8, 9, 26-28] have developed a powerful analytical tool of real-rime Fourier-transform infrared (RT-IR) spectroscopy, which enables us to observe *in situ* the progress of polymerization of various types of vinyl compounds and epoxy derivatives.[3, 4] By pursuing the time-dependent absorbance change of the monomer and the initiator simultaneously, we can discuss the monomer to polymer conversion in relation to the decomposition of photoinitiator. This analytical method can be applied to solid-state polymerization as well as solution polymerization.

Usefulness of photopolymerization in polymer matrix has been shown in preparation of interpenetrating polymer networks by Decker and his coworkers.[29, 30] They studied the influence of the nature of polymer matrix on the photopolymerization behaviors of various acrylic compounds and found faster polymerization in poly(vinyl chloride) matrix.[30] They suggested an importance of chain-transfer reaction to polymer matrix.

The presence of a solid matrix in polymerization profoundly influences the polymerization rate through restricted diffusion of monomers and growing polymer chains. In such a situation, reaction diffusion process is sometimes considered to be the dominant termination mechanism.[31-33] As conversion increases, due to the difficulty of segmental movement of propagating radical, diffusion of radical through unreacted double bonds becomes faster than segmental diffusion and reaction diffusion process dominates the termination mechanism. In such a case, the termination rate constant, k_t, and the propagation rate constant, k_p, are related with each other by the following equation:[31-33]

$$k_t = R k_p [M]$$

where R is the reaction diffusion parameter, [M] is the concentration of monomer.

Bowman, et al.[34-36] had shown experimentally the validity of above relationship in highly crosslinked methacrylates. Mateo and his coworkers[37-41] reported the photopolymerization of methacrylates in various polymer matrices and the importance of reaction diffusion mechanism was explained by them. However, various types of termination mechanisms, including reaction diffusion, should be prevailing in variety of actual polymerization systems. Decker and Moussa[9] have reported a linear dependence of R_p on the light intensity for photopolymerization of acrylate , in which unimolecular termination process due to radical occlusion was involved. On the other hand, Scherzer and Decker[42] and Lecamp, et al.[43] have reported independently that R_p is proportional to the square root of light intensity, showing the occurrence of bimolecular termination process.

New type of printing plate utilizes photopolymerization in polymer matrix. [44-47] A photopolymerizable layer containing multifunctional monomers and a polymer matrix is coated on an anodized aluminum plate. Irradiation of laser light induces photopolymerization at the irradiated spots to three-dimensional polymer network on the aluminum surface. The laser-irradiated plate is developed in a usual way. The common disadvantage in the existing printing plate comes from the necessity of coating the surface of photopolymerizable layer with poly(vinyl alcohol) film to prohibit oxygen penetration during the photopolymerization process. The presence of such overcoat makes two successive coating processes necessary and deteriorates the image quality significantly due to laser-light scattering. The present author has been interested in creation of a highly effective photopolymerization system which is insensitive to atmospheric oxygen, leading to the elimination of overcoat. To attain this porpose, photopolymerization of particular styrene derivatives in suitable polymer matrix has

been investigated and it is the subject of this doctral thesis.

1-4. Background of the present thesis

The pre-organized state of monomer which Jansen[10, 11] has postulated to explain his experimental results should be closely related to topochemical polymerization[48-52] and polymerization in liquid crystalline state.[53-56] Topochemical polymerization has gained special attentions for obtaining well-defined ultra-high molecular weight polymers with highly regulated structures by the so-called crystal engineering. Polymerization in liquid crystalline state is also a recent topic to obtain highly ordered polymer materials. In pursuit of novel LC phase behavior and properties, a number of polymer-LC composites have been developed. Among them polymer stabilized LC systems[57] have been of considerable research interest due to their great potential in LC display applications.[58]

Thermotropic LC polymers have gained special attentions due to their excellent mechanical properties and physical anisotropy and applied for engineering plastics. The author had been interested in developing some new thermotropic LC polyesters which show relatively wide temperature range of LC phase and decreased melting points.[59-61] Commonly known thermotropic LC polyesters shows relatively high melting points and narrow temperature ranges of LC phase and when they are applied for polymerization media as an anisotropic matrix, inappropriately high temperature for polymerization and insufficient stability of LC phase usually make such an usage difficult to operate. These high melting points can be decreased by several types of structural modifications including either the introduction of a flexible spacer group in the main chain, or the placement of lateral substituents on the repeating units, or the introduction of molecular kinks or bends in their units, or by copolymerization with other rodlike comonomers.[62,

[63] Flexible spacers have been most extensively used to decrease polymer melting points and improve their stability, [64,65] and the role of these flexible spacer groups within the main chain had been under intensive investigations for both theoretical[66, 67] and experimental[62, 68] aspects. Lateral substituents on main chain LC polymers generally reduce both the melting points, T_m, and the isotropization temperature, T_i, but their relative effects on decreasing T_m and T_i are quite different and unpredictable.

In general, the effects of substituents on T_i can be divided into two categories: steric and polar effects. That is, lateral substituents may either decrease molecular anisotropy and destabilize the LC phase because of steric interference or, through dipolar intermolecular interactions, they may contribute to the stabilization of the LC phase. However, it had also been proposed that steric effects can, in some case, increase the thermal stability of the LC phase by interlocking effects.[69]

The author had prepared a series of thermotropic polyesters based on a triad ester mesogenic unit containing an arylsulfonyl substituted hydroquinone group and a decamethylene spacer group of the following structure: [59]

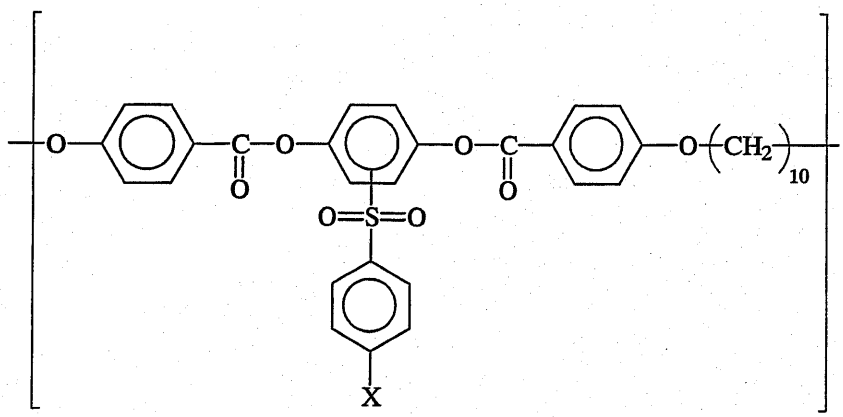

in which X is H, CH_3, F, Cl, Br, I, NO_2 and OCH_3. The arylsulfonyl groups were expected to show large steric and polar effects, which should follow a consistent pattern

as a function of the size and either the electron withdrawing or the electron donating effects of the X substituents. All polymers formed nematic melts at 77 to 101 °C depending on the nature of the X substituents, and showed a fairly wide temperature range of nematic phase; i.e., 40 to 70 °C. A regular decrease in T_i, ΔH_i and ΔS_i was observed with increasing molecular radius of the substituted hydroquinone group. However, a polarity or polarizability effect was superimposed on these relationships. The observed result indicated the importance of these polarity or polarizability effect on the stability of the ordered phase.

Further approach had been made in an attempt to decrease T_m down to near room temperature which would enable us to carry out photopolymerization in an ordered phase by incorporating photopolymerizable monomers into these LC polymer matrix. The following thermotropic polyesters were prepared and their LC properties were investigated: [60, 61]

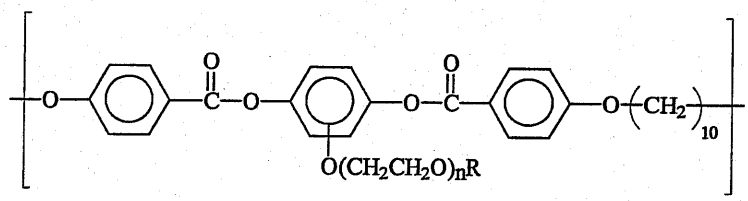

in which n = 0, 1 or 2 and R = CH_3 or C_2H_5. Although all of the polymers showed T_m at around 70 to 80 °C, which was still higher than we anticipated, T_i was increased much higher than those observed in the case of the arylsulfonyl groups described above.

We believe that these thermotropic LC polyesters would be useful for the anisotropic matrix for the photopolymerization of various LC monomers and incorporation of such LC monomers may lead to a novel unique polymer LC materials.

Kinetic analysis of polymerization process is indispensable for understanding of

polymerization mechanism and for attaining improved effectiveness of polymerization. Polymerization process is mainly divided into four elementary steps, namely initiation, propagation, chain transfer and termination reactions. Each step determines the polymerization behavior and kinetic analyses must be done with using reliable analytical tools to investigate all these elementary reactions. One of the most important parameters to be estimated is the concentration of propagating species in any kinds of polymerization processes. In cationic polymerization, the author had been interested in determining the concentration of propagating carbocation in cationic polymerization of styrene in solution. A new end-capping method, with sodium 2-naphthoxide as capping agent, had been developed by us[70, 71] and used for determining the concentration ([P*]) and chain-length distribution of the propagating species in cationic polymerization of styrene. In the reactions initiated by acetyl perchlorate ($AcClO_4$) at 0 °C, the added naphthoxide combined quantitatively and instantaneously with the growing chains to form 2-naphthoxy-capped polymers that exhibited a UV absorption of the end group at ca. 330 nm. On the basis of this band, [P*] and propagating rate constant (k_p) was determined; the initiation efficiency ([P*]/[$AcClO_4$]) and the k_p values depended strongly not only on the polarity of polymerization solvents but on the initial monomer concentration. GPC analysis (UV at 330 nm), monitoring the naphthoxyl end group of the product polymers, provided the chain-length distribution of the propagating species. Constant values of [P*] in the polymerization process revealed a steady-state condition of the polymerization and dependence of [P*] and k_p on the initial monomer concentration suggested the complex nature of the polymerization mechanism.

As for radical polymerization in solution, ESR (electron spin resonance spectroscopy) has been the most powerful tool to determine the propagating radical concentration.

However, in the photopolymerization in bulk, the detection of the propagating radical was sometimes impossible due to the strong dependence of the thermodynamic stability of propagating radicals on their chain-length, or due to the accumulation of trapped radical which do not contribute to the polymerization.[24, 72] RT-IR spectroscopy, which we used for the investigation of solid-state photopolymerization of styrenyl compounds, is a powerful tool to observe *in situ* the progress of polymerization as described in section 1-3.

1-5. Outline of the present thesis

In this thesis, the experimental results of the synthesis and the photopolymerization behavior in polymer matrix of a series of styrenyl monomers bearing 1,3,4-thiadiazole group are presented and discussed.

In Chapter 2, various types of styrenyl monomers were prepared and their reactivities in solid-state photopolymerization were investigated. Photopolymerizability of these styrenyl compounds are discussed in terms of London dispersion force and hydrogen bonding with polymer matrix. Effect of atmospheric oxygen on the polymerization behavior was also investigated.

In Chapter 3, photodecomposition process of the photoinitiator, 2-substituted-3,4-bis(trichloromethyl)-1,3,4-triazine, was analyzed by RT-IR spectroscopy and the effects of the initiator concentration and light intensity on the rate of photodecomposition were discussed. Photopolymerization rate of the styrenyl compounds and photodecomposition rate of the photoinitiator were concurrently measured and kinetic analysis was carried out.

In Chapter 4, the effect of monomer concentration on the photopolymerization

behavior of the styrenyl compound was investigated.

In Chapter 5, the effects of photoinitiator concentration and light intensity on the photopolymerization of the styrenyl compound were investigated, partly aiming at estimation of the number of the monomer molecules incorporated in the preorganized structure.

In Chapter 6, the size of alkyl substituent on the styrenyl compounds was systematically altered and its effect on the photopolymerization behavior was investigated. The nature of the preorganized structure was discussed in reference to the effect of polymer matrix on photopolymerization.

In Chapter 7, polymers having pendant styrenyl groups were prepared for the use of the reactive polymer matrix and their photopolymerization behavior was investigated. Copolymerization of the pendant styrenyl groups with free monomers was also investigated and participation of preorganized structure of pendant styrenyl groups as well as monomer molecules in the graft polymerization is discussed.

In Chapter 8, the experimental results obtained in this thesis are briefly summarized.

References

1. Crivello, J. V., Adv. in Polym. Sci., 1984, 62, 1.
2. Decker, C., Macromol. Symp. 1999, 143, 45.
3. Crivello, J. V.; Ortiz, R. A., J. Polym. Sci. Part A. Polym. Chem., 2001, 39, 2385.
4. Crivello, J. V.; Ortiz, R. A., ibid., 2001, 39, 3578.
5. Crivello, J. V.; Ortiz, R. A., ibid., 1983, 21, 1097.
6. Pappas, S. P. ; Pappas, B. C. ; Gatechair, L. R., ibid., 1984, 22, 69.
7. Pappas, S. P. ; Gatechair, L. R. ; Jilek, J. H. , ibid., 1984, 22, 77.
8. Moussa, K. ; Decker, C., ibid., 1993, 31, 2197.
9. Decker, C. ; Moussa, K. , Makromol. Chem., 1988, 189, 2381.
10. Jansen, J.F.G.A. ; Dias, A. A. ; Dorschu, M. ; Coussens, B., Polym. Prepr., 2001, 42, 769.
11. Jansen, J.F.G.A. ; Dias, A. A. ; Dorschu, M. ; Coussens, B., Macromolecules, 2002, 35, 7529.
12. Du Pont, U. S. Patent 2,448,828 (1946).
13. Dietrich, R., DAS 1 298 414 (1969).
14. Bonham, J. A.; Petrellis, P. C., US patent 3,954,475 (1976).
15. Smith, G. H. ; Bonham, J. A., US patent 3,779,778 (1973).
16. Buhr, G. ; Dammel, R. ; Lindley, C. R., Polym. Mat. Sci. Eng., 1989, 61, 269.
17. MacDonald, S. A. ; McKean, D. R., J. Photopolym. Sci. Tech., 1990, 3, 375.
18. Pohlers, G. ; Scaiano,; Sinta, R. J. C., Chem. Mater., 1997, 9, 3222.
19. Pawlowski, G. ; Dammel, R., J. Photopolym. Sci. Tech., 1991, 4, 389.
20. Frechet, J. M. J., Pure & Appl. Chem., 1992, 64, 1239
21. Pohlers, G. ; Scaiano, J. C. ; Step, E. ; Sinta, R., J. Am. Chem. Soc., 1999, 121,

6167.

22. Decker, C. ; Xuan, H. L. ; Viet, T. N. T., J. Polym. Sci. Part A. Polym. Chem., 1995, 33, 2759.

23. Decker, C. ; Viet, T. N. T., Macromol. Chem. Phys., 1999, 200, 358.

24. Mizuta, Y. ; Morishita, N. ; Kuwata, K., Appl. Magn. Reson., 2000, 19, 93.

25. Williams, R. M. ; Khudyakov, I. V. ; Purvis, M. B. ; Overton, B. J. ; Turro, N. J., J. Phys. Chem. B, 2000, 104, 10437.

26. Decker, C. ; Moussa, K. , Macromolecules. 1989, 22, 4455.

27. Decker, C., Macromolecules. 1990, 23, 5217.

28. Decker, C. ; Moussa, K. , Eur. Polym. J., 1990, 26, 393.

29. Kaczmarek, H. ; Decker, C., J. Polym. Sci. Part A. Polym. Chem., 1994, 54, 2147.

30. Moussa, K. ; Decker, C., ibid., 1993, 31, 2633.

31. Schulz, G. V., Z. Phys. Chem. (Munich), 1956, 8, 290.

32. Buback, M. ; Huckestein, B. ; Russel, G. T., Macromol. Chem. Phys., 1994, 195, 539.

33. Stickler, M., Macromol. Chem., 1983, 184, 2563.

34. Anseth, K. S. ; Anderson, K. J. ; Bowman, C. N., Macromol. Chem. Phys., 1996, 197, 833.

35. Lovell, L. G. ; Stansbury, J. W. ; Syrpes, D. C. ; Bowman, C. N., Macromolecules, 1999, 32, 3913.

36. Young, J. S. ; Bowman, C. N., ibid., 1999, 32, 6073.

37. Mateo, J. L. ; Serrano, J. ; Bosch, P., ibid., 1997, 30, 1285.

38. Bosch, P.; Serrano, J.; Mateo, J. L.; Guzman, J.; Calle, P.; Sieiro, C. J Polym Sci Part A. Polym Chem 1998, 36, 2785.

39. Mateo, J. L.; Calbo, M.; Bosch, P., ibid., 2001, 39, 2049.

40. Mateo, J. L.; Calbo, M.; Bosch, P., ibid., 2001, 39, 2444.

41. Mateo, J. L.; Calbo, M.; Bosch, P., ibid., 2002, 40, 120.

42. Scherzer, T. and Decker, U. Rad. Phys. Chem., 1999, 55, 615.

43. Lecamp, L.; Youssef, B.; Bunel, C.; Lebaudy, P., Polymer, 1997, 38, 6089.

44. Herting, H. P. ; Goodman, R. M. In Proceedings of the Technical Association of the Graphic Arts, TAGA 1998, TAGA, Rochester, New York, N. Y., p.312.

45. Li, B. ; Zhang, S. ; Tang, L. ; Zhou, Q., Polym. J. 2001, 33, 263.

46. Zhang, S. ; Li, B. ;Tang, L. ; Wang, X. ; Liu, D. ;Zhou, Q., Polymer, 2001, 42, 7575

47. Urano, T. ; Nagao, T. ; Takada, A. ;Itoh, H., Polym. Adv. Technol., 1999, 10, 244.

48. Matsumoto, A. ; Matsumura, T. ; Aoki, S., J. Chem. Soc., Chem. Commun., 1994, 1389.

49. Tashiro, K. ; Kamae, T. ; Kobayashi, M. ; A. Matsumoto, A. ; Yokoi, K. ; Aoki, S., Macromolecules, 1999, 32, 2449.

50. Odani, T. ; Matsumoto, A., Macromol. Rapid Commun., 2000, 21, 40.

51. Matsumoto, A. ; Nagahama, S. ; Odani, T., J. Am. Chem. Soc., 2000, 122, 9109.

52. Matsumoto, A. ; Odani, T. ; Sada, K. ; Miyata, M. ; Tasiro, K., Nature, 2000, 405, 328.

53. Williamson, S. E. ; Kang, D. ; Hoyle, C. E., Macromolecules, 1996, 29, 8656.

54. Andersson, H. ; Trollsas, M. ; Gedde, U. W. ; Hult, A., Macromol. Chem. Phys., 1995, 196, 3667.

55. Guymon, C. A. ; Hoggan, E. N. ; Clark, N. A. ; Rieker, T. P. ; Walba, D. M. ; Bowman, C. N., Science, 1997, 275, 57.

56. Guymon, C. A. ; Bowman, C. N., Macromolecules, 1997, 30, 5271.

57. McCormick, D. T. ; Chavers, R. ; Guymon, C. A., Macromolecules, 2001, 34, 6929.

58. Walba, D. M., Science, 1995, 270, 250.

59. Furukawa, A. ; Lenz, R. W., Macromol. Chem., Macromol. Symp., 1986, 2, 3.

60. Lenz, R. W.; Furukawa, A. ; Wu, C. N., Polymers for Advanced Technologies, Ed. by Lewin, M., VCH Publishers, NY, 1988, p. 491.

61. Lenz, R. W.; Furukawa, A.; Bhowmik, P. ; Garay, R. O.; Majnusz, J., Polymer, 1991, 32, 1703.

62. Ober, C. K. ; Jin, J.-I. ; Lenz, R. W., Adv. Polym. Sci., 1984, 59, 103.

63. Lenz, R. W., Polym. Symp., 1985, 72, 1.

64. Jackson, W. J., Macromolecules, 1983, 16, 1027.

65. Jackson, W. J. ; Kuhfuss, H. F., J. Polym. Sci. Part A. Polym. Chem., 1976, 14, 2043.

66. Vasilenko, S. V. ; Khokhlov, A. R. ; Shibaev, V. P., Macromolecules, 1984, 17, 2270.

67. Abe, A., Macromolecules, 1984, 17, 2280.

68. Samulski, E. T. ; Gauthier, M. M. ; Blumstein, R. B. ; Blumstein, A., Macromolecules, 1984, 17, 479.

69. Dewar, M. J. S. ; Griffin, A. C., J. Am. Chem. Soc., 1975, 97, 6662.

70. Sawamoto, M. ;Furukawa,A.;Higashimura,T., Proc.IUPAC, I.U.P.A.C.,Macromol. Symp.,28th, 1982, 148

71. Sawamoto, M.; Furukawa, A.; Higashimura, T., Macromolecules,1983, 16, 518.

72. Bosch, P. ; Serrano, J. ; Mateo, J. L. ; Calle, P. ; Sieiro, C., J. Polym. Sci. Part A. Polym. Chem., 1998, 36, 2775.

Chapter 2

Design and synthesis of highly photopolymerizable styrenyl compounds in the solid-state photoinitiated polymerization

2-1. INTRODUCTION

The importance of photopolymerization has now been well recognized through various industrial applications including photocurable coatings, adhesives, printing inks and recording materials. Photoinitiated polymerization may be classified into two groups, i.e., photoinitiated cationic polymerization[1] and photoinitiated radical polymerization.[2] In either of them, developments of highly photosensitive systems are required and under extensive investigations. Recently, Crivello and Ortiz[3, 4] have developed highly photoactive epoxy monomers. These monomers undergo a fast cationic polymerization involving radical-induced decomposition of onium-salt photoinitiator.[1, 5-7] One of the most distinct advantages in cationic photopolymerization as compared with radical photopolymerization is the insensitivity to oxygen. As for radical photopolymerization, various types of effective photoinitiators have been developed. In combination with specially designed acrylate monomers, ultra-fast radical photopolymerization was demonstrated by Decker and Moussa.[2, 8]

In both types of photopolymerizations little attention has been paid to styrene derivatives, which is due to the relatively low polymerizability of styrene derivatives. On the other hand, incorporation of styrenyl units into polyacrylates renders improved physical and chemical properties such as mechanical properties, chemical resistance and

elevated T_g to the copolymers, which opens the way to industrial applications. Since styrenyl monomers could be polymerized in either cationic or radical mechanism, discovery of photoactive styrene monomers would create a new photopolymerization system. According to our preliminary investigation,[9] we considered styrene derivatives carrying heterocyclic substituent linked to the phenyl group through a methylthio group, expecting intermolecular interactions between the heterocyclic groups to align solid monomers in favorable way for photopolymerization, large free volume due to rotation around the linking group in the solid polymer and chain transfer to polymers yielding accessible radical to consume remaining monomers. In the preliminary investigation, we tested thiadiazole, triazine, benzthiazole and benzimidazole groups and found that thiadiazole group was the best to yield high polymerization reactivity in the presence of a suitable photoinitiator.[9] As a photoinitiator, we compared various types of photoinitiators for effectiveness to initiate photopolymerization of such styrenyl monomers and focused our attention on 2-(4'-methoxystyryl)-4,6-bis(trichloromethyl)-1,3,5-triazine[10-12] (PMS), which absorbs at 365 nm with a large absorption coefficient and can be sensitized to longer wavelengths in the presence of suitable dye and amines.[13, 14] This type of photoinitiator is a possible candidate for highly sensitive photopolymerization system in visible to near infrared region.

The present article reports the reactivity of novel styrenyl monomers, 5-substituted 2-(4'-vinylbenzyl)thio-1,3,4-thiadiazole, in photoinduced solid-state polymerization and discusses the effectiveness of these monomers in photoinduced radical polymerization and the effect of polymer matrix on the monomer reactivity.

2-2. EXPERIMENTAL

Materials

2-(4'-Methoxystyryl)-4,6-bis(trichloromethyl)-1,3,5-triazine (PMS) and 2-(4'-methoxynaphthyl)-4,6-bis(trichloromethyl)-1,3,5-triazine (TRB) were purchased from Panchim (Cedex, France) and used without further purification. 9-Phenylacridine (PA) and Luna TPO (2,4,6-trimethylbenzoyldiphenylphosphine oxide) (TPO) were obtained from Nihon Siber Hegner K. K. (Tokyo, Japan) and used without further purification. Polystyrene ($M_w = 2.1\times10^5$) was obtained from Wako Chemicals Ind. Ltd., (Osaka, Japan) and purified by precipitation from 1,4-dioxane solution with methanol. Poly(methyl methacrylate) (Wako Chemicals Ind. Ltd.) was purified by precipitation from 1,4-dioxane solution with hexane. 1,4-Dioxane (Wako Chemicals Ind. Ltd.) was used without further purification. 2,5-Dimercapto-1,3,4-thiadiazole was purchased from Tokyo Kasei Kogyo Co., Ltd.(Tokyo, Japan) and used without further purification. 4-Chloromethyl styrene was purchased from Seimi Chemical Co. Ltd. (Kanagawa, Japan) and used without further purification.

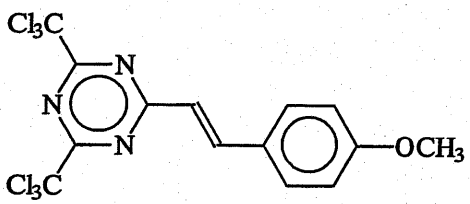

PMS

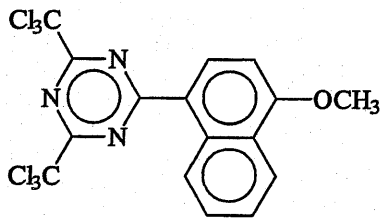

TRB

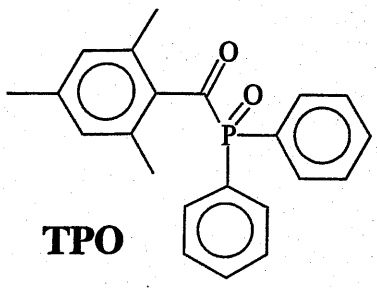

TPO

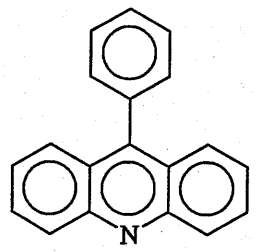

PA

Monomer preparations

All the monomers studied in this paper were prepared by the procedure as shown in Schemes 1 and 2.

Scheme1

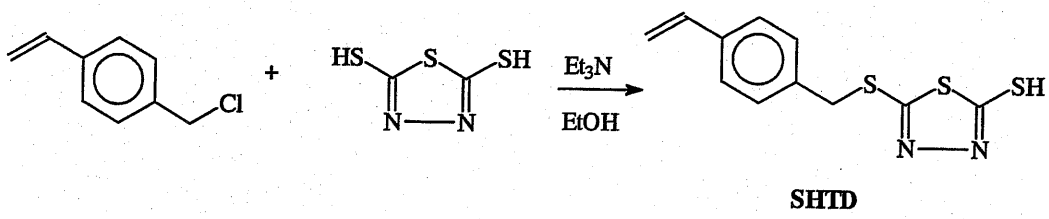

SHTD

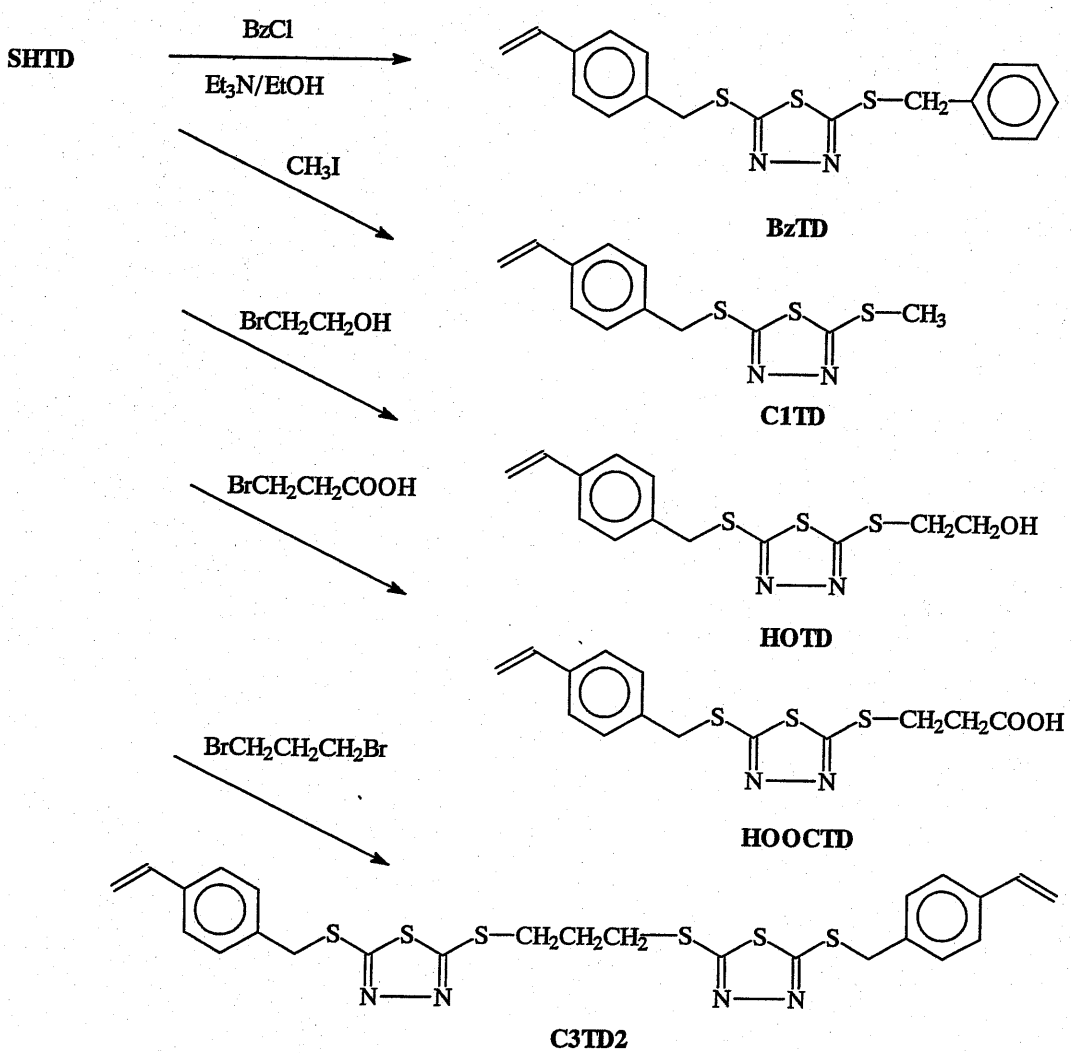

BzTD

C1TD

HOTD

HOOCTD

C3TD2

Scheme 2

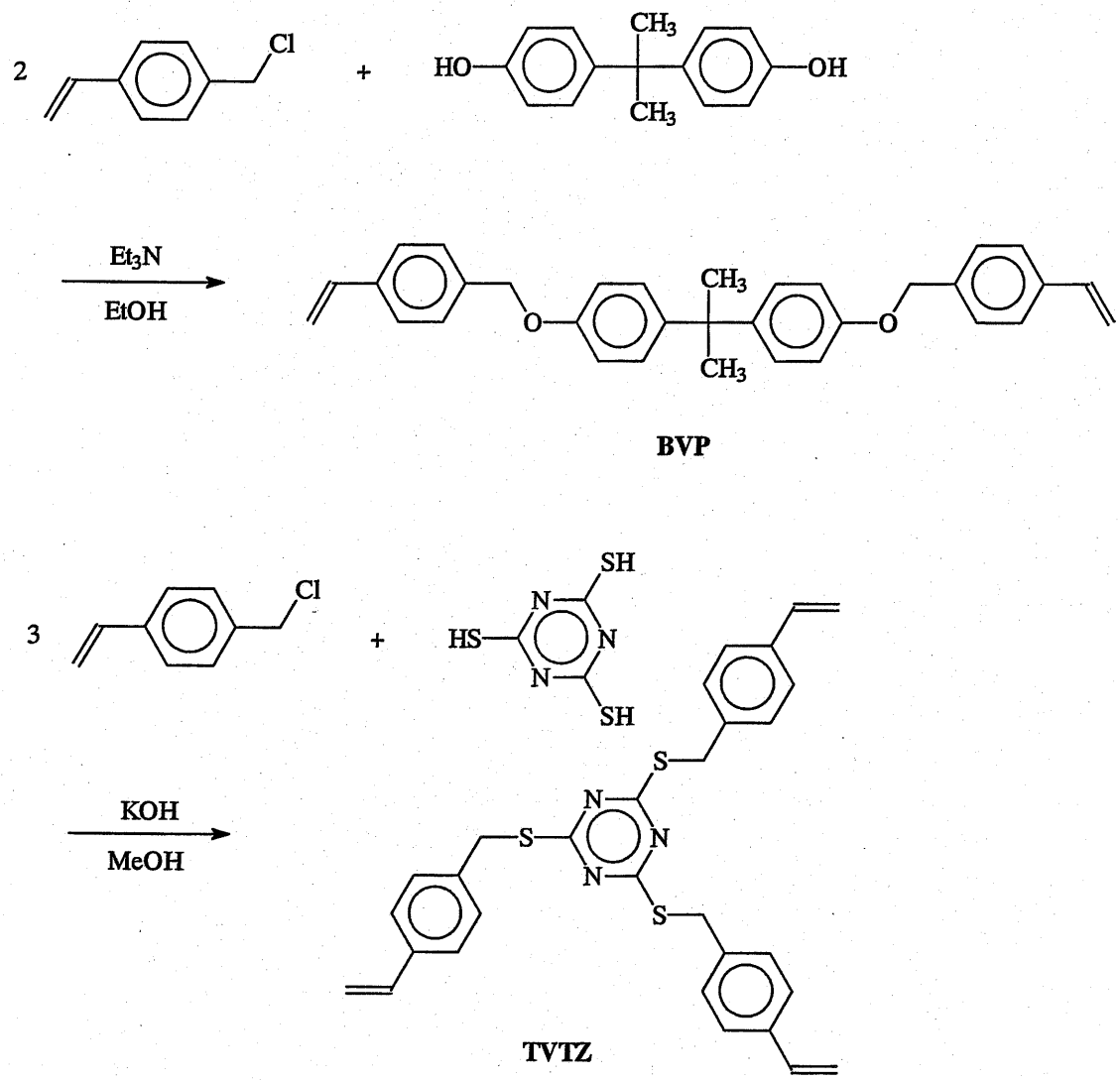

Preparation of 5- (4'-vinylbenzyl)thio-1,3,4-thiadiazole-2-thiol (SHTD)

2,5-Dimercapto-1,3,4-thiadiazole (100 g, 0.666 mole) was dispersed in ethanol (500 mL) and an equimolar amount of triethylamine was added under nitrogen atmosphere at 50 °C. To the mixture, 4-chloromethyl styrene (100 g, 0.655 mole) was added dropwise under stirring over 30 min. The reaction mixture became turbid gradually and white powder precipitated. The reaction was continued for further 3 h at 50 °C and then left at

room temperature. The slightly yellowish precipitate was filtered and washed twice with methanol and once with diisopropyl ether. Recrystallization from benzene gave colorless crystal. The yield was 101 g (57 %).

Elemental analysis: Calcd. for 5- (4'-vinylbenzyl)thio-1,3,4-thiadiazole-2-thiol (SHTD), C, 49.55; H, 3.75; N, 10.51. Obsd. C, 49.98; H, 3.84; N,10.53.

^{1}H NMR (200 MHz in $CDCl_3$, δ, ppm): 4.4(s, CH_2(benzyl), 2H); 5.23 (d, H_a, J = 11 Hz, 1H); 5.72 (d, H_b, J = 17.6Hz, 1H); 6.67 (dd, H_x, J = 11, 17.6 Hz, 1H); 7.34 (m, phenyl, 4H); 11.3 (b, SH, 1H).

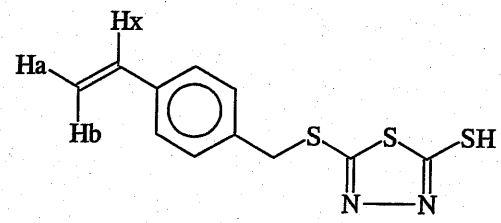

SHTD

Preparation of 2-(4'-vinylbenzyl)thio-5-benzylthio-1,3,4-thiadiazole (BzTD)

SHTD (13.3 g, 0.05 mol) was placed in a 300 mL flask and ethanol (150 mL) was added. Under stirring, triethylamine (6 g, 0.06 mol) was added and the mixture was gently heated on a stirrer-hot plate. At 55 °C the mixture became a clear solution and it was kept at 55 °C. Benzyl chloride (6 g, 0.05 mol) was then added to this solution, which became turbid after 5 to 10 min. After 30 min the flask became full of white precipitate and the mixture was stirred for another 30 min at 55 °C. Then, the flask was removed from the stirrer-hot plate and kept at room temperature. The precipitate was filtered, washed well with ethanol (100 mL) and diisopropyl ether (50 mL), and recrystallized from ethanol. The yield of the product was 14.3 g (80 %). Melting point was 103 °C.

Elemental analysis: Calcd. for 2-(4'-vinylbenzyl)thio-5-benzylthio-1,3,4-thiodiazole (BzTD), C, 60.59; H, 4.49; N, 7.85 . Obsd. C, 60.78; H, 4.45; N, 7.93.

^{1}H NMR (200 MHz in $CDCl_3$, δ, ppm): 4.47(s, CH_2(benzyl), 2H); 4.49(s, CH_2(benzyl), 2H); 5.24 (d, H_a, J = 11 Hz, 1H); 5.74 (d, H_b, J = 17 Hz, 1H); 6.67 (dd, H_x, J = 11, 17 Hz, 1H); 7.26-7.41 (m, phenyl, 9H)

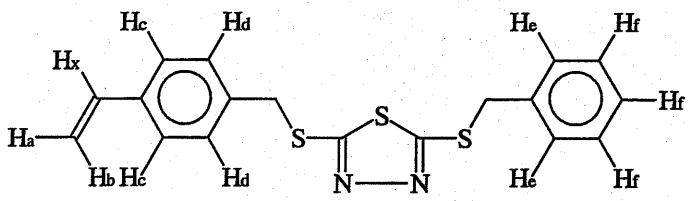

BzTD

Preparation of poly(BzTD)

Poly(BzTD) was synthesized by radical polymerization of BzTD and used as a polymer matrix in photopolymerization of the styrenyl monomers. BzTD (50 g) was placed in a 4-neck, round-bottom flask (500 mL) equipped with a reflux condenser, a thermometer, a nitrogen inlet and an overhead mechanical stirrer, and 1,4-dioxane (150 mL) and ethanol (50 mL) were added. The flask was kept in a hot-bath of 70 °C. Polymerization was initiated by adding 2,2'-azobisisobutyronitrile (0.5 g) and continued for 7 h at 70 °C. The polymerization mixture was then poured into methanol (2000 mL) and the precipitate was separated by decantation. The product was purified by repeated precipitation from 1,4-dioxane solution with methanol. After drying overnight in vacuum, slightly yellowish powder was obtained. The NMR analysis showed the formation of poly(BzTD). From GPC measurement equipped with a multi-angle laser light scattering detector (DAWN E, with operating/analysis software, Astra 4.73.04, both from Wyatt Technology Corp., Santa Barbara, CA), weight-average molecular

weight, M_w, of poly(BzTD) was found to be 1.6×10^5.

^{1}H NMR (200 MHz in $CDCl_3$, δ, ppm): 1.0 –1.5 (b, CH_2 in the main chain, 2H); 1.5 –1.8 (b, CH in the main chain, 1H); 4.3 – 4.6 (b, CH_2, 4H); 6.2 – 6.6 (b, H_d, 2H); 6.8 – 7.2 (b, H_c, 2H); 7.2–7.3 (b, H_f, 3H) and 7.3–7.5 (b, H_e, 2H).

Preparation of 2-(4'-vinylbenzyl)thio-5-methylthio-1,3,4-thiadiazole (C1TD) and its polymerization

C1TD was investigated to compare with BzTD for size effect of 5-substituent. C1TD was prepared by a procedure similar to that of BzTD. SHTD (26.6 g, 0.10 mol) was reacted with methyl iodide (14.2 g, 0.10 mol) in the presence of an equimolar amount of triethylamine (0.10 mol) in ethanol (200 mL) for 3 h at 10 °C. Recrystallization from ethanol gave colorless crystal. The yield was 17.4 g (62 %). Melting point was 48.7 °C.

Elemental analysis: Calcd. for 2-(4'-vinylbenzyl)thio-5-methylthio-1,3,4-thiodiazole (C1TD), C, 51.35; H, 4.28; N, 9.99. Obsd. C, 51.16; H, 4.22; N, 9.97.

^{1}H NMR (200 MHz in $CDCl_3$, δ, ppm) :2.73(s, CH_3, 3H); 4.46(s, CH_2, 2H); 5.24 (d, H_a, J = 11 Hz, 1H); 5.72 (d, H_b, J = 17 Hz, 1H); 6.67 (dd, H_x, J = 11, 17 Hz, 1H); 7.34 (s, phenyl, 4H)

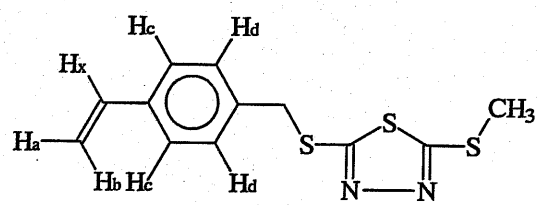

C1TD

Solution polymerization of C1TD was carried out by exactly the same way as that in the polymerization of BzTD for use in DSC measurements. After purification the formation of poly(C1TD) was confirmed by NMR analysis. From GPC measurement, M_w of poly(C1TD) was found to be 6.1×10^4.

Preparation of 2-(4'-vinylbenzyl)thio-5-(2'-hydroxyethyl)thio-1,3,4-thiadiazole (HOTD) and its polymerization

HOTD was prepared to investigate hydrogen bonding interactions of 5-substituent. SHTD (26.6 g, 0.10 mol) was reacted with 2-bromoethanol (12.5 g, 0.10 mol) in the presence of an equimolar amount of triethylamine (0.10 mol) in ethanol (200 mL) for 5 h at 70 °C. Recrystallization from benzene/ethanol (2/1) gave colorless crystal. The yield was 14.0 g (45 %). Melting point was 57.0 °C.

Elemental analysis: Calcd. for 2-(4'-vinylbenzyl)thio-5-(2'-hydoroxyethyl)thio-1,3,4-thiadiazole (HOTD), C, 50.25; H, 4.51; N, 9.02. Obsd. C, 50.11; H, 4.54; N, 8.91.

^{1}H NMR (200 MHz in $CDCl_3$, δ, ppm): 3.54 (t, CH_2(f), 2H); 4.40 (t, CH_2(g), 2H); 4.48(s, CH_2(e), 2H); 5.25 (d, H_a, J = 11 Hz, 1H); 5.74 (d, H_b, J = 17 Hz, 1H); 6.68 (dd, H_x, J = 11, 17 Hz, 1H); 7.35 (s, phenyl, 4H)

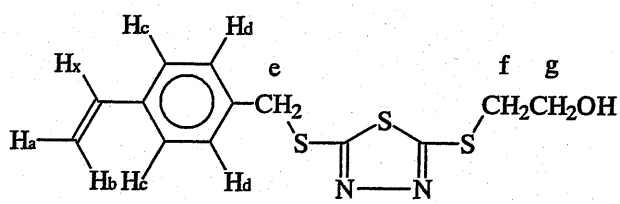

HOTD

Solution polymerization of HOTD was carried out by exactly the same way as that in the polymerization of BzTD for use as a polymer matrix. After purification the

formation of poly(HOTD) was confirmed by NMR analysis. From GPC measurement, M_w of poly(HOTD) was found to be 2.0×10^5.

Preparation of 2-(4'-vinylbenzyl)thio-5-(2'-carboxyethyl)thio-1,3,4-thiadiazole (HOOCTD) and its polymerization

HOOCTD was prepared to investigate hydrogen bonding interactions of 5-substituent. SHTD (26.6 g, 0.10 mol) was reacted with 3-bromopropionic acid (15.3 g, 0.10 mol) in the presence of triethylamine (0.22 mol) in ethanol (200 mL) for 5 h at 70 °C. The reaction mixture was acidified by concentrated hydrochloric acid and the precipitate was filtered and washed with water. Recrystallization from chloroform /ethanol gave colorless crystal. The yield was 24.0 g (71 %). Melting point was 108.4 °C.

Elemental analysis: Calcd. for 2-(4'-vinylbenzyl)thio-5-(2'-carboxyethyl)thio-1,3,4-thiodiazole (HOOCTD), C, 49.64; H, 4.14; N, 8.27. Obsd. C, 49.45; H, 4.22; N, 8.36.

^{1}H NMR (200 MHz in $CDCl_3$, δ, ppm): 2.94 (t, CH_2(g), 2H); 3.52 (t, CH_2(f), 2H); 4.47(s, CH_2(e), 2H); 5.24 (d, H_a, J = 11 Hz, 1H); 5.73 (d, H_b, J = 17 Hz, 1H); 6.68 (dd, H_x, J = 11, 17 Hz, 1H); 7.34 (s, phenyl, 4H).

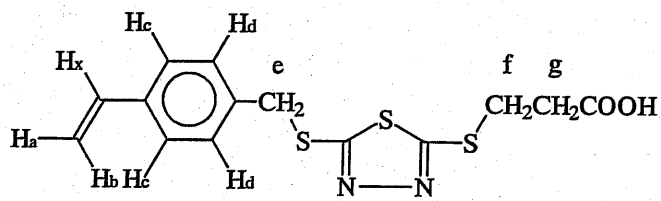

HOOCTD

Solution polymerization of HOOCTD was carried out by exactly the same way as that in the polymerization of BzTD for use as a polymer matrix. After purification the formation of poly(HOOCTD) was confirmed by NMR analysis. From GPC

measurement, M_w of poly(HOOCTD) was found to be 6.6×10^4.

Preparation of 1,3-bis[5-(4'-vinylbenzyl)thio-1,3,4-thiadiazole)-2-thio]propane (C3TD2)

C3TD2 is a bifunctional thiadiazole-substituted styrene derivative and should be useful to obtain crosslinked polymers. SHTD (26.6 g, 0.10 mol) was reacted with 1,3-dibromopropane (10.1 g, 0.05 mol) in the presence of triethylamine (12 g, 0.12 mol) in ethanol (200 mL) for 3 h at 65 °C. Recrystallization from benzene /ethanol gave colorless crystal. The yield was 49 g (86 %). Melting point was 76 °C.

Elemental analysis: Calcd. for 1,3-(bis(5-(4-vinylbenzyl)thio-1,3,4-thiadiazole)-2-thio)-propane (C3TD2), C, 53.07; H, 4.59; N, 9.53. Obsd. C, 53.10; H, 4.29; N, 9.97.

^{1}H NMR (200 MHz in $CDCl_3$, δ, ppm): 2.25 – 2.38 (m, CH_2(g), 2H); 3.42 (t, CH_2(f), 4H); 4.49(s, CH_2(e), 4H); 5.25 (d, H_a, J = 11 Hz, 2H); 5.73 (d, H_b, J = 17 Hz, 2H); 6.69 (dd, H_x, J = 11, 17 Hz, 2H); 7.36 (s, phenyl, 8H).

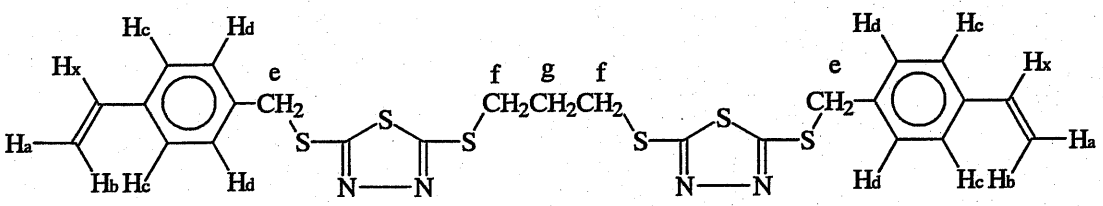

C3TD2

Preparation of 2,2-bis[4-(4'-vinylbenzyloxy)phenyl]propane (BVP)

BVP is bifunctional styrene derivative analogous to C3TD2 without thiadiazole group and useful to assess the contribution of thiadiazole group in the solid-state photopolymerization. 2,2-Bis(4-hydroxyphenyl)propane (50 g, 0.22 mol) was reacted

with 4-chloromethyl styrene (70 g, 0.46 mol) in the presence of triethylamine (48 g, 0.47 mol) in ethanol (400 mL) for 5 h at 65 °C. Recrystallization from benzene /ethanol gave colorless crystal. The yield was 70 g (69 %). Melting point was 115 °C.

Elemental analysis: Calcd. for 2,2-bis(4-(4'-vinylbenzyloxy)phenyl)propane (BVP), C, 85.97; H, 6.94. Obsd. C, 85.79; H, 6.97.

^{1}H NMR (200 MHz in $CDCl_3$, δ, ppm): 1.63(s, CH_3, 6H); 5.00(s, CH_2, 4H); 5.24 (d, H_a, J = 11 Hz, 2H); 5.74 (d, H_b, J = 17 Hz, 2H); 6.72 (dd, H_x, J = 11, 17 Hz, 2H); 6.84-6.90 (m, H_d, 4H); 7.10-7.16 (m, H_e, 4H); 7.34-7.44 (m, H_c, 8H).

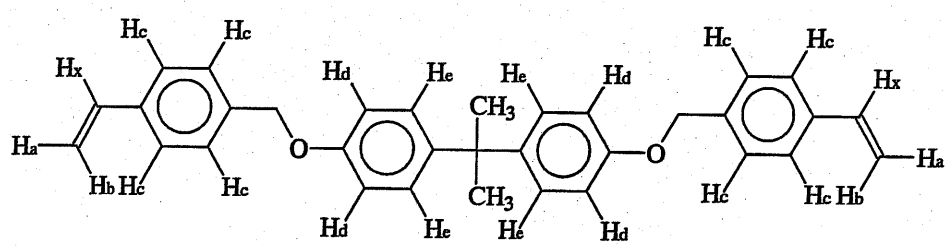

BVP

Preparation of 2,4,6-tris(4'-vinylbenzylthio)-1,3,5-triazine (TVTZ)

TVTZ is trifunctional triazine-substituted styrene derivative and useful to compare the contribution of thiadiazole group with triazine group in the solid-state photopolymerization. 2,4,6-Trimercapto-1,3,5-triazine (50 g, 0.28 mol) was reacted with 4-chloromethyl styrene (130 g, 0.85 mol) in the presence of potassium hydroxide (48 g, 0.85 mol) in methanol (900 mL) for 5 h at 50 °C. Recrystallization from benzene /ethanol gave colorless crystal. The yield was 130 g (88 %). Melting point was 130 °C.

Elemental analysis: Calcd. for 2,4,6-tris(4'-vinylbenzylthio)-1,3,5-triazine (TVTZ), C, 68.47; H, 5.14; N, 8.00. Obsd. C, 68.58; H, 6.97; N, 8.05.

^{1}H NMR (200 MHz in $CDCl_3$, δ, ppm): 4.31(s, CH_2, 6H); 5.23 (d, H_a, J = 11 Hz, 3H); 5.72 (d, H_b, J = 17 Hz, 3H); 6.68 (dd, H_x, J = 11, 17 Hz, 3H); 7.27-7.36 (m, phenyl, 12H).

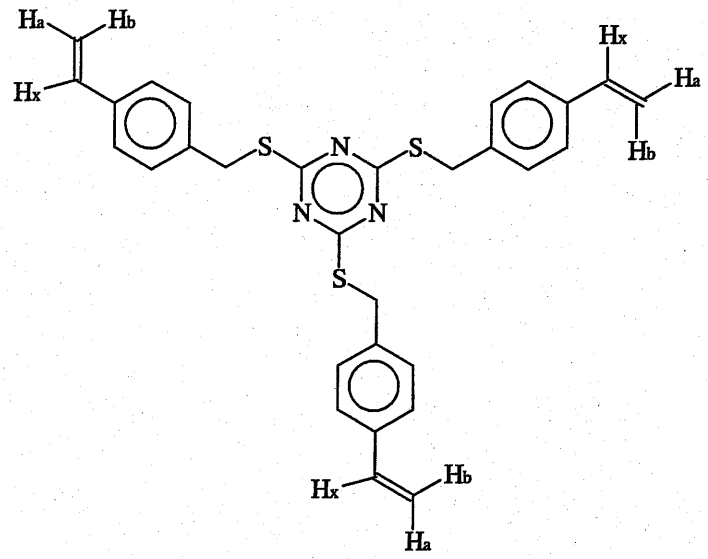

TVTZ

Photopolymerization

Photopolymerization of the styrene derivatives was carried out in the matrix of solid polymer and followed up to high monomer conversion by Fourier transform real-time infrared (RT-IR) [8, 15-18] spectroscopy, which was conducted on a Bio-rad FTS-40 (Bio-rad Laboratories, Inc., Hercules, CA) with an operating/analysis software, Win-IR. Polystyrene and poly(BzTD) were the most frequently used matrix polymers. The polymer (0.2 g) was dissolved in 1,4-dioxane (2 g) and monomer (0.1 g) and PMS (0.004 g) were added at room temperature. An exact amount (0.110 g) of the solution was eluted on KRS (KRS-5; TlBr (thallium bromide) (42 %) / TlI (thallium iodide) (58 %)) disk (diameter = 3 cm) and dried. The calculated thickness of cast film on KRS disk was 24 μm. KRS disk coated with the blend film was placed in the sample chamber of FT-IR spectrometer and IR spectra were recorded in the transmittance mode.

Monochromatic 365 nm light was irradiated on KRS disk through an interference filter attached to the end of optical fiber. The light source used was high-pressure Hg lamp (Spot-Cure, Ushio Inc., Tokyo, Japan) and the light intensity at the surface of KRS disk was measured by Radiometer IL1700 (International Light Lnc., Newburyport, MA) to be 1.61 $mW \cdot cm^{-2}$ (= 5.0×10^{-9} $einstein \cdot cm^{-2} \cdot s^{-1}$). All measurements were carried out at room temperature under argon atmosphere and RT-IR spectra were collected at the rate of 1 survey spectrum per 1.65 second with a resolution of 1 cm^{-1} over the spectra range of 450 cm^{-1} to 4000 cm^{-1}. The infrared absorption band at 990 cm^{-1} (vinyl, δCH, bending, out-of-plane) was monitored.

Monomer conversion was calculated according to the following equation:

$$conversion = \frac{A(990)_0 - A(990)_t}{A(990)_0}$$

in which $A(990)_0$ and $A(990)_t$ denote the peak absorbance at 990 cm^{-1} before UV-irradiation and at time t (s), respectively. The rate of polymerization, R_p, was calculated from the following equation;

$$R_p\,(mol\,l^{-1}\,s^{-1}) = -\frac{d[M]}{dt} = [M]_0 \frac{d(conversion)}{dt}$$

Since measured peak intensity at 990 cm^{-1} were somewhat scattered with time, the calculated value of R_p from the slope of time-conversion curve at an arbitrary time interval scattered significantly. 10th-order polynominal approximation was applied to all time-conversion curves and the polynominal curve fit was differentiated to obtain R_p at an arbitrary polymerization time.

DSC analysis

DSC analysis was carried out by using DSC 6200 (Seiko Instruments Inc., Chiba, Japan) with heating and cooling rate of 5 °C min^{-1} for the monomer and 10 °C min^{-1} for

the polymer and the blends.

2-3. RESULTS AND DISCUSSION

2-3-1. Influence of the photoinitiator

The choice of the photoinitiator is essential to achieve high polymerization rate and final conversion. For typical photoinitiators usable in photopolymerization studies, the following four types of photoinitiators were tested to find the most effective photoinitiator to induce fast polymerization of C1TD (2-(4'-vinylbenzyl)thio-5-methylthio-1,3,4-thiadiazole) in polystyrene matrix under the irradiation of monochromatic UV light at 365 nm; 2-(4'-methoxystyryl)-4,6-bis(trichloromethyl)-1,3,5-triazine (PMS), 2-(4'-methoxynaphthyl)-4,6-bis-(trichloromethyl)-1,3,5-triazine (TRB), 2,4,6-trimethylbenzoyldiphenylphosphine oxide (TPO)[19,20] and 9-phenylacridine (PA)[21]. In Figure 2-1, time-conversion curves for the polymerization of C1TD initiated by these photointiators are shown. Two bis(trichloromethyl)-triazine derivatives showed highest initiator activities and PMS was found to be the most effective photoinitiator of them. TPO, commonly known as one of the most effective photoinitiators for acrylic monomers, appears to be less effective than PMS under the irradiation of UV light at 365 nm. It might be due to smaller absorption coefficient of TPO at this wavelength as compared with those of PMS and TRB. PA caused long induction period and slow polymerization and was not suitable for the present investigations. PMS was found to have another distinctive advantage for determining the concentration of PMS in the polymerizing system by RT-IR as will be discussed in detail in Chapter 3. Photodecomposition rate of PMS can be quantitatively determined by monitoring the intensity of its characteristic absorption at 1171 cm^{-1}, which was assigned to a coupled asymmetric stretching vibration of two CCl_3 groups attached to

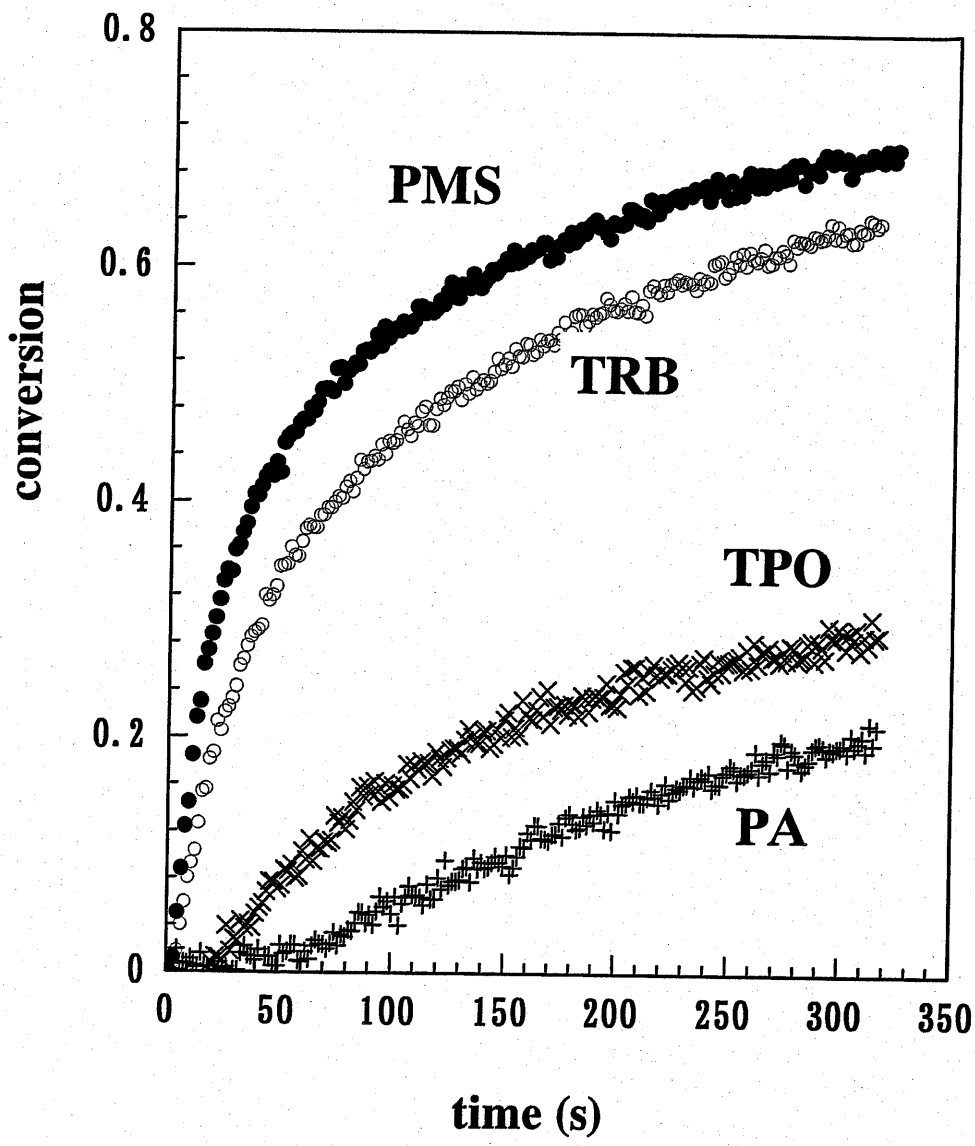

Figure 2-1. Comparison of the photoinitiators to induce the photopolymerization of C1TD in polystyrene matrix under 365-nm UV-irradiation. Photoinitiator/C1TD/polystyrene = 0.0016/0.12/0.20 (wt/wt/wt). Light intensity = 1.6 $mW \cdot cm^{-2}$. Photopolymerization was carried out at room temperature under argon atmosphere.

1,3,5-triazine ring based on molecular orbital calculations (force calculation by WinMOPAC v.2.0, Fujitsu Ltd.). This finding enabled us to study the polymerization behavior from either polymerization rate or decomposition of photoinitiator. Details on kinetic investigations based on such analysis will be discussed in Chapter 3. Consequently, we selected PMS as the most suitable photoinitiator for all of our investigations.

2-3-2. Photopolymerization reactivities of various types of styrenyl monomers in the polymer matrix

The polymerization reactivities of five types of styrenyl monomers (BzTD, C1TD, C3TD2, BVP and TVTZ) in polystyrene and poly(BzTD) matrices were investigated. As is seen in Figure 2-2, C3TD2 showed the highest polymerization reactivity and the final conversion reached up to 80 %, whereas BVP and BzTD showed very slow polymerization. The polymerization rate reached the maximum value at the initial stage of polymerization, and those for C3TD2 and C1TD were about 0.01 $mol \cdot L^{-1} \cdot s^{-1}$. It is rather surprising to note that the polymerization rate of C3TD2 and C1TD well exceeds that of trimethylolpropane triacrylate (TMPTA), since we expected that the intrinsic polymerization reactivity of these thiadiazole-substituted monomers should not be so much different from other styrene derivatives: *i.e.*, electron density and polarity at vinyl group of these styrenyl monomers are not influenced significantly by the nature of the substituents with are connected *via* methylene group at the 4-position of these styrenyl groups. In solution polymerization, conventional acrylate monomers usually polymerize much faster than styrene and other styrene derivatives. However, under the same experimental conditions, TMPTA polymerization was slow and the final conversion was low. BzTD was found to be incompatible with polystyrene matrix. All monomers except

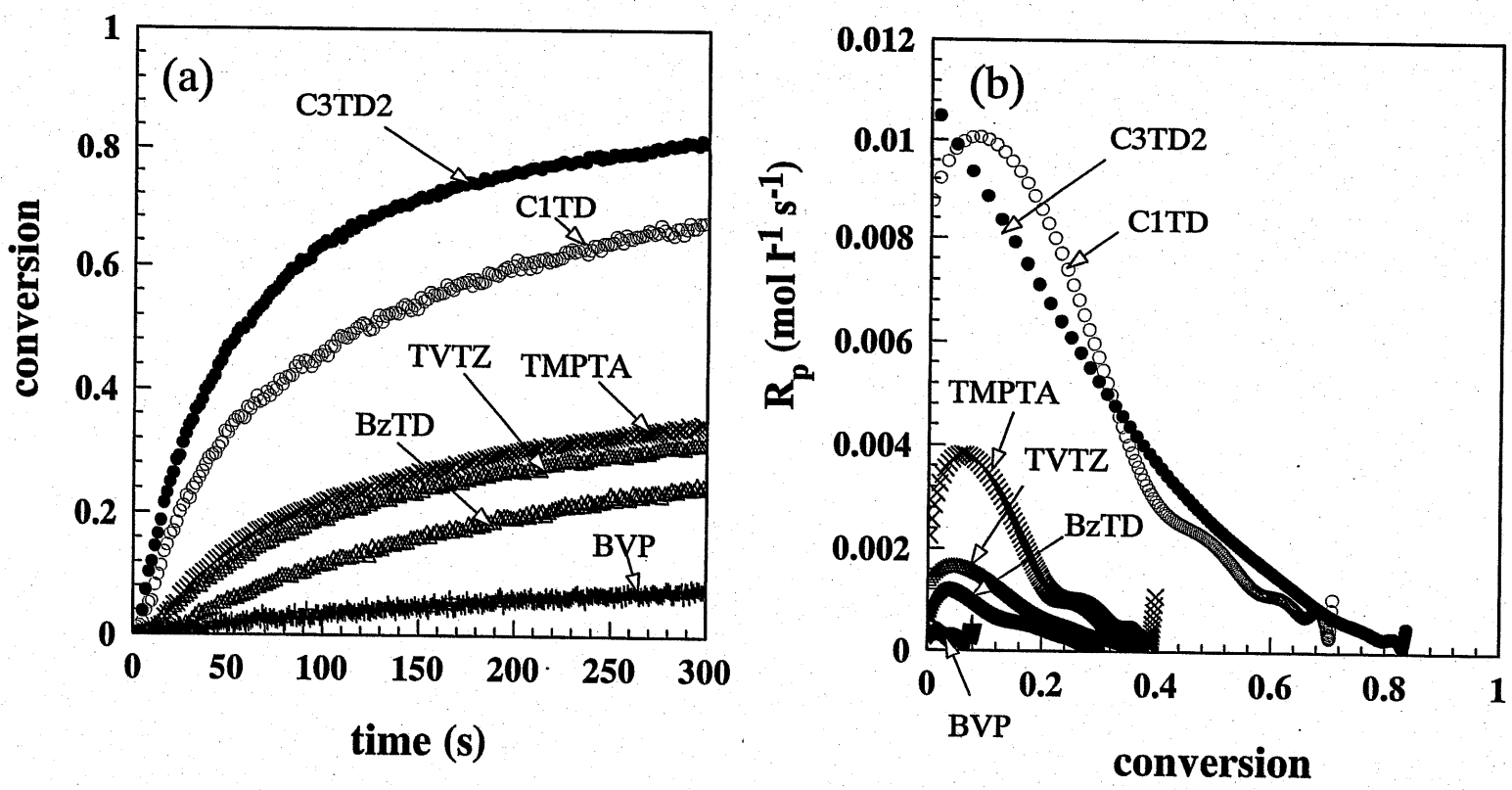

Figure 2-2. Time-conversion curves (a) and the rate of polymerization (b) of various styrene derivatives and trimethylolpropane triacrylate (TMPTA) in polystyrene matrix initiated by PMS under irradiation of 365 nm light at 20 – 25 °C. Ratio of monomer/polystyrene/PMS = 0.10/0.20/0.004 (wt/wt/wt) and the incident light intensity = 5.0×10^{-9} einstein·cm^{-2}·s^{-1}.

TMPTA are highly crystalline and no photopolymerization of these monomers was observed in bulk. The crystalline state of BzTD phase-separated from polystyrene matrix should be the cause for the poor polymerization reactivity. Except BzTD, other monomers and PMS seemed macroscopically to be homogeneously distributed in polystyrene matrix. Since BVP, which carries no thiadiazole group, was of low reactivity, a contribution of thiadiazole group in the fast polymerization is implied. We considered that these differences in polymerization reactivity must originate from the conformational characteristics and the state of microscopic distribution of these thiadiazole-substituted styrenyl monomers in polymer matrix.

It might be considered that aggregation of monomers caused by possible intermolecular interactions between monomers bearing thiadiazole group induce collocation of styrenyl groups in favor of polymerization. TVTZ, which carries triazine group, showed similar polymerization reactivity to TMPTA but far less reactive than C3TD2 and C1TD. Higher polymerization rates of C3TD2 and C1TD as compared with those of TVTZ, TMPTA and BVP might be due to some aggregate states in polymer matrix and molecular arrangements in such aggregations. Transmission electron microscopy on a thin film of polystyrene containing C1TD revealed the presence of such aggregations of C1TD molecules as shown in Figure 2-3. From such observation, C1TD must be distributed as clusters whose sizes are in the order of a few tens of nanometer in polystyrene matrix. Wide-angle x-ray diffraction patterns on the same polystyrene/C1TD blend gave only diffused weak diffraction patterns and no indication of crystalline state in such aggregates was observed. Therefore, C1TD molecules are existed in amorphous state inside the clusters.

Molecular orbital calculation based on the PM3 method[22] led to a polarizability as

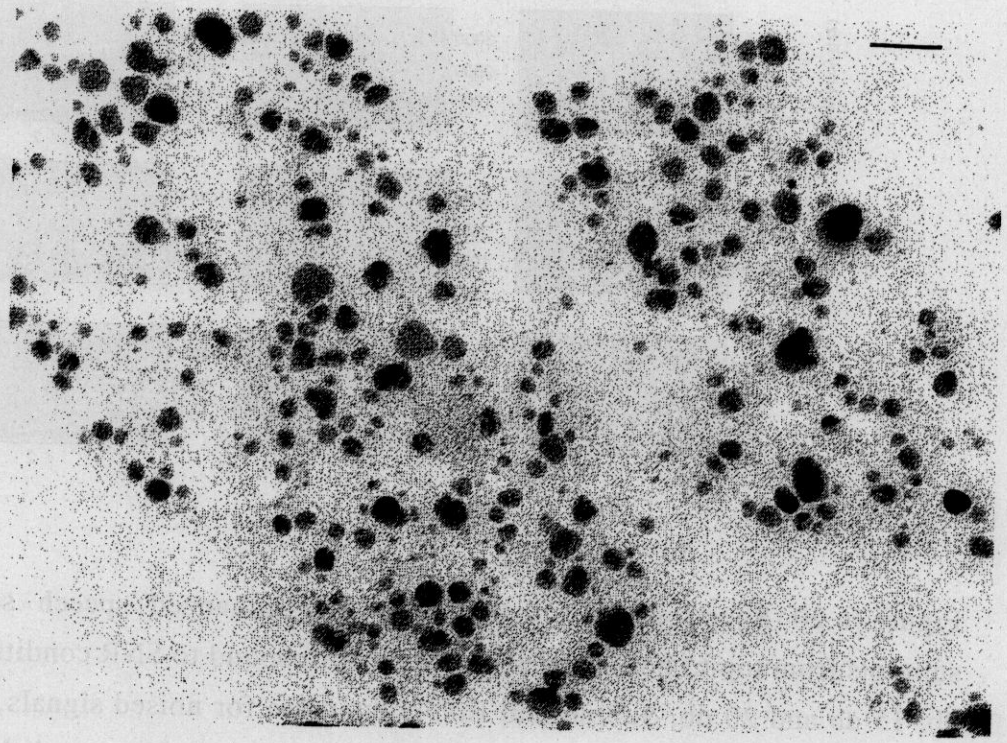

Figure 2-3. Clusters of C1TD molecules in polystyrene matrix observed by transmission electron microscope (magnification = *ca.* 2×10^5). A bar inside this figure indicates 50 nm. Sample was prepared from 1% solution of polystyrene and C1TD (2/1 wt/wt) dissolved in 1,4-dioxane, which was eluted on a Cu-mesh and air-dried. Thin film on Cu-mesh was immersed in 5% $AgNO_3$ aqueous solution for a few seconds and immediately washed with ion-exchanged water and dried. Ag ion is deposited selectively on thiadiazole group of C1TD molecule.

large as 172 a.u. and a relatively small value of dipole moment as 0.99 debye for C1TD. Intermolecular interactions between C1TD molecules, which must be responsible for aggregation, should be arisen principally from London dispersion force and dipole-dipole interaction should play in a minor part. Molecular shape of C1TD in its most stable conformation is shown in Figure 2-4(a). Rotation around methylenethio group is considered to occur rather freely even in solid state at room temperature from the molecular orbital calculations[22]. It is interesting to note that the characteristic molecular conformation in its energetically most stable state (C-1 and C-3) is a legless chair-like shape and molecular packing like stackable legless chairs seems to occur quite easily. A possible locally aligned structure of these monomers induced by intermolecular interactions is also schematically illustrated in Fig. 2-4(b).

Quite recently Jansen[23, 24] reported that some acrylate monomers exhibits high photopolymerization rate in bulk and their polymerization rates are directly related to the dipole moment of the acrylate monomers.[24] Some pre-organized structures due to the dipole-dipole interactions have been put forward by Jansen to explain the high reactivity of these acrylate monomers. In our case, London dispersion force instead of dipole-dipole interactions must play an important role to exhibit high polymerization reactivities for thiadiazole-substituted styrenyl monomers.

The similar experiments were carried out in poly(BzTD) matrix and the results are summarized in Figure 2-5. In this case the polymerization rate was remarkably increased especially for TMPTA, BzTD and C1TD as compared with those observed in polystyrene matrix. As shown in Fig. 2-5(b) the initial polymerization rate of C1TD was 0.036 $mol \cdot L^{-1} \cdot s^{-1}$, which is 3-fold higher than that observed in polystyrene matrix. As for C3TD2, the polymerization rate was not significantly affected by the polymer matrix.

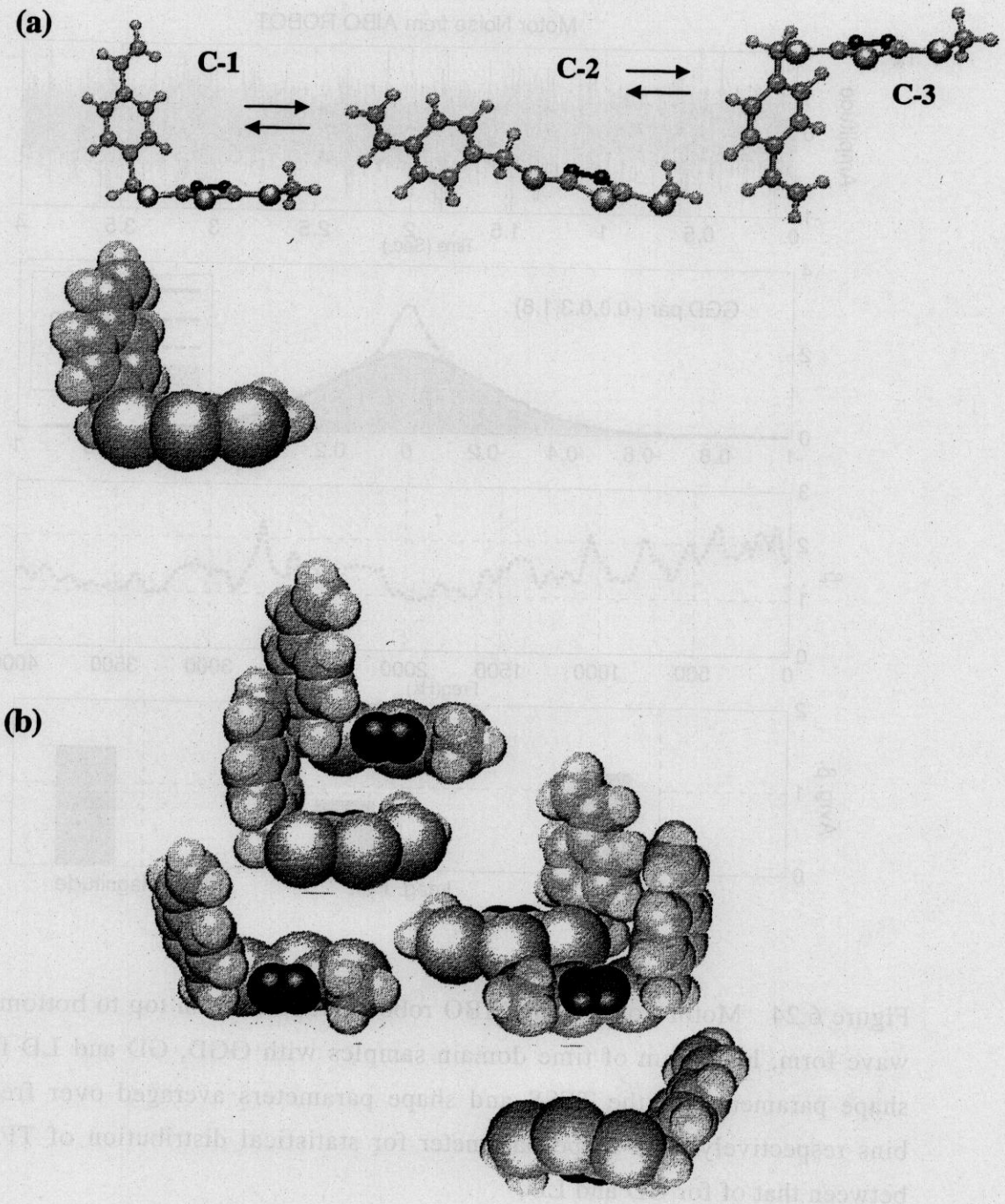

Figure 2-4. Energy minimized conformations (C-1 and C-3) of C1TD (a) and a possible locally aligned structure of C1TD molecules (b).

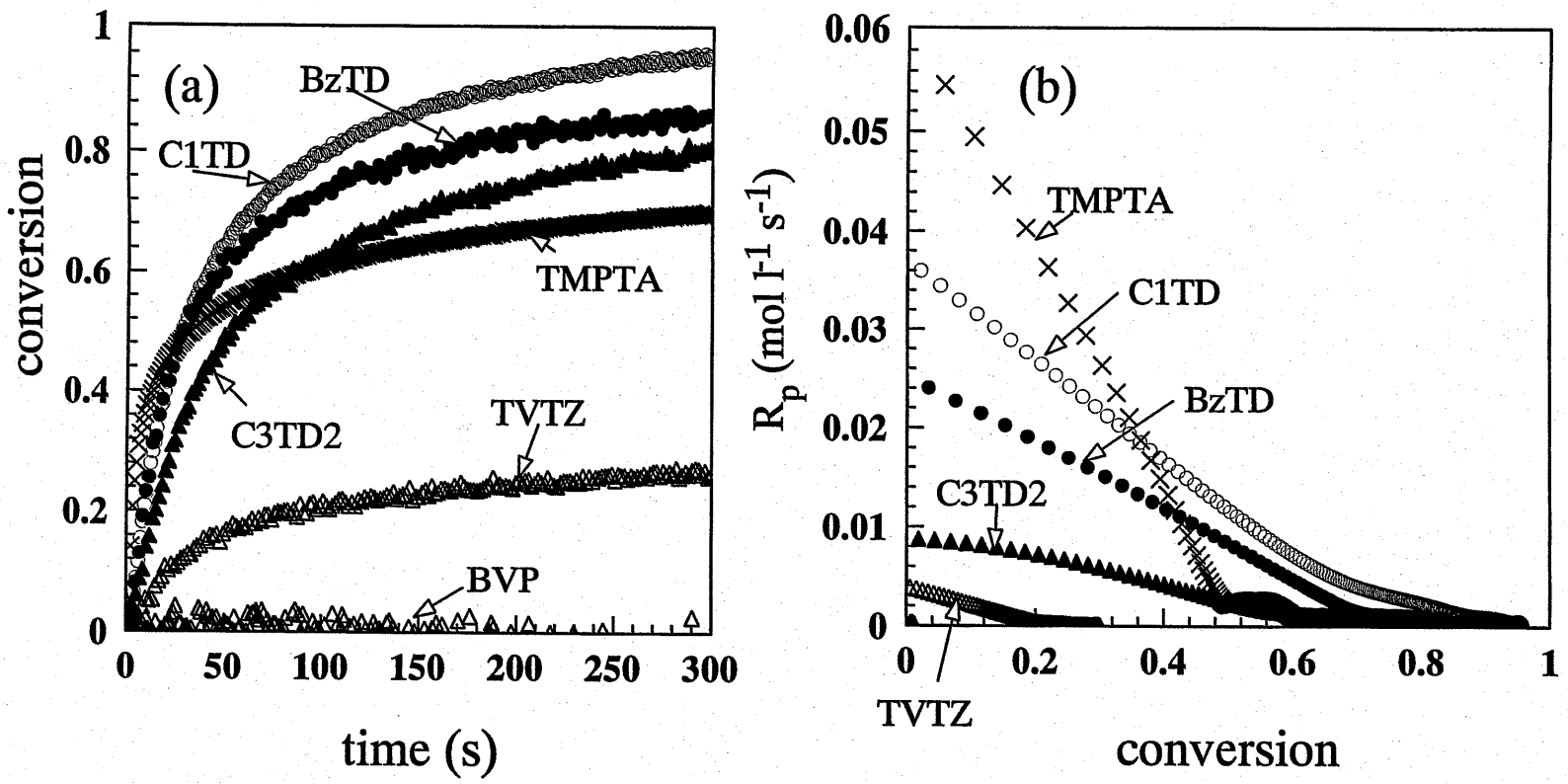

Figure 2-5. Time-conversion curves (a) and the rate of polymerization (b) of various styrene derivatives and TMPTA in poly(BzTD) matrix initiated by PMS under irradiation of 365 nm light at 20 – 25 °C. Ratio of monomer/poly(BzTD)/PMS = 0.10/0.20/0.004 (wt/wt/wt) and the incident light intensity = 5.0×10^{-9} einstein·cm^{-2}·s^{-1}.

The slow polymerization rate and the final conversion of TVTZ were as low as in polystyrene matrix.

Photopolymerization of TMPTA in poly(BzTD) matrix proceeded more quickly and reached higher conversion than that in polystyrene matrix. We can consider two explanations for the different effects of polymer matrix. One is that relatively low T_g of poly(BzTD) (see below and Table 2-1) should enhance diffusion-controlled photopolymerization of TMPTA. The other explanation is that poly(BzTD) acts as a powerful chain transfer agent for the presence of two methylenethio groups in a monomer unit. The radical species formed on the matrix polymer as a result of chain transfer reaction could migrate along the matrix to eventually encounter residual monomers to increase monomer conversion. The presence of heteroatom in the monomer structure had been found to increase the polymerization rate in bulk state.[25] Both of these two factors, effect of lower T_g and chain transfer to the labile hydrogen atoms, are considered to be the cause for enhanced polymerization rate. Nearly no polymerization reactivity of BVP in poly(BzTD) matrix should be ascribed to incompatibility of BVP with poly(BzTD) matrix.

In Figure 2-6, the effects of polymer matrices on the photopolymerization of TMPTA and C1TD are compared. It is seen that the photopolymerization of C1TD is more strongly dependent on the nature of polymer matrices than that of TMPTA. In poly(MMA) matrix, C1TD exhibited very poor reactivity and the monomer consumption virtually went off at about 20 % conversion. Polymerization behavior of C1TD in poly(MMA) is similar to that of TMPTA in the same matrix. C1TD polymerized much faster in other polymer matrices. In polystyrene matrix, the occurrence of locally aligned structures of C1TD in its aggregate phase as shown in Fig.

2-4(b) was considered. In poly(MMA) matrix, the local alignment of C1TD might be disturbed by the increased solubility in poly(MMA), causing a random distribution of C1TD and resulting in the reduced polymerization rate as observed in Fig. 2-6(b). It is assumed that in poly(BzTD) matrix, C1TD monomer could interact with pendant BzTD substituents to rearrange monomer orientation in favor of polymerization. A possible local rearrangement of C1TD molecules in the interstices of BzTD substituents is illustrated in Figure 2-7. In this case, C1TD molecules are considered to be allowed to rotate around its gravitational center and in one of their possible rearrangements, they could be aligned parallel in the same direction and their styrenyl groups face to each other in favor of polymerization as schematically illustrated in Figure 2-7(a).

Differential scanning calorimetry (DSC) measurements were carried out on polymer film containing monomer to determine glass transition temperature of the photopolymerization system. In Table 2-1, T_gs of typical samples are summarized. In the polymerization of BzTD in poly(BzTD) matrix, T_g of the photopolymerization system before irradiation is well below the room temperature and the polymerization proceeded in a rubbery state. Although, at the final conversion, T_g of the polymerization system increased to ca. 30 °C, the major part of the polymerization proceeded in a rubbery state. However, in the polymerization of C1TD in poly(BzTD) matrix or in polystyrene matrix, T_g of the photopolymerization system before irradiation was nearly the room temperature (20 – 25 °C). As the polymerization progressed, T_g of the polymerization system raised beyond the room temperature. Therefore, in this case, the photopolymerization must have proceeded in a glassy state. The faster polymerization of C1TD in a glassy state than that of BzTD in a rubbery state in the same poly(BzTD)

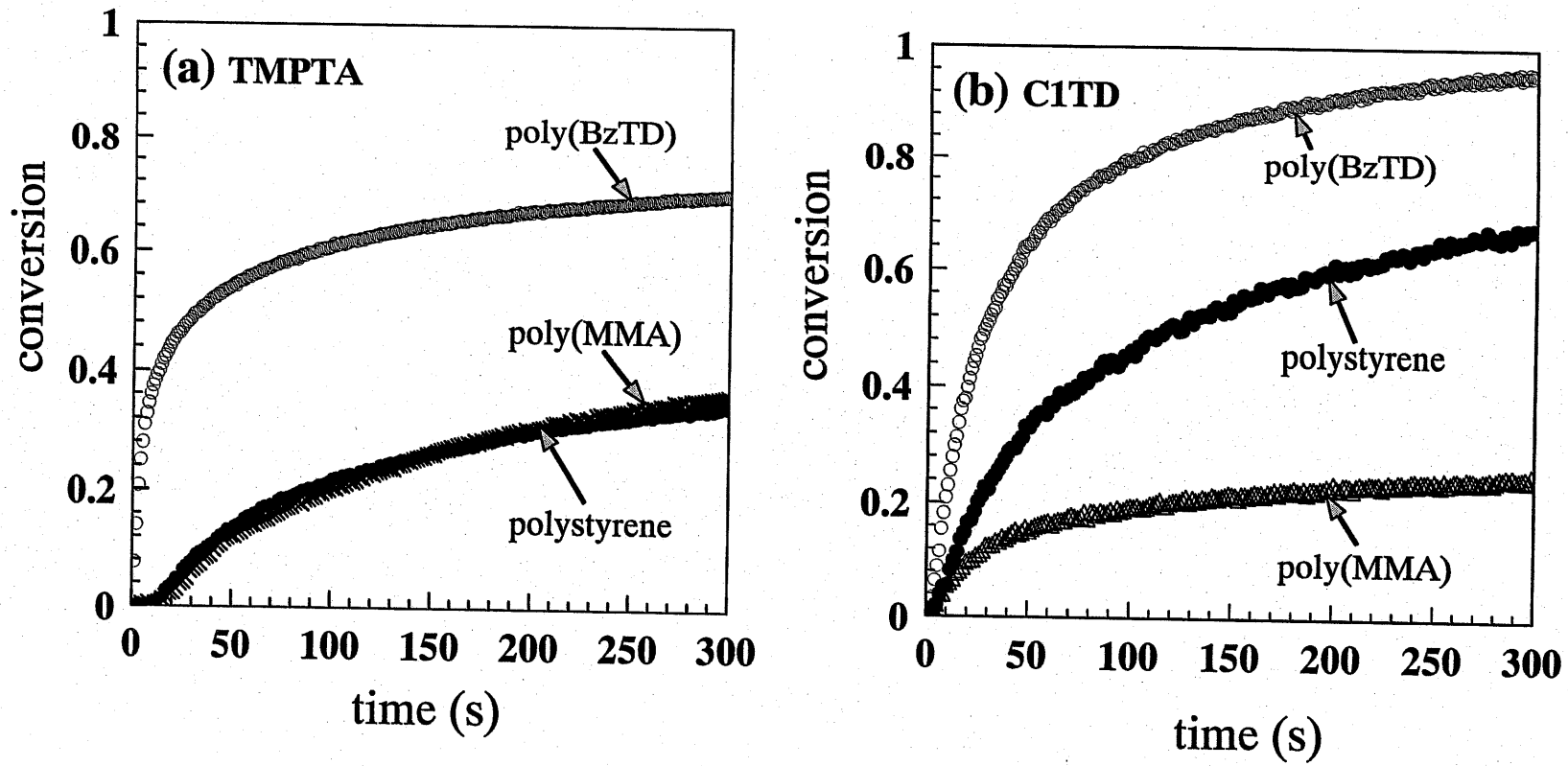

Figure 2-6. Influence of polymer matrix on the PMS-initiated photopolymerization of TMPTA (a) and C1TD (b) in the matrix of polystyrene (•), poly(BzTD) (o), and poly(MMA) (×). Ratio of monomer/matrix/PMS = 0.10/0.20/0.004 (wt/wt/wt) and the incident light intensity = 5.0×10^{-9} einstein·cm^{-2}·s^{-1}.

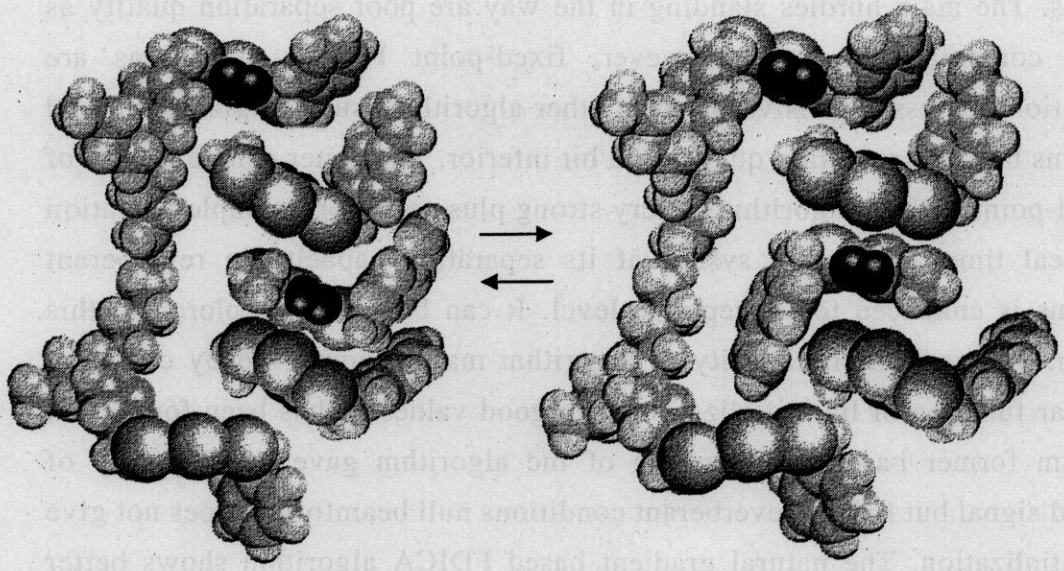

Figure 2-7. A schematic illustration showing a possible local rearrangement of C1TD molecules in the interstices of BzTD substituents.

Table 2-1. Glass transition temperatures of polymer and monomer/polymer blend.

polymer	monomer	polymer/monomer ratio	T_g (°C)
poly(BzTD)	none	-	30
poly(C1TD)	none	-	54
poly(BzTD)	BzTD	0.20/0.05	-1.8
poly(BzTD)	BzTD	0.20/0.10	-2.5
poly(BzTD)	C1TD	0.20/0.10	25
polystyrene	C2TD	0.20/0.05	32
polystyrene	C3TD	0.20/0.10	25

matrix could be explained by considering better orientation of C1TD in a glassy state than BzTD in a rubbery state. It has been reported in conventional photopolymerization of acrylate monomers that T_g seems to have dominant importance in determining the polymerization rate.[26] During the photopolymerization of initially liquid monomer systems, consumption of monomer and build-up of polymer networks sometimes result in notable slowdown of polymerization, which has sometimes been attributed to increasing T_g of the system. Lecamp et al.[27] have reported that the final conversion of polymerization of dimethacrylate oligomers was directly related with T_g and that in a glassy state polymerization did not occur. Molaire[26] had shown that in the photopolymerization system consisting of polymer matrix, trifunctional acrylate monomer and photoinitiator, the polymerization rate was strongly influenced by the reaction temperature. With decreasing polymerization temperature, polymerization slowed down and finally at T_g polymerization did not take place. He reported that the excess free volume is essential to initiate the photopolymerization and a high rate of

polymerization is expected for increasing conformational freedom of initiating species. In the present case, C1TD and BzTD, for instance, have two methylenethio groups and the rotation around the carbon – sulfur bond make various conformations of styrenyl group possible. Various types of conformational changes might be possible at temperatures below T_g and the polymerization might proceed in the remaining free volume via conformation-controlled reaction. This interpretation is to be confirmed in the future.

2-3-3. Polymerization reactivities of styrenyl monomers capable of hydrogen bonding with polymer matrix

The purpose of the present investigation is to explore solid-state photopolymerization system with favorable interactions between monomer and polymer matrix. We considered hydrogen-bonding interactions and prepared hydroxyl substituted monomer, HOTD, and carboxyl-substituted monomer, HOOCTD. When HOTD or HOOCTD was dissolved in poly(HOOCTD) matrix, hydrogen bonding between monomer and polymer side chain and a full compatibility are expected. In Figure 2-8, time-conversion curves in the photopolymerization of HOOCTD, HOTD and BzTD in three kinds of polymer matrices are shown. The polymerization in poly(HOOCTD) matrix (Figure 2-8(a)), HOTD and HOOCTD polymerized fast, whereas BzTD slowly. The lack of compatibility of BzTD in this polymer matrix should be the reason of the difference. The polymerization rates of HOTD and HOOCTD are nearly identical and the maximum polymerization rate was around 0.008 $mol \cdot L^{-1} \cdot s^{-1}$. When these monomers were polymerized in poly(HOTD) matrix, (Fig. 2-8(b)), HOTD and HOOCTD kept high reactivity, whereas BzTD showed surprisingly high polymerization rate. Since

BzTD is compatible with poly(HOTD) matrix, hydrogen bonding between monomer and polymer matrix should have enhanced the monomer reactivity. The effect of hydrogen bonding on polymerization behavior has been investigated in bulk polymerization of (meth)acrylate monomers and similar enhancement of reactivity was reported.[23,30]

These three monomers were photopolymerized also in poly(BzTD) matrix (Fig. 2-8(c)). Poor polymerization reactivity observed for HOOCTD is attributed to the lack of compatibility with the polymer matrix. It is feasible to say that the nature and possibly the size of substituents in monomer and matrix polymer play a very important role in this type of polymerization.

2-3-4. Effect of atmosphere on the photopolymerization of BzTD

Oxygen is known to inhibit radical polymerization, since it scavenges the initiator radicals effectively. The present photopolymerization systems are comprised solely of solid components and diffusion of atmospheric oxygen in the dry films should be considerably slower than in liquid acrylic monomers such as TMPTA.[28,29] Photopolymerization was carried out in the presence and in the absence of atmospheric oxygen and the polymerization profiles were compared as shown in Figure 2-9. The presence of atmospheric oxygen reduced the final conversion. However, the difference between the final conversions was as low as 5%. On the other hand, the polymerization rate was more profoundly affected by the presence of oxygen and the initial polymerization rate is suppressed to ca. 70% of that in argon atmosphere. In argon atmosphere the polymerization rate decreased linearly with conversion, whereas in the presence of atmospheric oxygen the polymerization deviated significantly from a linear

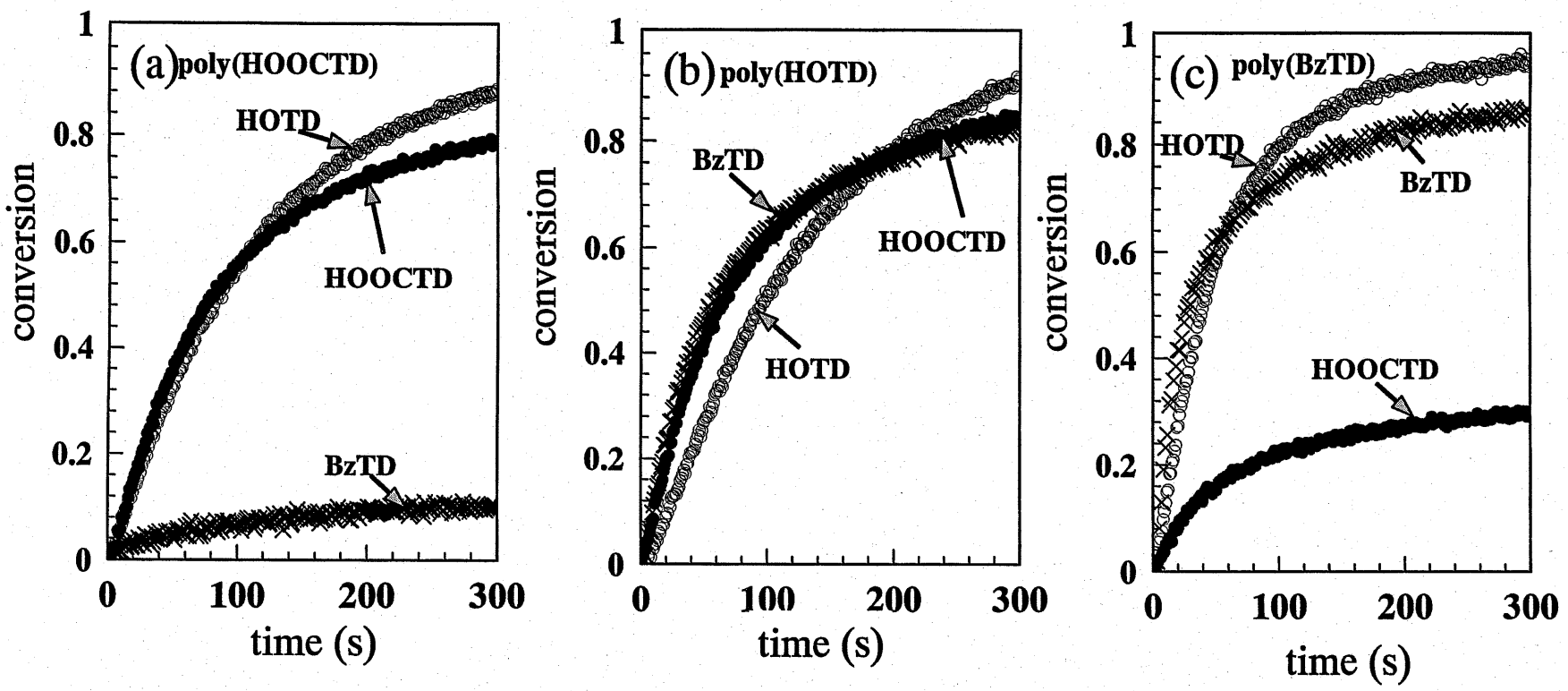

Figure 2-8. Photopolymerization of HOOCTD(•), HOTD(o) and BzTD(×) in poly(HOOCTD) (a), in poly(HOTD) (b), and in poly(BzTD) (c). Ratio of monomer/matrix/PMS = 0.10/0.20/0.004 (wt/wt/wt) and the incident light intensity = 5.0×10^{-9} einstein·cm^{-2}·s^{-1}.

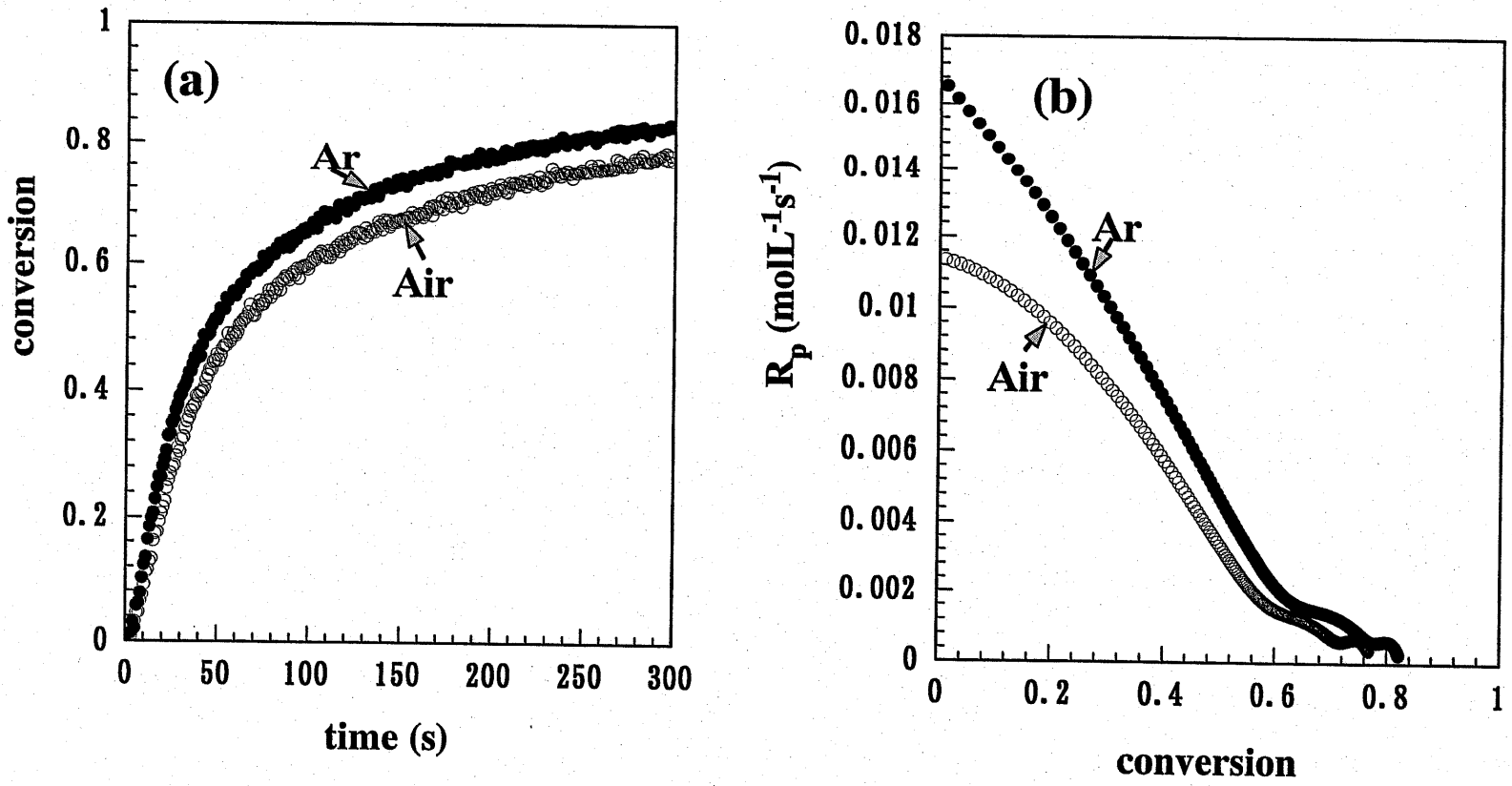

Figure 2-9. Time-conversion curves (a) and the rate of polymerization (b) of BzTD in poly(BzTD) matrix in argon and air, initiated by PMS under irradiation of 365 nm light at 20 – 25 °C. Ratio of BzTD/poly(BzTD)/PMS = 0.10/0.20/0.002 (wt/wt/wt) and the incident light intensity = 5.0×10^{-9} einstein·cm^{-2}·s^{-1}.

decrease with conversion. Evacuation of polymerization system was found to be necessary to obtain reproducible results in kinetic analysis of polymerization.

2-4. CONCLUSION

A series of styrenyl monomers bearing heterocyclic group, 1,3,4-thiadiazole ring, connected to styrenyl group through methylenethio group have been designed and synthesized. They showed high photopolymerization reactivity in polymer matrix. Even at temperatures below T_g, polymerization proceeded to high conversions. Molecular assembly caused by intermolecular interactions between thiadiazole groups in monomer molecules and high degree of rotational freedom arising from flexible methylenethio linkage are considered to explain high reactivity of these styrenyl monomers. Effects of matrix polymers on the polymerization behaviors were also remarkable. Polymers prepared from the present styrenyl monomers were found to be effective polymer matrices to increase the polymerization rate and the final conversion. The effect of atmospheric oxygen was also investigated and found to be negligible for the final conversion. The molecular orbital calculations based on the PM3 method revealed a relatively large value of polarizability (172 a.u.) for a typical styrenyl monomer, which could cause considerable molecular interaction through London dispersion force. The shape of the molecule is also unique and resembles a stackable legless chair. Molecular packing in aggregate phase, which was confirmed to exist in polystyrene matrix from the observation of transmission electron microscopy, could rearrange the styrenyl groups facing to each other in favor of effective photopolymerization in the solid state. The present solid-state photopolymerization system should be useful for wide range of applications by improvement of existing photopolymerization systems.

REFERENCES

1. Crivello, J. V., Adv. in Polym. Sci., 1984, 62, 1.
2. Decker, C. , Macromol. Symp. 1999, 143, 45.
3. Crivello, J. V. ; Ortiz, R. A., J. Polym. Sci. Part A. Polym. Chem., 2001, 39, 2385.
4. Crivello, J. V. ; Ortiz, R. A., ibid., 2001, 39, 3578.
5. Pappas, S. P. ; Pappas, B. C. ; Gatechair, L. R. , J. Polym. Sci. Part A. Polym. Chem., 1984, 22, 69.
6. Pappas, S. P. ; Gatechair, L. R. ; Jilek, J. H. , ibid., 1984, 22, 77.
7. Crivello, J. V. ; Lee, J. L., ibid., 1983, 21, 1097.
8. Decker, C. ; Moussa, K. , Makromol. Chem., 1988, 189, 2381.
9. unpublished results.
10. Buhr, G. ; Dammel, R. ; Lindley, C. R., Polym. Mat. Sci. Eng., 1989, 61, 269.
11. Pohlers, G. ; Scaiano, J. C., Chem. Mater., 1997, 9, 3222.
12. Pohlers, G. ; Scaiano, J. C. ; Step, E. ; Sinta, R., J. Am. Chem. Soc., 1999, 121, 6167.
13. Pawlowski, G. ; Dammel, R., J. Photopolym. Sci. Tech., 1991, 4, 389.
14. Urano, T. ; Nagao, T. ; Takada, A. ; Itoh, H. , Polym. Adv. Technol., 1999, 10, 244.
15. Decker, C. ; Moussa, K. , Macromolecules. 1989, 22, 4455.
16. Decker, C. ; Macromolecules. 1990, 23, 5217.
17. Decker, C. ; Moussa, K. ,Eur. Polym. J., 1990, 26, 393.
18. Rodriguez, M. ; Garcia-Moreno, I. ; Garcia, O. ; Sastre, R., Macromol. Chem. Phys., 2000, 201, 1345.
19. Mizuta, Y. ; Morishita, N. ; Kuwata, K., Appl. Magn. Reson., 2000, 19, 93.
20. Williams, R. M. ; Khudyakov, I. V. ; Purvis, M. B. ; Overton, B. J. ; Turro, N. J., J.

Phys. Chem. B, 2000, 104, 10437.

21. Braun, D. ; Studenroth, R., Angew. Makromol. Chem., 1979, 79, 79.

22. The polarizability and dipole moment are calculated as follows. All possible conformations are energy-minimized at the PM3 level using WinMOPAC v.2.0, Fujitsu Ltd. with the creterion for the maximum gradient (GNORM) less than 0.05. The resulting structures are sorted by the energy of formation. For a C1TD molecule, calculations converges to all possible conformations and the energy of formation in its most stable conformations, C-1 and C-3 in Figure 2-4(a) are lower than that in C-2 conformation by 0.7 kcal/mol in vacuum. This result suggests that at room temperature C1TD molecule could be in rapid equilibrium between these conformations as illustrated in Figure 2-4(a). Values of calculated polarizabilities and dipole moments are found to be not sensitive to these conformation changes.

23. Jansen, J.F.G.A. ; Dias, A. A. ; Dorschu, M. ; Coussens, B., Polym. Prepr., 2001, 42, 769.

24. Jansen, J.F.G.A. ; Dias, A. A. ; Dorschu, M. ; Coussens, B., Macromolecules, 2002, 35, 7529.

25. Andrzejewska, E. ; Andrzejewski, M., J. Polym. Sci. Part A. Polym. Chem., 1998, 36, 665.

26. Molaire, M. F. , J. Polym. Sci. Part A. Polym. Chem., 1982, 20, 847.

27. Lecamp, L. ; Youssef, B. ; Bunel, C. ; Lebaudy, P., Polymer, 1997, 38, 6089.

28. Moussa, K. ; Decker, C. , J. Polym. Sci. Part A. Polym. Chem., 1993, 31, 2633.

29. Decker, C. ; Moussa, K. , Macromol. Chem., 1990, 191, 963.

30. Matsumoto, A. ; Ueda, A. ; Aota, H. ; Ikeda, J., Macromol. Rapid Commun. 2000, 21, 701.

Chapter 3

Real-time monitoring of photodecomposition of initiator in polymer matrix and kinetic analysis of photopolymerization

3-1. INTRODUCTION

Photoinitiator is a key compound to determine the effectiveness of light-induced polymerization. Most of existing photoinitiators work in UV region and few are known to be sensitive to visible light.[1] Recent demands for visible-light sensitive photoinitiating system stem from evolving laser-imaging systems which utilizes moderate-power lasers including laser diodes to image photosensitive polymerizable media.[2-5] For such applications, high sensitivity and spatial resolution are indispensable to keep up with the demand for ever increasing recording density and throughput. Among few of visible-light sensitive photoinitiating systems, trichloromethyl triazine derivatives have been paid much interest. Trichloromethyl-substituted 1,3,5-triazines were found in the late 1960's[6] and are currently used in microelectronics. This type of photoinitiator can be used either as photo-radical initiator[7] or as photo-acid generator (PAG).[8-12] Upon UV-irradiation, trichloromethyl group connected to a triazine ring undergoes homolytic cleavage[13] of carbon-chlorine bond and the chlorine atom produced abstracts hydrogen atom from a donor, resulting in the formation of hydrogen chloride which acts as the acid catalyst in chemically amplified imaging system.[12, 14] On the other hand, the carbon radical produced adds to carbon-carbon double bond of monomer to initiate radical polymerization. We have been interested in trichloromethyl

triazine derivative as an unique photoinitiator working either as photo-radical initiator or as PAG. Furthermore, a high sensitivity of triazine derivatives to visible light by incorporating an appropriate dye and an amine has been reported.[15, 16] These unique advantages of triazine derivatives motivated our research interests to investigate photodecomposition behaviors of the triazines in solid state. Pohlers et al.[13] investigated the photodecomposition process of trichloromethyl triazine derivatives in solution. However, the photodecomposition process in solid state has not been investigated in details. In most of industrial applications of photopolymerization, usual photocurable formulation consists of a photoinitiator, a multi-functional oligomer and monomer. In the photopolymerization system, diffusion of reacting species dominates the polymerization kinetics. A number of investigations have dealt with photopolymerization kinetics in bulk phase and very important results have been obtained.[17-24] However, little is known about the initiation step of photopolymerization in bulk. Although the rate of initiation is directly related to the decomposition rate of photoinitiator and it determines the whole polymerization processes, only few are reported on actual photodecomposition processes of photoinitiator in bulk photopolymerization system. Decker et al. investigated the photodecomposition behaviors of typical photo-radical initiator, Lucirin TPO (from BASF) and of some PAG, triarylsulfonium salts, by monitoring the decrease of the UV absorbance of these photoinitiators.[25, 26] They found that these photoinitiators disappears according to a simple exponential law. However, such measurements on UV-spectroscopy might affect the photodecomposition of UV-sensitive photoinitiators and whole measurements should be carried out separately from the determination of polymerization rate. In order to investigate the relationship between polymerization rate and photodecomposition rate of photoinitiator, these should be determined at the same time in the polymerization

system. Other methods to measure photoinitiator decomposition have been explored such as laser flash photolysis and emission spectroscopy[13], time-resolved electron spin resonance[27] and time-resolved electron paramagnetic resonance[28]. However, these methods are useless to interpret the polymerization rate in terms of the initiator decomposition. We focused our attention in direct observation of photodecomposition of trichloromethyl-substituted triazine in photopolymerization system by monitoring simultaneously the change of monomer and photoinitiator concentration on real-time FT-IR (RT-IR) spectroscopy.[17-20] As for monomer, we selected a newly developed styrenyl monomer which bears 1,3,4-thiadiazole group as a substituent. Since this unique monomer exhibited very high polymerization reactivity, kinetic investigation of this polymerization is of great interest.

3-2. EXPERIMENTAL

Materials

2-(4'-Methoxystyryl)-4,6-bis(trichloromethyl)-1,3,5-triazine (**PMS**) was purchased from Panchim (Cedex, France) and used without further purification. Polystyrene (M_w = 3×10^5) was obtained from Wako Chemicals Ind. Ltd., (Osaka, Japan) and purified by precipitation from 1,4-dioxane solution with methanol. 1,4-Dioxane (Wako Chemicals Ind. Ltd.) was used without further purification.

Preparation of monomer and its polymerization

Preparation of 2-(4-vinylbenzyl)thio-5-benzylthio-1,3,4-thiodiazole (BzTD) and its polymer, poly(BzTD), were described in the previous chapter.

SEC/MALLS/RI/viscometry analysis[29] of poly(BzTD)

Molecular weight distribution (MWD) of poly(BzTD) obtained was determined by using SEC (size exclusion chromatography) system equipped with MALLS (multi-angle laser light scattering)(DAWN E, with operating/analysis software, Astra 4.73.04, both from Wyatt Technology Corp., Santa Barbara, CA), a differential refractometer (RI) and a differential viscometer (VISCOTEK model 300TDA with TriSEC data acquisition system operated by TriSEC 3.0 GPC software, Viscotek Corp., Richmond, CA). Separation columns were TSKgel G6000HHR + G3000HHR (Tosoh Corp., Tokyo, Japan) and SEC measurements were carried out with THF as eluent at a flow rate of 1.0 mL/min. The obtained MWD parameters are M_n = 40,800, M_w = 159,900, M_z = 392,200. Mark-Houwink-Sakurada parameters: a = 0.441, logK = –3.213.

DSC analysis of poly(BzTD), BzTD monomer and their blends

DSC analysis was carried out by using DSC 6200 (Seiko Instruments Inc., Chiba, Japan) with heating and cooling rate of 5 °C min^{-1} for the monomer and 10 °C min^{-1} for the polymer and the blends. BzTD monomer showed an endothermic peak at 103 °C (melting point) in the first heating run. Poly(BzTD) had T_g at 30 °C and the BzTD / poly(BzTD) blend at –1.8 °C (BzTD) / poly(BzTD) = 0.05/0.20 and –2.5 °C (0.10/0.20 wt/wt). The BzTD / poly(BzTD) blends are rubbery at room temperature (20 – 25 °C), although the surface of solution-cast film appears smooth without tackiness or stickiness.

General procedures for FT-IR measurements

Fourier transform real-time infrared (RT-IR)[17-20] spectroscopy were conducted on a Bio-rad FTS-40 (Bio-rad Laboratories, Inc., Hercules, CA) with an operating/analysis

software, Win-IR. Polystyrene or poly(BzTD) (0.2 g) was dissolved in 1,4-dioxane (2 g) and to this solution PMS (0.004 g or varied) and monomer (none or 0.0756 g) were added at room temperature. An exact amount (0.110 g) of the solution was eluted and dried on KRS (KRS-5; TlBr (42 %) / TlI (58 %)) disk. The thickness of cast film (15 ~ 24 μm) on KRS disk changed according to the proportion of PMS and monomer. A solution containing polymer, PMS and monomer (BzTD) were also eluted on a slide glass and after drying UV absorption spectrum was recorded on UV-VIS spectrometer model UV-2200 (Shimadzu Corp., Kyoto, Japan). A KRS disk coated with the sample was placed in the sample chamber of FT-IR spectrometer and IR spectra were recorded in the transmittance mode. Monochromatic 365 nm light was irradiated on KRS disk through an interference filter attached to the end of optical fiber. The light source used was high-pressure Hg lamp (Spot-Cure, Ushio Inc., Tokyo, Japan) and the light intensity at the surface of KRS disk was measured by Radiometer IL1700, (International Light Inc., Newburyport, MA.). The light intensity measured on the surface of KRS disk in the sample chamber was 1.61 $mW \cdot cm^{-2}$ = 5.0×10^{-9} $einstein \cdot cm^{-2} \cdot s^{-1}$. All measurements were carried out at room temperature under argon atmosphere and RT-IR spectra were collected at the rate of 1 survey spectrum per 1.65 second with a resolution of 1 cm^{-1} over the wavenumber range of 450 cm^{-1} to 4000 cm^{-1}.

3-3. RESULTS AND DISCUSSION

3-3-1. Determination of photodecomposition rate of PMS in polystyrene matrix by RT-IR

Infrared absorption spectrum of PMS shows an intense and characteristic absorption band at 1171 cm^{-1} which is assigned to a coupled asymmetrical stretching vibration of two CCl_3 groups connected to 1,3,5-triazine ring. If one of the chlorine atoms in CCl_3

groups is substituted by other atom or group, then symmetry of the substituent is lost and absorption band at 1171 cm^{-1} disappears or shifts to lower wavenumber from simulation based on molecular orbital calculations (force calculation by WinMOPAC v.2.0, Fujitsu Ltd.). Since this absorption band is quite intense and is not affected by absorptions due to polymer matrix and monomer, it was possible to determine quantitatively the concentration of PMS in the polymerization system under UV irradiation. FT-IR absorbance at 1171 cm^{-1} on the polystyrene film containing various concentrations of PMS obeyed the Lambert-Beer's law.

Photolysis of similar bis(trichloromethyl) triazine derivatives in solution was conducted by Buhr et al.[9] Using HPLC/MS spectroscopy, they determined the structures of major photodecomposition products of PMS in polymer matrix and proposed possible reaction pathway as illustrated in Scheme 3-1. Upon UV irradiation, PMS yields various kinds of photodecomposition products depending on the nature of polymer matrix. However, substitution of chlorine atom in CCl_3 group by hydrogen or other group is a common structural change. Such structural alternation should be accompanied by absorption change at 1171 cm^{-1}. Therefore, the absorption change at 1171 cm^{-1} should measure the concentration change of PMS upon UV irradiation. In Fig. 3-1, RT-IR spectral change of PMS in polystyrene matrix upon UV irradiation is shown. In this figure, the absorbance at 1171 cm^{-1} decreased monotonously, while the absorption at 1181 cm^{-1} due to polystyrene matrix was unchanged. These two absorptions were deconvoluted into two symmetrical absorptions and the intensity at 1171 cm^{-1} was monitored under UV irradiation to determine the time-dependent concentration change of PMS in polystyrene matrix. Photodecomposition ratio (*DR*) of PMS was calculated from Eq.(1).

$$DR = \frac{A(1171)_0 - A(1171)_t}{A(1171)_0} \qquad (1)$$

where $A(1171)_0$ and $A(1171)_t$ denote absorbance at 1171 cm^{-1} at the beginning and time t of UV irradiation, respectively.

Scheme 3-1

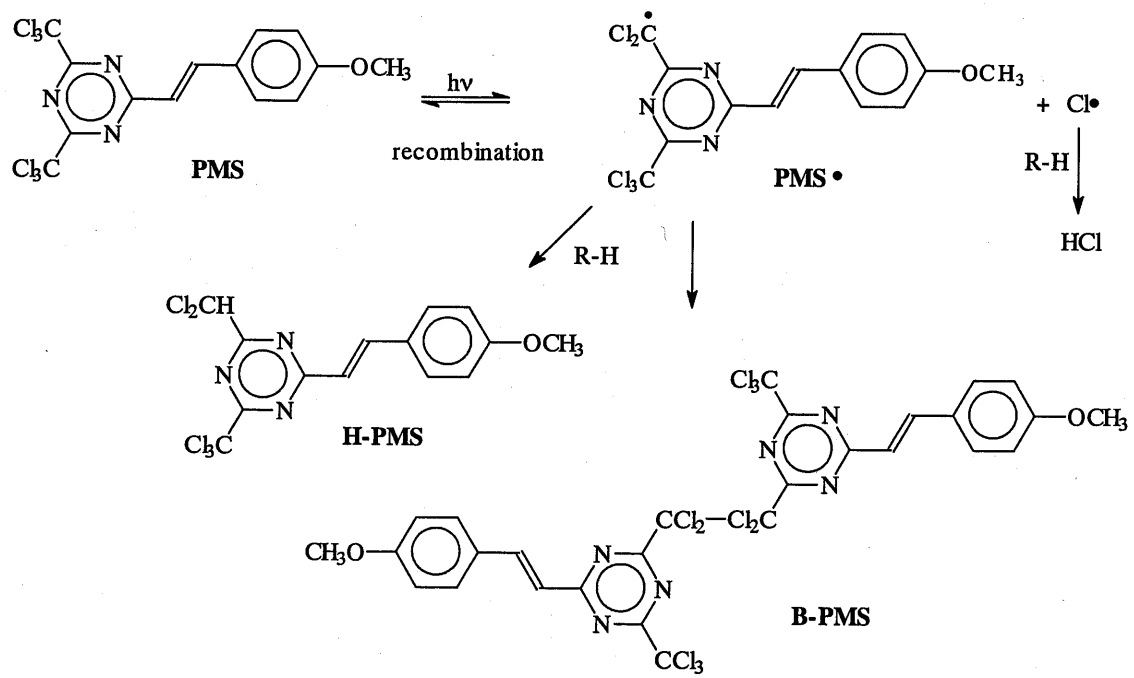

DR vs. time curves of PMS in polystyrene matrix with various initial PMS concentrations are plotted in Fig.3-2. As the initial concentration of PMS decreased, *DR* of PMS increased. Since the incident light intensity was kept constant, the ratio of photo-decomposed PMS to the initial PMS concentration should decrease as the initial concentration of PMS increases.

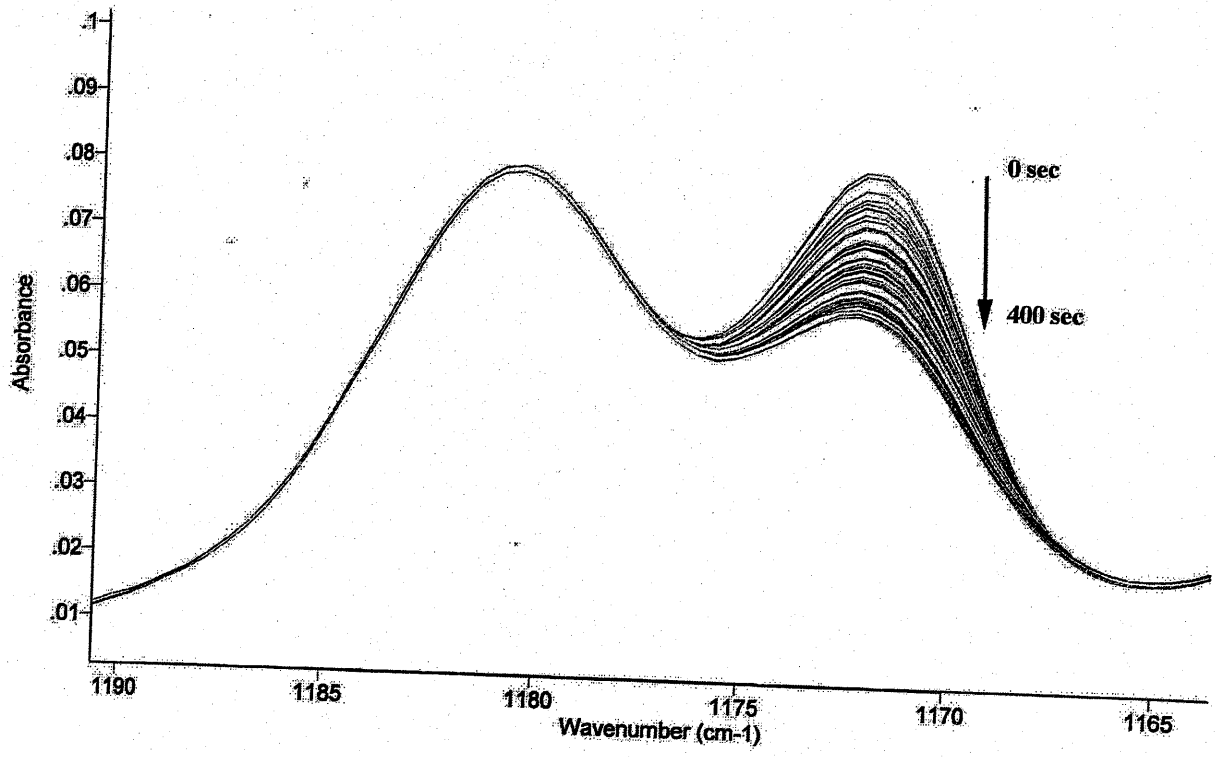

Figure 3-1. Photodecomposition of PMS in polystyrene matrix upon UV-irradiation at 365 nm as monitored by RT-IR spectroscopy.

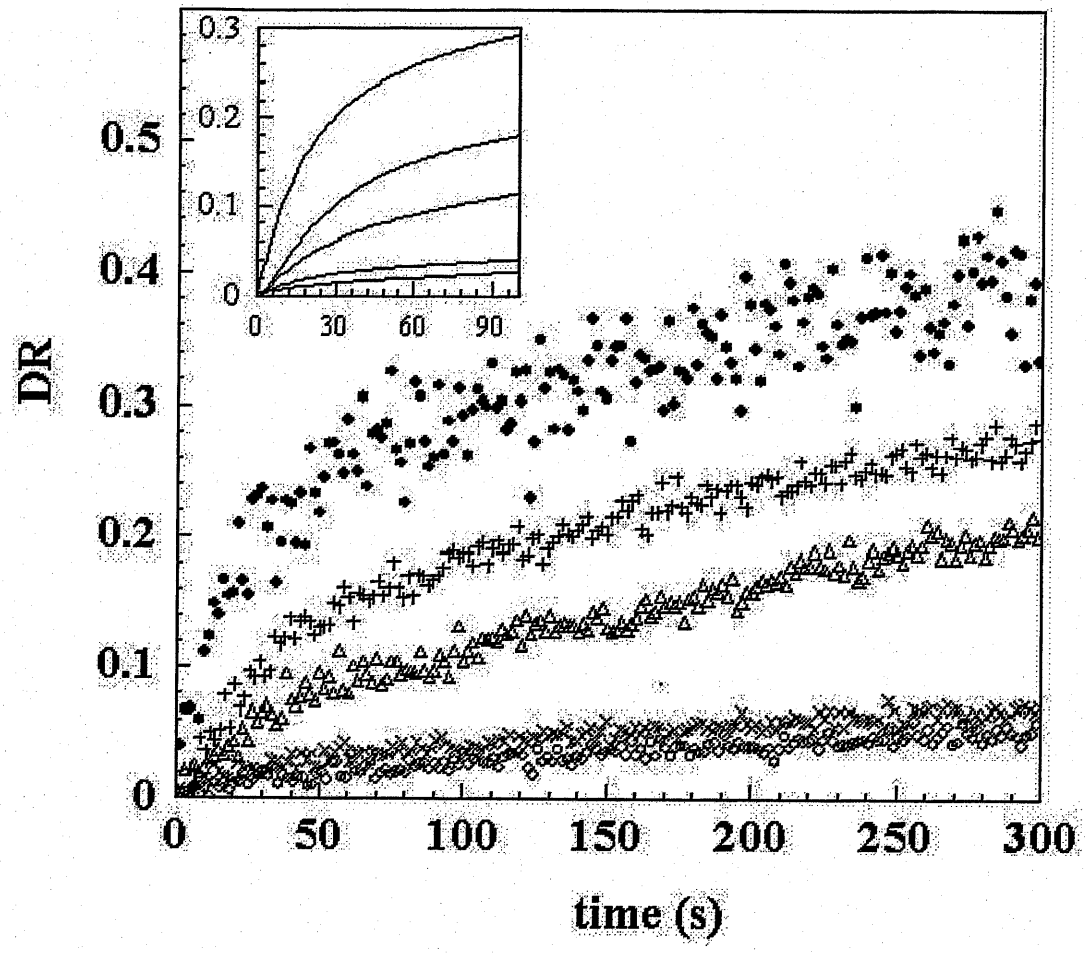

Figure 3-2. Decomposition ratio (*DR*) of PMS vs. time curves for various initial concentrations of PMS in polystyrene matrix. The inset shows curve fits to the experimental data points. The amount of PMS in 200 mg of polystyrene: (•) 1.4 mg, (+) 3.2 mg, (Δ) 4.2 mg, (¦) 7.7 mg, (×) 13 mg and (o) 37.6 mg.

Decomposition rate, R_d, of PMS was calculated from Eq.(2).

$$R_d\ (mol\,L^{-1}\,s^{-1}) = -\frac{d[PMS]}{dt} = [PMS]_0\,\frac{d(DR)}{dt} \qquad (2)$$

Quantum yield of photodecomposition (Φ_d) of PMS was calculated by Eq.(3):

$$\Phi_d = \frac{number\ of\ photodecomposed\ PMS\ molecules}{number\ of\ photons\ absorbed} = \frac{R_d}{I_a\ (einstein\,L^{-1}s^{-1})} = \frac{R_d \times \ell(cm)}{I_a\ (einstein\,cm^{-2}\,s^{-1}) \times 10^3} \qquad (3)$$

in which the light intensity absorbed by the sample, I_a, is expressed by the following equation:

$$I_a = I_0 \times (1 - \exp(-2.3\ \varepsilon l\ [\mathrm{PMS}\,]\,)\,) \qquad (4)$$

where I_0 denotes the incident light intensity, l is the thickness of polystyrene film and ε is the absorption coefficient of PMS in polystyrene matrix at 365 nm. The initial R_{d0} and Φ_{d0} values for different initial PMS concentrations were calculated from the initial slopes of the curve fits in *DR* vs. time plots. The results are summarized in Fig. 3-3(a) and (b). Although the obtained R_{d0} values are in the order of 2×10^{-4} mol·L^{-1}·s^{-1} and data points are rather scattered, R_{d0} seems to slightly increase with PMS concentration. On the other hand, Φ_{d0} is apparently independent on initial PMS concentrations. The average Φ_{d0} value is about 0.09 (±0.04). Buhr et al. had investigated the quantum yields of photodecomposition of similar bis-trichloromethyltriazines in novolak resin and reported the values in the range of 0.29 to 0.35. Pohlers et al.[13] estimated the quantum yield of 2-(4'-methoxynaphthyl)-4,6-bis(trichloromethyl)-1,3,5-triazines in cyclohexane solution to 0.11. They found that the polarity of the solvent affects the quantum yield significantly and showed that the quantum yield decreases with increase in solvent polarity.

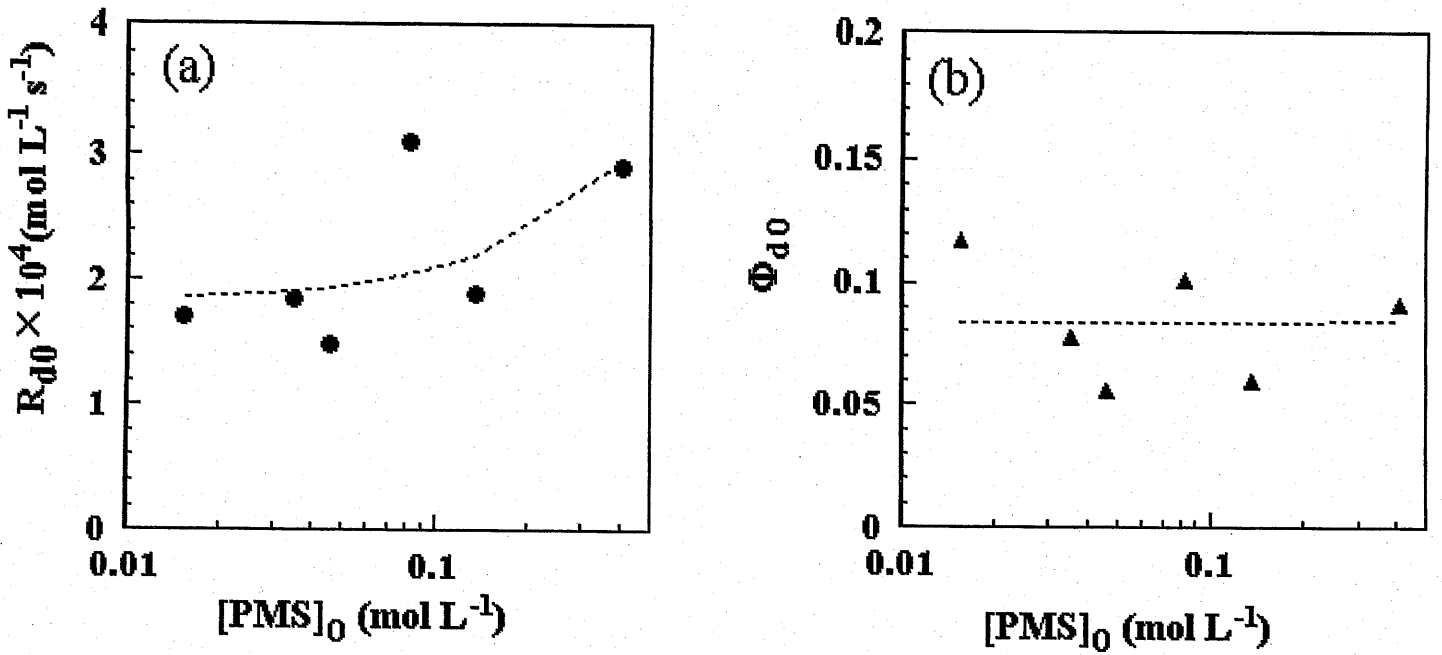

Figure 3-3. Dependence of R_{d0} (a) and Φ_{d0} (b) on the initial PMS concentration for the photodecomposition of PMS in polystyrene matrix.

Our result (0.09) is rather close to the value (0.11) obtained by Pohlers et al., though the difference in experimental conditions should be taken into consideration. Data scattering observed in Fig. 3-3(a) and (b) is considered to have arisen from the difficulty in controlling the thickness of the sample film on a KRS disk.

R_d of the photodecomposition for different initial PMS concentrations (Fig. 3-2) were calculated from Eq.(2) and are plotted against the residual PMS concentration, the latter being calculated according to the equation: [PMS] = $[PMS]_0 \times (1-DR)$, where $[PMS]_0$ denotes the initial PMS concentration. The results are summarized in Fig. 3-4. For all initial PMS concentrations, R_d decreased linearly with PMS concentration in the primary stage of photodecomposition process, and the slope of the linear part of each R_d vs. [PMS] plot appears to be independent on the initial PMS concentration. The relationship between R_d and [PMS] in the primary stage of photodecomposition can be expressed as follows:

$$R_d = k \times I_0(einstein\,L^{-1}s^{-1}) \times ([PMS] - C_f) \qquad (5)$$

where k (L·einstein^{-1}) denotes a decay constant and C_f represents a limiting PMS concentration attainable for the linear relation between R_d and PMS concentration. At the limiting PMS concentration the decomposition reaction ceases ($R_d = 0$). In other words, only a part of PMS molecules, ([PMS] – C_f), participate in the photodecomposition process and the remaining PMS (C_f mol·L^{-1}) are left unreacted for unknown reasons. A linear dependence of R_d on PMS concentration as expressed in Eq.(5) implies that photodecomposition is primarily determined by the probability of a photoinitiator molecule to be hit by a photon and is therefore proportional to the photoinitiator concentration. Similar results have been obtained by Decker et al. for the photolysis of TPO and a triarylsulfonium salt by monitoring UV-absorbance change of

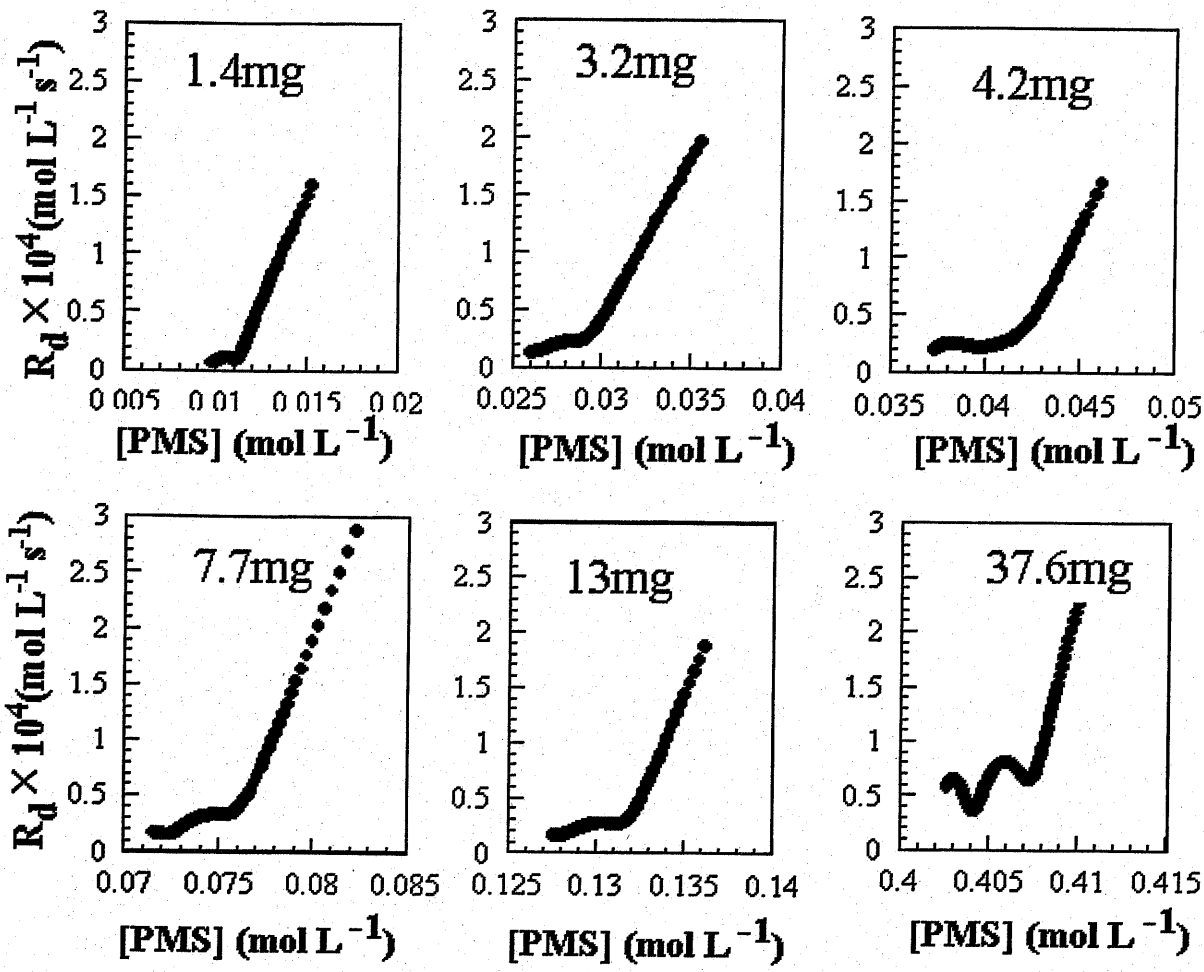

Figure 3-4. R_d *vs.* [PMS] plot for the photodecomposition process at various initial PMS concentrations. R_d was calculated from the results shown in Fig. 3-2.

these photoinitiators upon UV irradiation. It should be noted that k is approximately equal to $2.3\times\varepsilon l\Phi_d$, when absorbance is low, from Eq. (3) and (4) and directly related to Φ_d, if we neglect the contribution of inactive PMS, C_f, to the absorption of light and replace the term, [PMS], in Eq.(4) with [PMS] – C_f. It is beyond to the scope of this paper to argue the physical meanings of Eq. (5) in detail.

In Fig. 3-5(a), the decay constant, k, obtained from the slope of the linear part of R_d *vs.* [PMS] plot is plotted against $[PMS]_0$. In this figure, values of k are around 10 (L einstein^{-1}) and seemed to gradually increase with PMS concentrations. The problem to be solved is the reason why all PMS molecules do not participate in photodecomposition process. In Fig. 5(b), the effective PMS concentrations, ($[PMS]_0 - C_f$), are plotted against the initial PMS concentrations. The effective PMS concentration was independent of the initial PMS concentration and unchanged around 6×10^{-3} mol L^{-1}: this implies that no more than 6×10^{-3} mol L^{-1} of PMS molecules could decompose in polystyrene matrix.

In polystyrene matrix, PMS molecules are frozen in a glassy state and their diffusion is restricted. When a PMS molecule is photo-excited and dissociates into PMS radical and chlorine atom, their migration would be hindered by the surrounding polystyrene matrix and strong cage effect would enhance the recombination of these radical species. Therefore, in the bulk phase of polystyrene matrix, dissociation of PMS radical would be restrained by the cage effect. On the other hand, a part of PMS molecules should be located at the surface of the polystyrene matrix and these might be in different situation from the bulk. It is considered that only parts of PMS molecules happen to be in relatively mobile surroundings and these contribute the photodecomposition and others are virtually unable to dissociate into radicals.

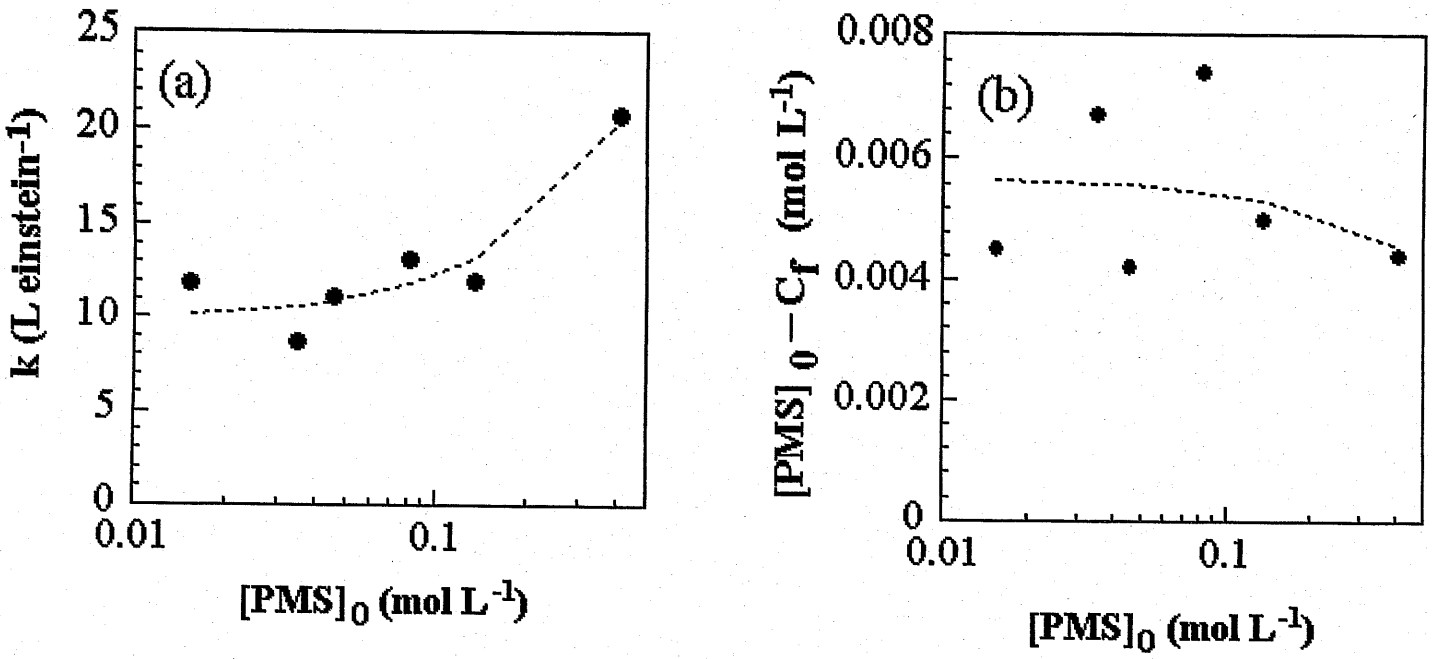

Figure 3-5. Dependence of k (a) and $[PMS]_0$-C_f (b) on the initial PMS concentration in the photodecomposition of PMS in polystyrene matrix. Data are based on the results shown in Fig. 3-2.

3-3-2. Effect of light intensity on photodecomposition rate of PMS

In polystyrene matrix, PMS was photodecomposed by the irradiation of 365 nm light with various intensities and the dependence of R_d and Φ_d on the light intensity was investigated to confirm the relationship given by Eq.(5). Under the experimental conditions, about 75 % of incident light were absorbed by the sample. As a matrix polymer, poly(BzTD) as well as polystyrene was used to investigate the effect of the nature of matrix polymer on photodecomposition behavior of PMS. In poly(BzTD) matrix, UV absorption of PMS shifted to longer wavelength by 10 nm (λmax = 395 nm) and absorption coefficient at 365 nm decreased by 75 % of that in polystyrene. This indicates an occurrence of some interactions between PMS and poly(BzTD). The results are summarized in Figures 3-6 and 7. In Fig. 3-6(a), R_{d0} depends linearly on incident light intensity as expected by Eq.(5) and R_{d0} is much higher in poly(BzTD) matrix than in polystyrene matrix. The dependence of R_{d0} on the light intensity is stronger in poly(BzTD) matrix than in polystyrene matrix. As shown in Fig.3-6(b), Φ_{d0} in polystyrene matrix decreases slightly with increasing the light intensity, whereas in poly(BzTD) matrix Φ_{d0} remained virtually constant. At any I_0 values, Φ_{d0} in poly(BzTD) matrix was larger than that in polystyrene matrix. The above-described experimental observations should be explained as follows. T_g of poly(BzTD) is found to be 30 °C as described in the previous chapter and PMS molecules in this matrix are relatively mobile as compared with those in polystyrene matrix. Cage effect which suppress the photo-dissociation of excited PMS molecules would be less eminent in poly(BzTD) matrix than in polystyrene matrix. In addition to such physical effect of matrix polymer, chemical features must affect the photodecomposition of PMS. Under an intense photo-irradiation, large numbers of PMS molecules decompose at the same

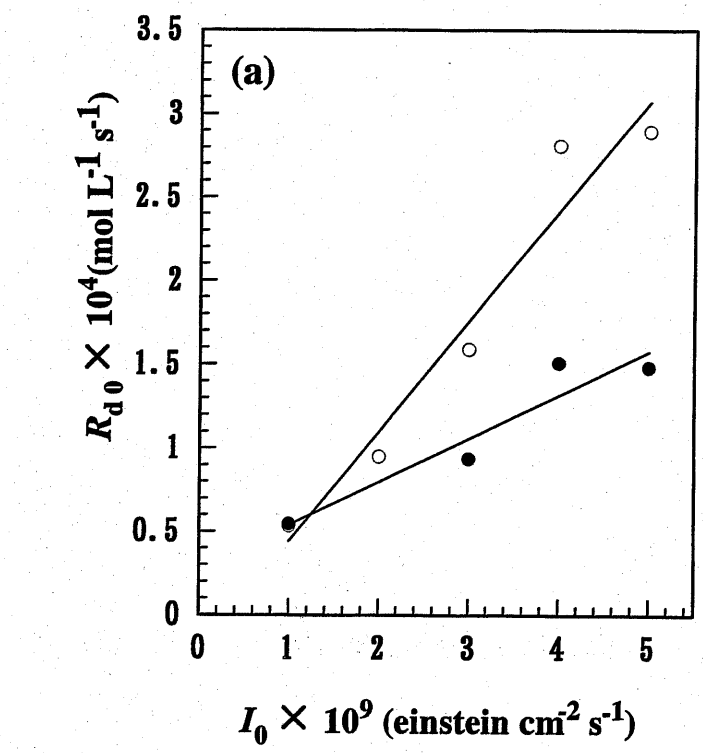

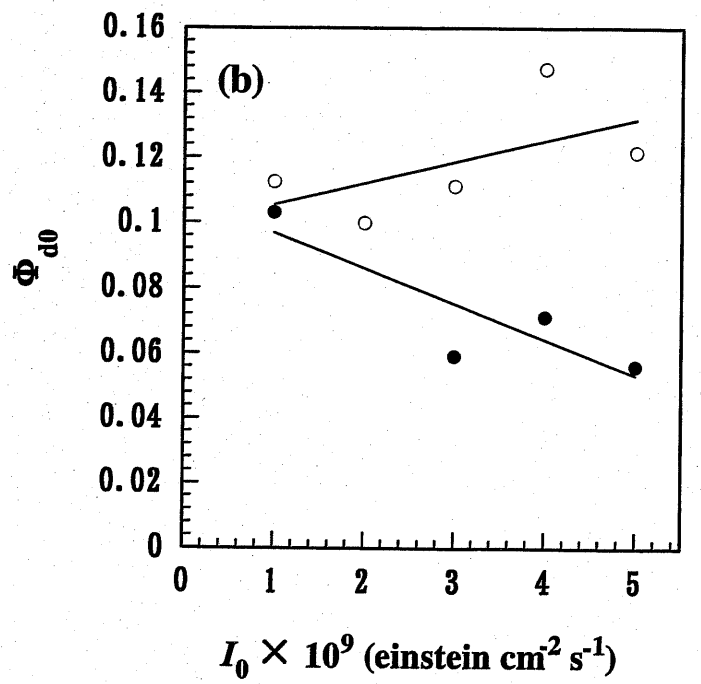

Figure 3-6. Dependence of R_{d0} (a) and Φ_{d0} (b) on the incident light intensity, I_0, in the photodecomposition of PMS in polystyrene matrix (•) and in poly(BzTD) matrix (o). PMS/polymer matrix = 0.0042/0.2 wt/wt.

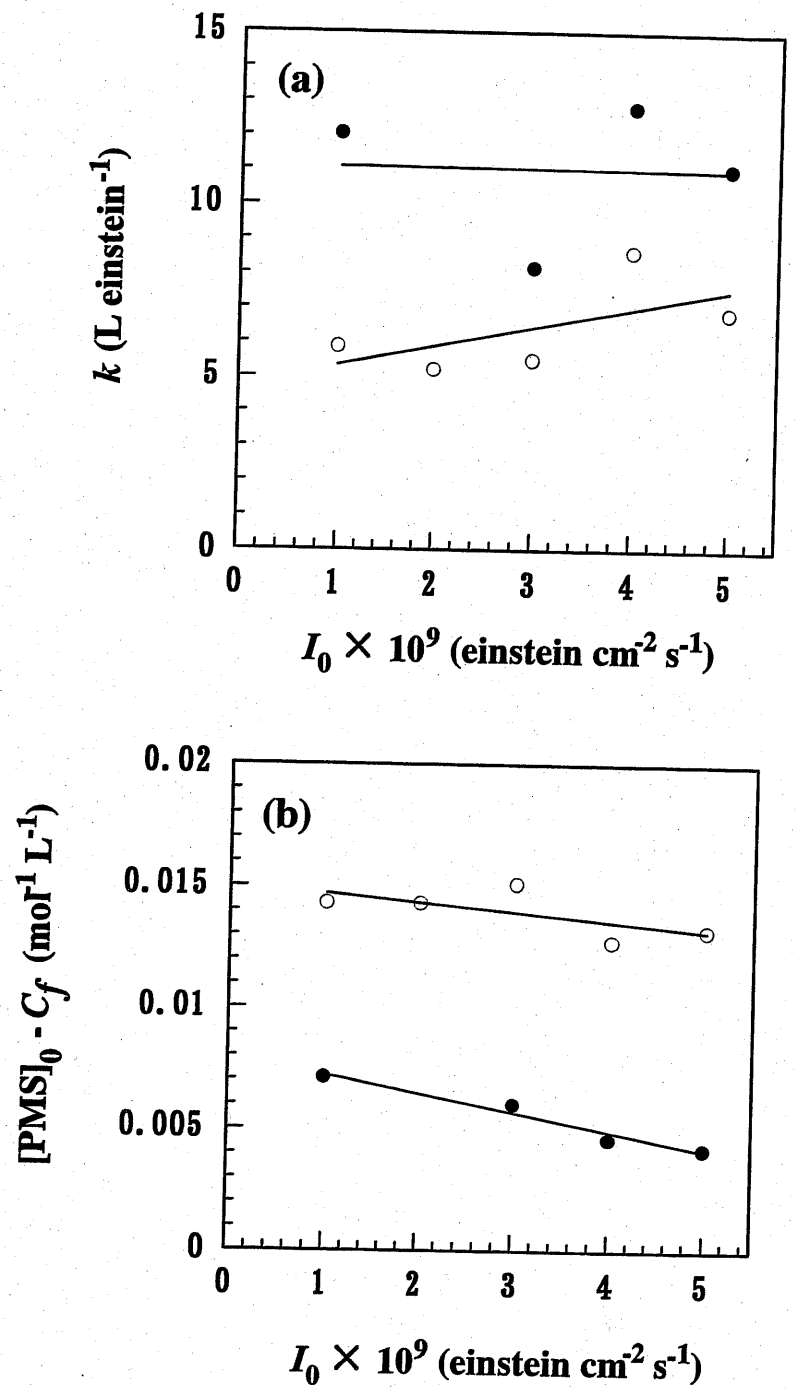

Figure 3-7. Dependence of k (a) and $[PMS]_0 - C_f$ (b) on the incident light intensity, I_0, in the photodecomposition of PMS in polystyrene matrix (•) and in poly(BzTD) matrix (o).

time to increase temporal concentration of chlorine atoms, which accelerates the back reaction, resulting in the decrease in the quantum yield of photodecomposition. On the other hand, under the condition that the concentration of hydrogen donor is high enough to scavenge chlorine atoms, the quantum yield of photodecomposition should not be affected by the light intensity. In the poly(BzTD) matrix the two thiobenzyl groups are powerful hydrogen donor to suppress radical recombination reaction effectively. This could account for higher values of R_{d0} and Φ_{d0} in poly(BzTD) matrix than in polystyrene matrix. Crivello et al.[36] have reported photoinduced ring-opening cationic polymerization of epoxide monomers bearing benzyl ether group initiated by diaryliodonium salts. They suggested that the aryl radical produced by photodecomposition of the onium salt abstracts labile benzyl hydrogens to yield benzyl radicals, which are in turn oxidized by the onium salt to benzyl cation as the real initiator of polymerization. The same activity of benzyl group should be applied to the present system.

Extensive hydrogen abstraction from benzyl groups is suggested from the SEC/MALLS/viscometry analysis[29, 31] of poly(BzTD) prepared by conventional solution polymerization. The Mark-Houwink-Sakurada parameter, which was determined using a differential viscometer in the GPC condition was 0.44, which is apparently lower than those for conventional linear polymers (0.5 – 0.8 depending on solvent), suggesting branched structure of poly(BzTD). The weight-average molecular weight (M_w) was determined by SEC/MALLS analysis and from the slope of the double logarithmic plot of the radius of gyration versus M_w, conformational coefficient[30, 32, 33] was found to be 0.34. This parameter reflects the polymer chain density inside the individual polymer coil, and the relatively low value also suggests extensive branching

in the polymer chain. The chain branching should have been caused by chain transfer reaction to polymer benzyl groups in solution polymerization of BzTD monomer. From a practical point of view, poly(BzTD) matrix is superior to polystyrene matrix with higher quantum yield and increased decomposition rate of PMS.

Values of decay constant, k, and effective concentration of photoinitiator, $[PMS]_0 - C_f$, are plotted against the incident light intensity in Fig. 3-7(a) and (b). Values of k obtained for poly(BzTD) matrix and polystyrene matrix are nearly independent of the light intensity. Smaller values of k in poly(BzTD) matrix than in polystyrene matrix do not agree with higher values of Φ_{d0} in poly(BzTD) matrix. However, as shown in Fig. 3-7(b), effective PMS concentration, $[PMS]_0 - C_f$, is two fold higher in poly(BzTD) matrix than in polystyrene matrix. This fact must have led to the higher decomposition rate and increased overall quantum yield of photodecomposition of PMS in poly(BzTD) matrix.

3-3-3. Photodecomposition behavior of PMS in the presence of BzTD monomer and kinetic analysis of photopolymerization processes in the solid state

PMS and BzTD monomer were dispersed in poly(BzTD) matrix. Monomer consumption was followed by the absorbance change at 990 cm^{-1} (vinyl, δCH, out-of-plane bending) and at the same time photodecomposition of PMS was simultaneously monitored by the absorbance change at 1171 cm^{-1}. In Fig. 3-8(a), the time-conversion curves of monomer (BzTD) and photoinitiator (PMS) under irradiation of 365-nm monochromatic light are plotted. While monomer conversion reached 90% conversion after 400-second irradiation, photoinitiator conversion (decomposition ratio, *DR*) reached only about 50% and further photodecomposition was suppressed.

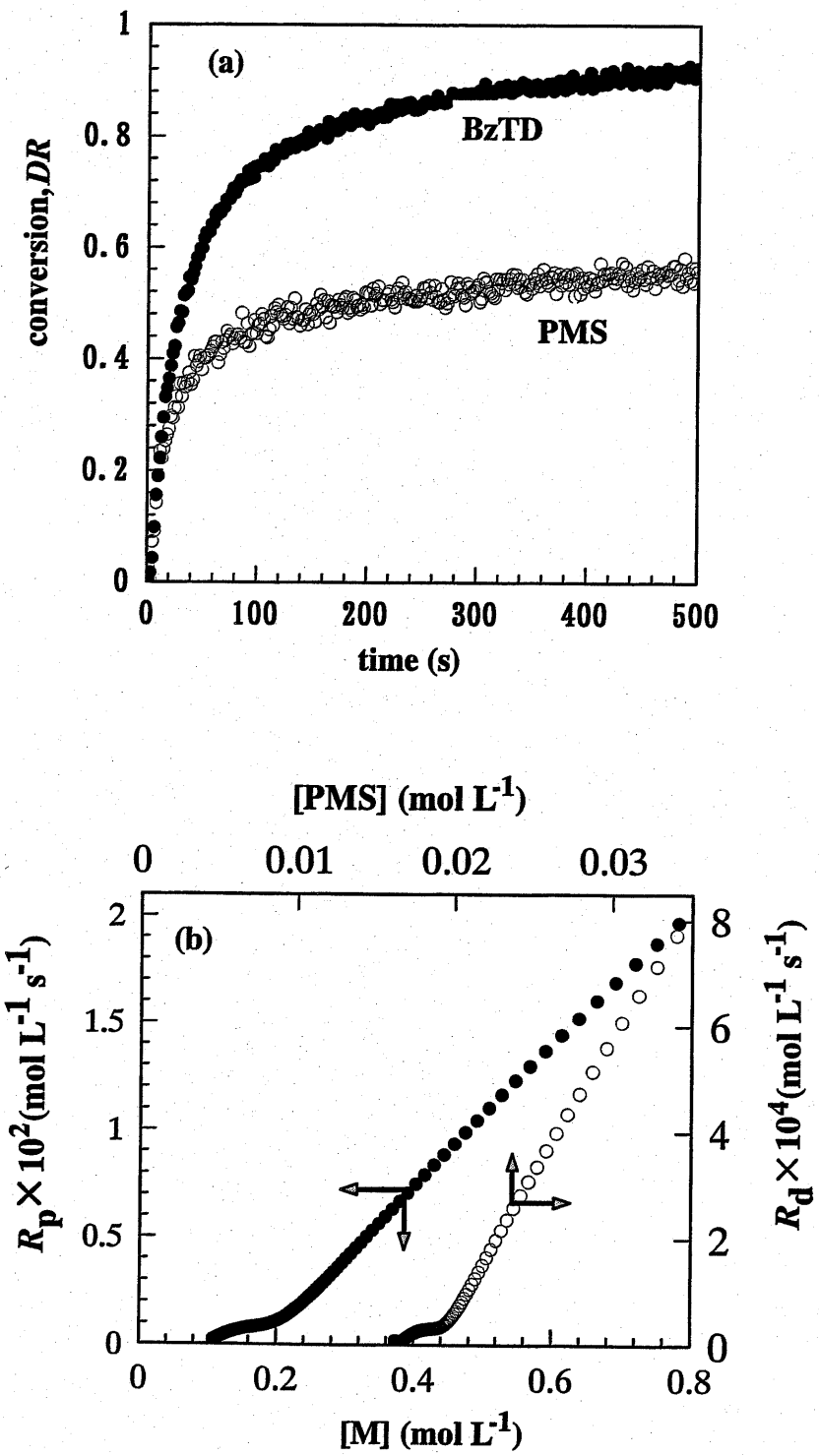

Figure 3-8. (a) Time-conversion curves of BzTD and PMS and (b) R_p *vs.* [M] and R_d vs. [PMS] plot for the photopolymerization of BzTD initiated by PMS in poly(BzTD) matrix. BzTD/PMS/poly(BzTD) = 0.0756/0.042/0.20 wt/wt/wt.

The polymerization rate (R_p) and photodecomposition rate (R_d) were determined by the differentiation of 8th-order polynominal curve fits and are plotted against each concentration as shown in Figure 3-8(b). It is found that both R_p and R_d decrease lineally with the corresponding concentrations during the major part of the polymerization. Initial photodecomposition rate, R_{d0}, was determined to be about 8×10^{-4} $mol\cdot L^{-1}\cdot s^{-1}$, which is about 3-fold larger than that obtained in the absence of BzTD monomer (in Fig. 3-6(a): $R_{d0} = 3\times10^{-4}$ $mol\cdot L^{-1}\cdot s^{-1}$). This fact suggests that in the presence of the monomer, PMS radical attacks to the neighboring monomer molecule and this initiation reaction would suppress the recombination of photo-dissociated PMS molecule, resulting in increased decomposition rate of PMS.

The linear dependence of R_p on monomer concentration proves that the first-order kinetics at the steady-state condition as expressed by Eq. (6) holds:

$$R_p = k_p [P\cdot] [M] \qquad (6)$$

where k_p designates the propagation rate constant, [P·] the concentration of propagating radical, and [M] the monomer concentration.

The linear dependence of R_d on [PMS] in the photopolymerization process supports the validity of Eq. (5). From the slope of the linear part in R_p vs. [M] plot, k_p[P·] was determined to be 0.33 s^{-1}. However, the experimental dependence of R_p on [M] is not expressed by Eq. (6) but by Eq. (7):

$$R_p = k_p [P\cdot] ([M] - C_m) \qquad (7)$$

where C_m denotes a concentration of monomer left unreacted.

The purpose of this study is to determine both the polymerization rate of styrenyl monomer and the photodecomposition rate of photoinitiator, PMS, concurrently in the solid state photopolymerization. The results obtained here revealed the fact that the

polymerization proceeds in a steady-state condition with a constant concentration of propagating radical, while the decomposition rate of the photoinitiator decreases with the progress of the photopolymerization. These two factors are apparently conflicting with each other, since the propagating radical must be supplied by the initiating PMS radical and the latter concentration decreases with the progress of the polymerization, while the former concentration is apparently constant during the polymerization. However, if the decrease in the decomposition rate of PMS is directly related to the decrease in the termination rate of the propagating radical, then steady-state condition should hold. In other words, if the termination reaction takes place between the propagating radical and the remaining PMS molecule, then the results obtained above would be satisfactorily explained.

A set of possible elementary steps are summarized in Scheme 3-2. In this Scheme, PMS· denotes the initiating radical produced by photodecopmposition of PMS and P· represents both the propagating polymer radical and the monomer radical produced by the addition of initiating radical. In this kinetic model, the reactivities of both polymer and monomer radicals are assumed to be the same and these two entities are not distinguished. D represents dead-polymer produced by the termination reaction between the propagating radical and the remaining PMS molecule. The rate constants, k_t and k_{tr} represent the termination rate constant and the chain transfer rate constant, respectively.

PMS has two types of labile sites for radical attack; i.e., trichloromethyl and styryl groups. The former definitely has a large chain transfer constant and by the abstraction of chlorine atom with the propagating radical P·, PMS· can easily be reproduced. This process is illustrated in Scheme 3-3. On the other hand, if the propagating radicals attack to the styryl group in the PMS molecule, then the addition of the propagating

Scheme 3-2

Photodecomposition :	$PMS \rightarrow PMS\bullet + Cl\bullet$	$:R_d = kI_0[PMS]$
Initiation :	$PMS\bullet + M \rightarrow P\bullet$	$:R_i = ki[PMS\bullet][M]$
Propagation :	$P\bullet + M \rightarrow P\bullet$	$:R_p = k_p[P\bullet][M]$
Termination :	$P\bullet + PMS \rightarrow D$	$:R_t = k_t[P\bullet][PMS]$
Chain Transfer :	$P\bullet + PMS \rightarrow D + PMS\bullet$	$:R_{tr} = k_{tr}[P\bullet][PMS]$
2nd Initiation:	$Cl\bullet + M \rightarrow P\bullet$	
Abstraction :	$Cl\bullet + RH \rightarrow R\bullet + HCl$	
3rd Initiation:	$R\bullet + M \rightarrow P\bullet$	

Scheme 3-3

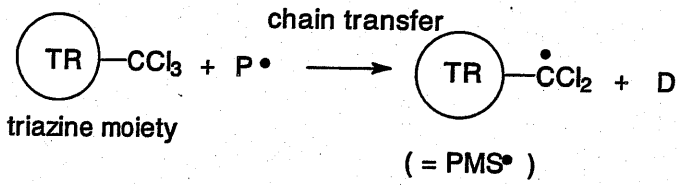

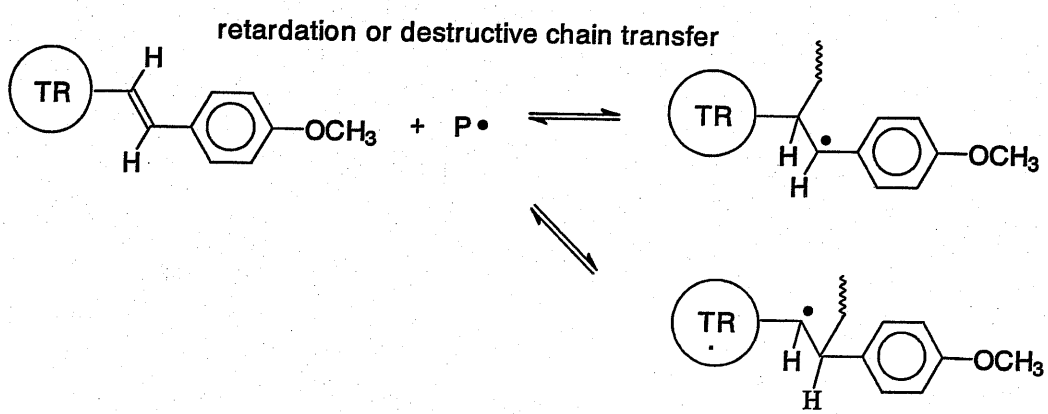

polymer chain to the styryl group would result in generation of relatively stable sterically hindered radicals as shown in Scheme 3-3. Harwood et al. [34] has found that in the benzoyl peroxide initiated polymerization of methyl methacrylate (MMA)-stilbene mixtures, stilbene acts as moderator for MMA polymerization and the resulted polymer had stilbene-end groups. Barson et al.[35] has also reported the high reactivities of stilbene derivatives towards the benzoyloxy radical. In our case, the concentration of PMS used was relatively high (0.0335 mol L^{-1}) and the mole % of PMS to the BzTD monomer ($[PMS]_0 / [M]_0$ = 4.4 mol %) may be high enough to trap the propagating radical by the remaining PMS molecule.

On an analogy of copolymerization reactivity of stilbene with MMA[34], it may be reasonable to consider that the trapped radical by PMS may show poor reactivity to the monomer and would slow down or rather terminate the polymerization in effect. Therefore we consider that a destructive chain transfer reaction as shown in Scheme 3 might be the dominant termination process for these particular polymerization systems with relatively high concentrations of PMS.

Based on the elementally steps shown in Scheme 3-2 and with an assumption of a steady-state condition for every intermediate radical species, the following equations can easily be derived.

$$[P\cdot] = \frac{2R_d}{k_t[PMS]} = \frac{2kI_0}{k_t} \tag{8}$$

$$[PMS\cdot] = \left(1+\frac{2k_{tr}}{k_t}\right)\frac{kI}{k_i}\frac{[PMS]}{[M]}$$

$$\left(\textit{experimentally}:[PMS\cdot] = \left(1+\frac{2k_{tr}}{k_t}\right)\frac{kI_0}{k_i}\frac{[PMS]-C_f}{[M]-C_m}\right) \tag{9}$$

$$R_p = \frac{2k_pkI_0}{k_t}[M]$$

$$\left(\textit{experimentally}:R_p = \frac{2k_pkI_0}{k_t}([M]-C_m)\right) \tag{10}$$

$$kcl \equiv \frac{R_p}{R_i} = \frac{R_p}{R_d} = \frac{2k_p}{k_t}\frac{[M]}{[PMS]}$$

$$\left(\textit{experimentally}:kcl \equiv \frac{R_p}{R_i} = \frac{2k_p}{k_t}\frac{[M]-C_m}{[PMS]-C_f}\right) \tag{11}$$

where *kcl* means *k*inetic *c*hain *l*ength which is defined as the number of monomer molecules polymerized by one initiating radical.

Kinetic chain length (*kcl*) is a very important parameter to describe the characteristics of the polymerization process and this parameter should be the measure of the validity of the kinetic equations. In Fig. 3-9(a), both *kcl* and k_p/k_t in the polymerization process are plotted. The value of k_p/k_t remained constant (= 0.32) up to conversion = 0.6 and then sharply dropped to zero. The obtained constant value of this ratio of two kinetic parameters, k_p and k_t, proves the validity of the discussion described above. On the other hand, as is seen in this Figure, the value of *kcl* increased gradually with conversion and at conversion = 0.65 it turned to decrease. A peak observed at conversion = 0.8 is thought to be an artifact caused by the polynominal approximation of time-conversion curve.

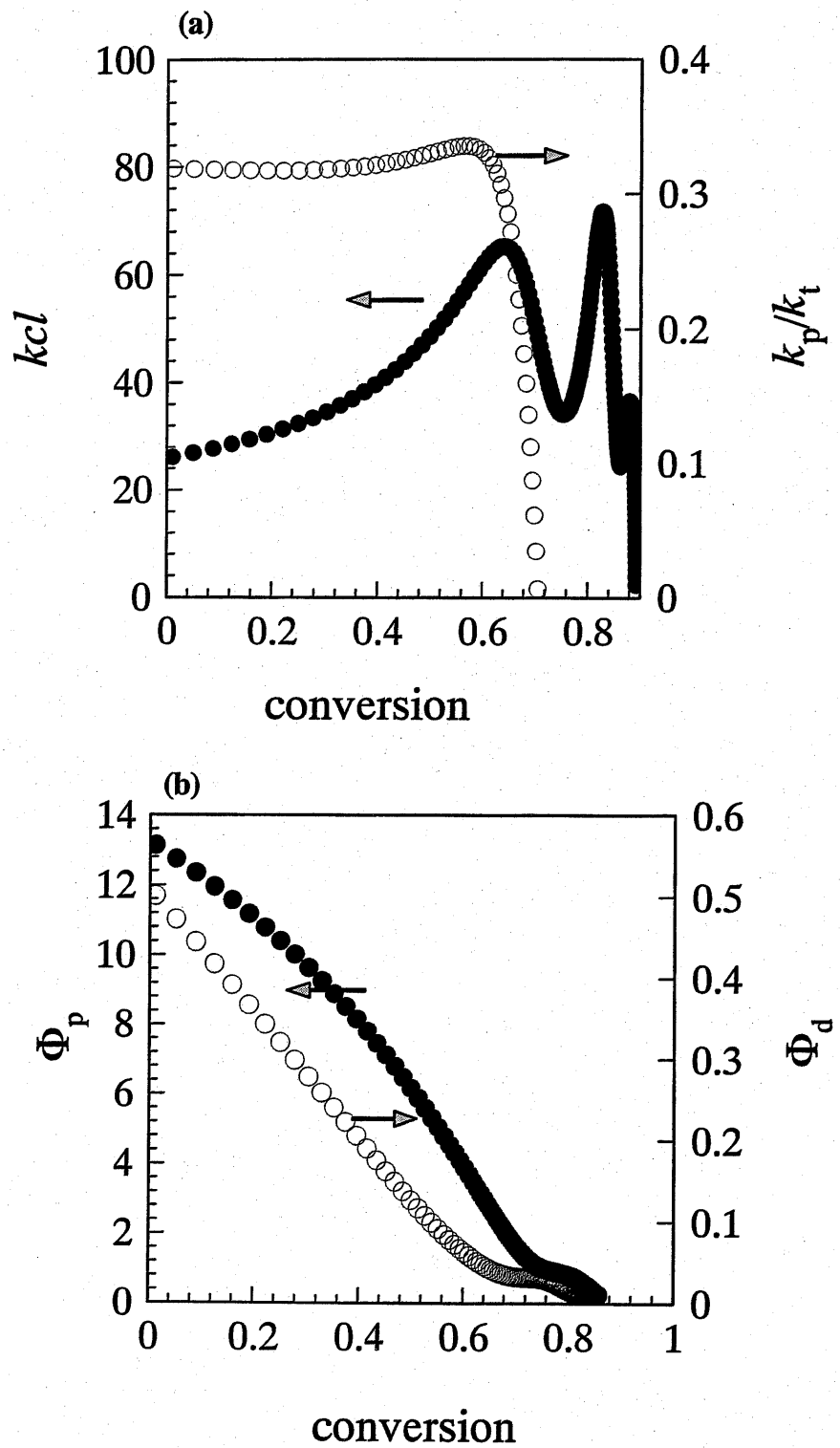

Figure 3-9. Dependence of *kcl* and k_p/k_t (a), and Φ_p and Φ_d (b) on conversion in the photopolymerization of BzTD initiated by PMS in poly(BzTD) matrix.

As is seen in Eq. (11), *kcl* is simply determined by the ratio of [M] to [PMS] and the observed tendency of increasing *kcl* with conversion does not imply any gel effect at all, but it is the result of relatively faster decrease of [PMS] than that of [M]. The value of kcl obtained in this study is in the order of 20~60 and this value is much smaller than those reported by Decker.[19] He reported *kcl* as large as 2000 to 10000 in polyurethane-acrylate photopolymerization system. This difference may be due to the difference in the diffusion coefficients of the monomers in both systems. In our system the monomer diffusion is restricted and only limited numbers of monomer molecules are available in the polymerization loci, so that it gives relatively very small values of *kcl*. Decker and Moussa[20] also studied the post-polymerization processes of above mentioned system and found k_p/k_t values are in the order of 0.2 to 0.37 and these are in good agreement with our value, 0.32, although they postulated a bimolecular termination process for their system. Reaction diffusion process,[36-45] which is frequently observed in polymerization in highly crosslinked system, predicts the following relationship:

$$k_t = R k_p [M]$$

where R is the reaction diffusion parameter, [M] is the concentration of monomer. If such reaction diffusion is the dominant termination process, values of k_p/k_t should not be constant in the polymerization process. The result obtained here indicates that reaction diffusion is not the dominant termination process in the polymerization of the styrenyl monomer.

Quantum yield of photopolymerization,[19] Φ_p, was also calculated based on the equation shown below:

$$\Phi_p = \frac{number\ of\ photopolymerized\ monomer\ molecules}{number\ of\ photons\ absorbed}$$
$$= \frac{R_p}{I_a\,(einstein\,L^{-1}s^{-1})} \qquad (13)$$
$$= \frac{R_p \times \ell(cm)}{I_a\,(einstein\,cm^{-2}\,s^{-1}) \times 10^3}$$

The result is shown in Fig. 3-9(b) together with Φ_d calculated by Eq.(3). Φ_p decreased gradually with conversion and the maximum value is around 13, which is again much smaller than 4000 reported by Decker.[19] The maximum Φ_d value obtained in the presence of BzTD monomer was around 0.5 and this value is about 5-fold larger than that obtained in the absence of the monomer. Apparently, the monomer can enhance the photodecomposition efficiency by reacting with the initiator radical.

3-4. CONCLUSION

Photodecomposition rate of initiator was monitored concurrently with photopolymerization rate of monomer first time. Polymerization behavior was explained quite well in connection with the photodecomposition rate of the initiator. Monitoring of photodecomposition process of a bis(trichloromethyl)-1,3,5-triazine derivatives by RT-IR spectroscopy could be applied to various kinds of photopolymerization system including conventional acrylate monomers. This would give us a powerful tool to investigate the mechanisms of photopolymerization. In this article we studied the polymerization behavior of a newly developed styrenyl monomer and found very high reactivity of this monomer. Even in a dispersed phase in a polymer matrix, a solid-state photopolymerization proceeded rapidly and our interest is in clarifying the mechanism of polymerization processes for such particular systems.

In the present investigation it was found that both polymerization and photodecomposition rates depend linearly on monomer and initiator concentrations, respectively. The rate constant ratio, k_p/k_t was constant in the polymerization process and this indicates that reaction diffusion is not the dominant termination process.

These results indicate that the solid-state polymerization of the styrenyl monomer is essentially the same as conventional solution polymerizations except for unimolecular termination process.

REFERENCES

1. Scranton, A. B. ; Bowman, A. ; Peiffer, R. W., Eds.; Photopolymerization: Fundamentals and Applications, American Chem. Soc.,Washington DC, 1997.
2. Decker, C.; Fouassier, J. D. In Lasers in Polymer Science and Technology: Applications (III); Fouassier, J. D. ;Rabek, J. F., Eds.; CRC Press, Boca Raton, 1989, p.1.
3. Herting, H. P. ; Goodman, R. M. In Proceedings of the Technical Association of the Graphic Arts, TAGA 1998, TAGA, Rochester, New York, N. Y., p.312.
4. Li, B. ; Zhang, S. ; Tang, L. ; Zhou, Q., Polym. J. 2001, 33, 263.
5. Zhang, S. ; Li, B. ;Tang, L. ; Wang, X. ; Liu, D. ;Zhou, Q., Polymer, 2001, 42, 7575
6. Dietrich, R., DAS 1 298 414 (1969).
7. Bonham, J. A.; Petrellis, P. C., US patent 3,954,475 (1976).
8. Smith, G. H. ; Bonham, J. A., US patent 3,779,778 (1973).
9. Buhr, G. ; Dammel, R. ; Lindley, C. R., Polym. Mat. Sci. Eng., 1989, 61, 269.
10. MacDonald, S. A. ; McKean, D. R., J. Photopolym. Sci. Tech., 1990, 3, 375.
11. Pohlers, G. ; Scaiano,; Sinta, R. J. C., Chem. Mater., 1997, 9, 3222.
12. Pawlowski, G. ; Dammel, R., J. Photopolym. Sci. Tech., 1991, 4, 389.
13. Pohlers, G. ; Scaiano, J. C. ; Step, E. ; Sinta, R., J. Am. Chem. Soc., 1999, 121, 6167.
14. Frechet, J. M. J., Pure & Appl. Chem., 1992, 64, 1239
15. Grotzinger, C. ; Burget, D. ; Jacques, P. ; Fouassier, J. P., Macromol. Chem. Phys., 2001, 202, 3513.
16. Urano, T. ; Nagao, T. ; Takada, A. ;Itoh, H., Polym. Adv. Technol., 1999, 10, 244.
17. Decker, C. ; Moussa, K. , Makromol. Chem., 1988, 189, 2381.

18. Decker, C. ; Moussa, K. , Macromolecules. 1989, 22, 4455.

19. Decker, C., Macromolecules. 1990, 23, 5217.

20. Decker, C. ; Moussa, K. ,Eur. Polym. J., 1990, 26, 393.

21. Rodriguez, M. ; Garcia-Moreno, I. ; Garcia, O. ; Sastre, R., Macromol. Chem. Phys., 2000, 201, 1345.

22. Scherzer, T. ; Decker, U., Rad. Phys. Chem., 1999, 55, 615.

23. Scherzer, T. ; Decker, U., Polymer, 2000, 41, 7681.

24. Lecamp, L. ; Youssef, B. ; Bunel, C. ; Lebaudy, P., Polymer, 1997, 38, 6089.

25. Decker, C. ; Xuan, H. L. ; Viet, T. N. T., J. Polym. Sci. Part A. Polym. Chem., 1995, 33, 2759.

26. Decker, C. ; Viet, T. N. T., Macromol. Chem. Phys., 1999, 200, 358.

27. Mizuta, Y. ; Morishita, N. ; Kuwata, K., Appl. Magn. Reson., 2000, 19, 93.

28. Williams, R. M. ; Khudyakov, I. V. ; Purvis, M. B. ; Overton, B. J. ; Turro, N. J., J. Phys. Chem. B, 2000, 104, 10437.

29. For a general reference, Provder, T. ; Barth, H. G. ; Urban, M. W.,Eds. ; Chromatographic Characterization of Polymers, Am. Chem. Soc. Washington, DC.,1995.

30. ibid., Timpa, J. D., Chap.11. p.141.

31. Lew, R. ; Cheung, P. ; Balke, S. T. ; Mourey, T. H., J. Appl. Poly. Sci., 1993, 47, 1685.

32. Chen, M. H. ; Wyatt, P. J., Macromol. Symp., 1999, 140, 155.

33. Johann, C. ; Kilz, P., J. Appl. Polym. Sci. Appl. Polym. Symp., 1991, 48, 111

34. Harwood, H. J. ; Christov, L. ; Guo, M. M. ; Holland, T. V. ; Huckstep, A. Y. ; Jones, D. H. ; Medsker, R. E. ; Rinaldi, P. L. ; Saito, T. ; Tung, D. S., Macromol. Symp.,

1996, 111,25.

35. Barson, C. A. ; Bevington, J. C. ; Breuer, S. W., Polym. Bull., 1996, 36, 423.

36. Schulz, G. V., Z. Phys. Chem. (Munich), 1956, 8, 290.

37. Buback, M. ; Huckestein, B. ; Russel, G. T., Macromol. Chem. Phys., 1994, 195, 539.

38. Stickler, M., Macromol. Chem., 1983, 184, 2563.

39. Anseth, K. S. ; Anderson, K. J. ; Bowman, C. N., Macromol. Chem. Phys., 1996, 197, 833.

40. Lovell, L. G. ; Stansbury, J. W. ; Syrpes, D. C. ; Bowman, C. N., Macromolecules, 1999, 32, 3913.

41. Young, J. S. ; Bowman, C. N., ibid., 1999, 32, 6073.

42. Mateo, J. L. ; Serrano, J. ; Bosch, P., ibid., 1997, 30, 1285.

43. Bosch, P.; Serrano, J.; Mateo, J. L.; Guzman, J.; Calle, P.; Sieiro, C. J Polym Sci Part A. Polym Chem 1998, 36, 2785.

44. Mateo, J. L.; Calbo, M.; Bosch, P., ibid., 2001, 39, 2049.

45. Mateo, J. L.; Calbo, M.; Bosch, P., ibid., 2001, 39, 2444.

46. Mateo, J. L.; Calbo, M.; Bosch, P., ibid., 2002, 40, 120.

Chapter 4

Influence of monomer concentration in the solid-state photoinitiated polymerization of styrenyl compound bearing 1,3,4-thiadiazole group

4-1. INTRODUCTION

The highly photopolymerizabile styrenyl monomers bearing thiadiazole group have become the center of our research interests in the previous investigations described in Chapters 2 & 3. Their unique polymerization behaviors are considered to originate from molecular assembly caused by intermolecular interactions. Existence of monomer aggregates in polystyrene matrix was confirmed by transmission electron microscopy. The molecular orbital calculations based on the PM3 method led to a fairly large polarizabiloity for a typical styrenyl monomer as described in Chapter 2. Intermolecular interactions between the monomer molecules could rearrange the styrenyl groups facing to each other in favor of effective photopolymerization in the solid state. If such an assembled structure within monomer aggregates exists in the polymerization system, polymerization kinetics could be independent of initial monomer concentration. Under these situations, we planned to investigate the effect of monomer concentration on the polymerization of these thiadiazole-substituted styrene derivatives in solid state.

In Chapter 3, we described a new method using real-time FT-IR spectroscopy, which

enabled us to investigate the photodecomposition behavior of the photoinitiator, bis(trichloromethyl)-1,3,5-triazine derivatives. This powerful technique realized the real-time monitoring of both polymerization rate of monomer and photodecomposition rate of photoinitiator simultaneously *in situ* of photopolymerization system. Kinetic analysis based on such dual monitoring revealed a feature of steady-state polymerization. Kinetic chain length was found to be around 20 ~ 60. This result suggested that the possible assembled or preorganized structure might consist of such numbers of molecules. In this Chapter we investigated the effect of monomer concentration on the solid-state photopolymerization behavior and tried to clarify the possibility of the preorganized structure of these styrenyl compounds.

It should be noted that polymerization in ordered phase has been extensively conducted to obtain highly ordered polymeric materials. Polymerization in liquid crystalline phase[1-4] and topochemical polymerization[5-9] are both closely related to our present investigations. Furthermore, preorganization of monomer molecules suggested by Jansen, et al.[10,11] is closely related to the present investigation.

4-2. EXPERIMENTAL

Materials

2-(4'-methoxystyryl)-4,6-bis(trichloromethyl)-1,3,5-triazine (PMS) was purchased from Panchim (Cedex, France) and used without further purification. Other chemicals were described in Chapter 2.

Photopolymerization

Photopolymerization of the styrene derivatives was carried out in the matrix of solid

polymer and followed up to high monomer conversion by Fourier transform real-time infrared (RT-IR) [8, 14-17] spectroscopy, which was conducted on a Bio-rad FTS-40 (Bio-rad Laboratories, Inc., Hercules, CA) with an operating/analysis software, Win-IR.

Monomer conversion was calculated according to the following equation:

$$conversion = \frac{A(990)_0 - A(990)_t}{A(990)_0}$$

in which $A(990)_0$ and $A(990)_t$ denote the peak absorbance at 990 cm^{-1} before UV-irradiation and at time t (s), respectively. The rate of polymerization, R_p, was calculated from the following equation;

$$R_p\,(mol\,l^{-1}\,s^{-1}) = -\frac{d[M]}{dt} = [M]_0 \frac{d(conversion)}{dt}$$

Since measured peak intensity at 990 cm^{-1} were somewhat scattered with time, the calculated value of R_p from the slope of time-conversion curve at an arbitrary time interval scattered significantly. 10th-order polynominal approximation was applied to all time-conversion curves and the polynominal curve fit was differentiated to obtain R_p at an arbitrary polymerization time.

4-3. RESULTS AND DISCUSSION

4-3-1.Effect of initial monomer concentration on rate of polymerization

In Figure 4-1 (a), time-conversion curves for the photopolymerization of BzTD initiated by PMS with various initial monomer concentrations were plotted. As the initial monomer concentration decreased, time-conversion curves tended to shift upward. Rate of polymerization was calculated from the differential of curve-fit for each time-conversion curve and plotted against conversion as shown in Fig. 4-1(b). In all cases of initial monomer concentrations, R_p was found to decrease linearly with

conversion. Both the slope and intercept to R_p axis of the linear plot increased with the initial monomer concentration. The linear dependence of R_p on monomer conversion suggests the constant concentration of propagating radical in the steady-state polymerization as expressed by eq. (5);

$$R_p = k_p[P\cdot]([M]-C_m) \qquad (5)$$

where k_p designates the propagation rate constant, [P·], the concentration of propagating radical and [M], monomer concentration. C_m denotes the residual monomer concentration. From the slope of R_p vs. conversion plot in Fig. 4-1(b), (slope = $-k_p[P\cdot][M]_0$), values of $k_p[P\cdot]$ in the polymerization were calculated and dependence of these values on the initial monomer concentration was shown in Fig. 4-2(a). Thus obtained values of $k_p[P\cdot]$ are around 0.036 (s^{-1}) and independent on the initial monomer concentration. This result strongly suggests that concentration of propagating radical is independent on initial monomer concentration and also propagation rate constant, k_p, is independent on monomer concentration. On the other hand, from the intercept of R_p vs. conversion plot at conversion = 0, R_{p0} (initial rate of polymerization) is obtained and this value should be equal to $k_p[P\cdot]([M]_0 - C_m)$ from eq.(5). Thus, R_{p0} was plotted against $([M]_0 - C_m)$ and result is shown in Fig. 4-2(b). In this Fig., linear relationship between R_{p0} and $([M]_0 - C_m)$ was obtained and from the slope of this linear relationship $k_p[P\cdot]$ was found to be 0.036 (s^{-1}), which agreed well to the previously obtained value. From these results it is certain that both k_p and [P·] are independent on initial monomer concentration and both are constants throughout the polymerization.

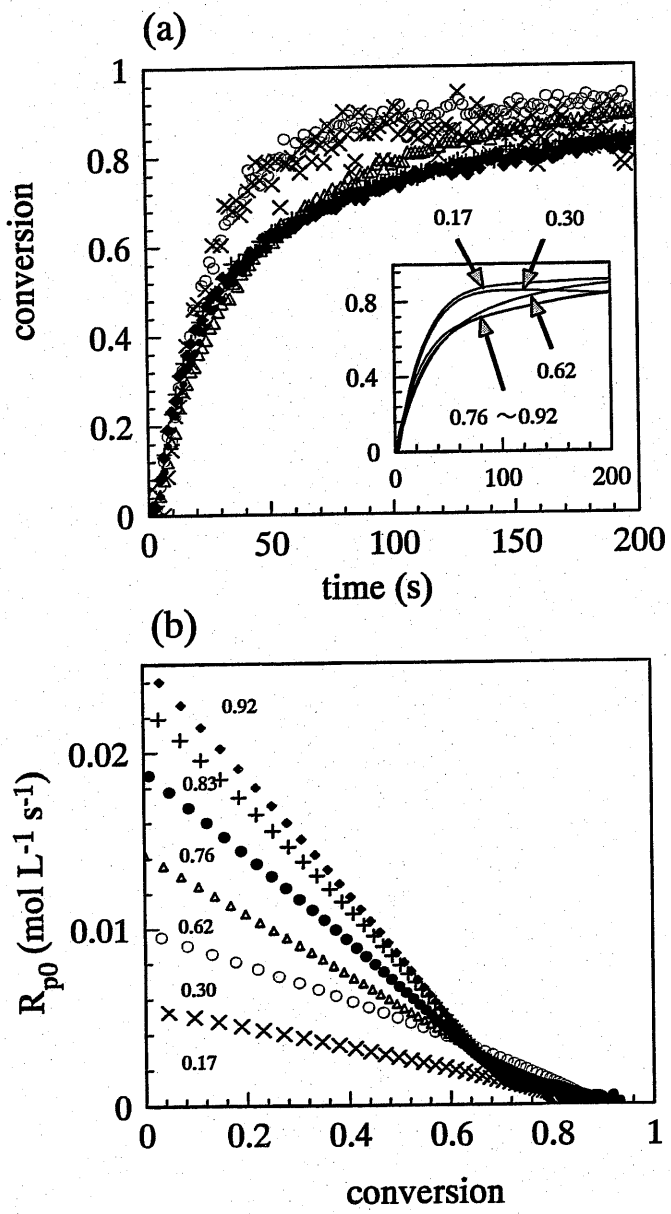

Figure 4-1. Effect of initial monomer concentration on the photopolymerization rate of BzTD in poly(BzTD) matrix initiated by PMS. Time-conversion curves (a) and R_p *vs.* conversion curves (b). The inset in (a) shows curve fits to the experimental data points. Figures indicated with arrows shows initial monomer concentrations in mol·L^{-1}. The incident light intensity = 5×10^{-9} einstein cm^{-2} s^{-1}. poly(BzTD) = 0.2 g (fixed) and PMS = 0.0042 g (fixed). BzTD = 0.013 g (×), 0.024 g (o), 0.057 g (Δ), 0.076 g (•), 0.086 g (+), and 0.10 g (*).

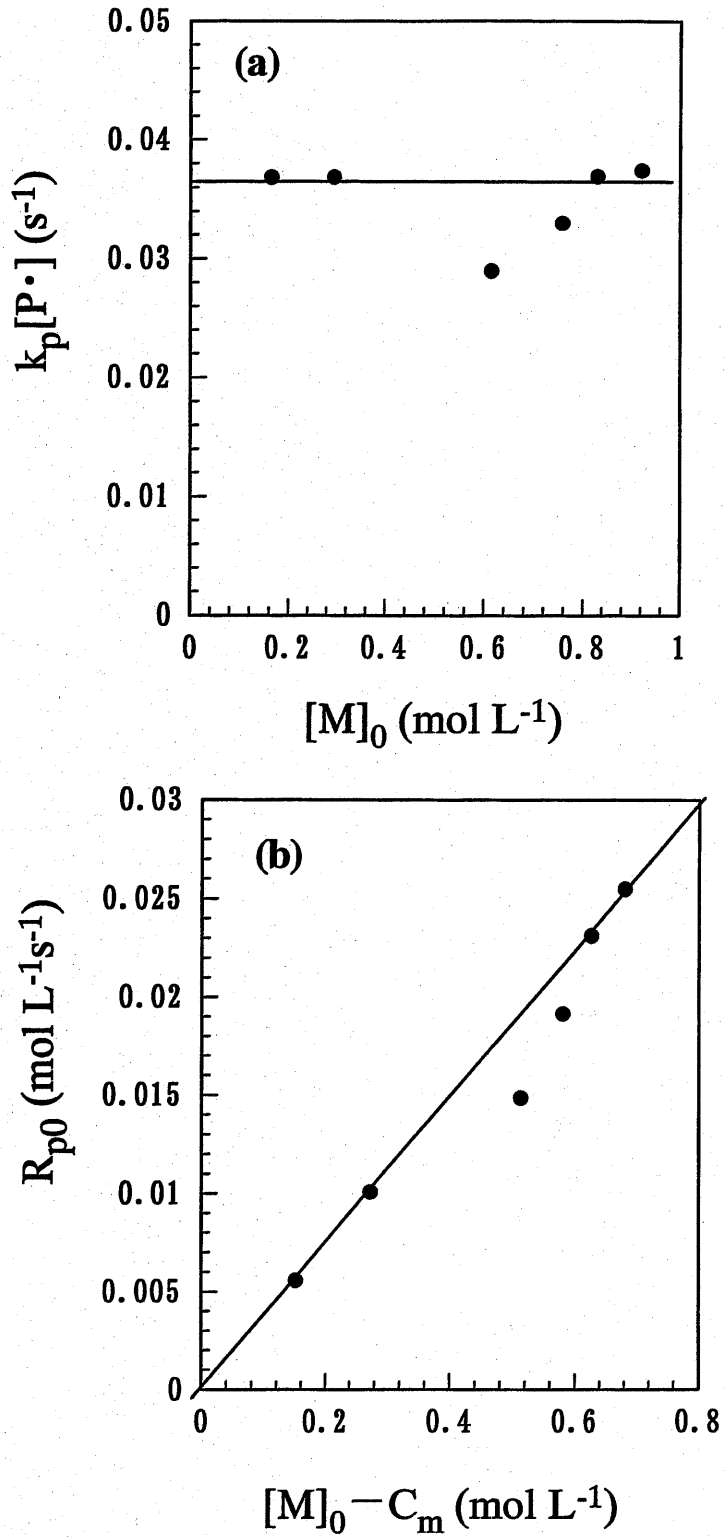

Figure 4-2. Values of $k_p[P\cdot]$ obtained for different initial monomer concentrations (a) and R_{p0} vs. $[M]_0 - C_m$ plot (b).

4-3-2.Effect of initial monomer concentration on residual monomer concentration

As for the residual monomer concentration, C_m defined in eq. (5), it was found that C_m can be related to the square of the initial monomer concentration and as shown in Fig. 4-3, a good correlation between C_m and $[M]_0^2$ was obtained. From this linear plot, the relationship between C_m and $[M]_0$ was found to be $C_m = 0.29[M]_0^2$. By integrating eq. (5), decrease of monomer concentration with time in the course of the photopolymerization is well expressed by the following equation.

$$\begin{aligned}\frac{[M]}{[M]_0} &= 0.29[M]_0 + (1-0.29[M]_0)\exp(-k_p[P\cdot]t) \\ &= 0.29[M]_0 + (1-0.29[M]_0)\exp(-0.036t)\end{aligned} \qquad (6)$$

In the above equation, the relative monomer concentration to initial monomer concentration is divided into two terms. The first term appears in eq. (6) implies that about 30 % of initial monomer concentration is unreactive toward photopolymerization. The second term in eq. (6) indicates that the rest of monomer is consumed with an ideal behavior as expected in steady state polymerization. The reason why 30 % of initial monomer is left from the polymerization is unknown and this ratio seems to be pre-determined before polymerization starts. As described later in this chapter, we considered that monomer molecules might be assembled in cluster structures and polymerization proceeds inside such clusters. The unreactive monomer molecules might be those distributed outside the clusters and mutual intermolecular distance between those expelled monomer molecules could inhibit the progress of effective polymerization.

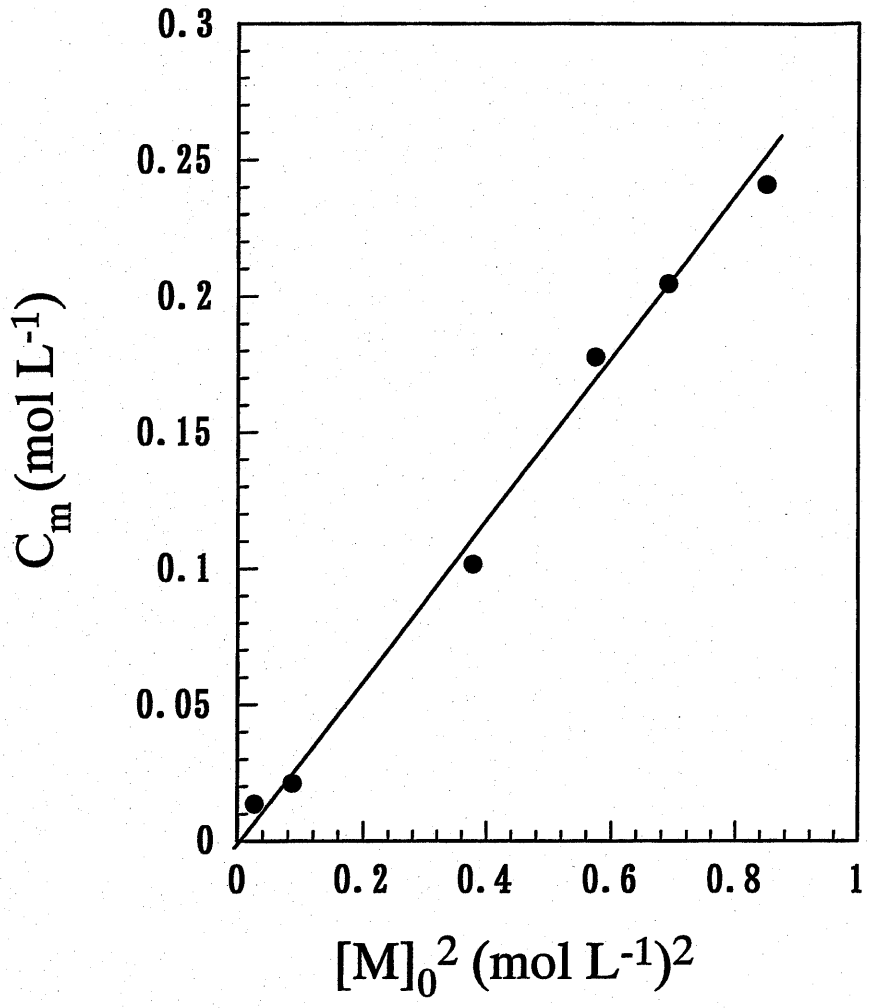

Figure 4-3. Relationship between the residual monomer concentration, C_m, and $[M]_0^2$.

4-3-3. Effect of initial monomer concentration on photodecomposition rate of photoinitiator

During the RT-IR observation of monomer consumption in polymerization process, concentration change of the photoinitiator, PMS, was also monitored at the absorption band of 1171 cm^{-1} which is assigned to a coupled asymmetrical stretching vibration of two CCl_3 groups attached to 1,3,5-triazine ring. The decomposition ratio (*DR*) of PMS was plotted against polymerization time as shown in Figure 4-4(a). The initial decomposition rate of PMS (R_{d0}) was calculated from the initial slope of the curve fit of experimental data points in the time *vs. DR* plot, and the results are summarized in Fig. 4-4(b). R_{d0} was found to be essentially independent on the initial monomer concentration and are in the order of 8 (± 1) × 10^{-4} $mol \cdot L^{-1} \cdot s^{-1}$, while the values of R_{p0} are around 1 × 10^{-2} $mol \cdot L^{-1} \cdot s^{-1}$, which are about one order larger than R_{d0}. The rate of monomer consumption is actually the sum of the rate of polymerization and the rate of initiation. If the initiation reaction proceeds faster than the photodecomposition rate (R_d), then initiation rate should be equal to R_d. Then, in order to obtain the actual rate of polymerization, it is necessary to subtract R_d from R_p. However, since the difference between R_d from R_p are enough large and subtraction of R_d from the previously obtained results of R_p did not affect so much, we neglected the contribution of R_d in obtaining R_p from the overall rate of monomer consumption.

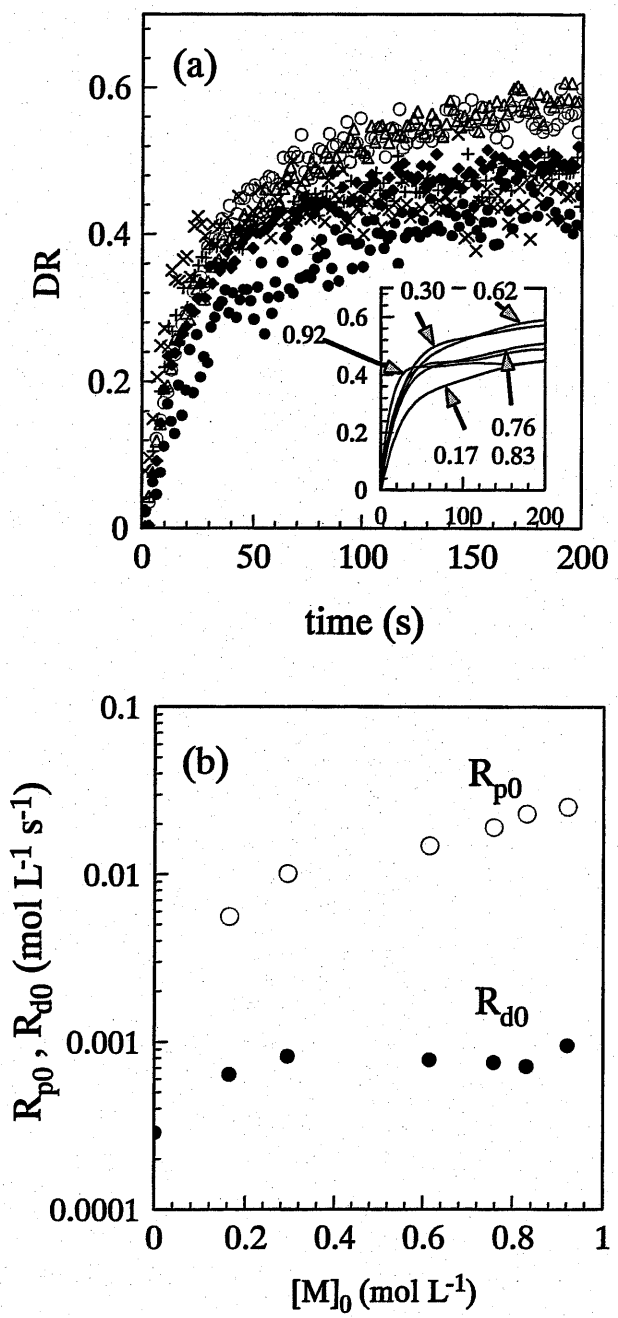

Figure 4-4. Effects of initial monomer concentrations on the photodecomposition rate of PMS during the photopolymerization of BzTD in poly(BzTD) matrix. Time-decomposition ratio (*DR*) curves (a) and dependences of R_{p0} and R_{d0} on the initial monomer concentration (b). The inset in (a) shows curve fits to the experimental data points. Figures indicated with arrows shows initial monomer concentrations in mol·L^{-1}.

4-3-4.Effect of initial monomer concentration on quantum yields of polymerization and photodecomposition of initiator

Quantum yields of polymerization (Φ_p) and photodecomposition of PMS (Φ_d) were calculated according to the equations (3) and (4):

$$\Phi_p = \frac{number\ of\ photopolymerized\ monomer\ molecules}{number\ of\ photons\ absorbed} = \frac{R_p}{I_a\ (einstein\,L^{-1}s^{-1})} = \frac{R_p \times \ell(cm)}{I_a\ (einstein\,cm^{-2}\,s^{-1}) \times 10^3} \quad (3)$$

$$\Phi_d = \frac{number\ of\ photodecomposed\ PMS\ molecules}{number\ of\ photons\ absorbed} = \frac{R_d}{I_a\ (einstein\,L^{-1}s^{-1})} = \frac{R_d \times \ell(cm)}{I_a\ (einstein\,cm^{-2}\,s^{-1}) \times 10^3} \quad (4)$$

in which the light intensity absorbed by the sample, I_a, is expressed by the following equation:

$$I_a = I_0 \times (1 - \exp(-2.3\,\varepsilon\,\ell[PMS])) \quad (5)$$

where I_0 denotes the incident light intensity of UV-irradiation, l is the thickness of polystyrene film and ε is the absorption coefficient of PMS in polystyrene matrix at 365 nm. In these polymerization conditions, about 60 % of the incident light was absorbed by the sample. The initial quantum yield of polymerization, Φ_{p0}, which was determined from the initial rate or polymerization according to Eq. (3), was found to increase linearly with the initial monomer concentration as shown in Figure 4-5(a). The initial

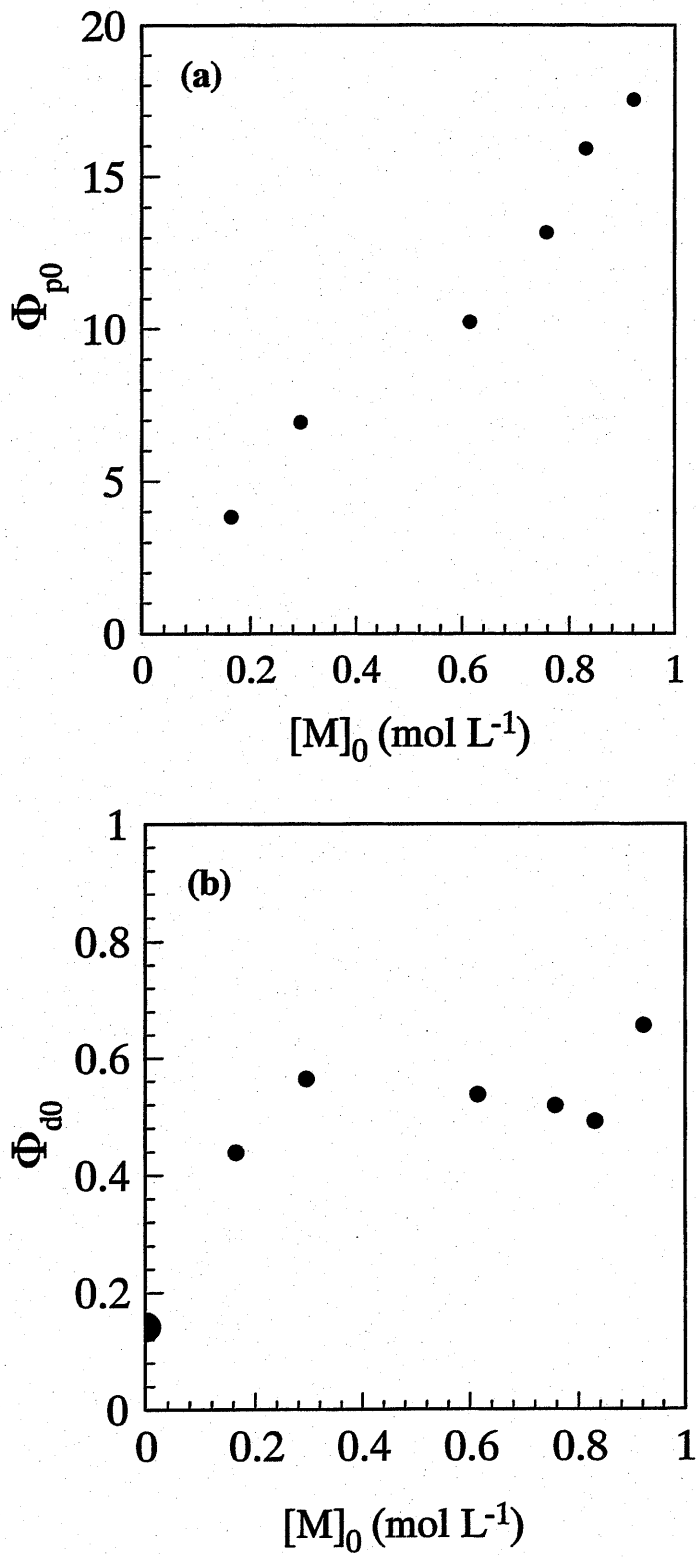

Figure 4-5. Dependence of Φ_{p0} (a) and Φ_{d0} (b) on the initial monomer concentration.

quantum yield of PMS photodecomposition, Φ_{d0}, was also plotted against the initial monomer concentration as shown in Figure 4-5(b). In the absence of monomer, Φ_{d0} was around 0.1 and this value was increased by ca. 5-fold in the presence of monomer. However, Φ_{d0} is almost independent on the initial monomer concentration and is in the range of 0.5 ± 0.1. Since the concentration of propagating radical and the quantum yield of photodecomposition were both found to be independent on the monomer concentration, the quantum yield of polymerization should be proportional to the number of monomer molecules available for the polymerization initiated by one initiating radical in each polymerization system. In other words, in each polymerization condition, monomer molecules might be assembled inside the cluster structure and these clusters would be consisted of the number of molecules which is proportional to the value of quantum yield of polymerization. On the contrary, if the monomer molecules are randomly distributed in the polymerization system, average intermolecular distance between monomer molecules should be inversely related to the volume fraction of the total monomer molecules in the system; i. e., average intermolecular distance $\propto [M]^{-1/3}$.[12]

. In the present polymerization condition, diffusion of monomer molecule is restricted due to the high melting point of the monomer (103°C), although T_g of the polymerization system is below a room temperature (–2.5 °C). Each monomer molecule should be fixed in the rubbery polymer matrix and as the volume fraction decreased, the average distance between monomer molecules should increase and polymerization would stop when there is no monomer molecules found in the vicinity of propagating radical. In such a situation propagating rate constant, k_p, would decrease with the decrease of monomer concentration and quantum yield of polymerization cannot be

proportional to the monomer concentration. However, the results obtained here are contrary to the expectation derived from random distribution of monomer molecules and would support the possibility of cluster structure of the monomer molecules.

4-3-5. Kinetic analysis on the polymerization system

As described in Chapter 3, a set of possible elementary steps are again summarized in Scheme 4-1. In this scheme, PMS· denotes the initiating radical produced by photodecopmposition of PMS and P· represents both the propagating polymer radical and the monomer radical produced by the addition of initiating radical. In this kinetic model, the reactivities of both polymer and monomer radicals are assumed to be the same and these two entities are not distinguished. D represents dead-polymer produced by the termination reaction between the propagating radical and the remaining PMS molecule. The rate constants, k, k_i, k_t and k_{tr} represent decay constant of photoinitiator, initiation rate constant, termination rate constant and chain transfer rate constant, respectively.

Scheme 4-1

Photodecomposition :	$PMS \rightarrow PMS\bullet + Cl\bullet$	$:R_d = kI_0[PMS]$
Initiation :	$PMS\bullet + M \rightarrow P\bullet$	$:R_i = k_i[PMS\bullet][M]$
Propagation :	$P\bullet + M \rightarrow P\bullet$	$:R_p = k_p[P\bullet][M]$
Termination :	$P\bullet + PMS \rightarrow D$	$:R_t = k_t[P\bullet][PMS]$
Chain Transfer :	$P\bullet + PMS \rightarrow D + PMS\bullet$	$:R_{tr} = k_{tr}[P\bullet][PMS]$
2nd Initiation:	$Cl\bullet + M \rightarrow P\bullet$	
Abstraction :	$Cl\bullet + RH \rightarrow R\bullet + HCl$	
3rd Initiation:	$R\bullet + M \rightarrow P\bullet$	

Based on the elementally steps shown in Scheme 4-1 and with an assumption of a steady-state condition for every intermediate radical species, the following equations can easily be derived.

$$[P\cdot] = \frac{2R_d}{k_t([PMS]-C_f)} = \frac{2kI_0}{k_t} \qquad (6)$$

$$[PMS\cdot] = \left(1+\frac{2k_{tr}}{k_t}\right)\frac{kI_0}{k_i}\frac{[PMS]-C_f}{[M]-C_m} \qquad (7)$$

$$R_p = \frac{2k_pkI_0}{k_t}([M]-C_m) \qquad (8)$$

$$kcl \equiv \frac{R_p}{R_i} = \frac{R_p}{R_d} = \frac{2k_p}{k_t}\frac{[M]-C_m}{[PMS]-C_f} \qquad (9)$$

where *kcl* indicates the *k*inetic *c*hain *l*ength which is defined as the number of monomer molecules polymerized by one initiating radical.

Among the above equations, *kcl* is one of the most useful kinetic parameters to correlate the polymerization rate with the decomposition rate of photoinitiator. Dependence of initial *kcl* value on the initial monomer concentration was determined by using Eq. (9), ($kcl_0 = R_{p0}/R_{d0}$), and is shown in Figure 4-6(a). The initial *kcl* value was found to be linearly dependent of the initial monomer concentration. It is interesting to observe the change of this parameter in the course of the photopolymerization process and *kcl* was plotted against conversion for the various initial monomer concentrations, as shown in Fig. 4-6(b). When the initial monomer concentration was 0.3 $molL^{-1}$ or lower, *kcl* was constant throughout the polymerization process. As the initial monomer concentration increases, *kcl* tends to increase with conversion and at the highest initial

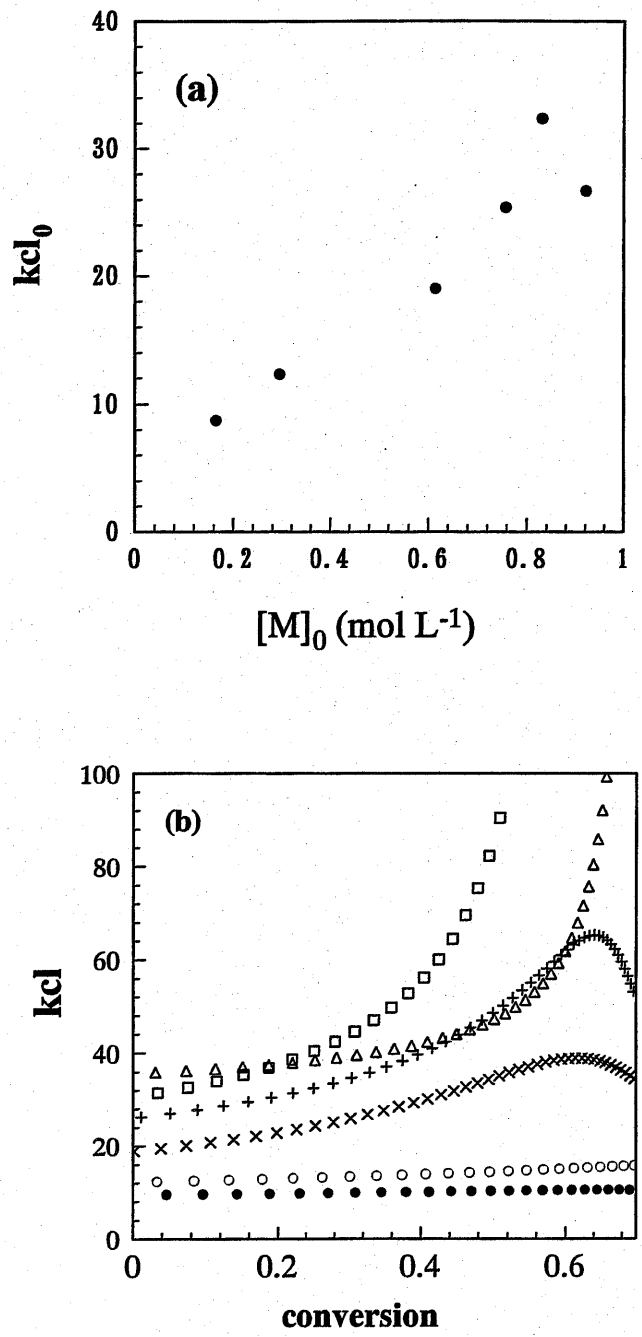

Figure 4-6. Dependence of initial *kcl* value on the initial monomer concentration (a) and change of *kcl* in the polymerization process (b): the initial monomer concentrations ($molL^{-1}$); (⊛)0.92, (Δ)0.83, (+)0.76, (×)0.62, (o)0.30, (•)0.17.

monomer concentration (= 0.92 molL^{-1}), *kcl* increased steeply with conversion. This observed tendency was simply due to the fast decrease in PMS concentration during the photopolymerization. However, at relatively high monomer concentration, domain structure might be inter-connected to give higher value of *kcl*. In the early stage of the photopolymerization (conversion up to 0.2), *kcl* is virtually independent of conversion and this implies that the number of photopolymerizable monomer molecules per one initiating radical species is only dependent on the initial monomer concentration and a possible domain structure of monomer molecules should be pre-organized before the polymerization is initiated.

It should be noted that the number of photopolymerizable monomer molecules per one initiating radical is also determined by the ratio of k_p/k_t as indicated in Eq. (9). This ratio of k_p/k_t was calculated according to Eq.(9) and plotted against the initial monomer concentration. Figure 4-7 shows the result and the ratio of k_p/k_t was found to be independent of the initial monomer concentration and agreed well with the result obtained in Chapter 3. Reaction diffusion mechanism, [13-23] which predicts k_p/k_t inversely depends on [M], does not dominate the termination process. This result suggests that the PMS molecules, which act as both photoinitiator and terminating agent, are uniformly distributed in the polymerization system. In Figure 4-8, the postulated domain structure of monomer molecules is schematically illustrated. Clusters of monomer molecules are considered to be distributed evenly in the polymer matrix and the size of such clusters are considered to be linearly dependent of monomer concentration. As the monomer concentration increases, the size of the cluster would increase. When polymerization starts inside each cluster, polymerization proceeds until it is terminated by the PMS molecule which may exist inside or near the cluster. If each cluster contains one PMS

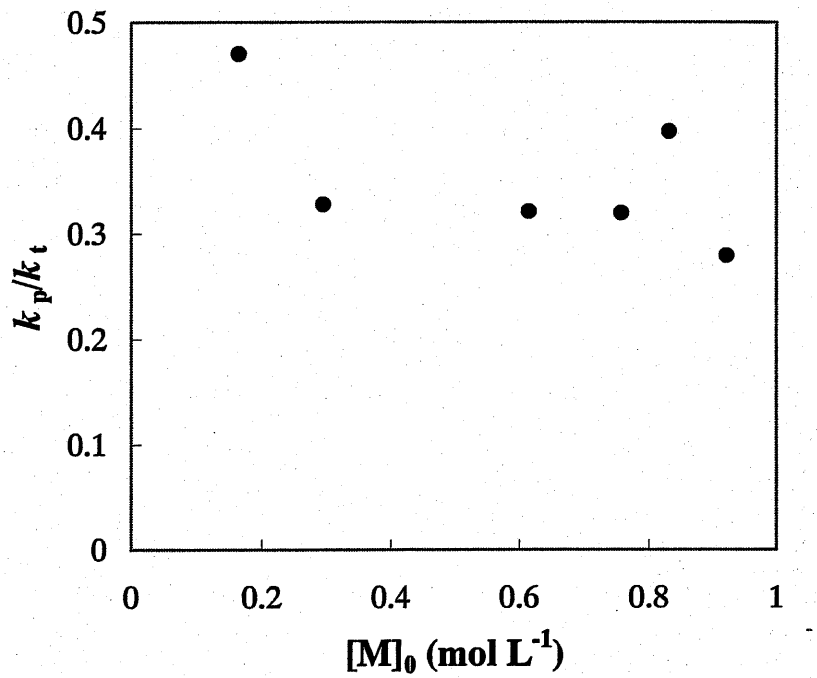

Figure 4-7. Dependence of k_p/k_t on the initial monomer concentration.

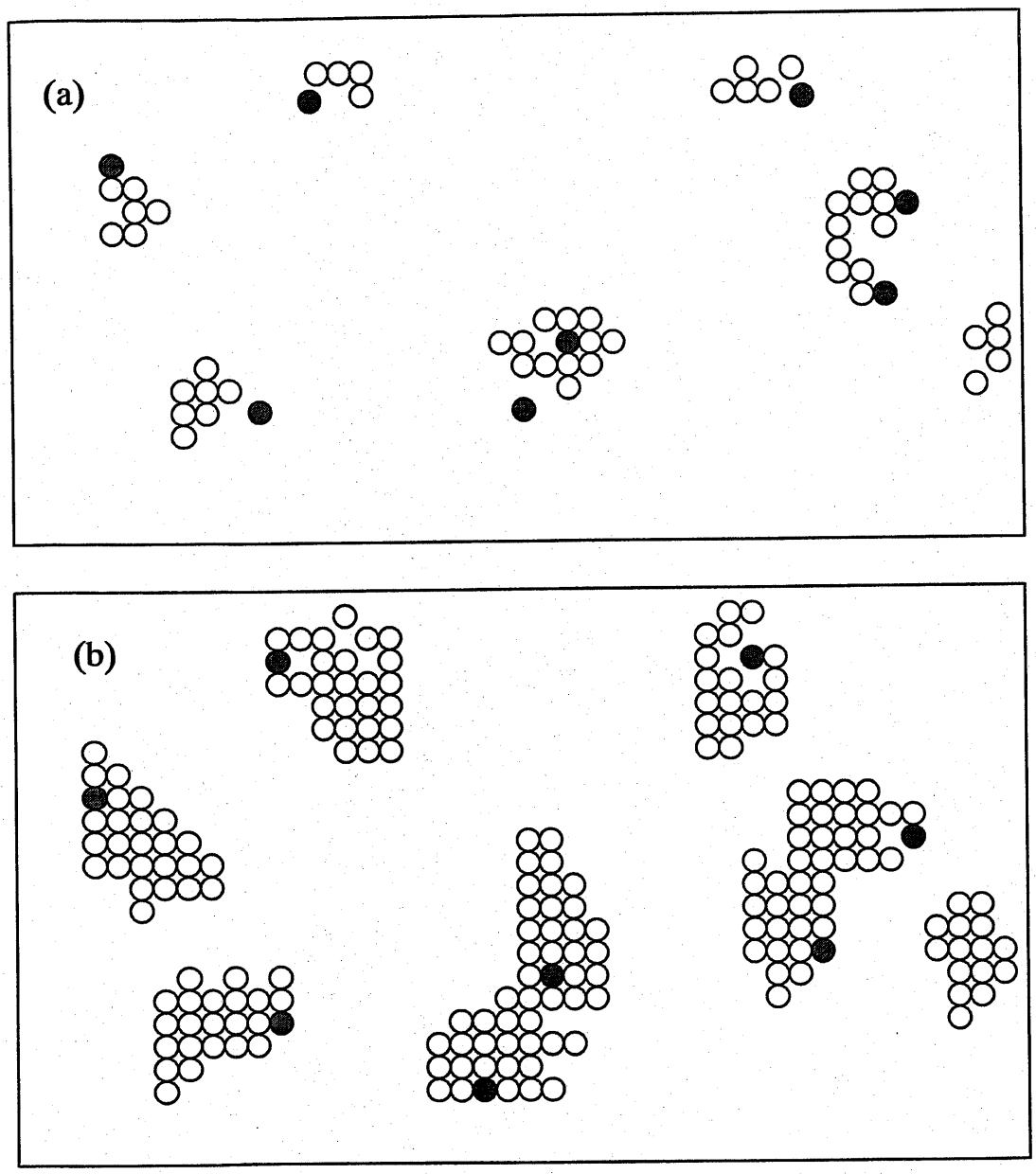

Figure 4-8. Schematic illustrations showing possible domain structures of monomer molecules at low monomer concentration (a) and at high monomer concentration (b). Filled circles indicate PMS molecules and open circles monomer molecules.

molecule in an average as illustrated in this figure, *kcl* value and the number of monomer molecules inside the cluster would be the same. However, if each cluster contains plural numbers of PMS molecules, then the actual size of such cluster must be larger than that expected from *kcl* value. In such a speculation, the size of the cluster estimated by the *kcl* value must be the minimum number of monomer molecules inside the cluster. If we reduce the initial concentration of PMS, *kcl* value would increase and would finally reach a maximum value which must correspond to the number of monomer molecules in the cluster. Therefore, in order to verify the validity of such speculation, we must carry out similar experiments with various concentrations of PMS and the results will be described in Chapter 5.

4-3-6. Polymerization of C1TD in polystyrene matrix

Comparative experiments were carried out to investigate the possibility of cluster structure and its effects on polymerization behavior for these thiadiazole-substituted styrenyl monomers in polymer matrix. The effects of initial monomer concentration on $k_p[P\cdot]$ and initial polymerization rate were summarized in Figure 4-9. Although $k_p[P\cdot]$ was found to decrease slightly as the initial monomer concentration decreases, polymerization rate was relatively insensitive to the initial monomer concentration as in the case of previously discussed polymerization system of BzTD in poly(BzTD) matrix. Linear dependence of initial polymerization rate, R_{p0} on $[M]_0 - C_m$ also indicates the steady-state polymerization and the applicability of the same polymerization kinetics described in the previous section 4-3-1 and 4-3-5. Decomposition rate of PMS was also monitored and values of kcl_0 were found to increase linearly with the initial monomer concentration as shown in Figure 4-10(a). The ratio of k_p/k_t decreased slightly with

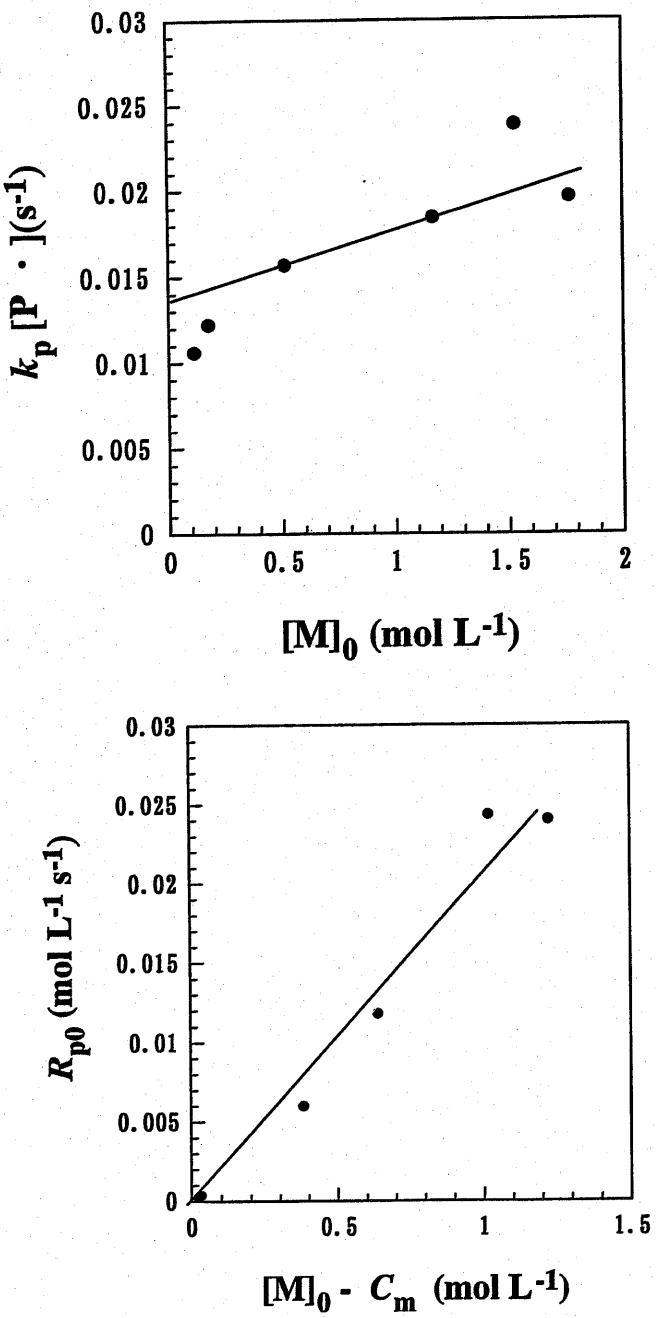

Figure 4-9. Values of k_p[P·] obtained for different initial monomer concentrations (a) and R_{p0} vs. $[M]_0 - C_m$ plot (b) for the polymerization of C1TD in polystyrene matrix initiated by PMS.

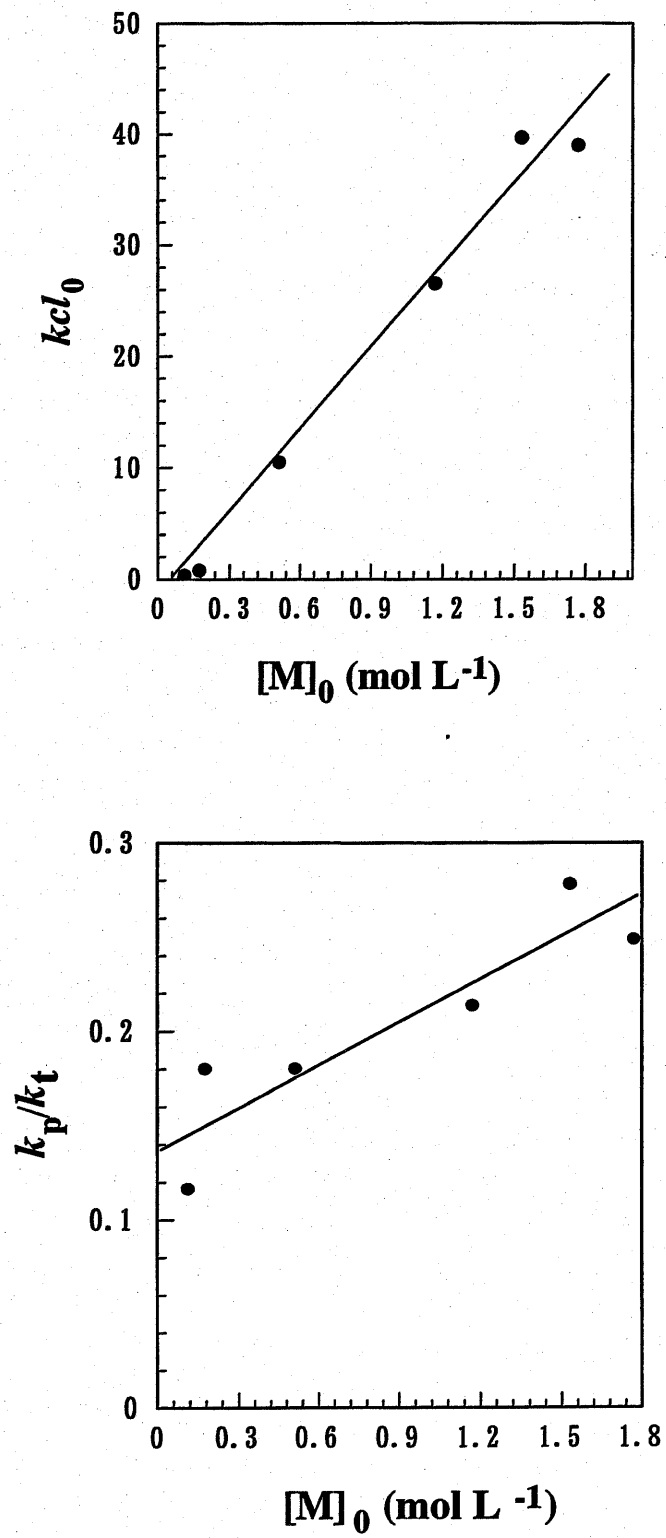

Figure 4-10. Dependence of initial *kcl* value (a) and k_p/k_t (b) on the initial monomer concentration.

the initial monomer concentration (Figure 4-10(b)). In consideration of the extent of the experimental errors, these results suggest that the polymerization of C1TD in polystyrene matrix is virtually unaffected to the initial monomer concentration and polymerization must progress inside the clusters of monomer aggregates also in this case.

GPC analysis of the photopolymerized system was carried out to confirm the validity of the kinetically estimated *kcl* value. In the polymerization process, *kcl* was calculated from the ratio of R_p to R_d as indicated by Eq. (9) and if chain transfer reaction is neglected, *kcl* should be equal to the degree of polymerization (*DP*). Each mole fraction of polymer chain which consists of *kcl* value of *DP* was calculated and plotted as shown in Figure 4-11. The calculated number average *DP* was 66.5. On the other hand, after the photopolymerization of C1TD in polystyrene matrix, the whole system was dissolved in THF and GPC analysis was carried out. The produced poly(C1TD) was selectively detected by UV absorption at 320 nm at which wavelength polystyrene do not show any detectable absorbance. The obtained GPC curve was shown together with that of polystyrene matrix in Figure 4-12. From this GPC analysis molecular weight of poly(C1TD) was found to be that M_w = 82000, M_n = 19000, number average *DP* = 68, which is very close to the value obtained above (66.5).

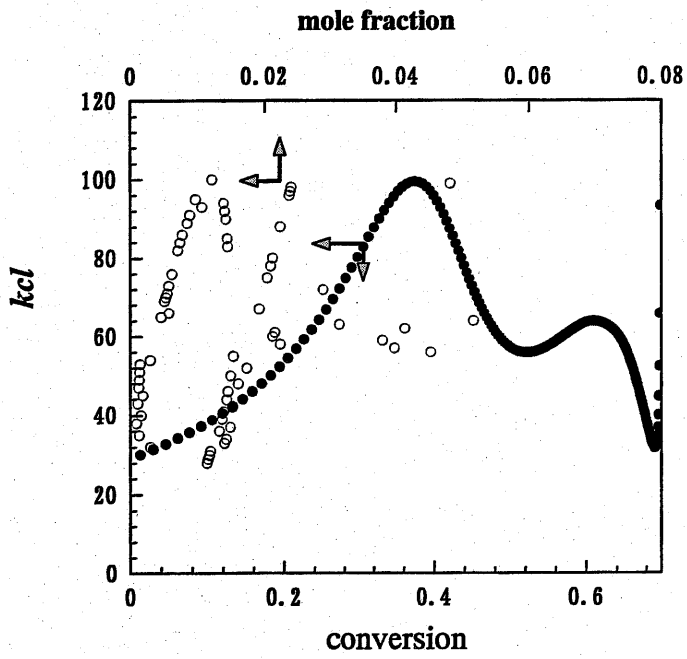

Figure 4-11. Dependence of *kcl* on conversion and mole fraction of each *kcl* fraction for the polymerization of C1TD in polystyrene matrix: C1TD/polystyrene/PMS = 0.1/0.2/0.0042 (wt/wt/wt).

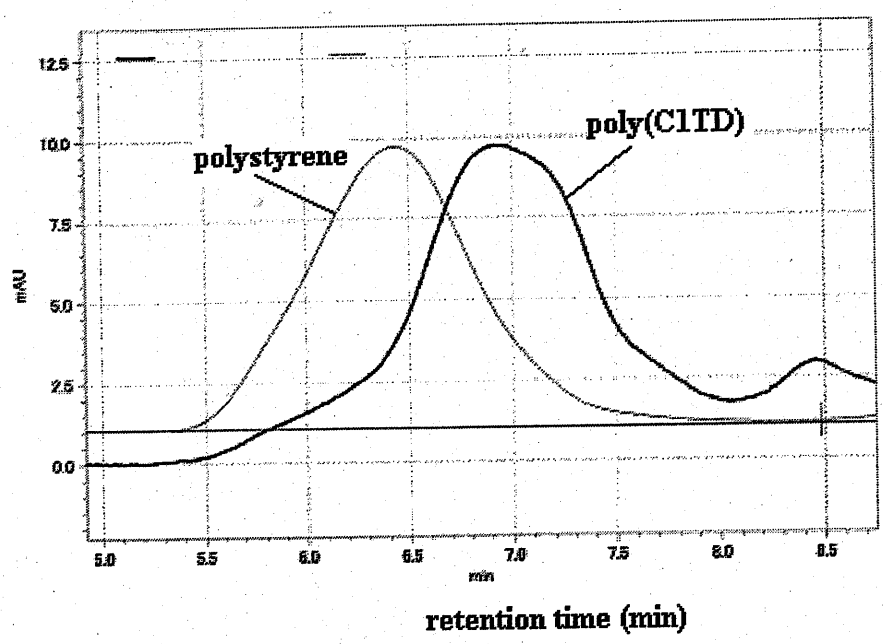

Figure 4-12. GPC analysis of poly(C1TD) obtained after photopolymerization of C1TD in polystyrene matrix. GPC curve for poly(C1TD) was obtained by monitoring UV absorbance at 320 nm. Polymerization condition was the same as that in figure 4-11.

4-3-7. Polymerization of TMPTA in poly(MMA)

Another comparative experiment was carried by using TMPTA as a typical acrylic monomer which should be completely miscible in poly(MMA) matrix and no possibility of cluster formation was anticipated in this case. When the initial monomer concentration was varied systematically, the observed rate of polymerization was changed as shown in Figure 4-13. The observed maximum rate of polymerization decreased drastically with the decrease in initial monomer concentration and at less than *ca.* 0.5 $mol \cdot L^{-1}$ of the initial monomer concentrations, polymerization seems not to proceed. As is seen in Figure 4-13(c), values of $k_p[P\cdot]$ also decrease with the decrease in initial monomer concentration. This result is contrasting to those obtained in the figures 4-2 and 4-9. In the present case, each monomer molecule should be fixed in the glassy polymer matrix and as the volume fraction decreased, the average distance between TMPTA molecules should increase and polymerization would stop when there are no monomer molecules found in the vicinity of propagating radical. In such a situation propagating rate constant, k_p, would decrease with the decrease of monomer concentration.

When compared with the previously obtained results on the effects of initial monomer concentration, it is apparent that thiadiazole-substituted styrenyl monomers behave quite differently from TMPTA and this might be due to the formation of cluster structures.

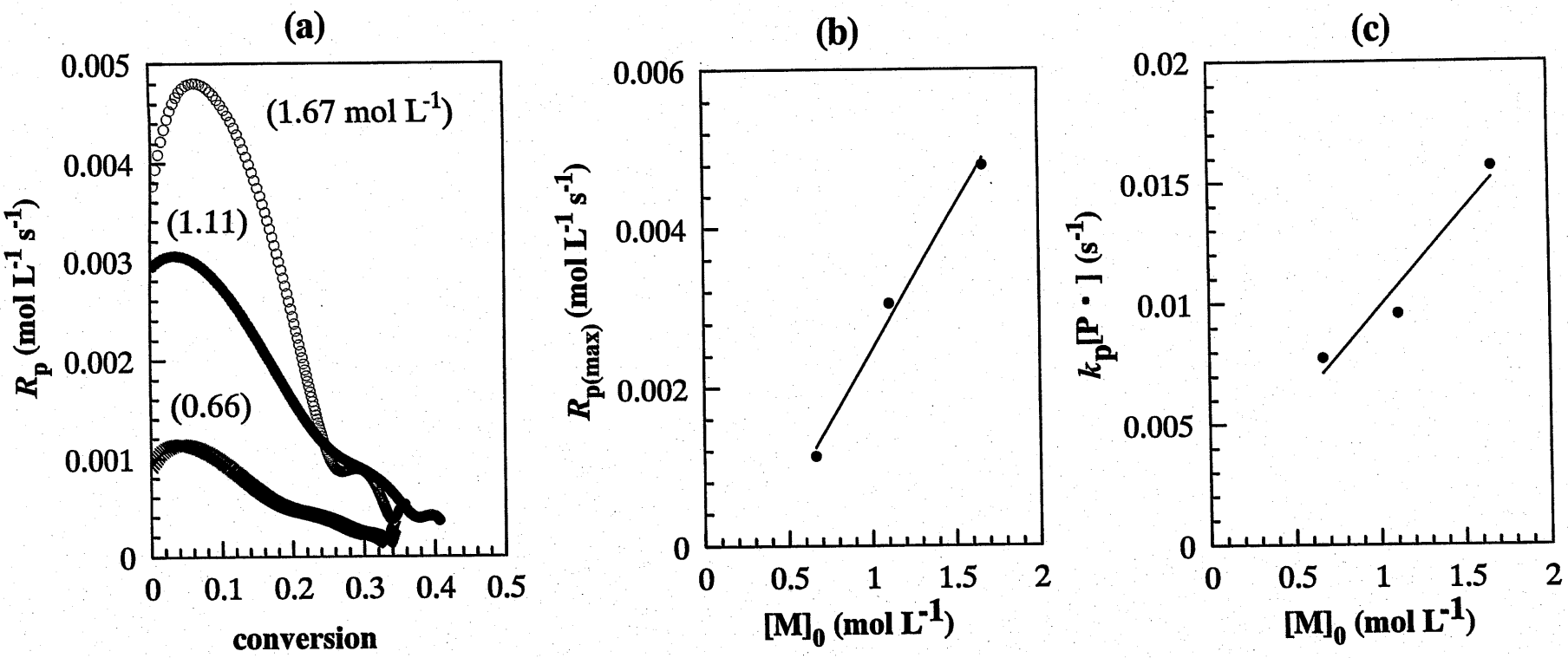

Figure 4-13. Photopolymerization behavior of TMPTA in poly(MMA) matrix with various initial monomer concentrations. Dependence of rate of polymerization on conversion (initial monomer concentration is indicated in the parenthesis),(a) and effects of initial monomer concentration on $R_{p(max)}$, (b) and $k_p[P\cdot]$, (c).

4-4. CONCLUSION

Photopolymerization of BzTD in poly(BzTD) matrix was found to proceed in the steady-state condition; $R_p = k_p[P\cdot]([M]-C_m)$, in which $k_p[P\cdot]$ was found to be constant (0.036 s^{-1}) and independent of the initial monomer concentration and monomer conversion. This result indicates that the density of monomer molecules in the polymerization locus is not affected by initial monomer concentration. Similar results were obtained also in the case of photopolymerization of C1TD in polystyrene matrix, in which cluster structure of C1TD molecules had been confirmed by transmission electron microscopy as described in Chapter 2. Independence of $k_p[P\cdot]$ on initial monomer concentration indicates that monomer molecules are assembled inside the cluster structures. On the other hand, in the polymerization of TMPTA in poly(MMA), $k_p[P\cdot]$ decreased with the decrease in initial monomer concentration and this result is reasonable when uniform distribution of monomer molecules in the polymer matrix is considered in this case.

Microscopically aggregated states of thiadiazole-substituted styrenyl monomers are supported by the present investigation and this should be one of the reasons of high polymerization reactivities of these monomers in polymer matrices.

REFERENCES

1. Williamson, S. E. ; Kang, D. ; Hoyle, C. E., Macromolecules, 1996, 29, 8656.
2. Andersson, H. ; Trollsas, M. ; Gedde, U. W. ; Hult, A., Macromol. Chem. Phys., 1995, 196, 3667.
3. Guymon, C. A. ; Hoggan, E. N. ; Clark, N. A. ; Rieker, T. P. ; Walba, D. M. ; Bowman, C. N., Science, 1997, 275, 57.
4. Guymon, C. A. ; Bowman, C. N., Macromolecules, 1997, 30, 5271.
5. Matsumoto, A. ; Matsumura, T. ; Aoki, S., J. Chem. Soc., Chem. Commun., 1994, 1389.
6. Tashiro, K. ; Kamae, T. ; Kobayashi, M. ; A. Matsumoto, A. ; Yokoi, K. ; Aoki, S., Macromolecules, 1999, 32, 2449.
7. Odani, T. ; Matsumoto, A., Macromol. Rapid Commun., 2000, 21, 40.
8. Matsumoto, A. ; Nagahama, S. ; Odani, T., J. Am. Chem. Soc., 2000, 122, 9109.
9. Matsumoto, A. ; Odani, T. ; Sada, K. ; Miyata, M. ; Tasiro, K., Nature, 2000, 405, 328.
10. Jansen, J.F.G.A. ; Dias, A. A. ; Dorschu, M. ; Coussens, B., Polym. Prepr., 2001, 42, 769.
11. Jansen, J.F.G.A. ; Dias, A. A. ; Dorschu, M. ; Coussens, B., Macromolecules, 2002, 35, 7529.
12. Turro, N. J., "Modern molecular photochemistry", Chapter 9, p.319, The Benjamin/Cummings Publishing Company, Inc., CA, (1978).

13. Schulz, G. V., Z. Phys. Chem. (Munich), 1956, 8, 290.

14. Buback, M. ; Huckestein, B. ; Russel, G. T., Macromol. Chem. Phys., 1994, 195, 539.

15. Stickler, M., Macromol. Chem., 1983, 184, 2563.

16. Anseth, K. S. ; Anderson, K. J. ; Bowman, C. N., Macromol. Chem. Phys., 1996, 197, 833.

17. Lovell, L. G. ; Stansbury, J. W. ; Syrpes, D. C. ; Bowman, C. N., Macromolecules, 1999, 32, 3913.

18. Young, J. S. ; Bowman, C. N., ibid., 1999, 32, 6073.

19. Mateo, J. L. ; Serrano, J. ; Bosch, P., ibid., 1997, 30, 1285.

20. Bosch, P.; Serrano, J.; Mateo, J. L.; Guzman, J.; Calle, P.; Sieiro, C. J Polym Sci Part A. Polym Chem 1998, 36, 2785.

21. Mateo, J. L.; Calbo, M.; Bosch, P., ibid., 2001, 39, 2049.

22. Mateo, J. L.; Calbo, M.; Bosch, P., ibid., 2001, 39, 2444.

23. Mateo, J. L.; Calbo, M.; Bosch, P., ibid., 2002, 40, 120.

Chapter 5

Effects of photoinitiator concentration and light intensity on the solid-state polymerization of styrenyl compound bearing thiadiazole group

5-1. INTRODUCTION

Light-induced polymerization and photocrosslinking reactions of various monomers in polymer matrix have gained special attention as a unique method for preparing polymer networks by simply illuminating the target with appropriate light source at ambient temperature. The rate and final conversion of such photopolymerization could be controlled by adjusting the light intensity and/or the concentration of photoinitiator. Intensive irradiation and relatively high concentration of photoinitiator could overwhelm the quenching effect of dissolved oxygen in the photopolymerization system. Especially in the solid state photopolymerization where photoactive monomer is dispersed in polymer matrix, even in the presence of air, photopolymerization sometimes proceeds without interference of oxygen[1-3]. In order to achieve the desired physical properties of photo-cured materials, the concentration of photoinitiator should carefully be optimized. As the concentration of photoinitiator increases, the apparent polymerization rate and conversions usually increases.[4] However, in some cases, overloaded photoinitiator causes insufficient polymerization due to the extensive

recombination of initiating radicals.[5] Mechanical properties of photocured materials are also significantly influenced by the concentration of photoinitiator and incident light intensity.[3, 6] Therefore, it is necessary to understand the effects of light intensity and photointiator concentration on photopolymerization behavior in every photopolymerization system for optimization of polymerization conditions.

Our present investigations are motivated by the necessity for optimizing the photopolymerization condition to achieve highest polymerization efficiency and we intended to investigate the effects of light intensity and photoinitiator concentration on the photopolymeriation behavior of these particular photopolymerization system.

5-2. EXPERIMENTAL

Materials

2-(4'-methoxystyryl)-4,6-bis(trichloromethyl)-1,3,5-triazine (PMS) was purchased from Panchim (Cedex, France) and used without further purification. All other materials used in this chapter are described in Chapter 2.

Preparations of monomer and polymer matrix

All the procedures were described in Chapters 2 and 3.

Photopolymerization

Photopolymerization of the styrene derivatives was carried out in the matrix of solid polymer and followed up to high monomer conversion by Fourier transform real-time infrared (RT-IR) [8, 14-17] spectroscopy as described in Chapter 3.

Monomer conversion was calculated according to the following equation:

$$conversion = \frac{A(990)_0 - A(990)_t}{A(990)_0}$$

in which $A(990)_0$ and $A(990)_t$ denote the peak absorbance at 990 cm^{-1} before UV-irradiation and at time t (s), respectively. The rate of polymerization, R_p, was calculated from the following equation;

$$R_p\,(mol\,l^{-1}\,s^{-1}) = -\frac{d[M]}{dt} = [M]_0\frac{d(conversion)}{dt}$$

Since measured peak intensity at 990 cm^{-1} were somewhat scattered with time, the calculated value of R_p from the slope of time-conversion curve at an arbitrary time interval scattered significantly. 10th order polynominal approximation was applied to all time-conversion curves and the polynominal curve fit was differentiated to obtain R_p at an arbitrary polymerization time.

5-3. RESULTS AND DISCUSSION

5-3-1. Photopolymerization of BzTD and photodecomposition of PMS at various initial PMS concentrations in poly(BzTD) matrix

In Figure 5-1 (a), time-conversion curves for the photopolymerization of BzTD initiated by various amounts of PMS were plotted. As the PMS concentration increased, time-conversion curves showed increased conversions at any polymerization time. Rate of polymerization, R_p, was calculated from the differential of the curve fit for each time-conversion curve and plotted against the monomer concentration as shown in Fig. 5-1(b). Except for the lowest two curves seen in this figure, R_p decreased linearly with monomer concentration and the slope of this linear relationship is almost independent on the initial PMS concentrations. In the case of relatively smaller initial PMS concentrations, i.e., 1.35 and 2.23× 10^{-3} mol·L^{-1}, polymerization started slowly at the

beginning and R_p vs. monomer concentration plots showed S-shaped curves for these cases. This might be caused by oxygen dissolved in the polymerization system and with higher concentrations of PMS, the effects of dissolved oxygen might have been overwhelmed by the large concentrations of generating PMS radical. Even in the case of two smallest initial PMS concentrations, R_p vs. monomer concentration plots were found to be well approximated by a linear relationship in the middle of polymerization. The observed linear relationship between R_p and monomer concentration indicates the constant concentration of propagating radical in a steady-state condition as expressed by Eq. (1);

$$R_p = k_p[P\cdot]([M]-C_m) \qquad (1)$$

where k_p designates the propagation rate constant, [P·], the concentration of propagating radical and [M], monomer concentration. C_m denotes the residual monomer concentration which does not contribute the polymerization. From the slope of R_p *vs.* monomer concentration plot in Fig. 5-1(b), values of k_p[P·] in the course of the polymerization were calculated and dependence of this value on the initial PMS concentration was plotted in Figure 5-2(a). The obtained values of k_p[P·] are around 0.030 to 0.036 (s^{-1}) when the initial concentration of PMS is over 6×10^{-3} mol·L^{-1} and virtually independent on the initial PMS concentration. When the initial PMS concentration is below 6×10^{-3} mol·L^{-1}, k_p[P·] decreased steeply to around 0.01 (s^{-1}). Since the propagation rate constant, k_p, is considered to be not affected by the initial PMS concentration, this result reflects directly the dependence of propagating radical concentration on the initial photoinitiator concentration. This result shows that polymerization rate was virtually independent on the photoinitiator concentration except

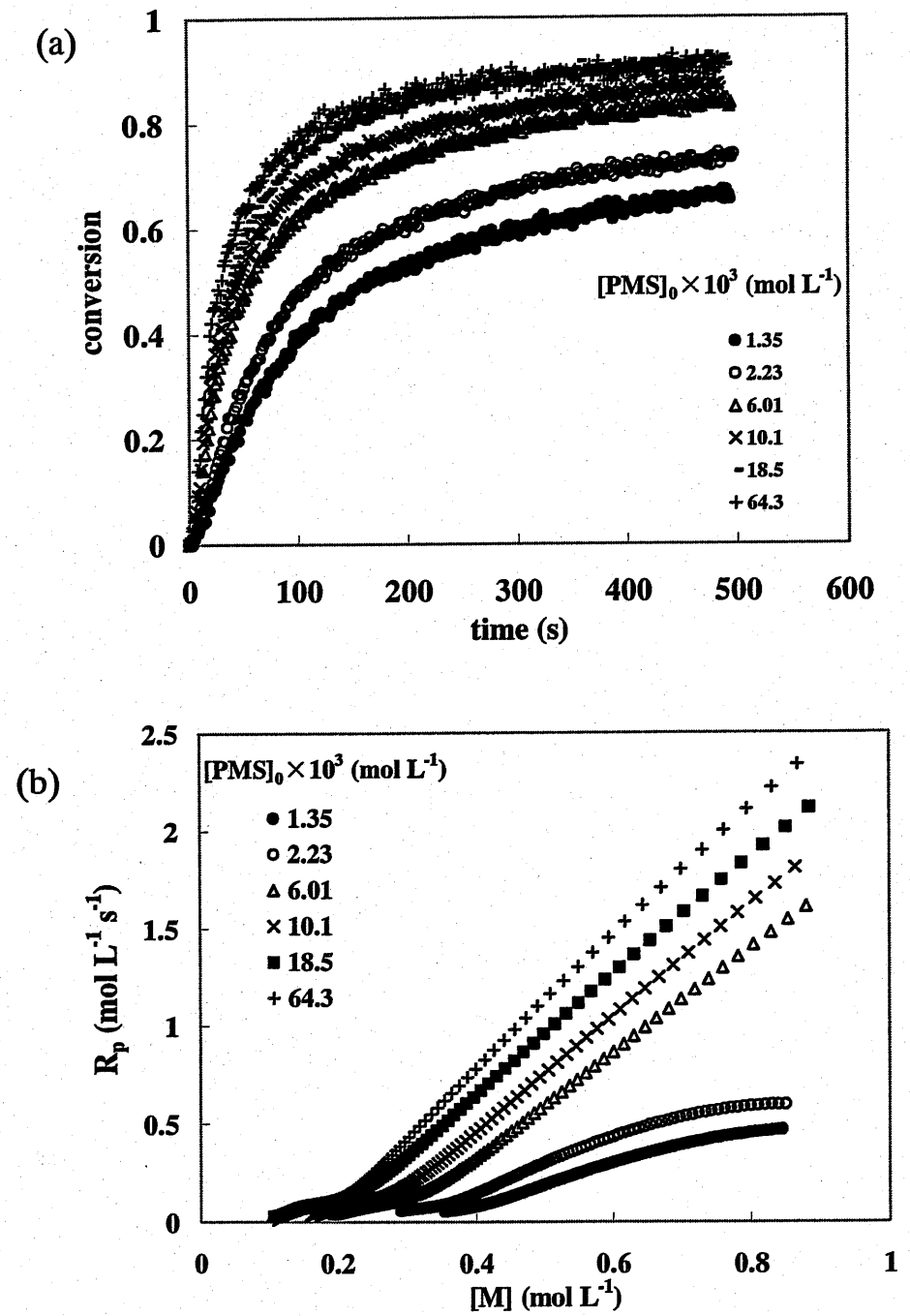

Figure 5-1. (a) Time-conversion curves for the polymerization of BzTD in poly(BzTD) matrix with various initial PMS concentrations and (b) R_p vs. monomer concentration plot. The initial PMS concentrations are indicated in the Figure. BzTD/poly(BzTD) = 0.086g/0.2g. The incident light intensity = 5×10^{-9} einstein cm^{-2} s^{-1}.

for the two smaller photoinitiator concentrations. Initial polymerization rate, R_{p0}, was plotted against the initial PMS concentration as is seen in Figure 5-2(b). R_{p0} seems to increase with the initial PMS concentration and this result is apparently conflicting with the result described above. However, the residual monomer concentration, C_m, was found to decrease with the increase in the initial PMS concentration (Fig. 5-3) and this implies that the total monomer concentration participating in the polymerization increases with PMS concentration and the overall polymerization rate as expressed in Eq. (1) also increases. The effect of initial initiator concentration on polymerization rate is manifested in decreasing the residual monomer concentration and it is important to observe that propagating radical concentration remained virtually constant when the initial PMS concentration is above 6×10^{-3} mol·L^{-1}. This result should be compared with the rate of the photoinitiator decomposition, since this process should determine the concentration of propagating radical. During the RT-IR measurements of monomer consumption in the polymerization process, the concentration change of the photoinitiator, PMS, was also monitored at the absorption band of 1171 cm^{-1} which was assigned to a coupled asymmetrical stretching vibration of two CCl_3 groups attached to1,3,5-triazine ring. The decomposition ratio (*DR*) of PMS was plotted against polymerization time as shown in Figure 5-4(a). Maximun decomposition ratio was around 0.3 to 0.5 and the rest of PMS was remained unreacted in this polymerization condition. In our experimental conditions, the minimum detectable concentration of PMS was around 10×10^{-3} mol·L^{-1} (ca. 0.4 % of total composition) and when the initial PMS concentration was below this value, RT-IR measurements of PMS decomposition was unable to carry out with a sufficient accuracy.

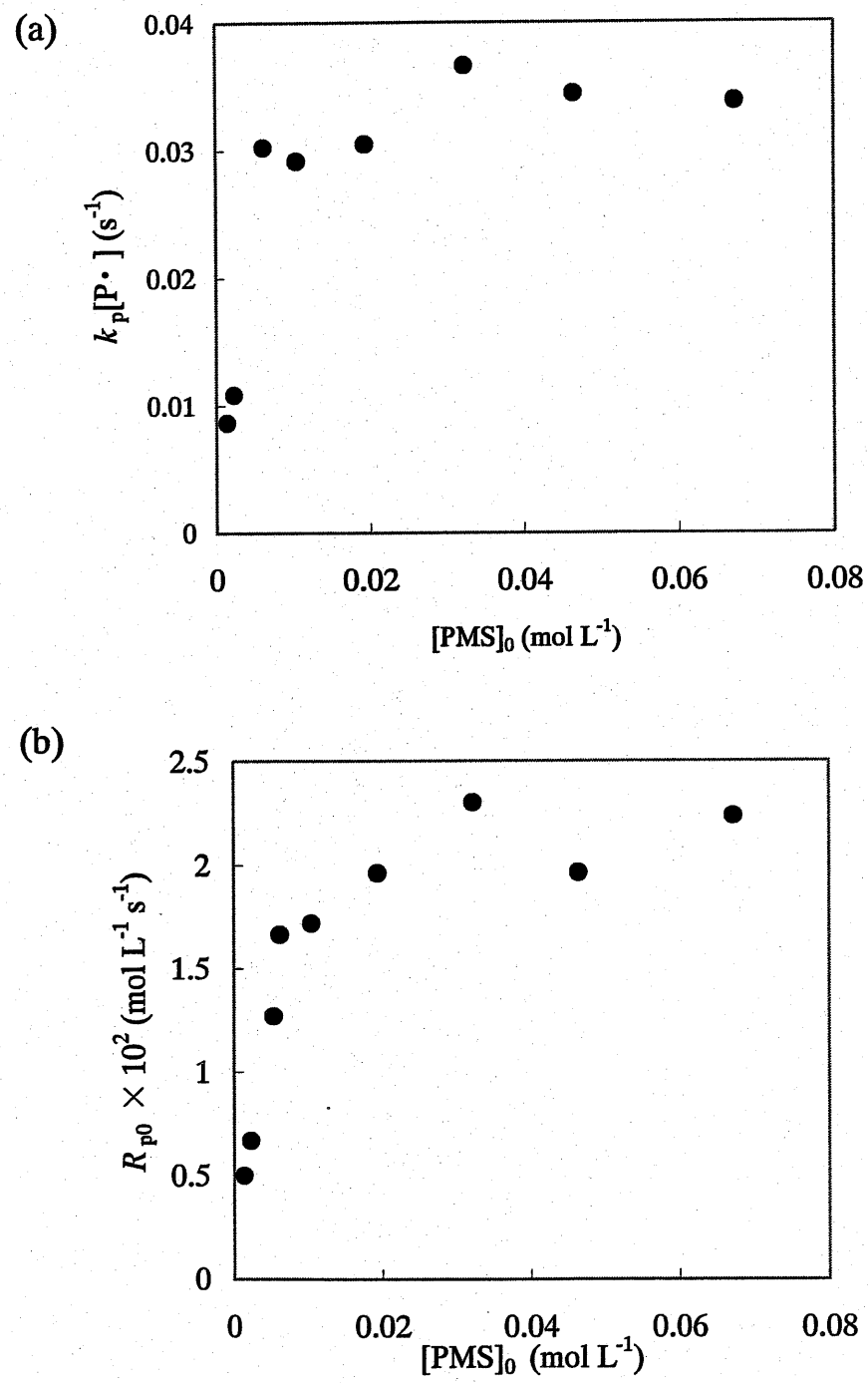

Figure 5-2. Dependence of $k_p[P\cdot]$ (a) and R_{p0} (b) on the initial PMS concentration.

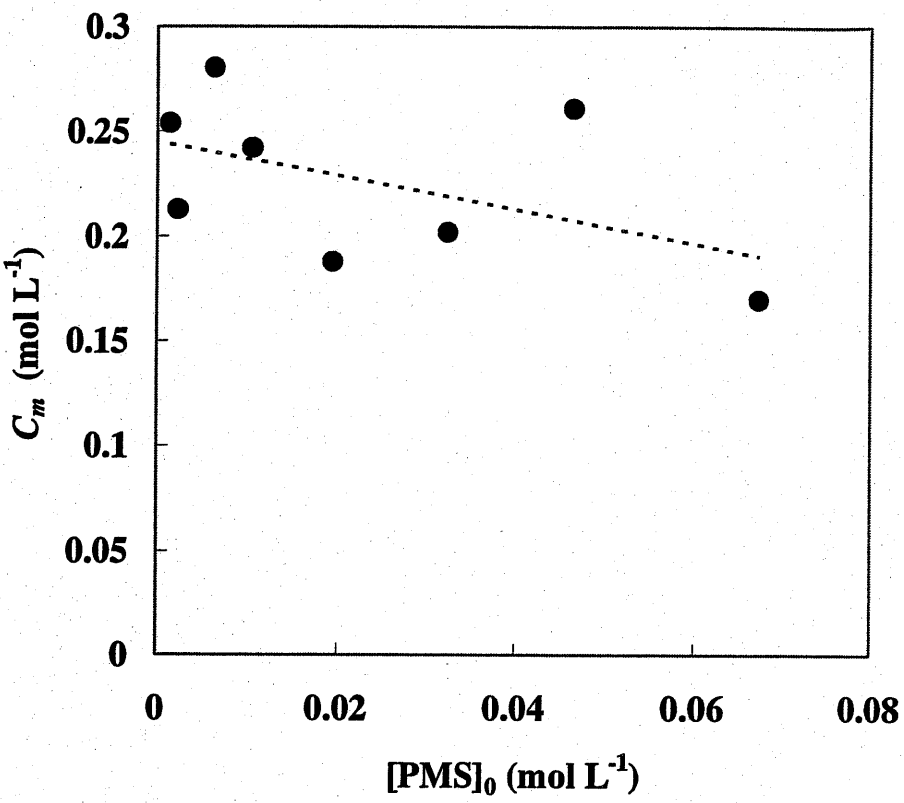

Figure 5-3. Dependence of C_m on the initial PMS concentration.

Decomposition rate, R_d, of PMS was calculated according to the equation;

$$R_d\ (mol\,L^{-1}\,s^{-1}) = -\frac{d[PMS]}{dt} = [PMS]_0\frac{d(DR)}{dt} \qquad (2)$$

Since the individual data points shown in Fig. 5-4(a) were rather scattered, 10th-order of polynominal approximation was applied for each DR vs. time curve and thus obtained curve fit was differentiated to obtain R_d according to Eq. (2). As shown in Fig. 5-4(b), R_d was plotted against PMS concentration. R_d decreased linearly with PMS concentration at the primary stage of photodecomposition process. The relationship between R_d and [PMS] can be expressed experimentally as follows:

$$R_d = k \times I_0(einstein \cdot L^{-1}\,s^{-1}) \times ([PMS] - C_f) \qquad (3)$$

where k (L·einstein^{-1}) represents a decay constant. C_f denotes a residual PMS concentration which could be reached if the decomposition proceeds linearly with PMS concentration as expressed in Eq. (3), at which concentration the decomposition would cease (R_d = 0). Only a part of PMS molecules, ([PMS] – C_f), were photoactive and C_f mol·L^{-1} of PMS was remained unreacted. In Figure 5-5(a), the decay constant, k, obtained from the slope of the linear part of R_d vs. [PMS] relationship was plotted against the initial PMS concentration. k was found to be ca. 20 and is independent on the initial PMS concentration. As for the residual PMS concentration, C_f, this was found to be linearly related to the initial PMS concentration, as is seen in Figure 5-5(b), and C_f is expressed approximately by $C_f = 0.61[PMS]_0$. Initial decomposition rate of PMS, R_{d0}, which can be found in Fig. 5-4(b) at the highest point of each linear dependence of R_d *vs.* [PMS] plot, was also found to decrease linearly with the initial PMS concentration and the relationship expressed in Eq. (3) is rewritten in the form as expressed in Eq.(4).

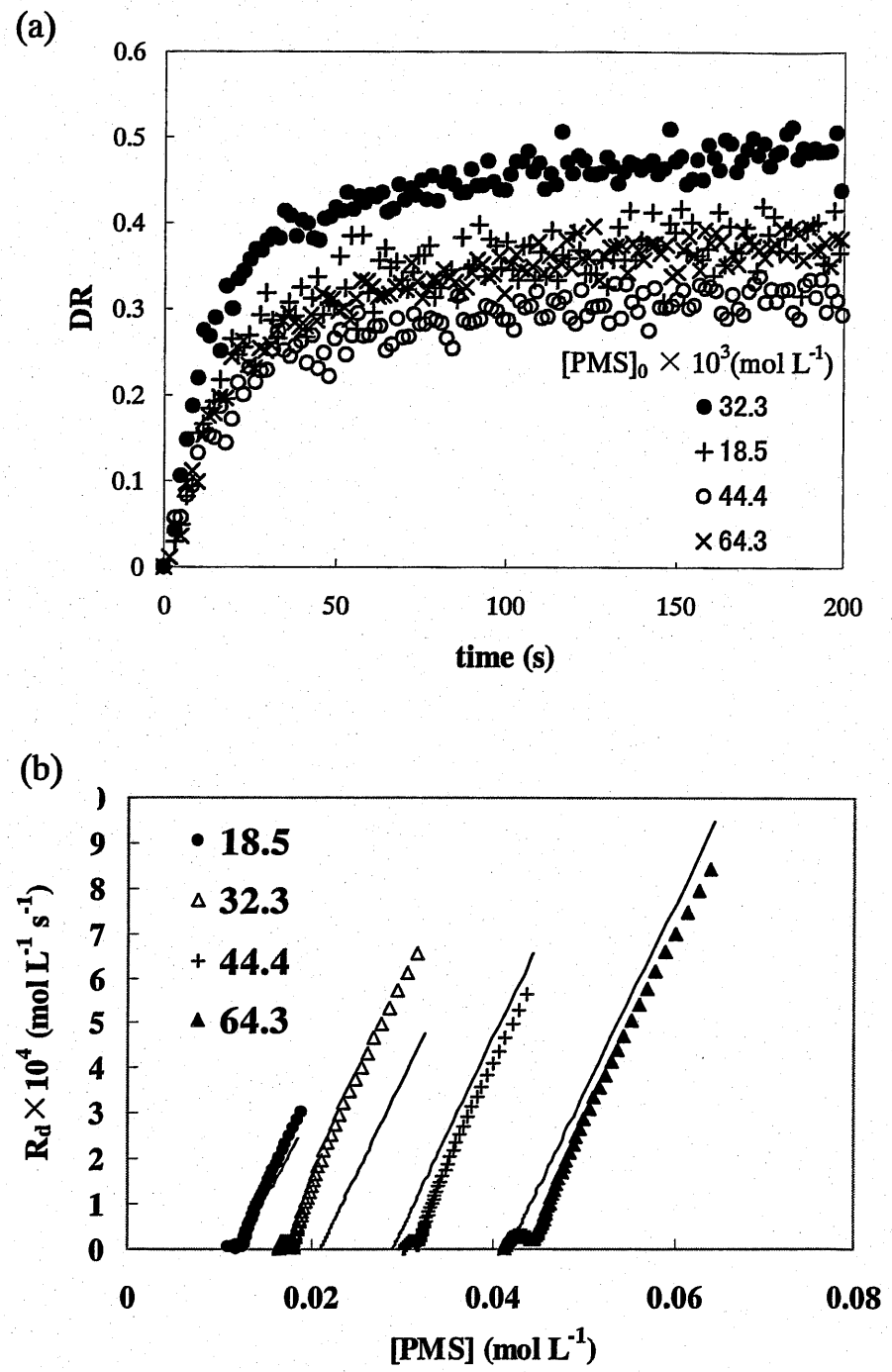

Figure 5-4. Decomposition rate (*DR*) *vs.* time (a) and R_d vs. [PMS] (b) plots for the polymerization of BzTD shown in Figure 5-1. Solid lines in (b) show the calculated values based on Eq. (4) (see text).

$$[PMS]\ (mol\,L^{-1}) = [PMS]_0\,(0.61+0.39\exp(-kI_0t)) = [PMS]_0\,(0.61+0.39\exp(-0.042t)) \quad (4)$$

In the above discussion, the polymerization of monomer and the decomposition of PMS were independently measured and analyzed. It is of great interest to discuss the relationship between polymerization rate and decomposition rate of the initiator. The previously obtained result on R_p indicates the constant value of propagating radical concentration in the course of the photopolymerization, whereas the decomposition rate of the initiator decreased at the same time. In a steady-state condition, the rate of termination should be the same as that of the initiation and the latter should be equal to R_d, if the initiation reaction takes place much faster than the decomposition reaction of the photoinitiator. In Eq. (3), R_d is proportional to the concentration of "photoactive" PMS. Therefore, if the termination rate is also proportional to the concentration of "photoactive" PMS, then this term is canceled out and the concentration of propagating radical become constant. This treatise implies that termination would take place between propagating radical and PMS. As described in Chapter 3, a set of possible elementary steps are again summarized in Scheme 5-1. In this Scheme, PMS· denotes the initiating radical produced by photodecopmposition of PMS and P· represents both the propagating polymer radical and the monomer radical produced by the addition of initiating radical. In this kinetic model, the reactivities of both polymer and monomer radicals are assumed to be the same and these two entities are not distinguished. D represents dead-polymer produced by the termination reaction between the propagating radical and the remaining PMS molecule. The rate constants, k, k_i, k_t and k_{tr} represent decay constant of photoinitiator, initiation rate constant, termination rate constant and chain transfer rate constant, respectively.

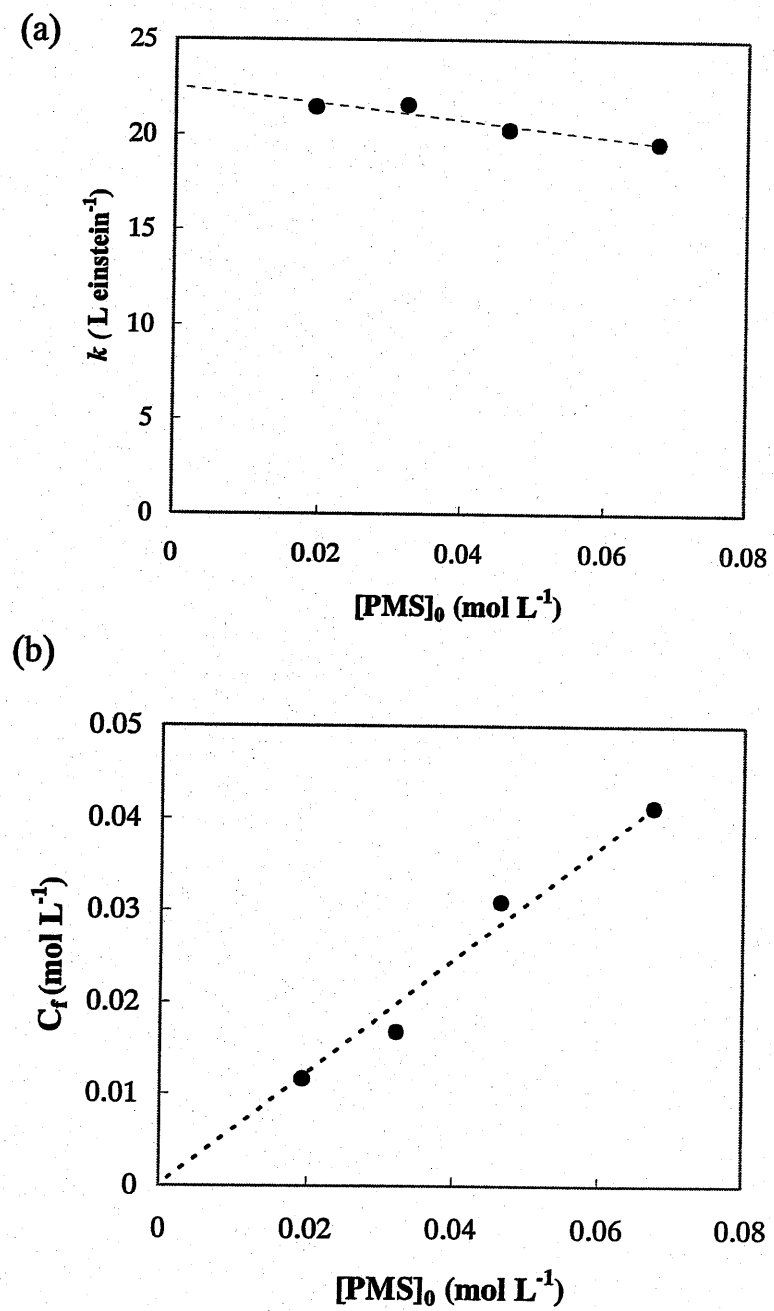

Figure 5-5. Dependence of decay constant, k, (a) and residual PMS concentration, C_f, (b) on the initial PMS concentration.

Scheme 5-1

Photodecomposition :	$PMS \rightarrow PMS\bullet + Cl\bullet$	$:R_d = kI_0[PMS]$
Initiation :	$PMS\bullet + M \rightarrow P\bullet$	$:R_i = k_i[PMS\bullet][M]$
Propagation :	$P\bullet + M \rightarrow P\bullet$	$:R_p = k_p[P\bullet][M]$
Termination :	$P\bullet + PMS \rightarrow D$	$:R_t = k_t[P\bullet][PMS]$
Chain Transfer :	$P\bullet + PMS \rightarrow D + PMS\bullet$	$:R_{tr} = k_{tr}[P\bullet][PMS]$
2nd Initiation:	$Cl\bullet + M \rightarrow P\bullet$	
Abstraction :	$Cl\bullet + RH \rightarrow R\bullet + HCl$	
3rd Initiation:	$R\bullet + M \rightarrow P\bullet$	

Based on the elementally steps in Scheme 5-1, the following relationship can easily be derived.

$$[P\cdot] = \frac{2R_d}{k_t([PMS]-C_f)} = \frac{2\Phi_d' I_0}{k_t} \qquad (4)$$

$$[PMS\cdot] = \left(1+\frac{2k_{tr}}{k_t}\right)\frac{\Phi_d' I_0}{k_i}\frac{[PMS]-C_f}{[M]-C_m} \qquad (5)$$

$$R_p = \frac{2k_p\Phi_d' I_0}{k_t}([M]-C_m) \qquad (6)$$

$$kcl \equiv \frac{R_p}{R_i} = \frac{R_p}{R_d} = \frac{2k_p}{k_t}\frac{[M]-C_m}{[PMS]-C_f} \qquad (7)$$

where *kcl* indicates the *k*inetic *c*hain *l*ength which is defined as the number of monomer molecules polymerized by one initiating radical.

In Chapter 4 we postulated that the monomer molecules might form clusters in the polymerization system and the size of the cluster was estimated by the values of *kcl*. From Eq. (7) initial value of *kcl* (kcl_0) was calculated as the ratio of R_{p0}/R_{d0} and plotted against the initial PMS concentration as shown in Figure 5-6(a). This value was found to increase with decreasing the initial PMS concentration and a polynominal approximation gave the value of ca. 200 at the zero concentration of PMS. This result indicates that the possible cluster of monomer molecules is consisted of ca. 200 molecules and as the PMS concentration increases, the each cluster contains increased number of PMS molecules, resulting in the decreased value of *kcl*. On the other hand, if the initial PMS concentration is less than 1/200 of monomer concentration, some of cluster does not contain PMS molecules and polymerization proceeds unevenly in the system. In such a case R_p should be decreased as compared with those higher PMS concentrations. In the present polymerization condition the initial monomer concentration is 0.83 $molL^{-1}$ and 1/200 of this concentration corresponds to 4×10^{-3} $molL^{-1}$. So that when the initial PMS concentration is less than this value, the polymerization rate should decrease abruptly. In Figure 5-1 and 5-2, R_p and $k_p[P\cdot]$ were found to decrease suddenly at the initial PMS concentration less than 6×10^{-3} $molL^{-1}$ and these results are well explained by considering the existence of cluster structure of monomer molecules, as described above.

Validity of the kinetic investigations described above was further checked over by calculating the ratio of the rate constants, k_p/k_t, according to Eq. (7). The result is shown in Fig. 5-6(b). This ratio was found to be constant (0.3 ~ 0.4) at the initial PMS concentration larger than 6×10^{-3} $molL^{-1}$ and this result proves the validity of such discussion.

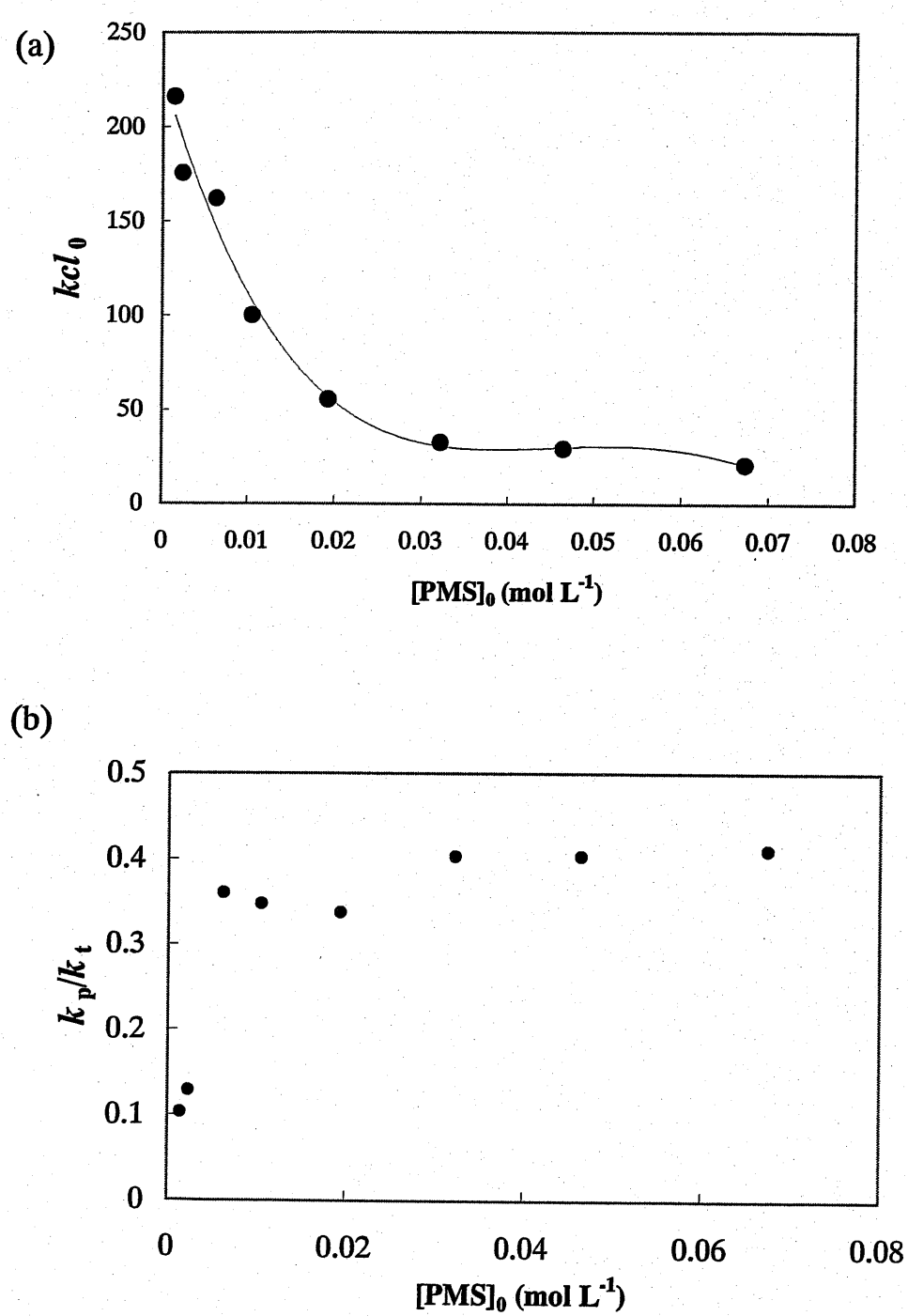

Figure 5-6. Dependence of kcl_0 (a) and k_p/k_t (b) on the initial PMS concentration.

Values of kcl_0 at $[PMS]_0 \leq 0.01$ molL^{-1} were calculated according to Eq. (4).

5-3-2. Effect of light intensity on the photopolymerization of BzTD and photo-decomposition of PMS in poly(BzTD) matrix

The intensity of the incident light was varied to observe the effect of light intensity both on the polymerization rate of BzTD and on the photodecomposition rate of PMS. From the kinetic equations, (3) and (6), both rates are expected to be linearly dependent on the incident light intensity. In Figure 5-7, polymerization rate of BzTD, R_p, and decomposition rate of PMS, R_d, is plotted against the corresponding concentrations at various light intensities. As for the polymerization rate, at the lowest incident light intensity, polymerization rate was initially lower than that expected from a linear dependence of R_p on monomer concentration and this was probably caused by oxygen dissolved in the polymerization system as in the case of the smaller initial PMS concentrations described in the previous section. The slope of the linear relationship between R_p and monomer concentration decreased gradually with the decrease in light intensity. Decomposition rate of PMS was also dependent on the incident light intensity and the linear dependence of R_d on PMS concentration during the photodecomposition process was maintained in this range of light intensity, suggesting that oxygen dissolved in the polymerization system affects the polymerization rate much more sensitively than the photodecomposition rate of PMS. Dependence of initial rate of polymerization, R_{p0}, and the intrinsic rate of polymerization, $k_p[P\cdot]$, during the polymerization on the incident light intensity was shown in Figure 5-8. Both plots show the identical dependence on the incident light intensity and are fairly deviated from the expected linear relationship of eq. (6). This result indicates that the concentration of propagating radical does not change linearly with the incident light intensity.

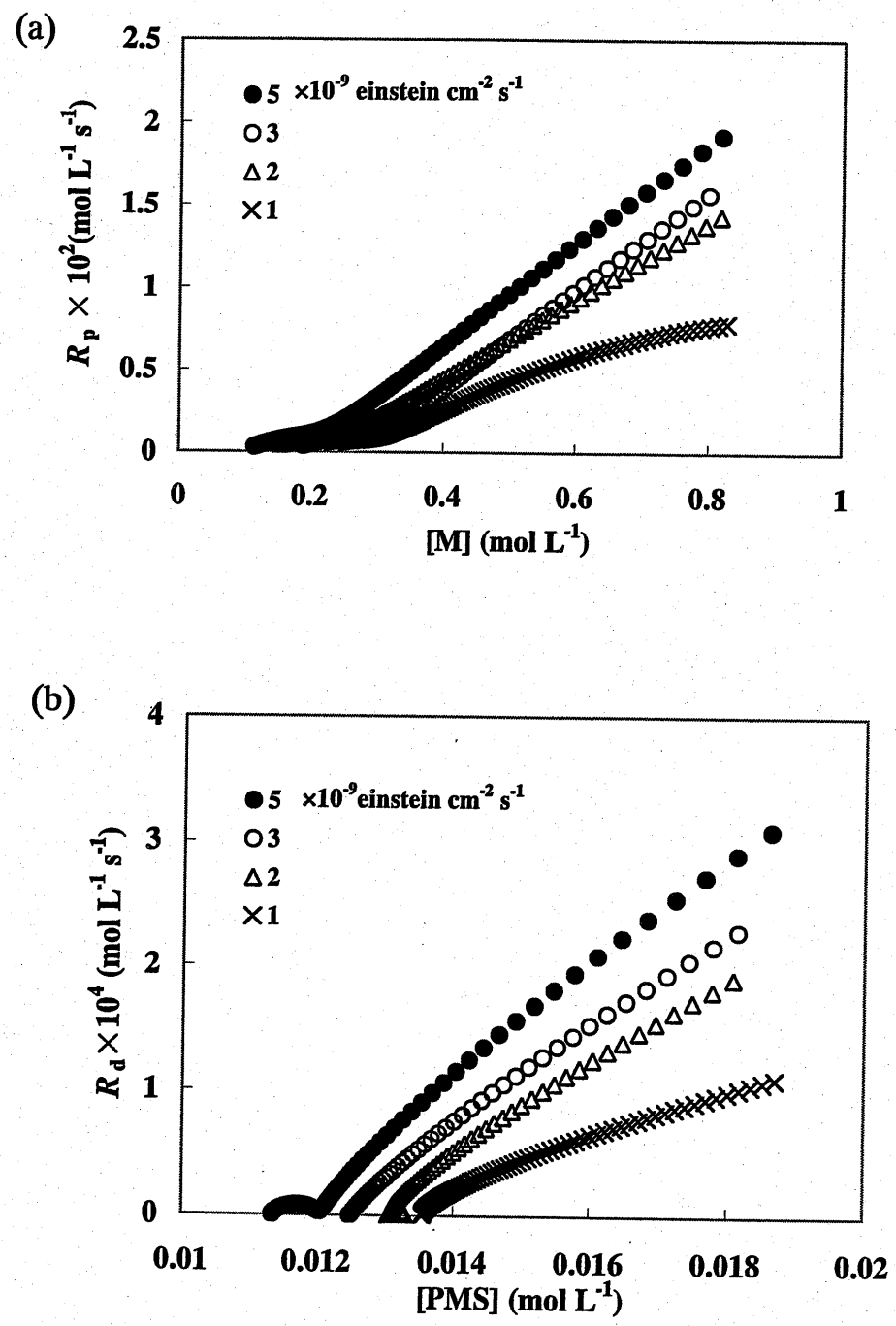

Figure 5-7. Effect of light intensity on R_p (a) and R_d (b) in the PMS initiated photopolymerization of BzTD in poly(BzTD) matrix. BzTD/poly(BzTD)/PMS = 0.086/0.2/0.0025 (wt/wt/wt).

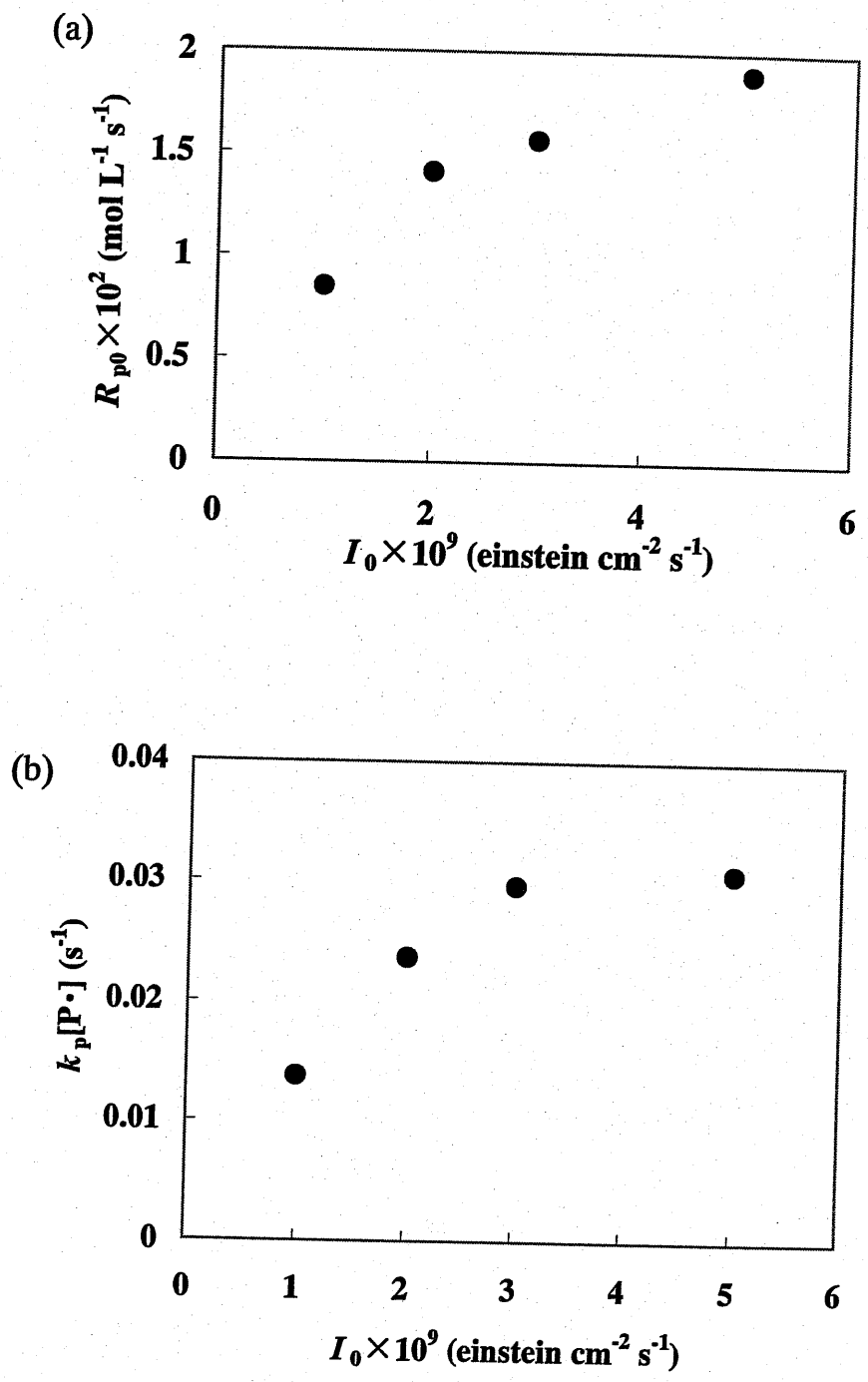

Figure 5-8. Dependence of R_{p0} (a) and k_p[P·] (b) on the incident light intensity.

Decomposition rate of PMS was also observed with non-linear dependency on the incident light intensity, as shown in Figure 5-9(a). The essential cause for these non-linear dependencies on the light intensity is seen in the change of the quantum yield of photodecomposition of PMS, Φ_{d0}, shown in Fig. 5-9(b). As the incident light intensity decreases, Φ_{d0} increases gradually and this affects both R_p and R_d in extents expected by Eq. (3) and (6), respectively. It is interesting to observe that the initial quantum yield of photodecomposition of PMS reaches almost unity at the lowest incident light intensity. In polymer matrix, PMS radical produced by the irradiation of UV light is considered to be in a rapid equilibrium with recombination reaction with chlorine radical which is generated at the same time of PMS radical via homolytic cleavage of carbon-chlorine bond in a trichloromethyl group of PMS molecule.[7-10] When the incident light intensity decreases, the concentration of the initiating PMS radical decreases and recombination of PMS radical with chlorine radical would decrease, resulting in the increase in quantum yield of photodecomposition of PMS. Light intensity seems to affect only the quantum yield of PMS photodecomposition and polymerization behavior itself remained unaffected. In Figure 5-10, kinetic chain length and k_p/k_t are plotted against the incident light intensity and it was found that these parameters were independent on the light intensity, suggesting that our discussions described above are appropriate.

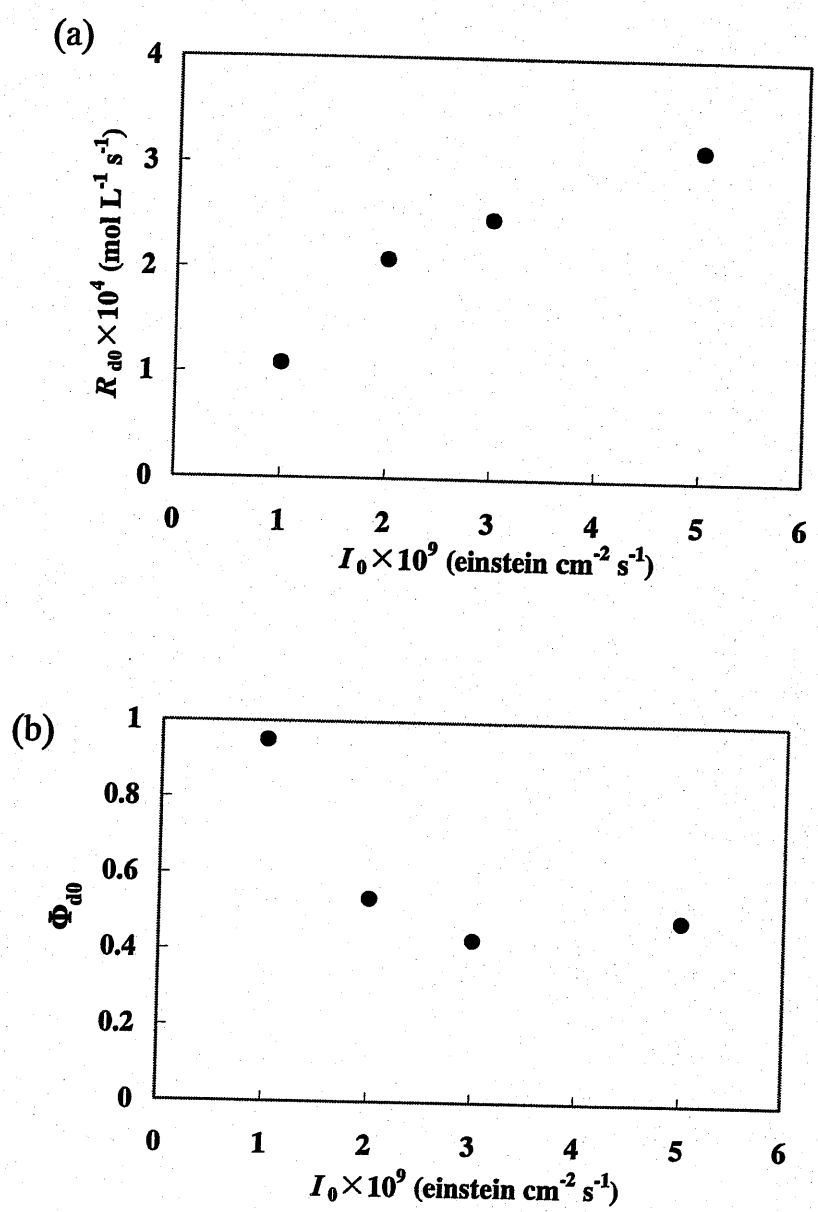

Figure 5-9. Dependence of R_{d0} (a) and Φ_{d0} (b) on the incident light intensity.

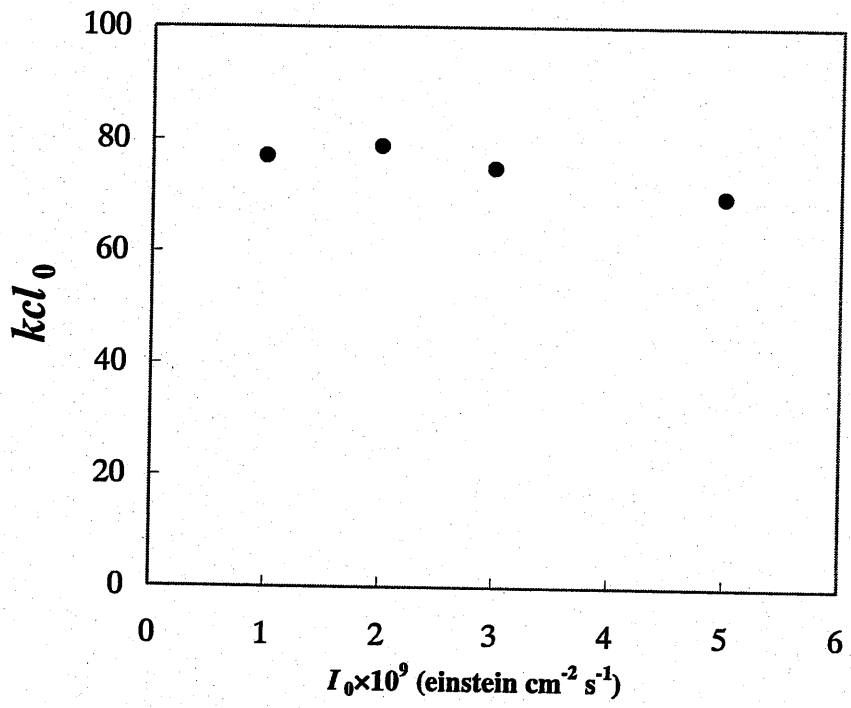

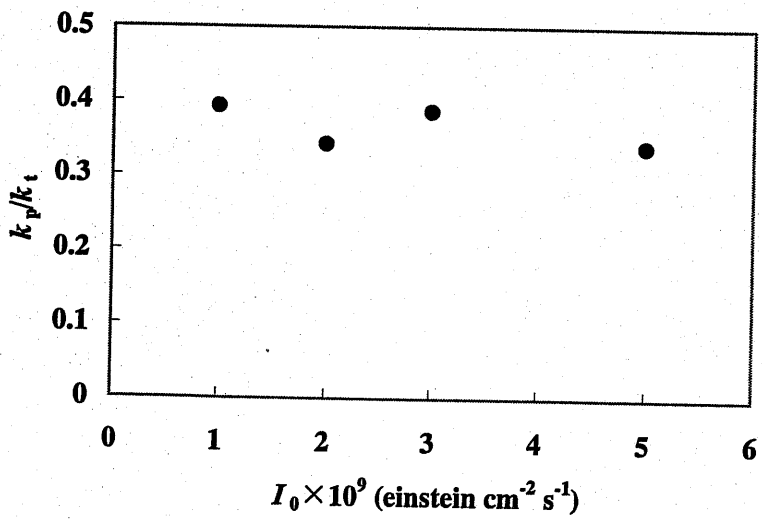

Figure 5-10. Dependence of kcl_0 (a) and k_p/k_t (b) on the incident light intensity.

5-4. CONCLUSION

The effects of photoinitiator concentration and light intensity on the photoinitiated polymerization of BzTD in poly(BzTD) matrix were investigated. From the dependence on the initial photoinitiator concentration, the maximum value of kinetic chain length (*kcl*) was estimated to be around 200 at the initial monomer concentration of 0.83 $mol \cdot L^{-1}$. This maximum *kcl* value is considered to represent the number of monomer molecules included in the monomer cluster formed in the polymerization system. When the initial photoinitiator concentration fell below 1/200 of the initial monomer concentration, polymerization rate decreased abruptly, suggesting the existence of cluster structure of monomer molecules. The quantum yield of photodecomposition of the photoinitiator increased with decreasing light intensity and finally reached unity. On the other hand, kinetic parameters such as k_p/k_t and kinetic chain length were shown to be independent of the light intensity.

REFERENCES

1. Chapter 2 in this thesis.

2. Moussa, K. ; Decker, C., J. Polym. Sci. Part A. Polym. Chem., 1993, 31, 2633.

3. Kaczmarek, H. ; Decker, C., J. Polym. Sci. Part A. Polym. Chem., 1994, 54, 2147.

4. Scherzer, T. and Decker, U. Rad. Phys. Chem., 1999, 55, 615.

5. Lecamp, L. ; Youssef, B. ; Bunel, C. ; Lebaudy, P., Polymer, 1997, 25,6089.

6. Decker, C. ; Viet, T. N. T., Macromol. Chem. Phys., 1999, 200, 358.

7. Buhr, G. ; Dammel, R. ; Lindley, C. R., Polym. Mat. Sci. Eng., 1989, 61, 269.

8. Pohlers, G. ; Scaiano,; Sinta, R. J. C., Chem. Mater., 1997, 9, 3222.

9. Pawlowski, G. ; Dammel, R., J. Photopolym. Sci. Tech., 1991, 4, 389.

10. Pohlers, G. ; Scaiano, J. C. ; Step, E. ; Sinta, R., J. Am. Chem. Soc., 1999, 121, 6167.

Chapter 6

Effect of alkyl chain length in 2-(4'-vinylbenzyl)thio-5-alkyl-thio-1,3,4-thiadiazole on its photopolymerization in polymer matrix

6-1. INTRODUCTION

In radical photopolymerization the polymerization rate is greatly influenced by the nature of the monomer and especially in the bulk state, the viscosity is a key factor to increase the rate of photopolymerization. However, the relationship between the chemical structure of the monomer and its photopolymerizability had not been investigated in detail until Decker[1] found that heterocyclic oxygen introduced into the structural unit of acrylate compound accelerated the polymerization reactivity. Quite recently Jansen, et al.[2, 3] reported that some acrylate compounds exhibited high photopolymerization reactivity in bulk and the rates of polymerization were directly related to the dipole moment of acrylate compounds. Some preorganized structures due to dipole-dipole interactions have been put forward by them to explain the high reactivity of these acrylate compounds. The effect of preorganized structure has been observed in the photopolymerization of monomers which are capable to form intermolecular hydrogen bonding.[2]

The pre-organized state of monomer which Jansen has postulated to explain his experimental results should be closely related to topochemical polymerization[4-8] and

polymerization in liquid crystalline state.[9-12] Topochemical polymerization has gained special attentions for obtaining well-defined ultra-high molecular weight polymers with highly regulated structures by the so-called crystal engineering. Polymerization in liquid crystalline state is also a recent topic to obtain highly ordered polymer materials. In a smectic phase, dramatically enhanced polymerization rates are observed for some acrylate monomers photopolymerized in a smectic media.[11, 12] In such a LC phase, ordering of monomers can significantly alter the polymerization behavior and kinetics.

In the previous chapters we investigated the various aspects of photopolymerization behavior of the styrenyl monomers bearing 1,3,4-thiadiazole group in polymer matrix. In this Chapter, we report the size effect of the substituent on the photopolymerization behavior of such styrenyl monomers. In Chapter 2, we found the existence of cluster structure of C1TD (2-(4'-vinylbenzyl)thio-5-methylthio-1,3,4-thiodiazole) in polystyrene matrix. Intermolecular interactions between such monomer molecules could induce locally assembled structures of these monomer molecules. From the kinetic investigations described in Chapter 4 and 5, aggregated phase structures of monomer molecules seemed to be probable. We are now interested in seeing the effect of the size of alkyl substituent on thiadiazole group on the polymerization behavior, since the bulkiness of such alkyl substituent must affect the nature of the cluster considerably. We considered that the formation of the monomer cluster might be assisted by the polymer matrix which possesses the same 1,3,4-thiadiazole groups in the side chain. In such a point of view, the effect of matrix polymer was also investigated to clarify the polymerization mechanism of such unique photopolymerization system.

6-2. EXPERIMENTAL

Materials

2-(4'-Methoxystyryl)-4,6-bis(trichloromethyl)-1,3,5-triazine (PMS) was purchased from Panchim (France) and used without further purification. Polystyrene (M_w = 3×10^5) was obtained from Wako Chemicals Ind. Ltd., (Osaka, Japan) and purified by precipitation from 1,4-dioxane solution with methanol. 1,4-Dioxane (Wako Chemicals Ind. Ltd.) was used without further purification. Methyl iodide, ethyl iodide , propyl iodide and buthyl to decyl bromides were purchased from Tokyo Kasei Kogyo Co., Ltd.(Tokyo, Japan) and used without further purification. 4-Chloromethyl styrene was purchased from Seimi Chemical Co. Ltd. (Kanagawa, Japan) and used without further purification.

Monomer preparations

All the monomers studied in this chapter were prepared by the procedure as shown in Scheme 6-1.

Scheme 6-1

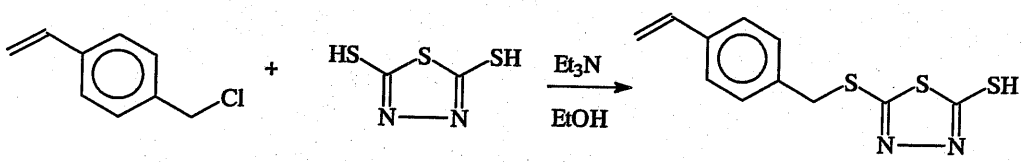

SHTD

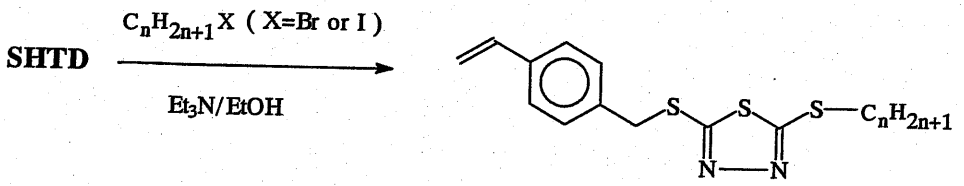

CnTD

Synthesis of 2-(4'-vinylbenzyl)thio-5-alkylthio-1,3,4-thiadiazole (CnTD)

"Cn" in CnTD implies the number of alkyl carbon substituted in 5-position of 1,3,4-thiadiazole. CnTD's were investigated to compare with each other for size effect of 5-substituent. Preparation of 5- (4'-vinylbenzyl)thio-1,3,4-thiadiazole-2-thiol (SHTD) was described in Chapter 2. C1TD was prepared by the following procedure. SHTD (26.6 g, 0.10 mol) was reacted with methyl iodide (14.2 g, 0.10 mol) in the presence of an equimolar amount of triethylamine (0.10 mol) in ethanol (200 mL) for 3 h at 10 °C. Recrystallization from ethanol gave colorless crystal. The yield was 17.4 g (62 %). Melting point was 48.7 °C.

Elemental analysis: Calcd. for 2-(4'-vinylbenzyl)thio-5-methylthio-1,3,4-thiodiazole (C1TD), C, 51.35; H, 4.28; N, 9.99. Obsd. C, 51.16; H, 4.22; N, 9.97.

^{1}H NMR (200 MHz in $CDCl_3$, δ, ppm) :2.73(s, CH_3, 3H), 4.46(s, CH_2(benzyl), 2H), 5.23 (d, H_a, J = 11 Hz, 1H), 5.72 (d, H_b, J = 17.6Hz, 1H), 6.67 (dd, H_x, J = 11, 17.6 Hz, 1H), 7.34 (m, phenyl, 4H).

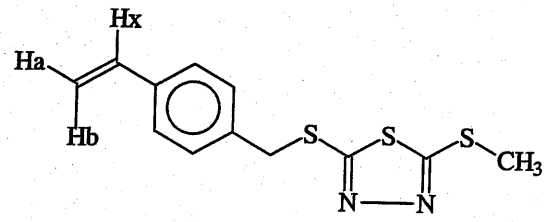

C1TD

C2TD and C3TD were prepared by a procedure similar to that of C1TD. SHTD was reacted with ethyl iodide (for C2TD) or propyl iodide (for C3TD) in the presence of equimolar amount of triethylamine (0.10 mol) in ethanol (200 mL) for 8 h at 10 °C. Other monomers from C4TD to C10TD were prepared by a procedure similar to that

described above except that 1-bromoalkane was used instead of 1-iodoalkane and reaction was carried out at 70 °C for 5 h.

C2TD:

Recrystallized from methanol / diisopropyl ether (3/1 v/v). The yield was 53 %. Melting point was 34.5 °C.

Elemental analysis: Calcd. for 2-(4'-vinylbenzyl)thio-5-ethylthio-1,3,4-thiodiazole (C2TD), C, 52.98; H, 4.75; N, 9.51. Obsd. C, 53.12; H, 4.65; N, 9.59.

^{1}H NMR (200 MHz in $CDCl_3$, δ, ppm) :1.40 (t, CH_3, J = 7.4 Hz, 3H), 3.24 (q, CH_2, J = 7.4 Hz, 2H), 4.46(s, CH_2(benzyl), 2H), 5.23 (d, H_a, J = 11 Hz, 1H), 5.72 (d, H_b, J = 17.6Hz, 1H), 6.67 (dd, H_x, J = 11, 17.6 Hz, 1H), 7.34 (m, phenyl, 4H).

.

C3TD:

Recrystallized from methanol / diisopropyl ether (3/1 v/v). The yield was 32 %. Melting point was 11.2°C.

Elemental analysis: Calcd. for 2-(4'-vinylbenzyl)thio-5-propylthio-1,3,4-thiodiazole (C3TD), C, 54.46; H, 5.19; N, 9.08. Obsd. C, 54.12; H, 5.22; N, 9.25.

^{1}H NMR (200 MHz in $CDCl_3$, δ, ppm) :1.03(t, CH_3, J = 7.2 Hz, 3H), 1.79(m, CH_2, J = 7.2, 7.4 Hz, 2H), 3.23 (t, CH_2, J = 7.4 Hz, 2H), 4.46(s, CH_2(benzyl), 2H), 5.23 (d, H_a, J = 11 Hz, 1H), 5.72 (d, H_b, J = 17.6Hz, 1H), 6.67 (dd, H_x, J = 11, 17.6 Hz, 1H), 7.34 (m, phenyl, 4H).

C4TD:

Recrystallized from methanol / diisopropyl ether (3/1 v/v). The yield was 34 %.

Melting point was 23.0 °C.

Elemental analysis: Calcd. for 2-(4'-vinylbenzyl)thio-5-butylthio-1,3,4-thiodiazole (C4TD), C, 55.81; H, 5.58; N, 8.68. Obsd. C, 56.26; H, 5.80; N, 8.93.

^{1}H NMR (200 MHz in $CDCl_3$, δ, ppm) :0.91 (t, CH_3, J = 7.2 Hz, 3H), 1.44 (m, CH_2, 2H), 1.72 (m, CH_2, 2H), 3.25 (t, CH_2, J = 7.4 Hz, 2H) 4.46(s, CH_2(benzyl), 2H), 5.23 (d, H_a, J = 11 Hz, 1H), 5.72 (d, H_b, J = 17.6Hz, 1H), 6.67 (dd, H_x, J = 11, 17.6 Hz, 1H), 7.34 (m, phenyl, 4H).

C5TD:

Recrystallized from ethanol. The yield was 67 %. Melting point was 28.5 °C.

Elemental analysis: Calcd. for 2-(4'-vinylbenzyl)thio-5-pentylthio-1,3,4-thiodiazole (C5TD), C, 57.05; H, 5.94; N, 8.32. Obsd. C, 57.42; H, 6.09; N, 8.51.

^{1}H NMR (200 MHz in $CDCl_3$, δ, ppm) : 0.88 (t, CH_3, J = 7 Hz, 3H), 1.35 (m, CH_2, 4H), 1.76 (m, CH_2, 2H), 3.24 (t, CH_2, J = 7 Hz, 2H) 4.46(s, CH_2(benzyl), 2H), 5.23 (d, H_a, J = 11 Hz, 1H), 5.72 (d, H_b, J = 17.6Hz, 1H), 6.67 (dd, H_x, J = 11, 17.6 Hz, 1H), 7.34 (m, phenyl, 4H).

C6TD:

Recrystallized from ethanol. The yield was 71 %. Melting point was 33.4 °C.

Elemental analysis: Calcd. for 2-(4'-vinylbenzyl)thio-5-hexylthio-1,3,4-thiodiazole (C6TD), C, 58.19; H, 6.28; N, 7.99. Obsd. C, 58.04; H, 6.32; N, 8.11.

^{1}H NMR (200 MHz in $CDCl_3$, δ, ppm) : 0.86 (t, CH_3, 3H), 1.2 – 1.5 (b, CH_2, 6H), 1.75 (m, CH_2, 2H), 3.24 (t, CH_2, 2H), 4.46(s, CH_2(benzyl), 2H), 5.23 (d, H_a, J = 11 Hz, 1H), 5.72 (d, H_b, J = 17.6Hz, 1H), 6.67 (dd, H_x, J = 11, 17.6 Hz, 1H), 7.34 (m, phenyl, 4H).

C7TD:

Recrystallized from ethanol. The yield was 69 %. Melting point was 38.8 °C.

Elemental analysis: Calcd. for 2-(4'-vinylbenzyl)thio-5-heptylthio-1,3,4-thiodiazole (C7TD), C, 59.25; H, 6.58; N, 7.68. Obsd. C, 59.14; H, 6.71; N, 7.70.

^{1}H NMR (200 MHz in $CDCl_3$, δ, ppm) : 0.88 (t, CH_3, 3H), 1.2 – 1.5 (b, CH_2, 8H), 1.76 (m, CH_2, 2H), 3.25 (t, CH_2, 2H), 4.46(s, CH_2(benzyl), 2H), 5.23 (d, H_a, J = 11 Hz, 1H), 5.72 (d, H_b, J = 17.6Hz, 1H), 6.67 (dd, H_x, J = 11, 17.6 Hz, 1H), 7.34 (m, phenyl, 4H).

C8TD:

Recrystallized from ethanol. The yield was 82 %. Melting point was 41.2 °C.

Elemental analysis: Calcd. for 2-(4'-vinylbenzyl)thio-5-octylthio-1,3,4-thiodiazole (C8TD), C, 60.22; H, 6.87; N, 7.40. Obsd. C, 60.41; H, 6.73; N, 7.77.

^{1}H NMR (200 MHz in $CDCl_3$, δ, ppm) : 0.88 (t, CH_3, 3H), 1.2 – 1.5 (b, CH_2, 10H), 1.75 (m, CH_2, 2H), 3.26 (t, CH_2, 2H), 4.46(s, CH_2(benzyl), 2H), 5.23 (d, H_a, J = 11 Hz, 1H), 5.72 (d, H_b, J = 17.6Hz, 1H), 6.67 (dd, H_x, J = 11, 17.6 Hz, 1H), 7.34 (m, phenyl, 4H).

C9TD:

Recrystallized from ethanol. The yield was 83 %. Melting point was 49.0 °C.

Elemental analysis: Calcd. for 2-(4'-vinylbenzyl)thio-5-nonylthio-1,3,4-thiodiazole (C9TD), C, 61.13; H, 7.13; N, 7.13. Obsd. C, 61.01; H, 7.28; N, 7.28.

^{1}H NMR (200 MHz in $CDCl_3$, δ, ppm) : 0.88 (t, CH_3, 3H), 1.2 – 1.5 (b, CH_2, 12H), 1.75 (m, CH_2, 2H), 3.25 (t, CH_2, 2H), 4.46(s, CH_2(benzyl), 2H), 5.23 (d, H_a, J = 11 Hz,

1H), 5.72 (d, H_b, J = 17.6Hz, 1H), 6.67 (dd, H_x, J = 11, 17.6 Hz, 1H), 7.34 (m, phenyl, 4H).

C10TD:

Recrystallized from ethanol. The yield was 80 %. Melting point was 52.3 °C.

Elemental analysis: Calcd. for 2-(4'-vinylbenzyl)thio-5-decylthio-1,3,4-thiodiazole (C10TD), C, 61.97; H, 7.38; N, 6.89. Obsd. C, 61.92; H, 7.36; N, 7.07.

^{1}H NMR (200 MHz in $CDCl_3$, δ, ppm) : 0.88 (t, CH_3, 3H), 1.2 – 1.5 (b, CH_2, 14H), 1.75 (m, CH_2, 2H), 3.25 (t, CH_2, 2H), 4.46(s, CH_2(benzyl), 2H), 5.23 (d, H_a, J = 11 Hz, 1H), 5.72 (d, H_b, J = 17.6Hz, 1H), 6.67 (dd, H_x, J = 11, 17.6 Hz, 1H), 7.34 (m, phenyl, 4H).

Preparation of poly(C3TD)

Poly(C3TD) was synthesized by radical polymerization of C3TD and used as a polymer matrix in photopolymerization of CnTD. C3TD (30 g) was placed in a 4-neck, round-bottom flask (300 mL) equipped with a reflux condenser, a thermometer, a nitrogen inlet and an overhead mechanical stirrer, and 1,4-dioxane (100 mL) and ethanol (10 mL) were added. The flask was kept in a hot-bath of 70 °C. Polymerization was initiated by adding 2,2'-azobisisobutyronitrile (0.2 g) and continued for 7 h at 70 °C. The polymerization mixture was then poured into methanol (1000 mL) and the precipitate was separated by decantation. The product was purified by repeated precipitation from 1,4-dioxane solution with methanol. After drying overnight in vacuum, slightly yellowish powder was obtained. The NMR analysis showed the formation of poly(C3TD). From GPC measurement equipped with a multi-angle laser

light scattering detector (DAWN E, with operating/analysis software, Astra 4.73.04, both from Wyatt Technology Corp., Santa Barbara, CA), weight-average molecular weight, M_w, of poly(C3TD) was found to be 5.8×10^5.

^{1}H NMR (200 MHz in $CDCl_3$, δ, ppm): 1.03(t, CH_3, J = 7 Hz, 3H), 1.2 –1.6 (b, CH_2 in the main chain, 2H), 1.6 –2.1 (b, CH in the main chain, 1H), 1.79(m, CH_2, J = 7 Hz, 2H), 3.23 (t, CH_2, J = 7 Hz, 2H), 4.3 – 4.6 (b, CH_2(benzyl), 2H), 6.2 – 6.6 (b, phenyl H, 2H); 6.8 – 7.2 (b, phenyl H, 2H).

Preparation of 2-(4'-vinylbenzyl)thio-5-benzylthio-1,3,4-thiadiazole (BzTD) and its polymerization

BzTD and its homopolymer, poly(BzTD) were prepared by the procedures as described in Chapter 2.

Photopolymerization

Photopolymerization of the styrene derivatives was carried out in the matrix of solid polymer and followed up to high monomer conversion by Fourier transform real-time infrared (RT-IR) [8, 14-17] spectroscopy, which was conducted on a Bio-rad FTS-40 (Bio-rad Laboratories, Inc., Hercules, CA) with an operating/analysis software, Win-IR. Sample preparations and photopolymerization procedures were described in detail in Chapter 2 and 3.

Monomer conversion was calculated according to the following equation:

$$conversion = \frac{A(990)_0 - A(990)_t}{A(990)_0}$$

where $A(1171)_0$ and $A(1171)_t$ denote absorbance at 1171 cm^{-1} at the beginning and time t of UV irradiation, respectively.

The rate of polymerization, R_p, was calculated from the following equation;

$$R_p\,(mol\,L^{-1}\,s^{-1}) = -\frac{d[M]}{dt} = [M]_0\,\frac{d(conversion)}{dt}$$

Since individual data points of peak intensities at 990 cm^{-1} were somewhat scattered, the calculated value of R_p from the relative differences of peak intensities at an arbitrary time interval scattered significantly. Therefore, 10th-order polynominal approximation was applied to all time-conversion curves and such polynominal curve fit was differentiated to obtain R_p at an arbitrary polymerization time.

6-3. RESULTS AND DISCUSSION

6-3-1. Photopolymerization of CnTD in polystyrene matrix

Photopolymerization reactivities of CnTD monomers were investigated in polystyrene matrix. The number of alkyl carbons in the alkylthio group at 5-position of 1,3,4-thiadiazole group was systematically varied and the effect of the size of this alkyl substituent on their polymerization reactivity was investigated. Time-conversion curves obtained for these monomers were shown in Figure 6-1. In all cases, polymerization started without any noticeable induction period and proceeded with moderate polymerization rate. Final conversions attained were in the range of 0.7 ~ 0.8 for all monomers. C9TD and C10TD showed the highest final conversions among others. Maximum polymerization rate, $R_{p(max)}$, observed for each CnTD monomer was plotted against the number of carbon atoms in the alkyl substituent of CnTD as is seen in Figure 6-2(a). Highest polymerization rate was obtained for C2TD and others were around 0.01 $mol{\cdot}L^{-1}{\cdot}s^{-1}$ and seems not to depend on the number of carbon atoms in the alkyl substituent. Therefore, the size of the alkyl substituent was found not to affect essentially the polymerization reactivity of CnTD monomers in polystyrene matrix. Photodecomposition process of PMS was concurrently observed by monitoring the

absorption intensity at 1171 cm^{-1} of polymerization system and photodecomposition rate was calculated by the differential of time-photodecomposition ratio curve of PMS. Maximum photodecomposition rate, $R_{d(max)}$, of PMS, which was attained in the beginning of the irradiation, was plotted in order to compare the effect of the structure of CnTD monomers on the photodecomposition rate of PMS, as shown in Fig. 6-2(b). Lowest value of $R_{d(max)}$ was observed for the polymerization of C1TD and highest value of $R_{d(max)}$ was obtained for C7TD. These differences in $R_{d(max)}$ are considered to reflect the reactivity of each monomer to the initiating radicals derived from photodecomposition of PMS molecules.

In the absence of these monomers, photodecomposition rate of PMS was determined separately and the obtained value of $R_{d(max)}$ was ca. 2×10^{-4} $mol\cdot L^{-1}\cdot s^{-1}$ in polystyrene matrix. This value is much lower than those obtained in the presence of these monomers and the increase of $R_{d(max)}$ should imply the contribution of initiation reaction to prevent recombination of initiating PMS radical with chlorine atom which is by-produced by the photodecomposition of PMS molecule. Except for C1TD, other monomers showed almost identical effects on photodecomposition rate of PMS and values of $R_{d(max)}$ were around 1×10^{-3} $mol\cdot L^{-1}\cdot s^{-1}$, which is about 5-fold of that in the absence of monomer. Kinetic chain length, $kcl_{(max)}$, determined by the ratio of $R_{p(max)}$ to $R_{d(max)}$, is a measure of polymerization efficiency and represents the number of monomer molecrized per one molecule of photodecomposed PMS.

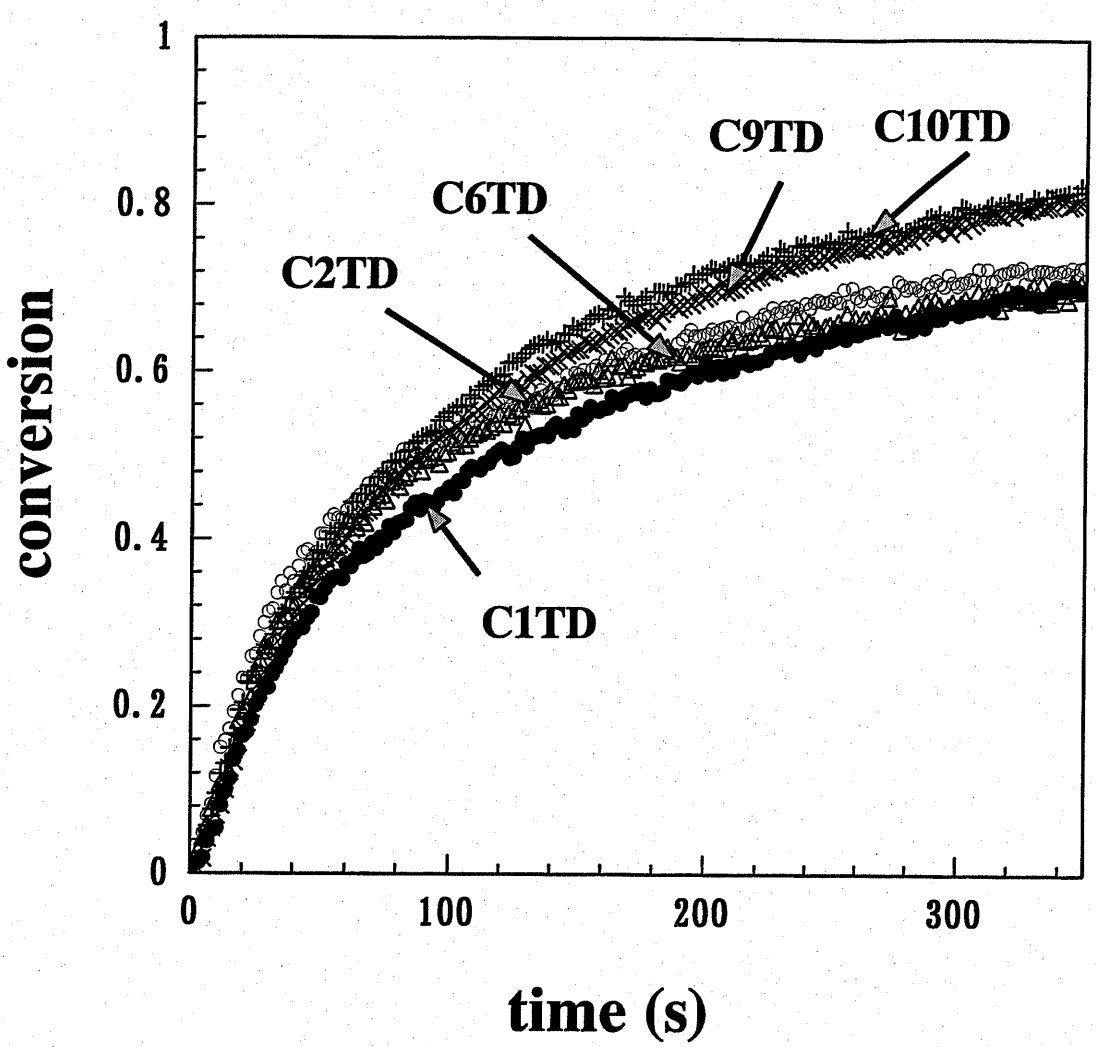

Figure 6-1. Photopolymerization profiles of CnTD monomers in polystyrene matrix initiated by PMS under the irradiation of 365-nm light. PMS/CnTD/polystyrene = 0.0042/0.10/0.20 (wt/wt/wt). Light intensity = 1.6 $mW \cdot cm^{-2}$. Photopolymerization was carried out at room temperature under argon atmosphere.

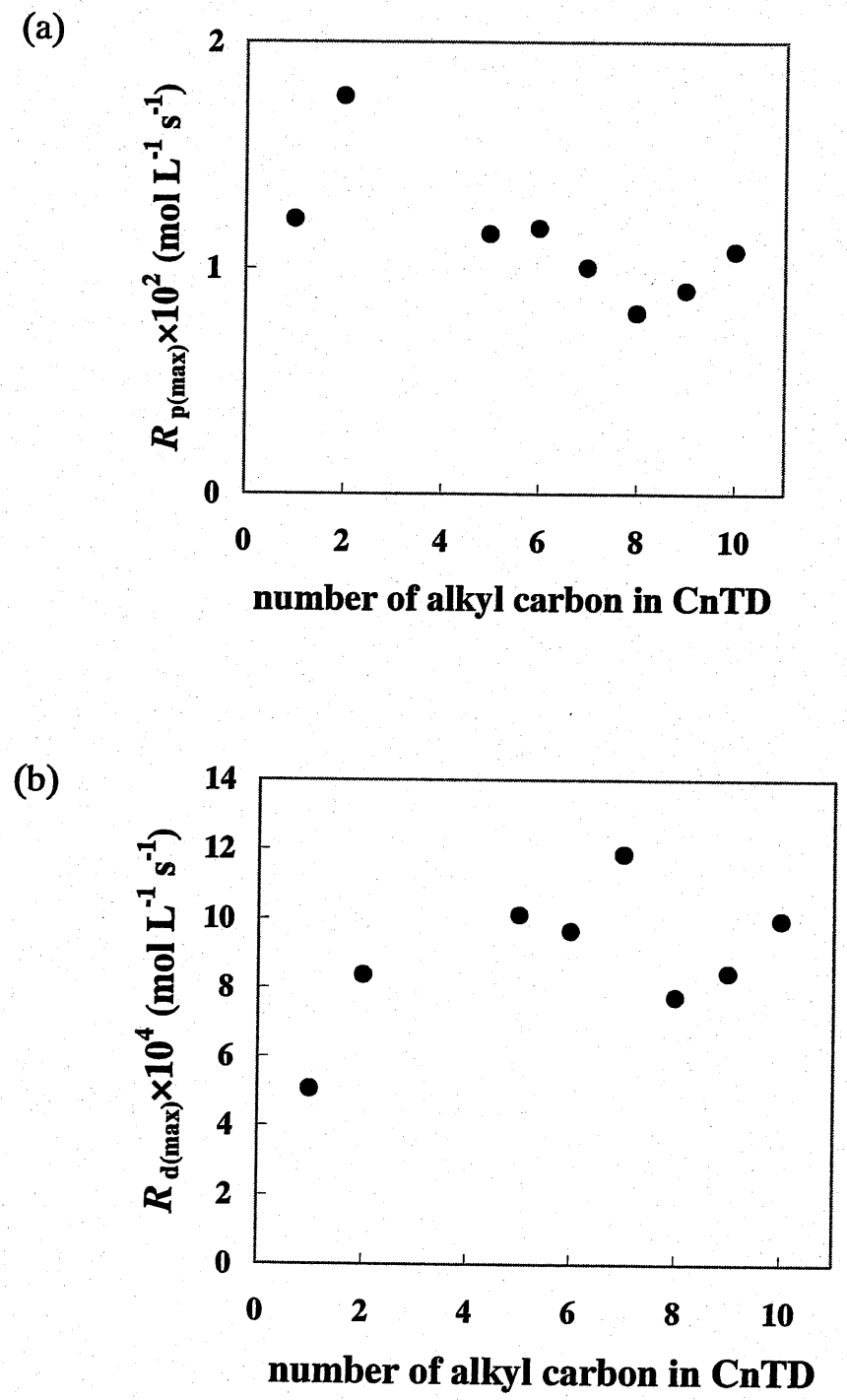

Figure 6-2. Dependence of maximum polymerization rate, $R_{p(max)}$, (a) and maximum decomposition rate of PMS, $R_{d(max)}$, (b) on alkyl chain length of CnTD in polystyrene matrix.

In Figure 6-3, the calculated values of $kcl_{(max)}$ were plotted against the number of carbon atoms in the alkyl substituent of CnTD. C1TD and C2TD are found to be polymerized with ca. 20 molecules of these monomers per a PMS molecule photodecomposed. Others are less efficient and obtained values of $kcl_{(max)}$ were around 10. These relatively smaller values as compared with those reported by Decker et al. indicate that average numbers of monomer molecules available to each initiating radical are limited to such smaller values and the existence of polystyrene matrix restricts the propagation of radical chain within ten to twenty of monomer molecules, which may not be appropriate to be called as photopolymerization.

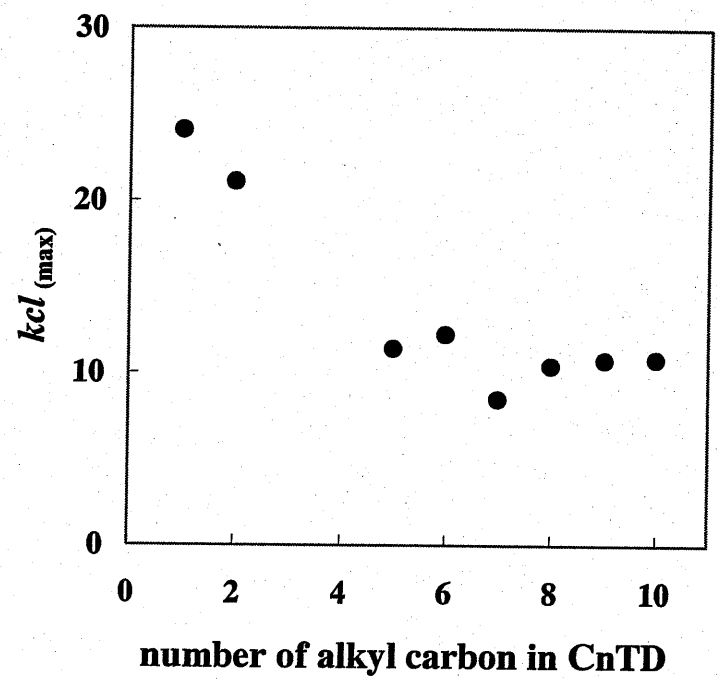

Figure 6-3. Dependence of kinetic chain length on the alkyl chain length in CnTD for the PMS-initiated photopolymerization of CnTD in polystyrene matrix. Polymerization condition was the same as that in Fig. 6-2.

6-3-2. Photopolymerization of CnTD in poly(C3TD) matrix

Comparisons of polymerization behavior of CnTD were also carried out in poly(C3TD) matrix. Drastic difference in polymerization behavior of CnTD was observed as shown in Figure 6-4. Highest polymerization efficiency was observed in the case of C1TD and as the size of the alkyl substituent in CnTD monomer increases, both polymerization rate and final conversion are decreased. In particular, final conversions reached almost 100% for the polymerization of C1TD and C4TD. On the other hand, C9TD and C10TD were found to be the least photopolymerizable monomers in poly(C3TD) matrix, although these two monomers showed highest polymerization reactivity in polystyrene matrix as described before. In Figure 6-5, both maximum photopolymerization rate, $R_{p(max)}$, and maximum photodecomposition rate, $R_{d(max)}$, of PMS are plotted. Polymerization rate of C1TD in poly(C3TD) matrix is about 3 times higher than that in polystyrene matrix. However, C6TD and other homologues with the increased number of the alkyl carbon showed decreased polymerization reactivity in poly(C3TD) than those in polystyrene matrix. As for the photodecomposition rate of PMS, a similar tendency is seen in Fig. 6-5(b). Apparently, both photopolymerization reactivity and initiation efficiency are decreased for the monomers of C6TD and higher homologues. Kinetic chain length (Figure 6-6) obtained for C1TD was increased up to ca. 40, which is about 2-fold of that in polystyrene matrix. C9TD and C10TD showed values of $kcl_{(max)}$ as low as ca. 5 and this small number indicates that true polymerization did not take place for these two monomers. From C4TD to C8TD, values of $kcl_{(max)}$ were around the same of those obtained in polystyrene matrix. In summary, poly(C3TD) matrix enhances the polymerization reactivity of C1TD and deactivates the polymerization reactivity of

both C9TD and C10TD. The increase of kcl in the case of C1TD indicates that in poly(C3TD) matrix, C1TD monomer molecules might be oriented in a favorable way to the photopolymerization.

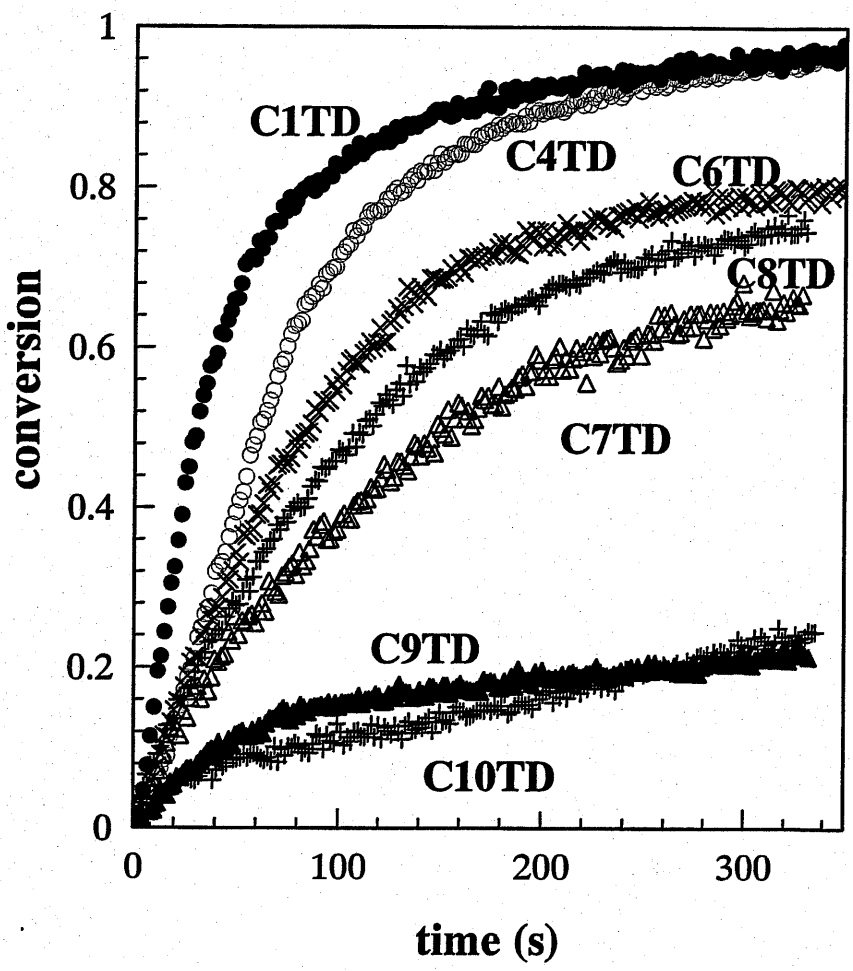

Figure 6-4. Photopolymerization behaviors of CnTD monomers in poly(C3TD) matrix initiated by PMS under the irradiation of 365 nm light. PMS/CnTD/poly(C3TD) = 0.0042/0.10/0.20 (wt/wt/wt). Light intensity = 1.6 $mW \cdot cm^{-2}$. Photopolymerization was carried out at room temperature under argon atmosphere.

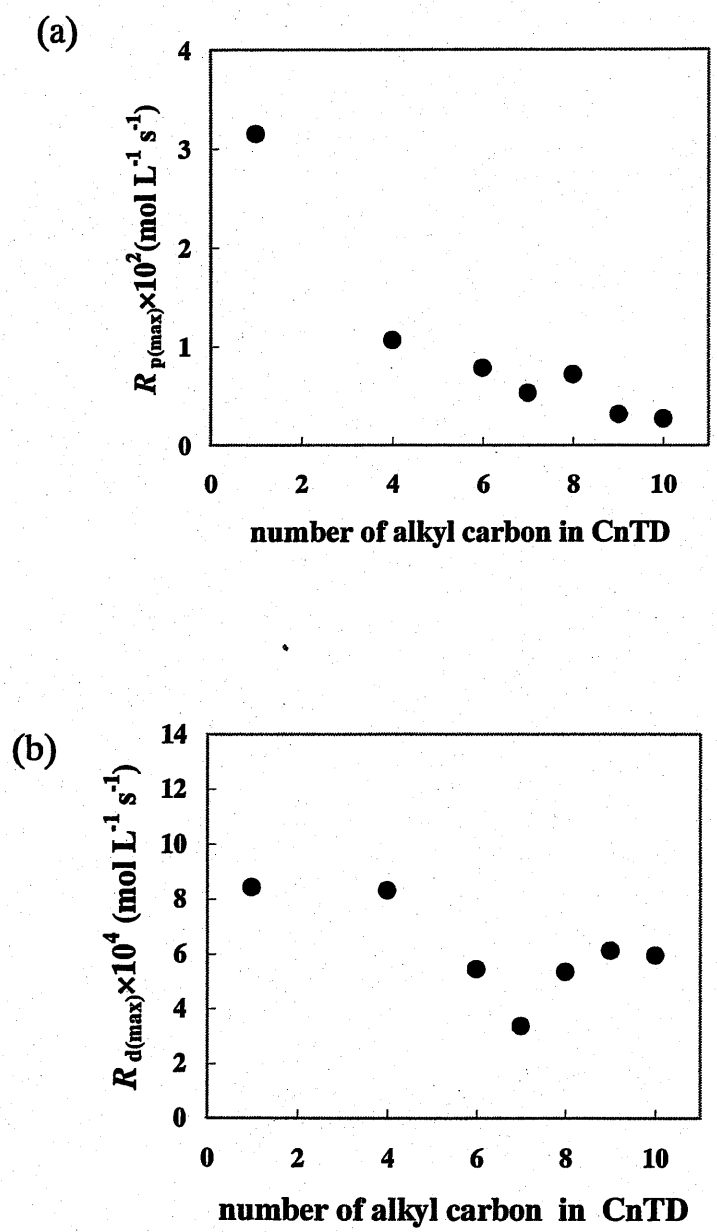

Figure 6-5. Dependence of maximum polymerization rate, $R_{p(max)}$, (a) and maximum decomposition rate of PMS, $R_{d(max)}$, (b) on alkyl chain length of CnTD in poly(C3TD) matrix.

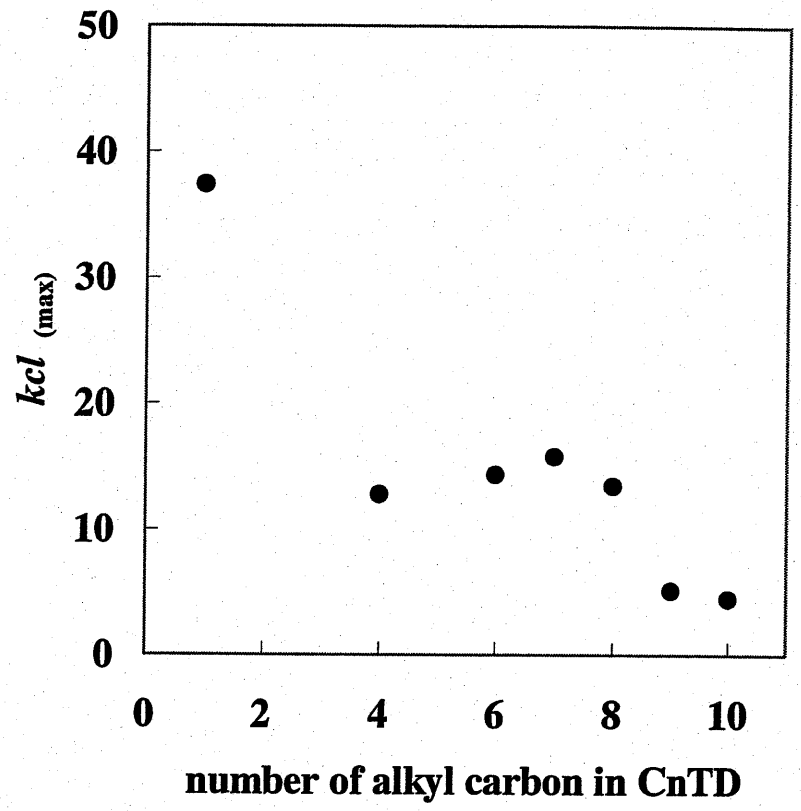

Figure 6-6. Dependence of kinetic chain length on the alkyl chain length in CnTD for the PMS-initiated photopolymerization of CnTD in poly(C3TD) matrix.

6-3-3. Photopolymerization of CnTD in poly(BzTD) matrix

Comparisons of polymerization behavior of CnTD were again carried out by using poly(BzTD) matrix. The pendant substituent of benzylthio group was introduced to investigate the effect of phenyl ring attached to the pendant thiadiazole group on the polymerization behavior of CnTD in comparison with propyl substituent in poly(C3TD). Drastic acceleration of polymerization rate of C1TD and deactivation for C9TD and C10TD were observed also in this polymer matrix, as shown in Figure 6-7. C6TD showed decreased polymerization reactivity as compared with the result obtained in poly(C3TD) matrix. In Figure 6-8, maximum polymerization rate was decreased linearly with the increase in the number of carbon atoms in the alkyl substituent of CnTD and from C6TD to C10TD except C8TD the polymerization rate of these monomers in poly(BzTD) matrix were smaller than those in polystyrene matrix. The maximum polymerization rate of C1TD was further increased up to ca. 0.04 $mol \cdot L^{-1} \cdot s^{-1}$ which is about 4-fold of that in polystyrene matrix. In Figure 6-8(b), maximum photodecomposition rate, $R_{d(max)}$, of PMS are plotted against the number of alkyl carbons in CnTD. It is characteristic that for C6TD to C10TD except C8TD, the decomposition rates of PMS were suppressed as compared with those for other monomers. Kinetic chain length (Figure 6-9) obtained for C1TD was ca. 40, which is same as that in poly(C3TD) matrix. C9TD and C10TD showed values of $kcl_{(max)}$ as low as ca. 5, again and this small number indicates that no effective polymerization takes place for these two monomers. In summary, poly(BzTD) matrix enhances the polymerization reactivity of CnTD of smaller alkyl substituents (C1 and C2) and deactivates the polymerization reactivity of both C9TD and C10TD.

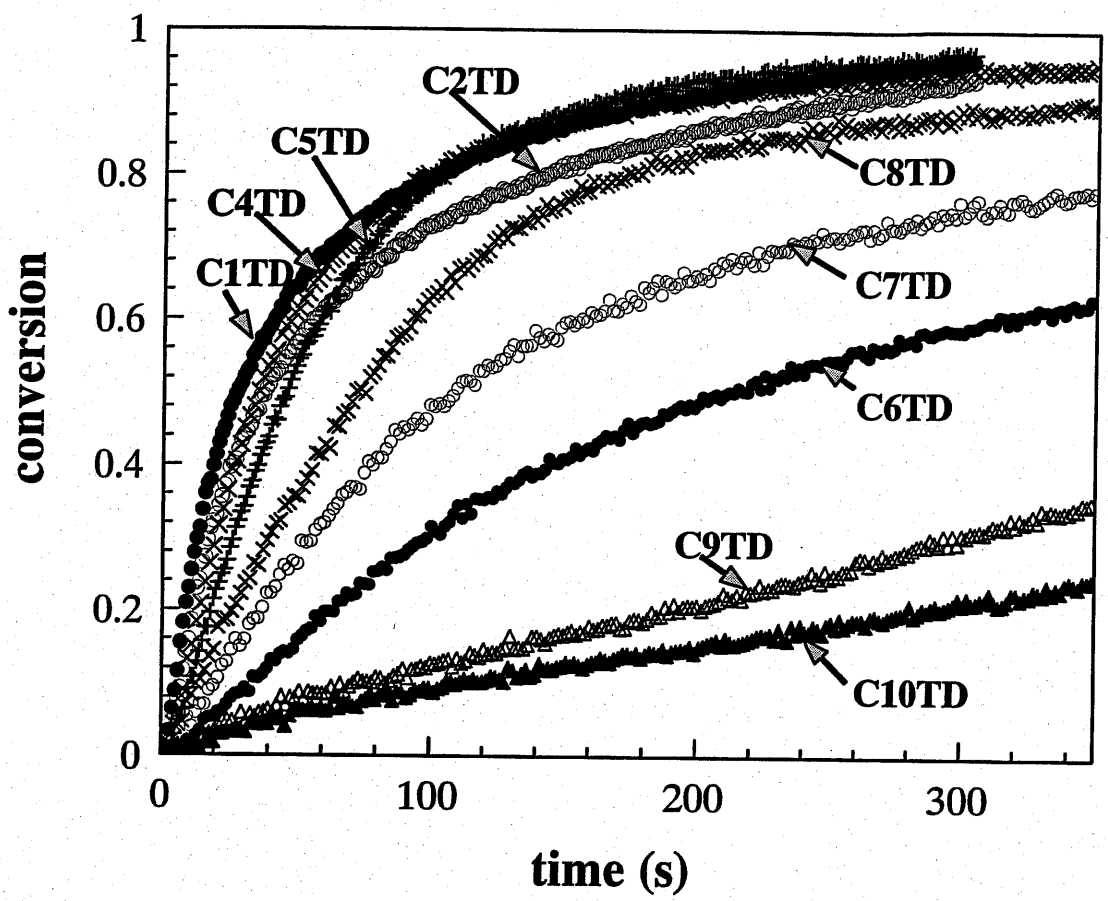

Figure6-7. Photopolymerization behaviors of CnTD monomers in poly(BzTD) matrix initiated by PMS under the irradiation of 365 nm light. PMS/CnTD/poly(BzTD) = 0.0042/0.10/0.20 (wt/wt/wt). Light intensity = 1.6 $mW \cdot cm^{-2}$. Photopolymerization was carried out at room temperature under nitrogen atmosphere.

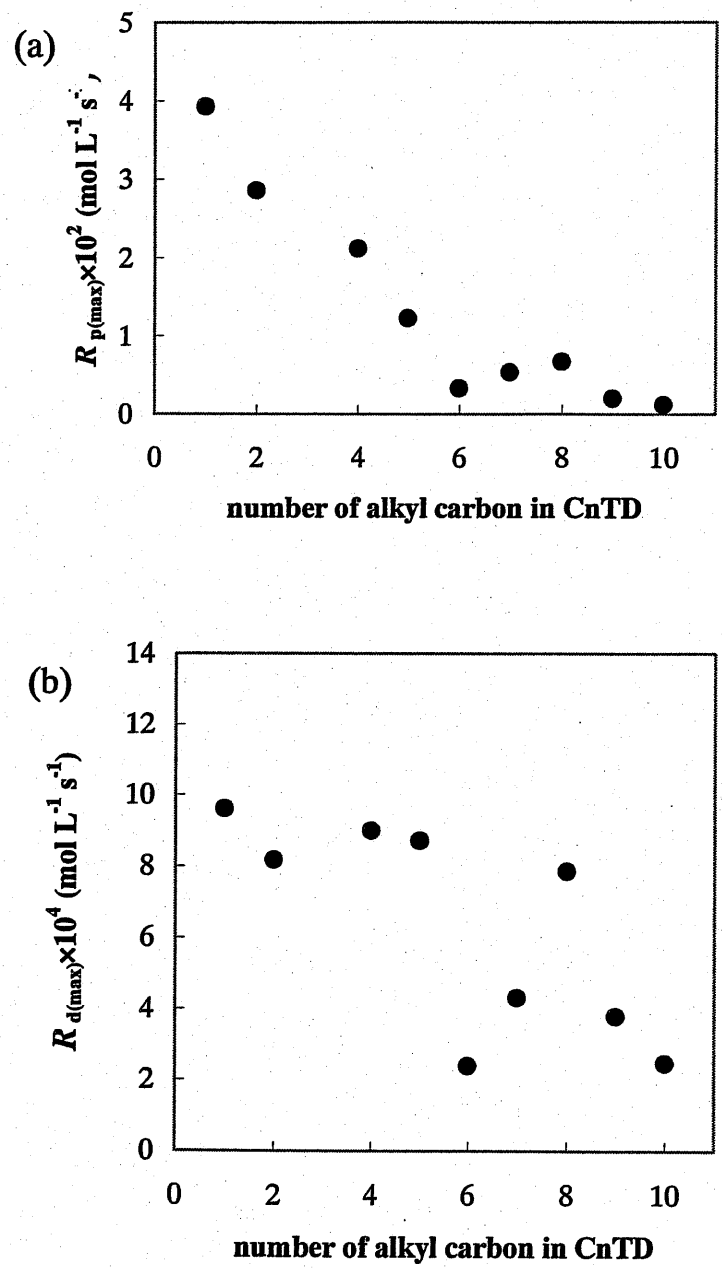

Figure 6-8. Dependence of maximum polymerization rate, $R_{p(max)}$, (a) and maximum decomposition rate of PMS, $R_{d(max)}$, (b) on alkyl chain length of CnTD in poly(BzTD) matrix.

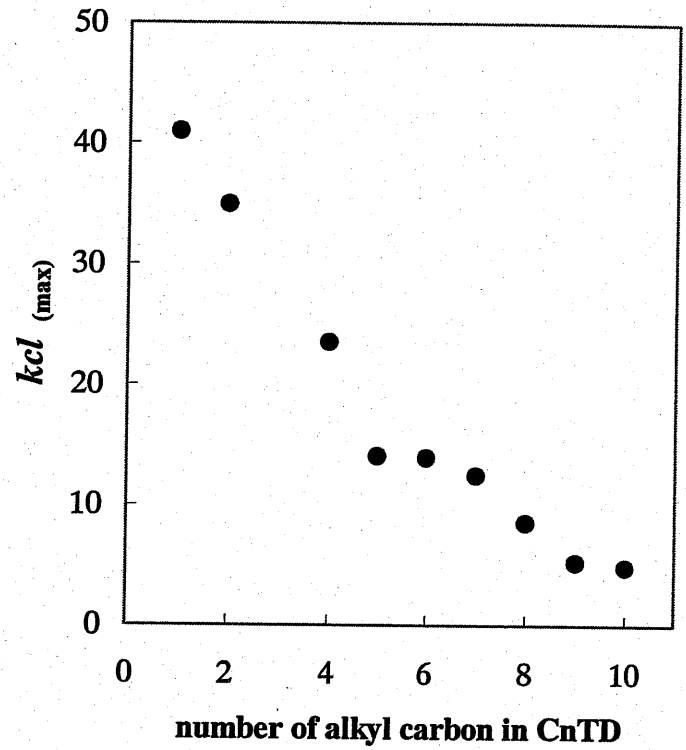

Figure 6-9. Dependence of kinetic chain length on the alkyl chain length in CnTD for the PMS-initiated photopolymerization of CnTD in poly(BzTD) matrix.

In order to explain all the data obtained so far, specific interactions between polymer matrix and CnTD monomers are considered. In the cases of poly(C3TD) and poly(BzTD), these polymers have pendant 1,3,4-thiadiazole groups which are believed to assemble with each other and with CnTD monomers through intermolecular interactions caused by London dispersion force characteristic to highly polarizable benzylthio-substituted 1,3,4-thiadiazole group. Molecular orbital calculation based on the PM3 method gave a value of polarizability as large as 172 a.u. for a C1TD molecule in its most stable conformation. This result suggests both possibilities of locally assembled structures of these monomers themselves and another assembled structures of those incorporated with the pendant thiadiazole groups of the polymer matrix. In polystyrene matrix, cluster structure of aggregated monomer molecules had been confirmed as described in Chapter 2 and in this case, polymerization rate was not affected by the size of the alkyl substituent. Inside the aggregates dispersed in the glassy matrix of polystyrene, monomer molecules might be frozen and their mutual alignments should be at random fashion; therefore the polymerization proceeded at moderate rate and no size effect was observed. On the other hand, in poly(C3TD) and poly(BzTD) matrices, monomer molecules should interact with pendant thiadiazole groups of the matrix polymer (which is apparent from the observed decrease in T_g, see Table 2-1 in Chapter 2 of this thesis) and aggregation of monomer molecules should incorporate such pendant substituents. Since T_gs of the monomer/polymer blends are close to room temperature (*e.g.*, 25 °C for C1TD/poly(BzTD) blend), rotational and vibrational freedom of molecular motions should be greatly increased. We considered that when the size of the alkyl substituent in CnTD is relatively small, then CnTD molecules might be allowed to rotate inside the interstices of the pendant groups of the

polymer matrix such as poly(C3TD) or poly(BzTD), rearranging themselves with alkyl group headed toward the backbone chain, as schematically illustrated in Figure 6-10(a). Since styrenyl groups are located outside of the congested pendant groups of the matrix polymer in this case, rotational degree of freedom for these styrenyl groups would be retained and polymerization of these styrenyl groups would proceed efficiently. On the other hand, when the size of the alkyl substituent in CnTD is relatively large, such rotation and rearrangements of molecules inside the interstices of the pendant groups of the matrix polymer would be difficult to occur and molecular assembly would be fixed at random fashion. In such a case, polymerization would be difficult to proceed within the densely packed molecular assembly inside the interstices of pendant groups of the polymer matrix.

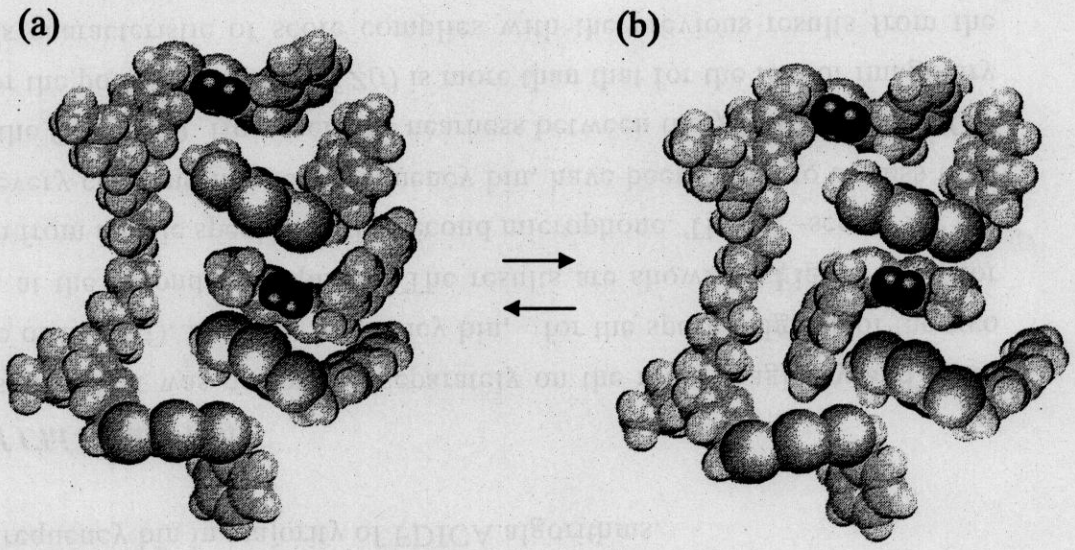

Figure 6-10. Schematic illustrations indicating possible mutual alignments of C1TD monomer molecules inside the interstices of the pendant thiadiazole groups in poly(BzTD) matrix. C1TD molecules are allowed to rotate and mutual alignments such as (a) and (b) are in rapid equilibrium.

6-4. CONCLUSION

Our initial purpose of establishing an efficient photopolymerization system, which consists of styrenyl monomer in combination with an appropriate photoinitiator in a suitable polymer matrix, was attained by optimizing the size of alkyl substituent at 5-position of 1,3,4-thiadiazole group with a choice of PMS as photoinitiator and poly(BzTD) as matrix polymer. High polymerization rate and reduced concentration of residual monomer were attained in this study. When the size of alkyl substituent is relatively small, polymerization proceeded rapidly and kinetic chain length (*kcl*) increased up to ca. 40, whereas larger alkyl substituents resulted in decreased polymerization reactivity and smaller *kcl* values. A possible explanation to the observed experimental results should be that monomer molecules are assembled with the pendant groups of matrix polymer and molecular rearrangements inside the assembled structure would determine the polymerization reactivity. These obtained results are fully consistent with previously obtained results described in the preceding chapters.

REFERENCES

1. Moussa, K. ; Decker, C., J. Polym. Sci. Part A. Polym. Chem., 1993, 31, 2197.
2. Jansen, J.F.G.A. ; Dias, A. A. ; Dorschu, M. ; Coussens, B., Polym. Prepr., 2001, 42, 769.
3. Jansen, J.F.G.A. ; Dias, A. A. ; Dorschu, M. ; Coussens, B., Macromolecules, 2002, 35, 7529.
4. Matsumoto, A. ; Matsumura, T. ; Aoki, S., J. Chem. Soc., Chem. Commun., 1994, 1389.
5. Tashiro, K. ; Kamae, T. ; Kobayashi, M. ; A. Matsumoto, A. ; Yokoi, K. ; Aoki, S., Macromolecules, 1999, 32, 2449.
6. Odani, T. ; Matsumoto, A., Macromol. Rapid Commun., 2000, 21, 40.
7. Matsumoto, A. ; Nagahama, S. ; Odani, T., J. Am. Chem. Soc., 2000, 122, 9109.
8. Matsumoto, A. ; Odani, T. ; Sada, K. ; Miyata, M. ; Tashiro, K., Nature, 2000, 405, 328.
9. Williamson, S. E. ; Kang, D. ; Hoyle, C. E., Macromolecules, 1996, 29, 8656.
10. Andersson, H. ; Trollsas, M. ; Gedde, U. W. ; Hult, A., Macromol. Chem. Phys., 1995, 196, 3667.
11. Guymon, C. A. ; Hoggan, E. N. ; Clark, N. A. ; Rieker, T. P. ; Walba, D. M. ; Bowman, C. N., Science, 1997, 275, 57.
12. Guymon, C. A. ; Bowman, C. N., Macromolecules, 1997, 30, 5271.

Chapter 7

Preparation of polymers bearing pendant styrenyl group and its photopolymerization behavior in solid state

7-1. INTRODUCTION

In various industrial applications, reactive prepolymer having at least two polymerizable groups serves to produce the necessary viscosity and performance for effective crosslinking. Photopolymerizable prepolymers can be divided into three types, depending on the positions of the reactive groups in the polymer molecules:[1]

(1) Where the reactive groups form part of the polymer chain as in the case of unsaturated polyesters as described before. Other examples classified in this category include epoxidized natural rubber (effective in cationic polymerization).[2-6]

(2) Where the reactive groups are present in the endgroups of a linear or branched polymer, and as for example so-called epoxy acrylates are the representatives for this category.[1]

(3) Where the reactive groups are introduced in the pendant groups of a polymer. Such polymers can be prepared, for instance, by the reaction of a precursor polymer with a compound which possesses both a polymerizable group and a second reactive group of a different kind to combine with the precursor polymer.[1]

A variety of polymers classified to the last category are most extensively investigated, since the most effective and dense crosslinking of the polymerization system can be

attained by the reactions between the pendant reactive groups. Both cationically and radically photopolymerizable groups are introduced to various types of backbone polymers. Polydimethylsiloxanes (PDMSs) are one of the most extensively utilized polymers as starting materials to prepare various types of photoactive polymers, since they present unique characteristics such as high thermal and chemical stabilities, high flexibility and hydrophobicity. Glycidyl ether[7] and cyclohexane oxide[8] were introduced to the siloxane backbone by the hydrosilation method. PDMSs containing acrylic and methacrylic ester groups, linked to the siloxane backbone, have been synthesized.[9-15] PDMSs bearing pendant styrenyl groups have been prepared[16,17] and its photo-crosslinking via a cationic mechanism using mainly onium salts as photoinitiators has been investigated.[18] Natural rubber is also another example for modification of its structure with pendant acrylic esters.[19, 20] All these polymers are effective to obtain highly crosslinked materials by themselves or through the blends of these polymers with monomers dispersed in such photoactive matrices.

In the previous chapters, photopolymerizability of styrenyl monomers bearing 1,3,4-thiadiazole group was discussed in relation to their structures and interaction with polymer matrix. We attempted to introduce such styrenyl group onto polymer backbone to make reactive polymer matrix in an aiming to concretize a highly effective photopolymerization system which can produce three-dimensional polymer network upon irradiation of UV light. In such a case, pendant styrenyl group would polymerize in the presence of photoinitiator and intermolecular crosslinking would be instantly formed. Photopolymerization behavior of pendant styrenyl group is investigated in comparison with corresponding low-molecular-weight styrenyl monomers and then copolymerization of these different types of styrenyl groups is attempted in this Chapter.

7-2. EXPERIMENTAL

7-2-1. Materials

2-(4'-methoxystyryl)-4,6-bis(trichloromethyl)-1,3,5-triazine (PMS) was purchased from Panchim (Cedex, France) and used without further purification. 1,4-Dioxane (Wako Chemicals Ind. Ltd.) was used without further purification. 2,5-Dimercapto-1,3,4-thiadiazole was purchased from Tokyo Kasei Kogyo Co., Ltd.(Tokyo, Japan) and used without further purification. 4-Chloromethyl styrene was purchased from Seimi Chemical Co. Ltd. (Kanagawa, Japan) and used without further purification. Poly(4-hydroxystyrene) (PHM–C) was obtained from Maruzen Petrochemical Co. Ltd. (Tokyo, Japan) and used as received. Methanol solution containing 40 wt% of TBAH(tetra(n-butyl)ammonium hydroxide)(350g, 0.54 mole) was obtained from Nippon Fine Chemical Co. Ltd.(Tokyo, Japan). As a polymerization inhibitor, N-nitrosophenylhydroxylamine aluminium salt, $[(C_6H_5N(NO)O]_3Al$, (Q-1301, Wako Chemicals Ind. Ltd.) was used without further purification.

7-2-2. Preparation of monomers

C1TD, BzTD and C3TD2 were prepared according to the procedures described in Chapter 2.

C1TD

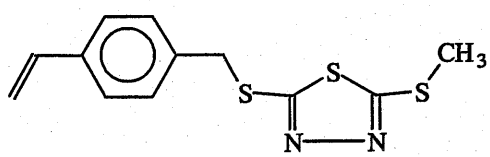

BzTD

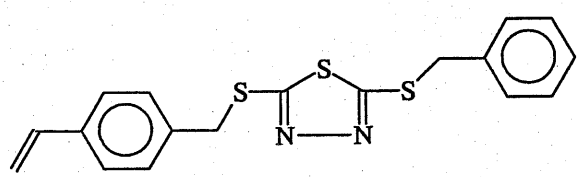

C3TD2

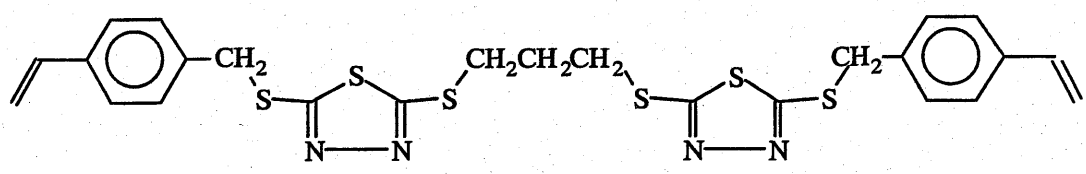

7-2-3. Preparation of homopolymers bearing pendant styrenyl group

Two types of homopolymers bearing pendant styrenyl group were prepared. One was prepared by the polymerization of triethylamine salt of SHTD followed by the addition of 4-chloromethyl styrene. Another homopolymer was prepared by the reaction of poly(4-hydroxystyrene) with 4-chloromethy styrene.. The purpose of preparations of these two polymers was to investigate the effect of linking group on the photopolymerization reactivity of styrenyl group attached to the polymer chain.

7-2-3(a) Preparation of poly[4-methylenethio-1',3',4'-thiadiazolyl-2'-(4"-vinylbenzylthio) styrene] (poly(VBzTD))

SHTD (50g, 0.188 mol) was placed in a 4-neck, round-bottom flask (500 mL) equipped with a reflux condenser, a thermometer, a nitrogen inlet and an overhead mechanical stirrer, and ethanol (150 mL) and distilled water (25 mL) were added. Under nitrogen atmosphere, triethylamine (20g, 0.198 mol) was added and SHTD was dissolved completely. The flask was kept in a hot-bath of 70 °C. Polymerization was initiated by adding 2,2'-azobisisobutyronitrile (0.5 g) and continued for 10 h at 70 °C.

The polymerization mixture was then transferred to a 1000 mL flask on a stirrer-hot plate and stirred at room temperature. 4-Chloromethyl styrene (30g, 0.2 mol) and Q-1301(polymerization inhibitor, 0.1g) were gradually added to the mixture under

vigorous stirring. As the reaction proceeded, the resulted polymer was precipitated from the solution and then, 1,4-dioxane (200mL) was added to keep the reaction mixture homogeneous. The solution temperature was raised to 50 °C and the reaction was continued for 5 h at this temperature and then left at room temperature overnight.

The reaction mixture was poured into methanol (2000 mL) and the precipitate was separated by decantation. The product was purified by repeated precipitation from 1,4-dioxane solution with methanol. After drying overnight in vacuum, slightly yellowish rubbery solid was obtained. The nmr analysis showed the formation of poly(VBzTD). Poly(VBzTD) had been found to form insoluble gel in a few weeks when stored in bulk even in a refrigerator. Therefore, the obtained polymer was dissolved in 1,4-dioxane (20 wt %) together with N-nitrosophenylhydroxylamine aluminium salt, Q-1301 (0.1 wt % relative to the amount of the polymer) and stored in a refrigerator.

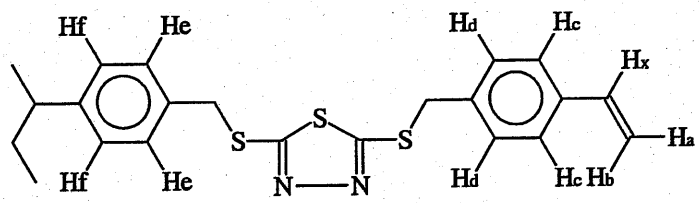

poly(VBzTD)

^{1}H NMR (200 MHz in $CDCl_3$, δ, ppm): 1.0 –1.5 (b, CH_2 in the main chain, 2H); 1.5 –2.2 (b, CH in the main chain, 1H); 4.3 – 4.5 (b, CH_2, 4H); 5.2 (d, Ha, 1H); 5.65 (d, Hb, 1H);6.1 – 6.6 (b, Hf, 2H); 6.4 – 6.8 (b, Hx, 1H);6.8 – 7.2 (b, He, 2H); 7.2–7.35 (b, Hc, Hd, 4H).

From GPC measurement equipped with a multi-angle laser light scattering detector (DAWN E, with operating/analysis software, Astra 4.73.04, both from Wyatt

Technology Corp., Santa Barbara, CA), weight-average molecular weight, M_w, and number-average molecular weight, M_n of poly(VBzTD) was found to be 1.4×10^6 and 5.5×10^5, respectively.

7-2-3(b) Preparation of poly[4-(4'-vinylbenzyloxy)styrene] (poly(VBzS))

Poly(4-hydroxystyrene) (PHM–C, 60g) was dissolved in THF (200g) and methanol solution containing 40 wt% of TBAH(tetra(n-butyl)ammonium hydroxide)(350g, 0.54 mole) at 60 °C. Into this solution 4-chloromethyl styrene (82g, 0.54mol) and Q-1301(0.1g) were added under vigorous stirring. The reaction was carried out at 60 °C for 20 h. Then the reaction mixture was left at room temperature and poured into methanol (2000mL). The precipitated polymer was collected by decantation and dissolved in acetone (300mL). This acetone solution was poured into methanol (2000mL) again and the precipitated polymer became powdery and recovered by filtration and washed with methanol several times. The polymer was dried under reduced pressure and stored in a refrigerator.

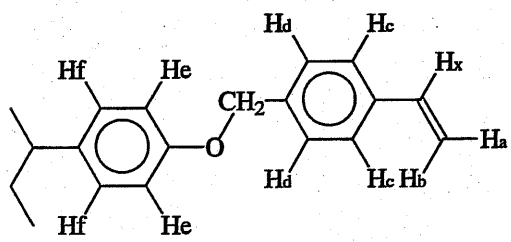

poly(VBzS)

^{1}H NMR (200 MHz in $CDCl_3$, δ, ppm): 1.0 –1.6 (b, CH_2 in the main chain, 2H); 1.5 –2.4 (b, CH in the main chain, 1H); 4.7 – 5.1 (b, CH_2, 2H); 5.2 (d, Ha, 1H); 5.7 (d, Hb, 1H);6.2 – 7.0 (b, He, Hf, Hx, 5H); 7.2–7.35 (b, Hc, Hd, 4H).

7-2-3(c) Preparation of copolymer, poly(VBzTD-co-BzTD)

In the preparation of poly(VBzTD) described above, both vinylbenzyl and benzyl groups were introduced with various molar ratios to the precursor, poly(SHTD), in an attempt to investigate the effect of molar ratio of pendant styrenyl group.

Solution of triethylamine salt of poly(SHTD) was prepared by the same procedure as described in the preparation of poly(VBzTD). The obtained solution was divided into four portions and in each portion an equimolar amount of mixture of 4-chloromethyl styrene and benzyl chloride with different molar ratios (varied from 0.2/0.8 to 0.8/0.2) was added at 50°C. In each run, the reaction was continued for 5 h and left at room temperature overnight. The reaction mixture was then poured into large amounts of methanol and the precipitate was separated by decantation. The products were purified by repeated precipitation from 1,4-dioxane solution with methanol. After drying overnight in vacuum, slightly yellowish rubbery solids were obtained. The obtained copolymers were dissolved in 1,4-dioxane together with Q-1301 as polymerization inhibitor and stored in a refrigerator.

7-2-4. Photopolymerization

Photoinitiated polymerization of pendant styrenyl group was carried out in a dry film casted on KRS (KRS-5; TlBr (thallium bromide) (42 %) / TlI (thallium iodide) (58 %)) disk (diameter = 3 cm) from a solution of polymer obtained by the procedures described above. A solution of polymer (1.0 g, containing 0.20 g of solid polymer) was diluted with 1,4-dioxane (1 g) and photoinitiator, 2-(4'-methoxystyryl)-4,6-bis(trichloromethyl)-1,3,5-triazine, (PMS), (0.0042 g or varied), was added into this solution. An exact amount (0.110 g) of the solution was eluted on KRS disk and dried.

The thickness of cast film on KRS disk was calculated to ca.15 μm. Real-time FT-IR (RT-IR) spectroscopy[19-25] was conducted as described in Chapter 2.

All measurements were carried out at room temperature under argon atmosphere. The infrared absorption band at 990 cm^{-1} (vinyl, δCH, bending, out-of-plane) was monitored.

Conversion of vinyl group was calculated according to the following equation:

$$conversion = \frac{A(990)_0 - A(990)_t}{A(990)_0}$$

in which $A(990)_0$ and $A(990)_t$ denote the peak absorbance at 990 cm^{-1} before UV-irradiation and at time t (s), respectively. The rate of polymerization, R_p, was calculated from the following equation;

$$R_p\,(mol\,L^{-1}\,s^{-1}) = -\frac{d[M]}{dt} = [M]_0\frac{d(conversion)}{dt}$$

7-3. RESULTS AND DISCUSSION

7-3-1. Characterization of polymers bearing pendant styryl groups

Figure 7-1 shows ^{1}H-nmr charts of poly(VBzS) and poly(VBzTD) in $CDCl_3$ solutions and these spectra are agreed well with the expected structures of the polymers. The molecular weight distribution of poly(VBzS) and the precursor, poly(4-hydroxystyrene) were determined as; $M_w = 11\times10^3$, $M_n = 7.4\times10^3$ for poly(VBzS) and $M_w = 5.4\times10^3$, $M_n = 2.8\times10^3$ for poly(4-hydroxystyrene). The calculated increase in molecular weight is ca. 2-fold of that of the precursor polymer and the observed increase in wight average molecular weight agreed well with the expected value.

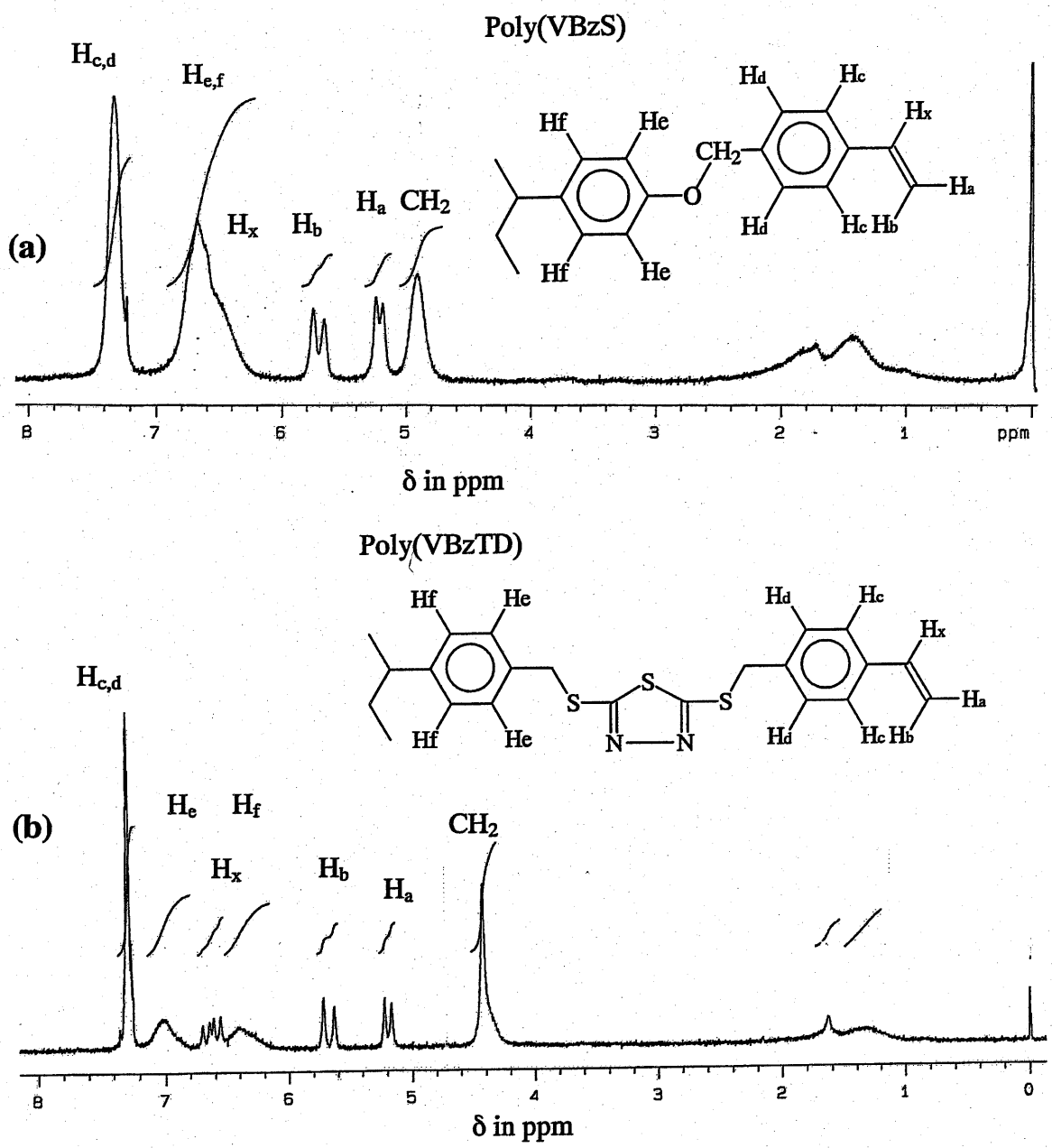

Figure 7-1. ^{1}H-nmr spectra of poly(VBzS) (a) and poly(VBzTD) (b) in $CDCl_3$.

Figure 7-2 shows the ^{1}H-nmr charts for poly(VBzTD-co-BzTD). The molar ratio of vinylbenzyl group actually introduced into the polymer chain was determined by the ratio of vinyl protons to benzyl protons observed in the ^{1}H NMR analyses and agreed well with the fed molar ratio of 4-chloromethyl styrene.

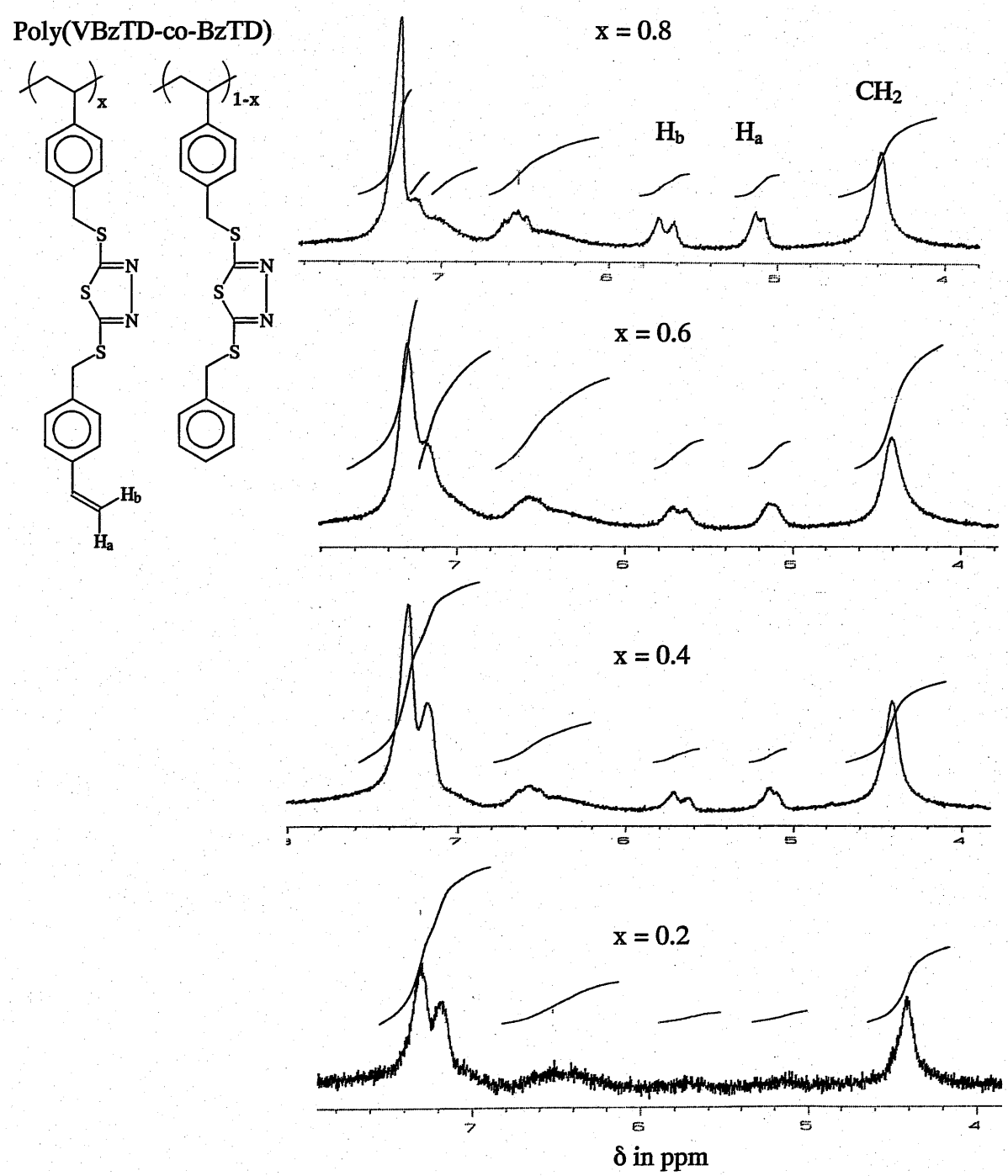

Figure 7-2. ^{1}H-nmr spectra of poly(VBzTD-co-BzTD) with varied copolymer compositions in deuterated dimethylformamide.

7-3-2. Comparison of polymerization reactivity of pendant styrenyl group attached to polymer chain via different linking groups

The two homopolymers, poly(VBzTD) and poly(VBzS) were compared to investigate the photopolymerization reactivity of pendant styrenyl groups attached to polystyrene backbone via thiadiazole group or CH_2O group, respectively. Photoinitiated polymerization of these pendant styrenyl groups in the presence of photoinitiator, PMS, was studied by RT-IR and the results were shown in Figure 7-3. The conversion of styrenyl group in poly(VBzTD) was gradually increased as the irradiation dose increased, whereas styrenyl group in poly(VBzS) showed no polymerization reactivity in this experimental condition. Poly(VBzTD) appeared rubbery at room temperature and styrenyl group attached to this polymer should be in an environment of rubbery matrix. This implies that the segmental movements of polymer chain and rotational movements of pendant styrenyl groups should be taking place extensively inside the polymerization system and this allows the polymerization to proceed effectively. On the other hand, poly(VBzS) appeared to be a glassy solid and the polymerization system was apparently in a glassy state. In such a case, styrenyl groups are frozen in a solid matrix and rotational movements of pendant styrenyl groups, which are assumed to be necessary to induce effective polymerization, should be restricted. In poly(VBzTD), a pendant styrenyl group is separated from the main chain via two flexible CH_2S groups attached to a thiadiazole group. Rotation around these two CH_2S groups may allow large free volume of pendant styrenyl group in a rubbery state of the polymerization system. However, the bulkiness of such pendant substituents would cause steric repulsion with each other and such steric hindrance might allocate styrenyl groups in unfavorable positions for polymerization. This might

explain the observed relatively slow rate of polymerization of styrenyl group in poly(VBzTD).

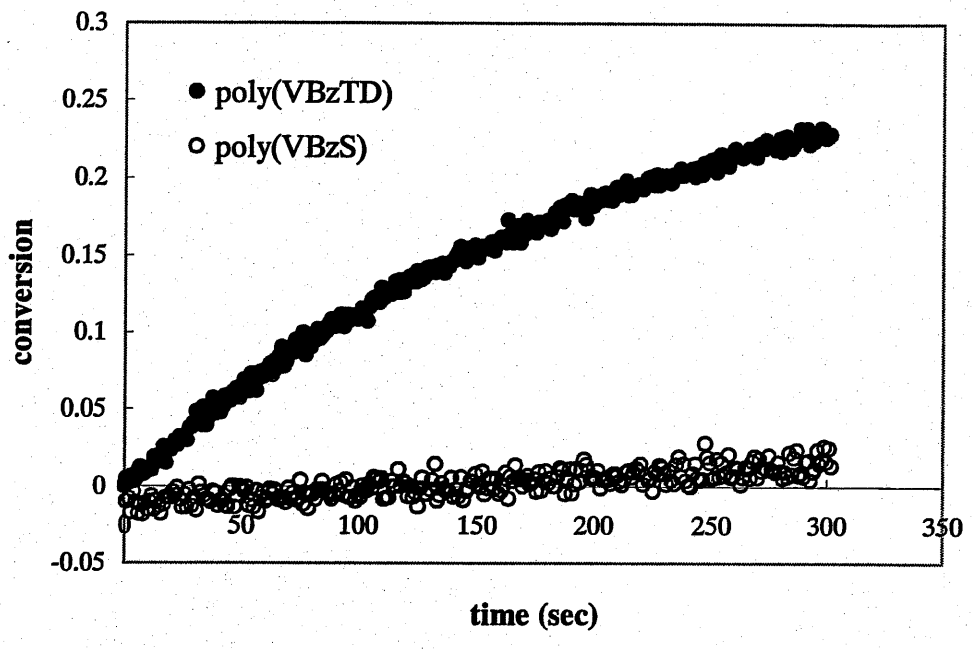

Figure 7-3. Comparison of polymerizability of pendant styrenyl groups attached in poly(VBzTD) and poly(VBzS). Polymerization was initiated by PMS under the irradiation of 365-nm light at 20 – 25 °C. Ratio of poly(VBzTD)/PMS = poly(VBzS)/PMS = 0.20/0.004 (wt/wt) and the incident light intensity = 5.0×10^{-9} einstein·cm^{-2}·s^{-1}.

7-3-3.Polymerization behavior of pendant styrenyl group in poly(VBzTD-co-BzTD)

The pendant styrenyl group in poly(VBzTD) was diluted by incorporating benzyl group instead of styrenyl group and the molar ratio of pendant styrenyl group was systematically altered from 0.2 to 1.0 with an interval of 0.2 in the obtained poly(VBzTD-co-BzTD). Time-conversion curves obtained for these copolymers were shown in Figure 7-4. As the molar ratio of pendant styrenyl group decreased, conversion was increased at any polymerization time. Highest conversion was attained with the styrenyl molar ratio of 0.2. This result was rather surprising, since in this particular case each styrenyl group connected to the polymer backbone via thiadiazole linking group is separated by four similar benzyl groups in an average and such mutual separation of styrenyl groups would result in decreased polymerization reactivity. The rate of polymerization was calculated from the differential of curve fit for each time-conversion curve. Figure 2(b) shows the plot of thus obtained R_p vs. concentration of remaining styrenyl group, [M]. Each plot showed almost linear relationship with curved edge at the initial stage of polymerization. In the beginning of the polymerization, possibly due to the presence of polymerization inhibitor and/or the dissolved oxygen, presence of induction period was observed except for the case of the smallest styrenyl content (0.2). The observed relationship between R_p and [M] was approximated by a equation (1).

$$R_p = k_p [P\cdot] ([M]-C_m) \qquad (1)$$

where C_m denotes a residual concentration of styrenyl group which could be reached if the polymerization proceeds linearly with the monomer concentration as expected by eq. (1), at which concentration the polymerization would terminate ($R_p = 0$).

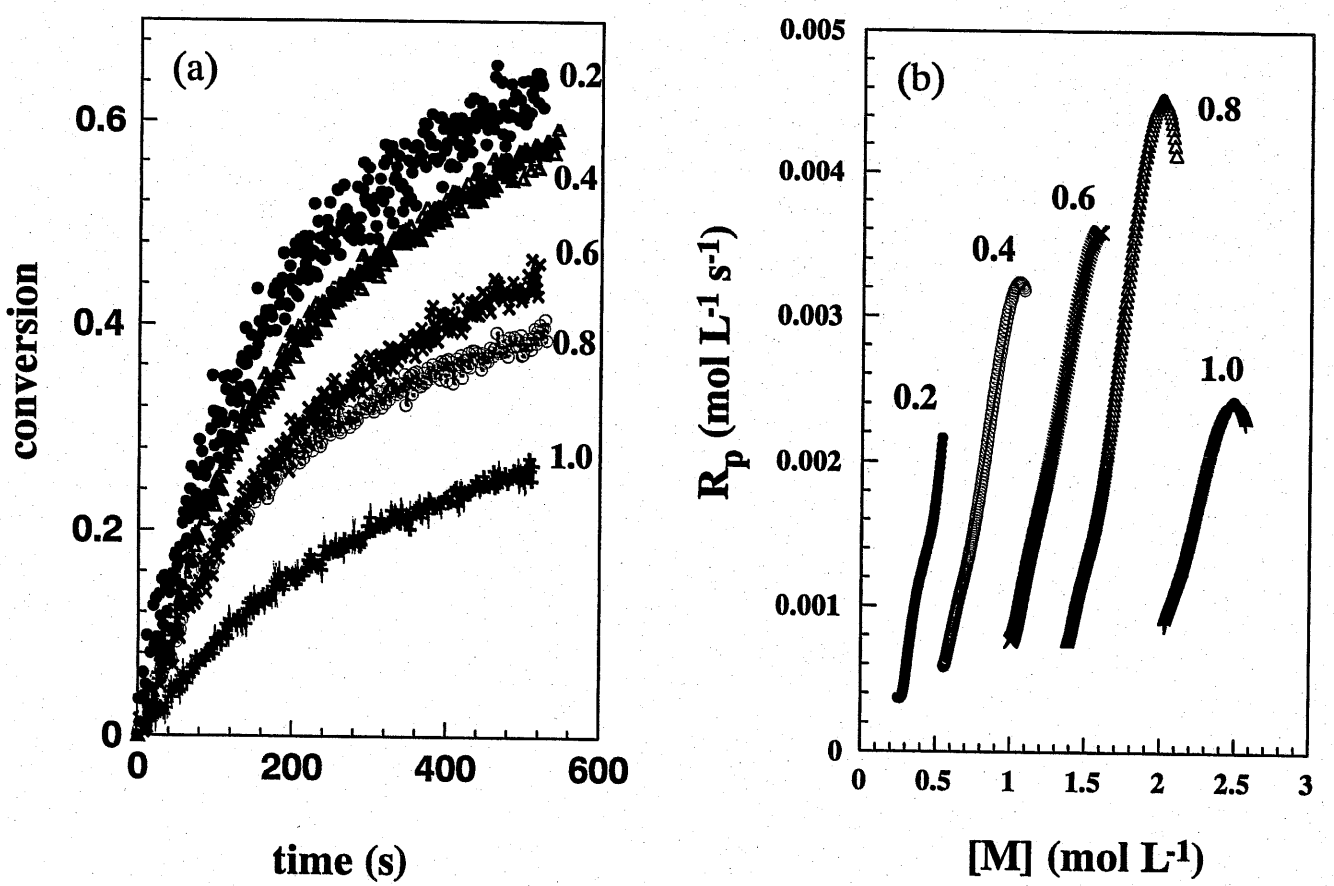

Figure 7-4. (a) Time-conversion curves and (b) R_p vs. pendant styrenyl concentration plot for the PMS-initiated photopolymerization of pendant styrenyl group in poly(VBzTD-co-BzTD). Numbers appears inside the Figures indicate the molar ratio of pendant styrenyl group in the copolymer.

From the slope and the intercept of this linear approximation, values of k_p [P·] and C_m was obtained. Figure 7-5 shows the relationship between k_p[P·] and the initial concentration of pendant styrenyl group. The lowest value of k_p[P·] was observed for the homopolymer of pendant styrenyl group and with the incorporation of benzyl substituted unit in the copolymer structure, the increase in k_p[P·] was observed. The value of k_p[P·] was apparently constant in the concentration range of pendant styrenyl group between 0.5 and 1.5 mol·L^{-1}. Polymerization reactivity of pendant styrenyl group is apparently increased by separating pendant styrenyl groups with similar and less bulky benzyl substituents. Steric hindrance between adjacent pendant styrenyl groups might be reduced by the presence of benzyl groups. Maximum rate of polymerization observed, $R_{p(max)}$, and the extrapolated value of the initial polymerization rate based on Eq. (1), $R_{p0(ex)}$ were plotted against the effective initial concentration of pendant styrenyl group, $[M]_0 - C_m$ as is seen in Fig. 7-5(b). Both values of $R_{p(max)}$ and $R_{p0(ex)}$ are increased with the increase in $([M]_0 - C_m)$ until the latter value reaches 0.7. Figure 7-6 shows the dependence of the residual unsaturation of styrenyl group, C_m, on square of the initial concentration of styrenyl group. From this linear plot, the relationship between C_m and $[M]_0$ was found to be $C_m = 0.30[M]_0^2$. By integrating Eq. (2), decrease in the concentration of pendant styrenyl group with time during the photopolymerization is well expressed by the following equation.

$$\frac{[M]}{[M]_0} = 0.30[M]_0 + (1 - 0.30[M]_0)\exp(-k_p[P\cdot]t) \qquad (2)$$
$$= 0.30[M]_0 + (1 - 0.30[M]_0)\exp(-0.0065t)$$

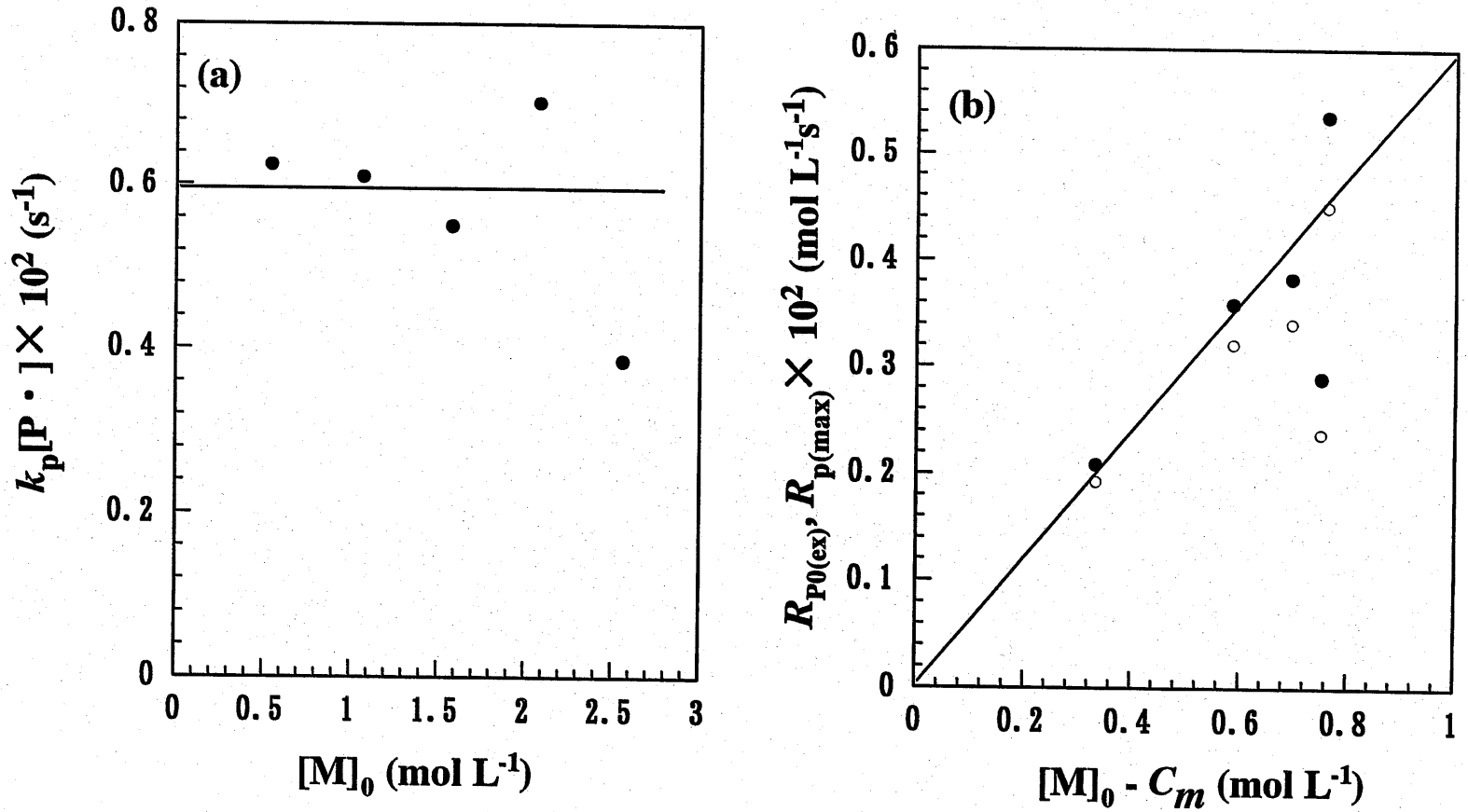

Figure 7-5. Dependence of $k_p[P\cdot]$ on the initial concentration of pendant styrenyl group (a) and $R_{p0(ex)}$ (•), $R_{p(max)}$ (o) *vs.* $[M]_0$– C_m plot (b).

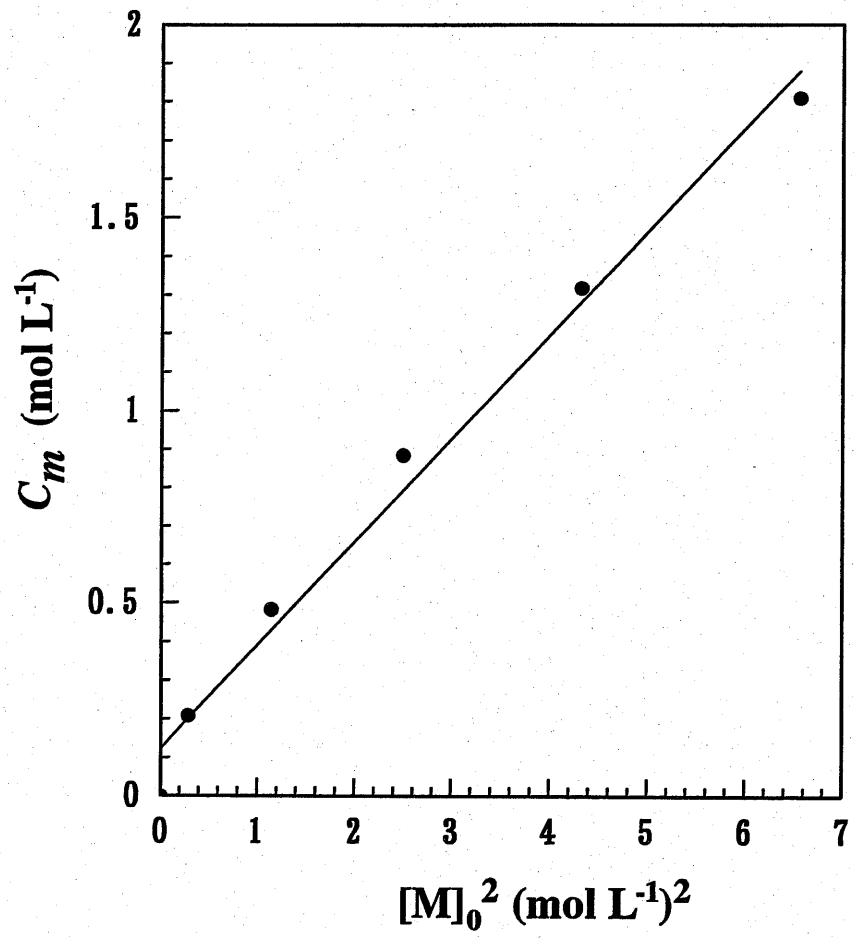

Figure 7-6. Relationship between the residual pendant styrenyl concentration and the initial pendant styrenyl concentration.

In the above equation, the ratio of concentration of pendant styrenyl group to the initial value is divided into two terms. The first term appears in Eq. (2) implies that about 30 % of initial concentration of pendant styrenyl group is unreactive toward the photopolymerization. The second term in Eq. (2) indicates that the rest of pendant styrenyl group is consumed with an ideal behavior as expected in a steady state polymerization. The reason why 30 % of pendant styrenyl group is left from the polymerization is unknown and this ratio seems to be pre-determined before polymerization starts. This result is essentially the same as that observed in the case of polymerization of BzTD in poly(BzTD) matrix as described in Chapter 4. Aggregation of pendant styrenyl groups might occur in this case and some of the pendant styrenyl groups are expelled outside the aggregates and might not contribute the polymerization.

During the RT-IR observation of monomer consumption in polymerization process, concentration change of photoinitiator, PMS, was also monitored at the absorption band of 1171 cm^{-1} which is assigned to a coupled asymmetrical stretching vibration of two CCl_3 groups attached to 1,3,5-triazine ring. The initial decomposition rate of PMS, R_{d0}, was determined and plotted against the initial concentration of pendant styrenyl group as shown in Figure 7-7. R_{d0} was found to be essentially independent on the initial concentration of pendant styrenyl group and are in the order of 2.5 (± 1) × 10^{-4} $mol \cdot L^{-1} \cdot s^{-1}$. The initial value of kinetic chain length, kcl_0, is defined by the following equation.

$$kcl_0 = R_{p0(ex)} / R_{d0} \qquad (3)$$

Figure 7-8 shows that kcl_0 is apparently independent of the initial concentration of pendant styrenyl group and around 15(± 5).

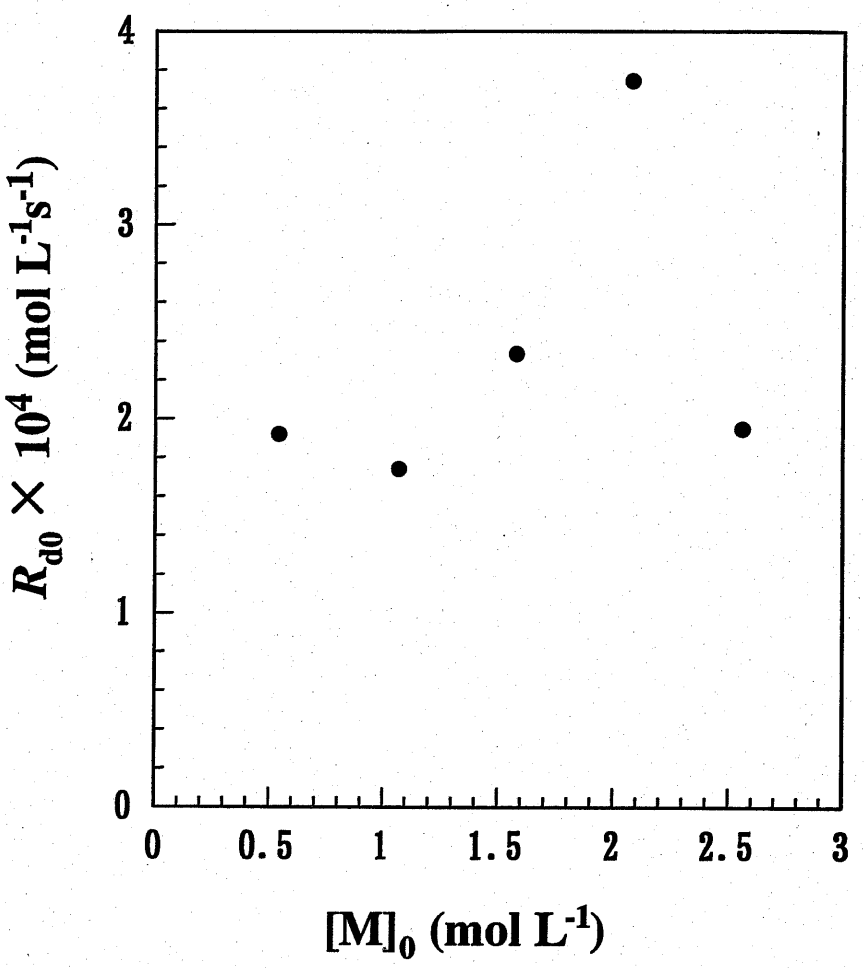

Figure 7-7. Relationship between R_{d0} and $[M]_0$.

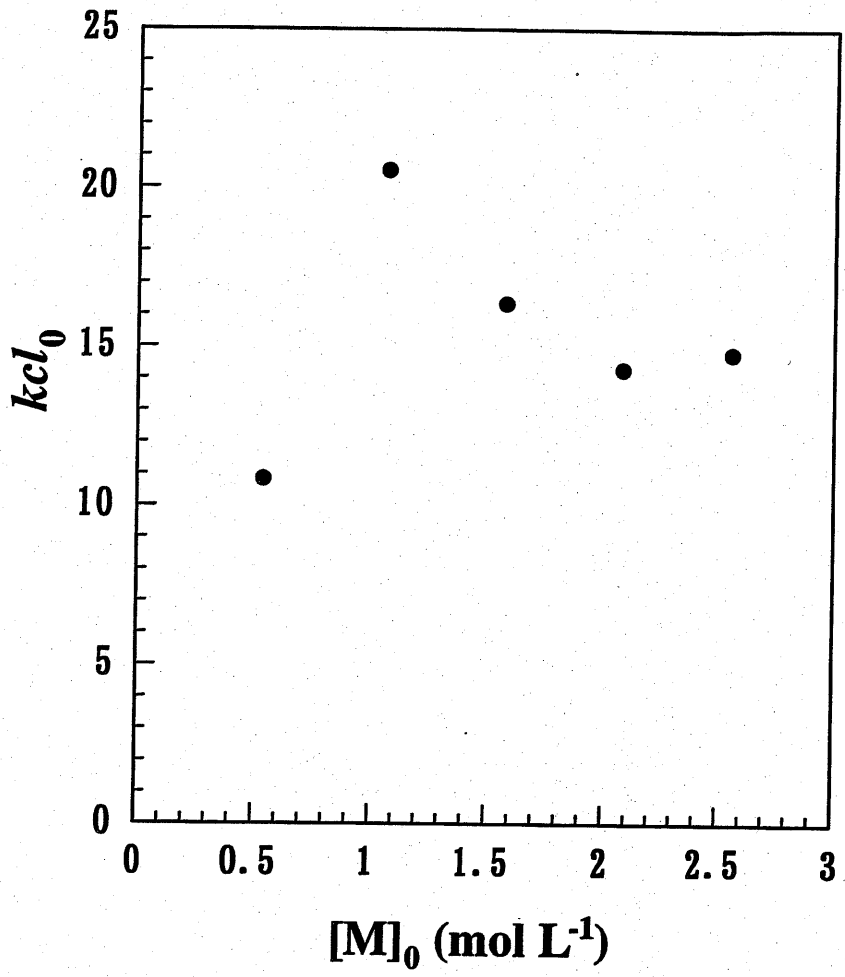

Figure 7-8. Relationship between kcl_0 and $[M]_0$.

7-3-4. Effects of photoinitiator concentration on polymerization reactivity of pendant styrenyl group

Photopolymerization behavior of pendant styrenyl group in the presence of various concentrations of photoinitiator (PMS) was investigated. Figure 7-9 shows the time-conversion curves (a) and the dependence of the initial polymerization rate, $R_{p0(ex)}$, on the initial concentration of PMS (b), respectively. The increase in conversion and polymerization rate with PMS concentration was eminent for the values up to 0.046 $mol \cdot L^{-1}$ and further increase in PMS concentration resulted in the decrease in both conversion and polymerization rate. Extensive recombination of initiating PMS radicals with by-produced chlorine atoms might be the cause of decreased polymerization efficiency at relatively high PMS concentration. Linear approximation of R_p *vs.* [M] plot, as described in the previous section, was applied also in this case and the obtained values of $k_p[P\cdot]$ and C_m were plotted against the initial concentration of PMS as seen in Figure 7-10. The values of $k_p[P\cdot]$ are independent of the initial concentration of PMS, whereas C_m decreased with PMS concentration. The latter could be explained as follows: as the initial concentration of PMS increased, the effective concentration of pendant styrenyl group participating in the polymerization also increases, and then the polymerization rate expressed in Eq. (1) also increases. The effect of initial PMS concentration on polymerization rate is manifested in decreasing residual styrenyl concentration and it is important to observe that the value of $k_p[P\cdot]$ are independent of the initial PMS concentration.

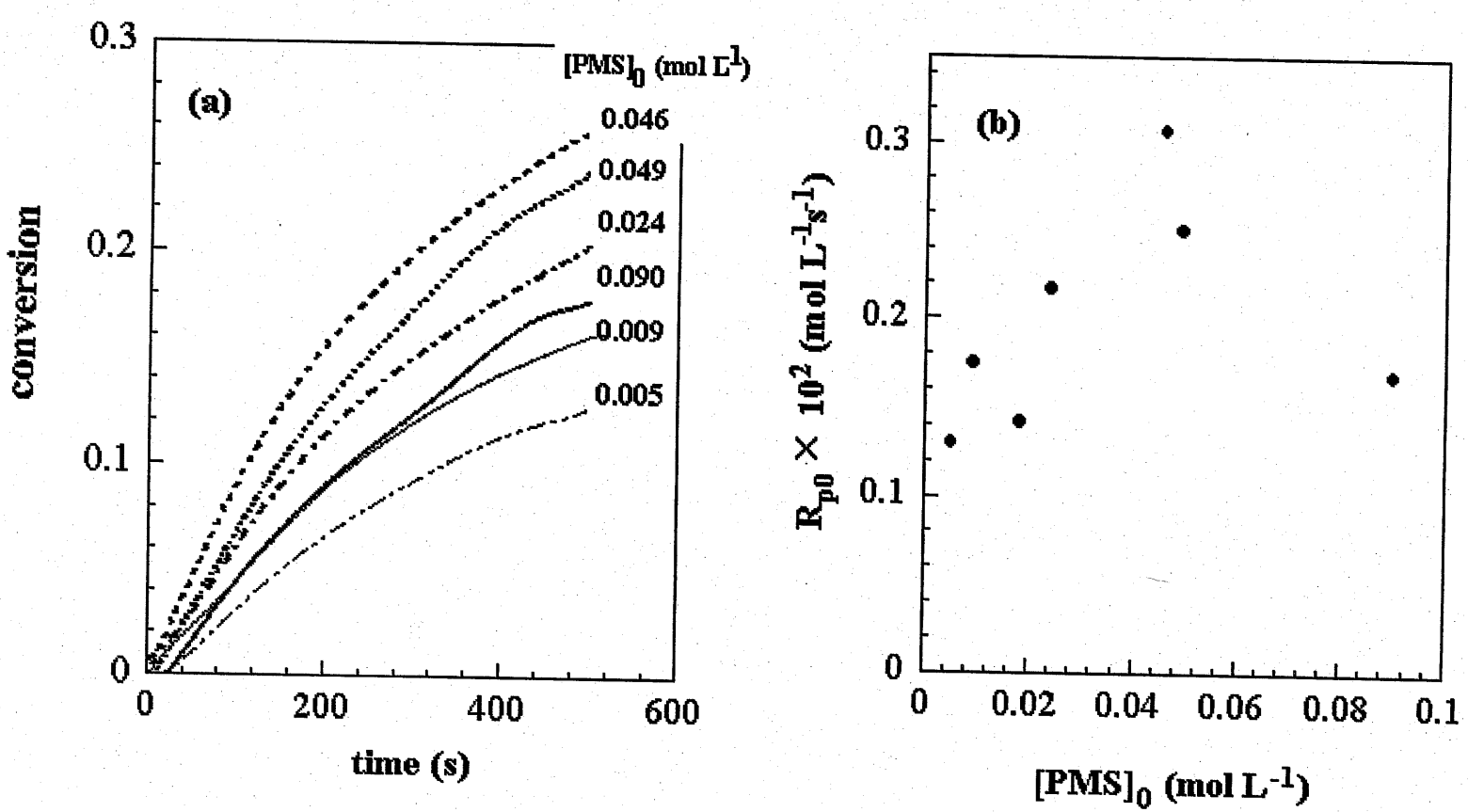

Figure 7-9. Time-conversion curves (a) and the dependence of the initial polymerization rate, $R_{p0(ex)}$, on the initial concentration of PMS (b) for the polymerization of pendant styrenyl group in poly(VBzTD).

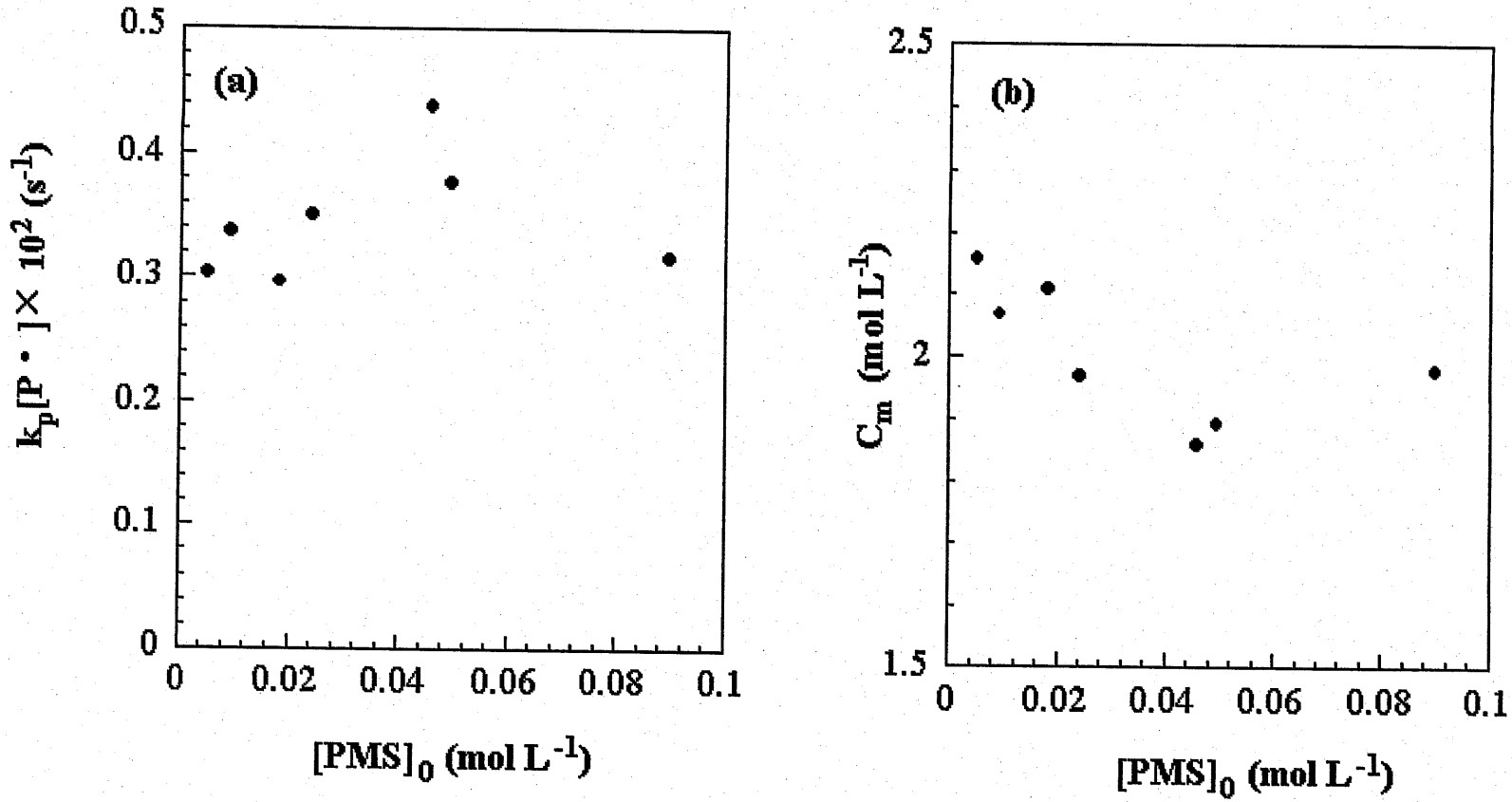

Figure 7-10. Dependence of $k_p[P\cdot]$ (a) and C_m on the initial concentration of PMS for the polymerization of pendant styrenyl group in poly(VBzTD).

7-3-5. Copolymerization of pendant styrenyl group with a free monomer

Pendant styrenyl groups connected to polymer backbone showed limited polymerization reactivity with relatively slow polymerization rate and insufficient final conversions. Therefore, it should be necessary to find a way to increase the polymerization reactivity of such pendant styrenyl group. Copolymerization of pendant styrenyl group with a low-molecular-weight monomer was investigated. As such monomers, C1TD, BzTD and C3TD2 were selected, since these monomers possess exactly the same structural characteristics as the pendant styrenyl group in poly(VBzTD) and complete miscibility of these monomers in poly(VBzTD) matrix was anticipated. C1TD and BzTD have been found to show high polymerization reactivity in poly(BzTD) matrix. In poly(VBzTD) matrix both monomer and pendant styrenyl group in poly(VBzTD) can participate the polymerization and overall conversion was the sum of each conversion. Figure 7-11 shows time-conversion curves of styrenyl group in the three different photopolymerization system. In the copolymerization system of BzTD and poly(VBzTD)(Figure 7-11(b)), the highest conversion was approximately 50 % and most of the remaining unsaturation was ascribed to the remaining pendant styrenyl group in poly(VBzTD). However, when the calculated polymerization rates were plotted against conversion (Figure 7-12), highest polymerization rate was observed in the copolymerization system, since increased concentration of styrenyl unsaturation was participated in this copolymerization system. The maximum polymerization rate was more than two-fold of that in the polymerization of BzTD in poly(BzTD) matrix. Figure 7-13 shows the actually photopolymerized concentration of styrenyl groups. In this Figure, the curve indicated as (2) + (3) shows the sum of the independently determined photopolymerized concentrations of styrenyl unsaturation of BzTD in poly(BzTD) and

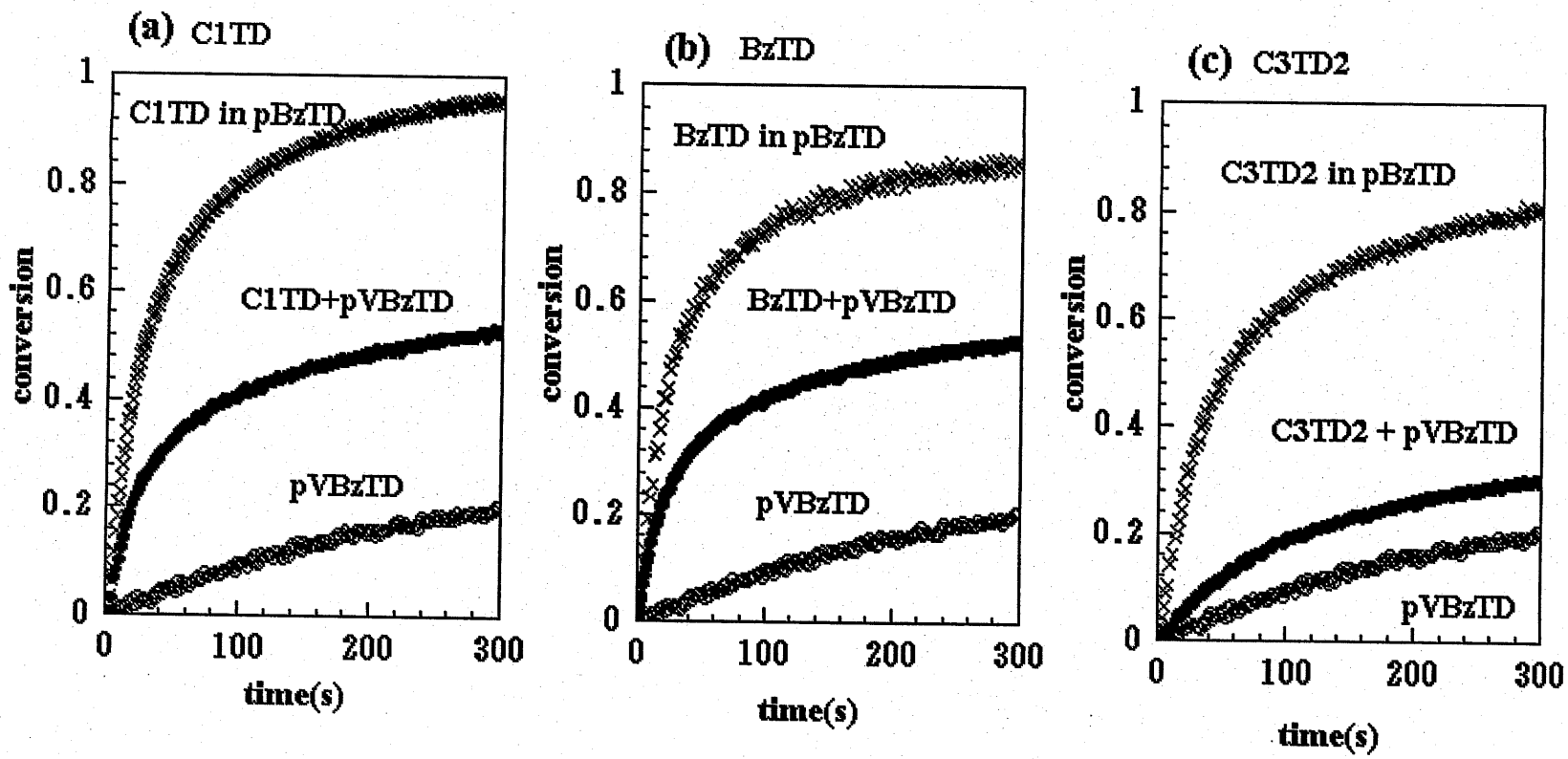

Figure 7-11. Photopolymerization behaviors of C1TD (a), BzTD (b) and C3TD2 in the matrix of poly(BzTD) and poly(VBzTD). Time-conversion curve for the homopolymerization of pendant styrenyl group in poly(VBzTD) is also drawn in each plot for comparison. Monomer/polymer matrix/PMS = 0.1/0.2/0.004 (wt/wt/wt).

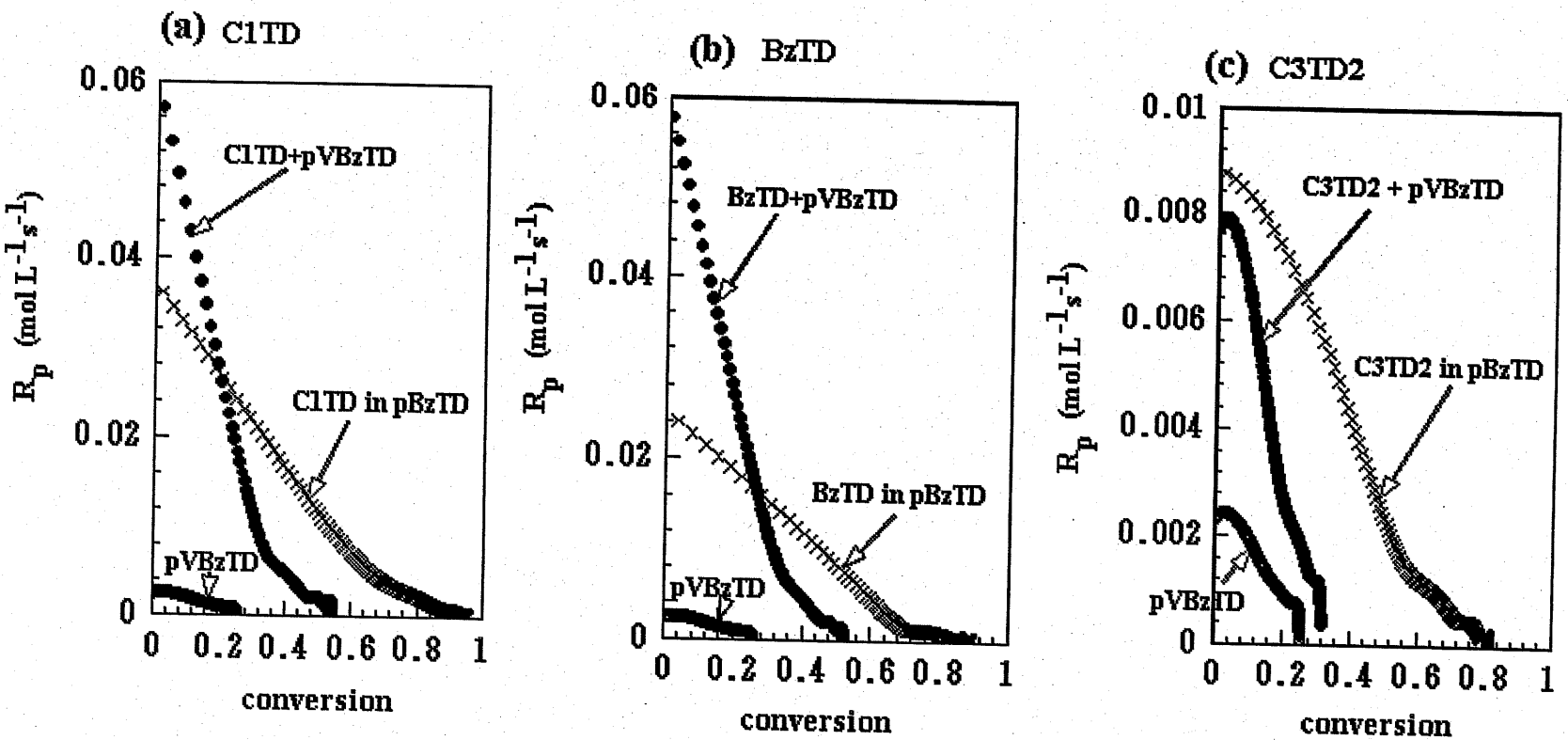

Figure 7-12. Rate of photopolymerization for C1TD (a), BzTD (b) and C3TD2 in the matrix of poly(BzTD) and poly(VBzTD). Polymerization rate for the homopolymerization of pendant styrenyl group in poly(VBzTD) is also drawn in each plot for comparison. Monomer/polymer matrix/PMS = 0.1/0.2/0.004 (wt/wt/wt).

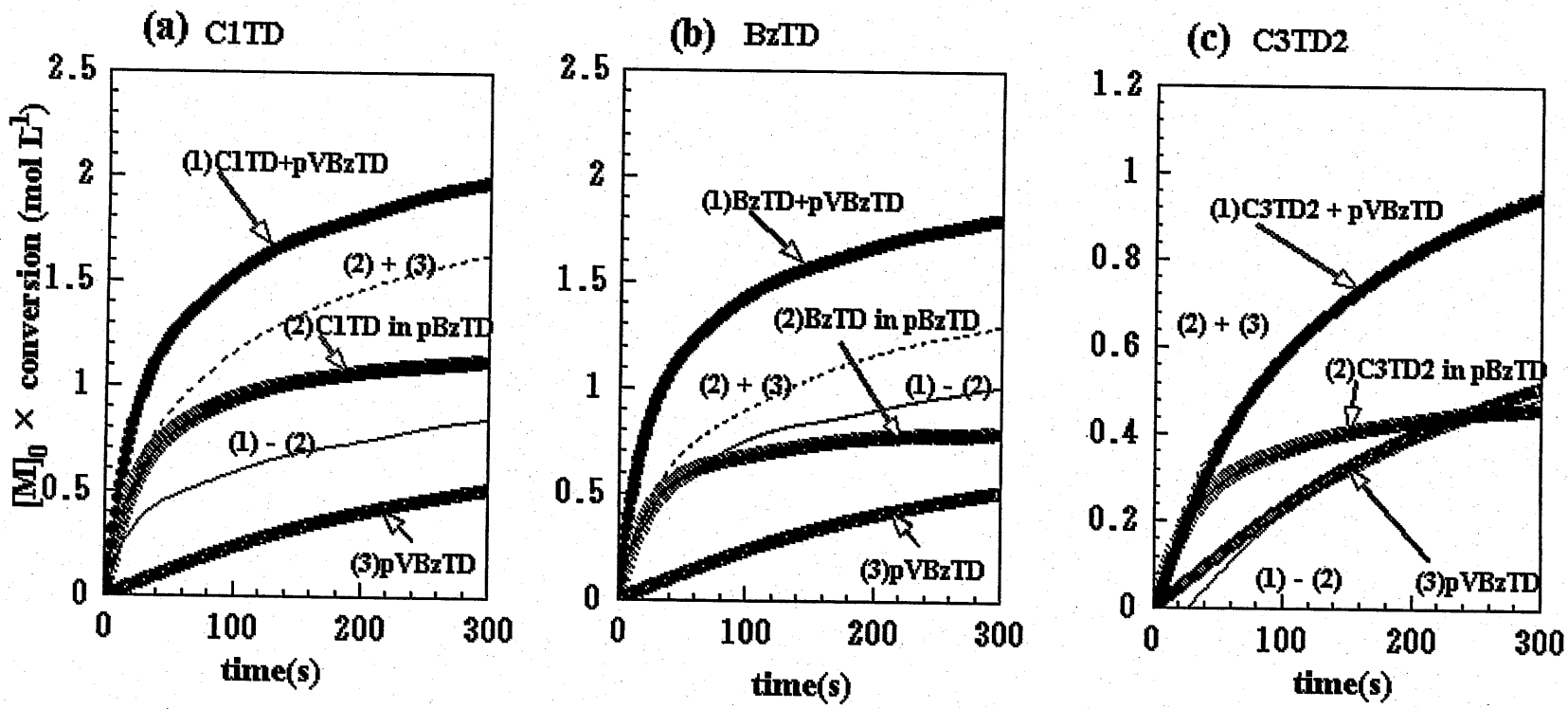

Figure 7-13. Plots for actually polymerized styrenyl concentration in the photopolymerization of C1TD (a), BzTD (b) and C3TD2 in the matrix of poly(BzTD) and poly(VBzTD). Data for the homopolymerization of pendant styrenyl group in poly(VBzTD) is also drawn in each plot for comparison.

that of poly(VBzTD). The curve (1) corresponding to the conversion of styrenyl unsaturation in the copolymerization system locates far above the curve, (2) + (3) and this indicates that styrenyl unsaturation in poly(VBzTD) should polymerized much faster than that in the homopolymerization of poly(VBzTD) represented by curve (3). In order to evaluate the polymerization reactivity of poly(VBzTD) in this copolymerization condition, curve (1) was subtracted by curve (2) and the resulted curve (1) – (2) should represent the polymerization reactivity of pendant styrenyl group in this copolymerization condition. It is quite surprising that the simulated polymerization profile of the pendant styrenyl group of poly(VBzTD) in the presence of BzTD shows an identical curve to that of BzTD in poly(BzTD) matrix. This result suggests that the pendant styrenyl group in poly(VBzTD) has the same reactivity as that of BzTD in the presence of BzTD and this result cannot be explained by a simple copolymerization mechanism.

Identical behavior is also seen in the case of C1TD (Figure 7-11(a), -12(a) and -13(a)). On the other hand, as for C3TD2, this monomer does not affect the polymerizability of pendant styrenyl group in poly(VBzTD) as is seen in Fig. 7-13(c). In this case, the actually photopolymerized concentration of styrenyl groups of C3TD2 and poly(VBzTD) in copolymerization are identical to the sum of the independently determined photopolymerized concentrations of styrenyl unsaturation of C3TD2 in poly(BzTD) and that of poly(VBzTD).

In our previous investigation on the polymerization behavior of similar types of styrenyl monomers, monomer molecules are considered to be assembled inside the interstices of pendant thiadiazole substituents of poly(BzTD) matrix (see Chapter 2 and 6). In the present polymerization system, BzTD monomer molecules might also be

assembled inside the interstices of pendant styrenyl-substituted thiadiazole groups of polymer matrix due to intermolecular interactions between thiadiazole groups of both moieties. As schematically illustrated in Figure 7-14, aligned structure of BzTD molecules and pendant styrenyl groups of poly(VBzTD) caused by large rotational degrees of freedom of monomer molecules in this system may explain the enhanced polymerization reactivity of this copolymerization system.

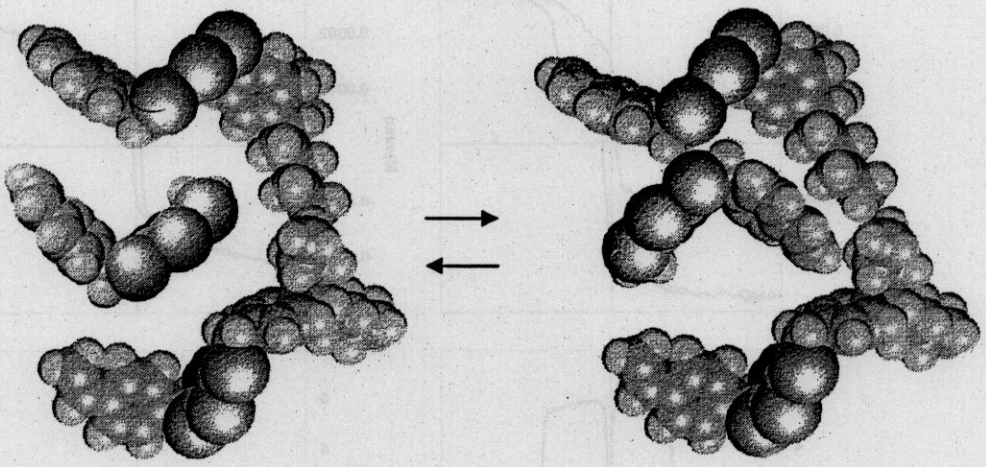

Figure 7-14. A schematic illustration showing possible rearrangements of C1TD molecules in the interstices of pendant styrenyl groups in poly(VBzTD).

7-4. CONCLUSION

The photoinitiated polymerization of pendant styrenyl group attached to the backbone chain *via* thiadiazole group was not very rapid and reached low final conversion. Taking the previously reported experimental findings into consideration, the low polymerization reactivity of pendant styrenyl group was improved by the addition of the analogous monomeric compound to the photopolymerization system. Copolymerization reactivity of the pendant styrenyl groups was remarkably increased and found to be equivalent to that of the anologous monomeric styrenyl compound. A possible mechanism for the observed experimental results could be that monomer molecules are assembled inside the interstices of the pendant styrenyl groups and large rotational degree of freedom might allow monomer molecules to align themselves in favor to effective progress of copolymerization with pendant styrenyl groups.

Further experimental proofs to discuss the validity of such speculation are necessary. However, the present investigation clearly showed the possibilities of highly effective photo-crosslinkable system which readily forms 3D network upon irradiation of UV light.

REFERENCES

1. Green, G. E. ; Stark, B. P. ; Zahir, S. A., J. Macro. Sci. –Revs. Macro. Chem., 1981-82, C21(2), 187.
2. Huang, W.-K. ; Hsiue, G.-H. ; Hou, W.-H., J. Polym. Sci. Part A. Polym. Chem., 1988, 26, 1867.
3. Puskas, J. E.; Kaszas, G. ; Kennedy, J. P., J. Macromol. Sci. –Chem., 1991, A28(1), 65.
4. Decker, C. ; Xuan, H. L. ; Viet, T. N. T., J. Polym. Sci. Part A. Polym. Chem., 1995, 33, 2759.
5. Decker, C. ; Xuan, H. L. ; Viet, T. N. T., ibid., 1996, 34, 1771.
6. Decker, C. ; Viet, T. N. T. ; Xuan, H. L., Eur. Polym. J., 1996, 32, 1319.
7. Harabagiu, V. ; Pinteala, M. ; Cotzur, C. ; Holerca, M. N. ; Ropot, M., J. Macromol. Sci. Pure Appl. Chem., 1995, A32, 1641.
8. Harabagiu, V. ; Pinteala, M. ; Cotzur, C. ; Simionescu, B. C. ; Simionescue, C. I., Polym. Bull., 1994, 1, 259.
9. Muller, U. ; Tempet, H. J. ; Neuegufeld, N., Eur. Polym. J., 1991, 27, 621.
10. Muller, U., J. Macromol. Sci. Pure Appl. Chem., 1996, A33, 33.
11. Bajdala, J. ; Muller, U. ; Wartewing, S. ; Winkler, K., Macromol. Chem. Phys., 1996, 197, 3093.
12. Muller, U., J. Macromol. Sci. Pure Appl. Chem., 1994, A31, 1905.
13. Muller, U. ; Jockusch, S. ; Timpe, H. J., J. Polym. Sci. Part A. Polym. Chem., 1992, 30, 2755.
14. Abdella, L. ; Dinia, M. N. ; Boutevin, B. ; Abadie, M. J. M., Eur. Polym. J., 1997, 33, 6.

15. Iojoiu, C. ; Abadie, M. J. M. ; Harabagiu, V. ; Pinteala, M. ; Simionescu, B. C., Eur. Polym. J., 2000, 36, 2115.

16. Abdellah, L.; Dinia, M. N. ; Boutevin, B. ; Abadie, J. M., Eur. Polym. J., 1997, 33, 869.

17. Abdellah, L.; Boutevin, B. ;Caporiccio, G. ; Guida-Pietrasanta, F., ibid., 2002, 38, 1515.

18. Pappas, S. P., "Encyclopedia of polymer science engineering", vol. 11. 1988, p. 186.

19. Xuan, H. L. ; Decker, C., J. Polym. Sci. Part A. Polym. Chem., 1993, 31, 769.

20. Decker, C. ; Viet, T. N. T. ; Xuan, H. L., Eur. Polym. J., 1996, 32, 549.

21. Moussa, K. ; Decker, C., J. Polym. Sci. Part A. Polym. Chem., 1993, 31, 2197.

22. Decker, C. ; Moussa, K. , Makromol. Chem., 1988, 189, 2381.

23. Decker, C. ; Moussa, K. , Macromolecules. 1989, 22, 4455.

24. Decker, C., Macromolecules. 1990, 23, 5217.

25. Decker, C. ; Moussa, K. , Eur. Polym. J., 1990, 26, 393.

Chapter 8

General summary

This thesis consists of an introductory chapter and six scientific chapters, each of which is summarized as follows.

Chapter 1. General introduction

Scientific and industrial significance and motif of photopolymerization of styrenyl compounds in polymer matrix are comprehensively described.

Chapter 2. Design and synthesis of highly photopolymerizable styrenyl compounds in the solid-state photoinitiated polymerization

A series of styrenyl compounds bearing 2,5-dithio-1,3,4-thiadiazole group were prepared and their reactivity in the solid-state photopolymerization initiated by 2-(4'-methoxystyryl)-4,6-bis-(trichloromethyl)-1,3,5-triazine was studied. These compounds exhibited high polymerization reactivity and the final conversion reached nearly completion despite of relatively high T_g of the polymer matrix. Even at temperatures below T_g, polymerization proceeded without ceiling conversion. These features were explained by considering intermolecular interactions between styrenyl compounds to induce molecular alignments effective for solid-state polymerization, large excess free volume arisen from rotation around methylenethio group, and/or intramatrix radical migration to encounter with standing-by monomers caused by chain transfer reaction to labile hydrogen atom.

Chapter 3. Real-time monitoring of photodecomposition of initiator in polymer matrix and kinetic analysis of photopolymerization

The photodecomposition process of the photoinitiator, 2-(4'-methoxystyryl)-4,6-bis(trichloromethyl)-1,3,5-triazine (PMS), dispersed in polymer matrix was monitored by real-time FT-IR (RT-IR) spectroscopy by tracing the absorbance at 1171 cm^{-1}, which is assigned to a coupled stretching absorption characteristic of bis(trichloromethyl) groups attached to 1,3,5-triazine ring. In polystyrene matrix, quantum yield of photodecomposition (Φ_d) of PMS was found to be 0.09 at the beginning of the photodecomposition and decayed rapidly with the consumption of PMS. The decomposition rate of PMS was found to depend linearly on the incident light intensity.

PMS-initiated photopolymerization of 2-(4-vinylbenzyl)thio-5-benzylthio-1,3,4-thiadiazole (BzTD) was monitored by RT-IR concurrently with the photodecomposition process of PMS. In poly(BzTD) matrix, BzTD monomer showed high polymerization rate under UV irradiation in the presence of PMS and the final conversion reached up to 90%, while ca. 50% of PMS remained unreacted. During the photopolymerization process, polymerization rate of BzTD and decomposition rate of PMS showed linear dependencies on the monomer and the PMS concentrations, respectively. From the kinetic analysis, termination process between the propagating polymer radical and PMS molecule was supposed to be the dominant termination process. Based on the kinetic model proposed, values of kinetic chain length (20～60) and rate constant ratio (k_p/k_t = 0.32) were obtained. Maximum quantum yield of the photopolymerization of BzTD was found to be 1.3, whereas Φ_d was ca. 0.5 which is about 5-fold higher than that observed in the absence of BzTD.

Chapter 4. Influence of monomer concentration in the solid-state photoinitiated polymerization of styrenyl compound bearing 1,3,4-thiadiazole group

Photopolymerization of BzTD in poly(BzTD) matrix was found to proceed in the steady-state condition; $R_p = k_p[P\cdot]([M]-C_m)$, in which $k_p[P\cdot]$ was found to be constant ($0.036\ s^{-1}$) and independent of the initial monomer concentration and monomer conversion. This result indicates that the density of monomer molecules in the polymerization locus is not affected by initial monomer concentration. Monomer molecules are considered to form cluster structure, the minimum size of which was estimated from the kinetic chain length to be 30 monomer molecules depending on the initial monomer concentration. The photopolymerization system of the styrenyl compounds in the polymer matrix is regarded as polymerization system in nanoscopically aggregated phase.

Chapter 5. Effects of photoinitiator concentration and light intensity on the solid-state polymerization of styrenyl compound bearing thiadiazole group

The effects of photoinitiator concentration and light intensity on the photoinitiated polymerization of BzTD in poly(BzTD) matrix were investigated. From the dependence on the initial photoinitiator concentration, the maximum value of kinetic chain length (*kcl*) was estimated to be around 200 at the initial monomer concentration of 0.83 $mol\cdot L^{-1}$. This maximum *kcl* value is considered to represent the number of monomer molecules included in the monomer cluster formed in the polymerization system. When the initial photoinitiator concentration fell below 1/200 of the initial monomer concentration, polymerization rate decreased abruptly, suggesting the existence of cluster structure of monomer molecules. The quantum yield of photodecomposition of

the photoinitiator increased with decreasing light intensity and finally reached unity. On the other hand, kinetic parameters such as k_p/k_t and kinetic chain length were shown to be independent of the light intensity.

Chapter 6. Effect of alkyl chain length in 2-(4'-vinylbenzyl)thio-5-alkyl-thio-1,3,4-thiadiazole on its photopolymerization in polymer matrix

The size of alkyl substituent at 5-position of 1,3,4-thiadiazole group was systematically altered and its effect on the photopolymerizability was investigated. In polystyrene matrix, those monomers polymerized efficiently and the size effect is not observed. On the other hand, in poly(BzTD) matrix the size effect is so eminent that small alkyl chain dramatically enhanced the polymerization rate, whereas longer alkyl chain depressed polymerization rate significantly. High polymerization rate and reduced concentration of residual monomer were attained in this study. When the size of alkyl substituent is relatively small, polymerization proceeded rapidly and kinetic chain length (*kcl*) increased up to ca. 40, whereas larger alkyl substituents resulted in decreased polymerization reactivity and smaller *kcl* values. A possible explanation to the observed experimental results should be that monomer molecules are assembled with the pendant groups of matrix polymer and molecular rearrangements inside the assembled structure would determine the polymerization reactivity.

Chapter 7. Preparation of polymers bearing pendant styrenyl group and its photopolymerization behavior in solid state

The photoinitiated polymerization of pendant styrenyl group attached to the backbone chain *via* thiadiazole group was not very rapid and reached low final conversion. Taking

the previously reported experimental findings into consideration, the low polymerization reactivity of pendant styrenyl group was improved by the addition of the analogous monomeric compound to the photopolymerization system. Copolymerization reactivity of the pendant styrenyl groups was remarkably increased and found to be equivalent to that of the anologous monomeric styrenyl compound. A possible mechanism for the observed experimental results could be that monomer molecules are assembled inside the interstices of the pendant styrenyl groups and large rotational degree of freedom might allow monomer molecules to align themselves in favor of effective progress of copolymerization with pendant styrenyl groups.

List of publications

Chapter 1.

End-capping analysis of styrene derivatives with sodium β-naphthoxide as capping agent. 1. Concentration and chain-length distribution of the propagating species in styrene polymerization
Sawamoto, Mitsuo ; Furukawa, Akira ; Higashimura, Toshinobu:
Macromolecules(1983), 16(4), 518-522

Liquid-crystal polymers. 23. Steric and polar effects of large substituents in thermotropic aromatic polyesters with decamethylene spacers
Furukawa, Akira ; Lenz, Robert W.
Macromol. Chem., Macromol. Symp.(1986), 2, 3-20

Synthesis and characterization of extended-rod thermotropic polyesters with poly(oxyethylene) pendant substituents
Lenz, Robert W. ; Furukawa, Akira ; Bhowmik, Pradip; Garay, Raul O.; Majnusz, Jerczy
Polymer (1991), 32(9), 1703-1712

Chapter 2.

Design and synthesis of highly photopolymerizable styrenyl compounds in the solid-state photoinitiated polymerization.

Furukawa, Akira; Imanishi, Yukio; Tanihara, Masao

accepted for publication in J. Polym. Sci., Polym. Chem. Ed.

Chapter 3.

Real-time monitoring of photodecomposition of initiator in polymer matrix and kinetic analysis of photopolymerization

Furukawa, Akira; Imanishi, Yukio; Tanihara, Masao

To be submitted

Chapter 4.

Influence of monomer concentration in the solid-state photoinitiated polymerization of styrenyl compound bearing 1,3,4-thiadiazole group

Furukawa, Akira; Imanishi, Yukio; Tanihara, Masao

To be submitted

Chapter 5.

Effects of photoinitiator concentration and light intensity on the solid-state polymerization of styrenyl compound bearing thiadiazole group

Furukawa, Akira; Imanishi, Yukio; Tanihara, Masao

To be submitted

Chapter 6.

Effect of alkyl chain length in 2-(4'-vinylbenzyl)thio-5-alkyl-thio-1,3,4-thiadiazole on its photopolymerization in polymer matrix

Furukawa, Akira; Imanishi, Yukio; Tanihara, Masao

To be submitted

Chapter 7.

Preparation of polymers bearing pendant styrenyl group and its photopolymerization behavior in solid state

Furukawa, Akira; Imanishi, Yukio; Tanihara, Masao

To be submitted

Other related publications which are not included in this thesis

1. Original papers

(1)Liquid-crystalline side chain phosphazenes

Singler, Robert E.; Willingham, Reginald A.; Lenz, Robert W.; Furukawa, Akira;Finkelmann, Heino

Polym. Prepr.(Am.Chem.Soc.,Div.Polym. Chem.), (1987), 28(1), 448-449

(2)Liquid-crystalline side chain phosphazenes

Singler, Robert E. ; Willingham, Reginald A. ; Lenz, Robert W. ; Furukawa, Akira; Finkelmann, Heino

Macromolecules (1987), 20(7), 1727-1728

(3)The effect of temperature on optical and viscoelastic properties of a homogenious thermotropic liquid crystalline polymer

Driscoll, Paul ; Fujiwara, Kenichi ; Masuda, Toshiro ; Furukawa, Akira ; Lenz, Robert W.

Polym. J. (1988), 20(4), 351-356

(4) A comparison of optical light transmission and dynamic viscoelastic properties for determining transitions in thermotropic liquid-crystalline polymers

Driscoll, Paul ; Masuda, Toshiro ; Furukawa, Akira ; Lenz, Robert W.

Polym. J. (1990), 22(7), 609-613

2. Review article

(1) Relationships between polymer structure and liquid crystalline phase behavior for thermotropic polyesters

Lenz, Robert W.; Furukawa, Akira ; Wu, C. N.

In 'Polymers for Advanced Technologies' (Ed. M. Lewin), VCH Publishers, NY, (1988), p. 491.

(2) Design of polymer particles

Furukawa, Akira

Kobunshi, (1991)、40(4), 240-243

3. Publication at international meetings

(1) A new end-capping analysis of cationic polymerization using sodium β-naphthoxide

Sawamoto, Mitsuo ; Furukawa, Akira ; Higashimura,Toshinobu

Proc.IUPAC, I.U.P.A.C.,Macromol. Symp.,28th (1982), 148

(2)Functional liquid toners and their applications for electrophotographic printing plates

Furukawa, Akira

Proc. SPIE-Int. Soc. Opt. Eng. (1990), 1253, 40-51

(3)Dispersion polymerization of styrene in the presence of mercapto containing polymer dispersants

Ojima, Chikako and Furukawa, Akira

Preprints in 5th SPSJ international polymer conference, 1994, 381.

Acknowledgements

I would like to express my sincere gratitude to Professor Emeritus Yukio Imanishi for his helpful comments and discussion during the preparation of this thesis. His sharp but warm comments had encouraged the author so much and without his guidance this study could never have been done.

I wish to express my grateful appreciation to Professor Masao Tanihara for his helpful advice and discussion. His kind acceptance of the author to study in his laboratory enabled the author to complete the present thesis.

I gratefully thank Professor Michiya Fujiki for his kind advices and encouragement.

I would like thank Professor Kiyomi Kakiuchi for his valuable comments.

I gratefully acknowledge Associate Professor Tamaki Nakano for his supports and valuable comments.

I would like to express my deepest thanks to Professor Emeritus Toshinobu Higashimura of Kyoto University. I owe him so much.

I would like to thank Professor Mitsuo Sawamoto of Kyoto University for his valuable comments and supports.

I would like to express my sincere thanks to Professor Emeritus Robert W. Lenz.

Grateful acknowledgement is made to all members of Biocompatible Materials Science Laboratory and Polymer Materials Science Laboratory of Nara Institute of Science and Technology.

Finally, I would like to express my acknowledgement to my parents and my wife, Yoshiko.

March 24, 2003

Akira Furukawa